## *Quantifying Palaeopathology Using Geometric Morphometrics*

PLOMP, KIMBERLY,ANNE

# Quantifying Palaeopathology Using Geometric Morphometrics

**Kimberly A. Plomp**

## Abstract:

Palaeopathology is the study of disease and injury in archaeological bone. Traditional methods rely heavily on macroscopic description which can have a high degree of subjectivity and error, as well as limiting the types of research questions possible. Geometric morphometrics are a suite of shape analysis techniques and provide an opportunity to investigate possible relationships between skeletal morphological variation and disease. This thesis aims to demonstrate the potential of applying these methods in palaeopathological research and the results illustrate the benefits of using quantifiable and objective shape analysis methods in palaeopathology. The first half of the thesis discusses the use of geometric morphometrics to investigate skeletal variation to identify possible aetiological factors in the development of Schmorl's nodes and osteoarthritis. There was a strong association found between vertebral morphology and Schmorl's nodes in the lower spine. These findings have great implications for both bioarchaeological interpretation and clinical understanding of the aetiology and pathogenesis of Schmorl's nodes. Joint morphology of the proximal ulna and distal humerus was found to have no identifiable relationship with osteoarthritis, indicating that joint morphology is not a predisposing factor in elbow osteoarthritis, nor does osteoarthritis deform the joints in a systematic manner. A tentative relationship between eburnation and knee joint morphology was identified, although these results need to be verified with future research. If the association can be supported, shape analyses may provide a way for clinicians to monitor the progression of the disease. Geometric morphometrics were also shown to objectively record pathological shape deformation resulting from leprosy and residual rickets. The ability to objectively describe lesions with quantified data will greatly strengthen palaeopathology by decreasing the subjectivity and error inherent in macroscopic based methods. This thesis represents promising groundwork for the incorporation of geometric morphometrics into palaeopathological research.

# Quantifying Palaeopathology Using Geometric Morphometrics

**Kimberly Anne Plomp**

***Submitted in accordance with the requirements for the degree of***

***Doctor of Philosophy***

**Department of Anthropology**

**Department of Archaeology**

**Durham University**

**March 2013**

## Table of Contents:

**Chapter:**

## Table List:

## Chapter:

2)



3)

6)



7)

8)

## Figure List:

## Chapter:

2)

5)

6)

Statement of Copyright

## Acknowledgments:

There are few words I could use to describe the appreciation I have for my supervisors, Dr. Una Strand Viðarsdóttir and Professor Charlotte Roberts. I was incredibly fortunate to have two extraordinarily supportive and motivational supervisors who actively guided me through this research and provided a friendly and comfortable atmosphere in which to learn new methods and develop my research skills. There was constant enthusiasm and encouragement for my thesis, as well as my future endeavors. If I continue in research, it will be because of these two exceptional women. We made a great team and I look forward to collaborative projects in the future.

This thesis would not have been possible without the support and guidance of my good friends, Dr. Joe Owen, Dr. Charlotte King, and Dr. Ross Barnett. Joe Owen has patiently explained (repeatedly) the methods and theory behind geometric morphometrics. I would have struggled without you, Joe, and I hope you know how grateful I am. Thank you, Charlotte King, for always being there through the good times and the not-so-good times with a shoulder to cry on or a song to dance to. And thank you to Ross Barnett for always being a friend, colleague, and a generally awesome person - you made the last three years a wonderful experience. The atmosphere of the bioinformatics lab was always encouraging and entertaining, whether we were chatting over coffee and chocolate or choreographing a dance, and I will miss you all until next we meet.

A very special thank you also goes to Ashley Tallyn for always keeping me sane, as difficult a task as that was. Thank you to Ophelie Lebrasseur, Dr. Greger Larson, Dr. Mike Church, and Dr. Anna Linderholm for always being there with encouragement and advice. A very grateful thank you also goes to the very patient and generous Helgi Pétur Gunnarsson, whose genius with software programming and statistics enabled many of the analyses throughout this thesis.

Finally, I would like to thank my parents and sisters for their constant support and encouragement throughout my education. Also, to all my friends not mentioned, thank you for being with me through this experience.

***Dedication***

*I would like to dedicate this thesis to three very important people in my life - My Dad and Mom, who have always encouraged and supported my dreams, and my Gran, who always wanted to be an archaeologist.*

# Chapter 1) Introduction

Palaeopathology is the study of disease and injury in historic and prehistoric peoples through the analysis of pathological lesions present on skeletal remains. It provides valuable insight into the health and quality of life of past populations, the global and temporal distribution and evolution of disease, as well as generating information which can be beneficial in clinical research (Roberts and Manchester 2005; Klepinger 1983; Buikstra and Roberts 2012). Palaeopathology is a growing research field which has seen the utilization of many innovative techniques to study past disease, such as ancient DNA, biochemical, and histological analyses (Monot et al. 2005; Bouwman and Brown 2005; Roberts and Ingham 2008; Von Hunnius 2009). However, palaeopathology relies heavily on macroscopic descriptions of lesions and subsequent differential diagnoses; these methods can be subjective and prone to error (Miller et al. 1996; Waldron and Rogers 1991; Davis et al. 2012). Geometric morphometrics is a collection of statistical techniques for the analysis of shape variability and change in three- and two-dimensional "objects" (Baab et al. 2012; O'Higgins and Jones 1998). Although having revolutionized shape analysis in related fields, their utility in palaeopathological research remains underexplored, but offer the potential of providing detailed descriptions of small-scale shape variation related to disease processes, as well as objectifying data.

The present research project aims to explore the possibility of using geometric morphometric analyses in palaeopathological research by applying the methods to several pathological conditions affecting the human skeleton. The conditions chosen

were those which affect the shape of skeletal elements and/or ones which have aetiologies which are not fully understood.

The first three manuscripts use geometric morphometrics to identify morphological characteristics of skeletal elements associated with pathological conditions of multiple aetiologies. Both osteoarthritis and Schmorl's nodes are commonaly identified in archaeological human remains and have aetiologies which are poorly understood clinically. Palaeopathologists have a unique opportunity to analyse human populations and skeletal elements without soft tissue; identifying shape differences associated with these conditions will contribute to understanding disease processes which many clinical studies are unable to see without highly detailed statistical shape analyses. Geometric morphometric techniques are also applicable to, and usable in, clinical research, allowing for both disciplines to communicate their results in a more comparative manner. This thesis illustrates the benefits of using geometric mophrometrics to investigate the relationship between vertebral shape and Schmorl's nodes (Manuscript 1-2) and joint shape and osteoarthritis (Manuscript 3). The aims of these studies were to identify possible morphological characteristics which may suggest aetiological factors, as well as explore the potential of using these methods to aid in collaboration between palaeopathological and clinical studies.

The final manuscript focuses on the use of geometric morphometrics to accurately record and describe pathological lesions on bones. Traditional macroscopic methods in palaeopathology are inherently subjective and are highly influenced by observer experience and skill (Miller et al. 1996). These methods also provide information about lesions which can be difficult to compare between different studies,

as use of language, terminology, and interpretation can differ substantially between researchers. The application of geometric morphometrics on the recording and description of pathological lesions will provide quantified and objective data which can be used in combination with macroscopic description to strengthen palaeopathological research and increase the scientific relevance of palaeopathological data. Manuscript 4 presents and discusses the results of analyses on the shape deformation of the nasal aperture due to rhinomaxillary syndrome in leprosy and of femora due to vitamin D deficiency. The aim of this study is to determine if geometric morphometrics can quantify pathological shape changes macroscopically identified on archaeological skeletons and to illuminate the benefits of having quantified data and virtual environments for illustrating pathological lesions in archaeological skeletons, both for research and teaching.

The manuscripts in this thesis have been formatted for publication in peer-reviewed research journals; the publication status of each manuscript is indicated in the individual section. The manuscripts are multi-authored with Kimberly A. Plomp, Charlotte A. Roberts, and Una Strand Viðarsdóttir as listed authors. All data collection and data analyses were carried out by Kimberly A. Plomp. Charlotte A. Roberts and Una Strand Viðarsdóttir were supervisors and involved in support, guidance, and editorial aid during the production of all manuscripts and this thesis. The thesis will first provide a detailed review of the background literature pertinent to this research (Chapter 2), as well as a detailed summary of all materials (Chapter 3) and methods (Chapter 4) used in each manuscript.

# Chapter 2) Background Information

The following chapter will provide a detailed discussion and overview of relevant literature pertaining to the pathological lesions and conditions under study in this thesis. The first section will discuss Schmorl's nodes, a spinal lesion analyzed in Manuscripts 1 and 2. The second section will provide a thorough discussion on osteoarthritis, which is the focus of Manuscript 3. The remaining two sections will discussion the infectious disease of leprosy and the metabolic disorder, rickets, the characteristic lesions of which are the focus of Manuscript 4.

## 2.1) Schmorl's nodes:

Schmorl's nodes are lytic depressions with scerlotic margins on the inferior or superior surface of the vertebral body, caused by a herniation of the nucleus pulposus of the intervertebral disc through the fibrous capsule into the vertebral endplate (Schmorl & Junghans 1971; Faccia & Williams 2008). The lesions were first described by Schmorl in 1927 (Schmorl 1927; Schmorl & Junghans 1971), and are commonly found in both archaeological and living human populations. Intervertebral disc herniation can occur without the formation of Schmorl's nodes when the nucleus pulposus is herniated in a lateral, medial, posterior or anterior direction (on the transverse plane); Schmorl's nodes will only develop when the herniated material is forced into the vertebral endplate. For clarity, the term "herniation" will be used when the general condition is discussed, and "Schmorl's nodes" when the herniation results in the recognized lesion.

**Intervertebral Disc:**

The intervertebral disc is composed of parallel concentric rings of fibrous tissue forming the annulus fibrosus (Figure 2.1); the inner and outer layers of the annulus differ in composition, with the outer layer having a higher proportion of Type I collagen, and the inner layer having a predominance of Type II collagen (Vernon-Roberts et al. 2007). The concentric arrangement of fibres in the annulus fibrosus provides resistance to torsion and flexion-extension during spinal movement, and strengthens the annulus fibrosus against rupture (Vernon-Roberts 1989). The nucleus pulposus is a semi-gelatinous substance enclosed by the annulus fibrosus which evenly distributes pressure on the annulus fibrosus and vertebrae; it is composed of water (≈80%), collagen, and protein-polysaccharide. The intervertebral disc slowly dehydrates with age, with a loss of 10-15% of the water content in both the annulus fibrosus and nucleus pulposus after the 3$^{rd}$ decade of life (Vernon-Roberts 1989). Disc herniation occurs when the nucleus pulposus ruptures through the annulus fibrosus, and Schmorl's nodes develop as a result of herniation of the nucleus pulposus into the vertebral endplate and vertebral body (Figure 2.2).

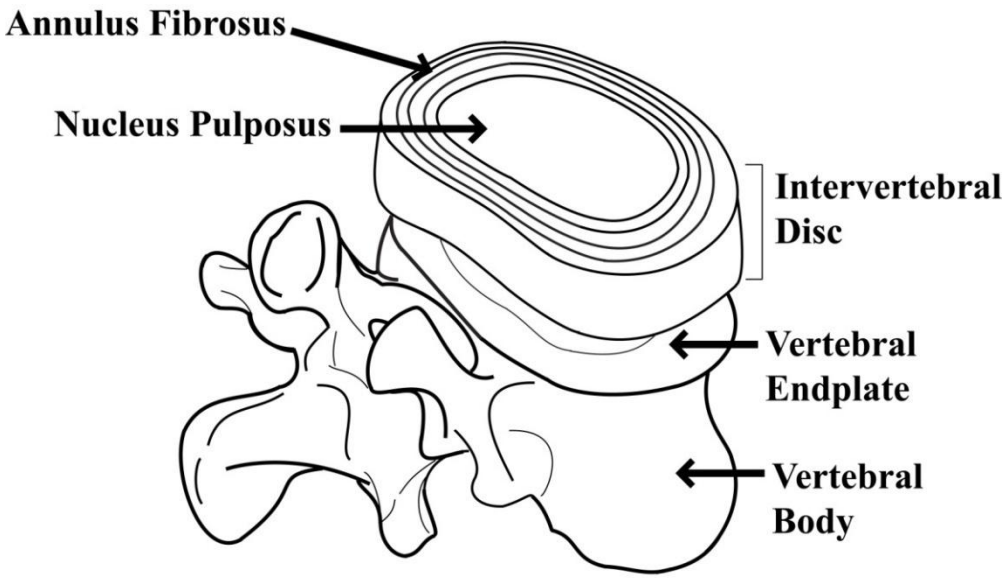


Figure 2.1) Diagram of vertebra and intervertebral disc with nucleus pulposus, annulus fibrosus, and vertebral endplate indicated.

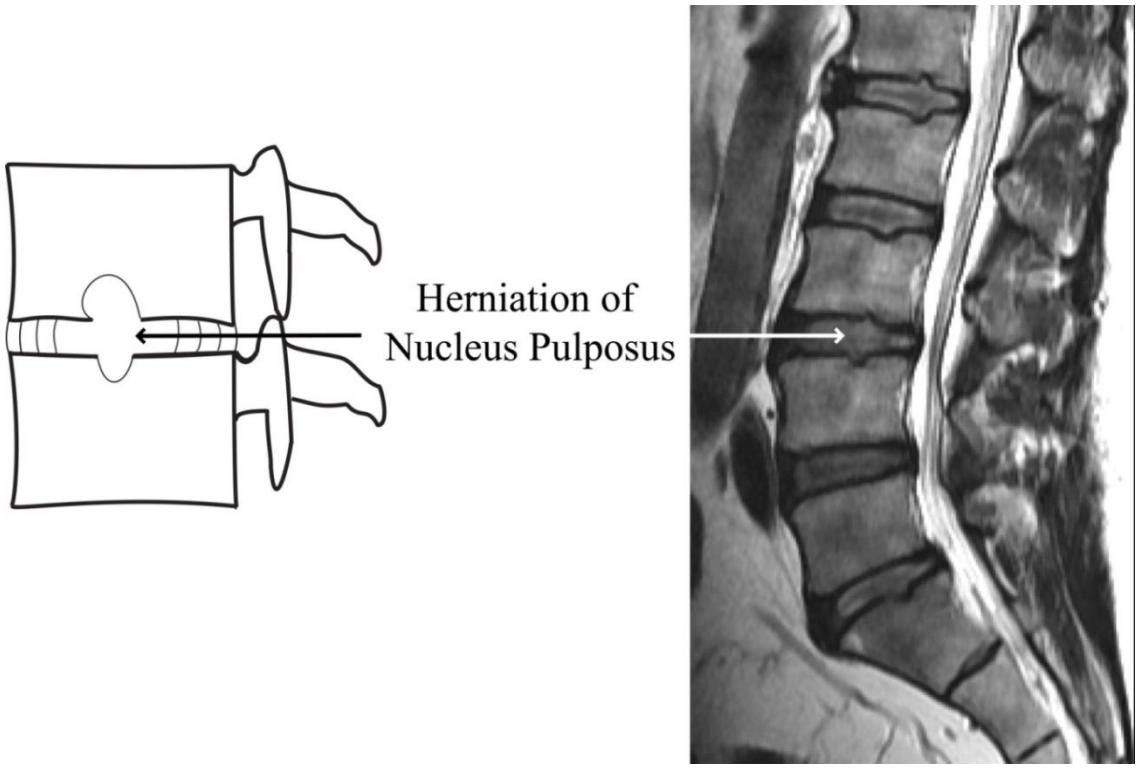


Figure 2.2) Left: Line drawing of intervertebral disc herniation which would result in Schmorl's nodes. Right: Radiograph of lumbar spine with intervertebral disc herniations producing Schmorl's nodes. (Radiograph image from Mok et al. 2010: 1945).

Pooni et al. (1986) discuss how the structure of the intervertebral disc can contribute to its ability to withstand movement without injury. They describe the thoracic vertebral disc as being more circular than the cervical and lumbar, which promotes an even distribution of strain on the disc in torsion, but the fibres would not be able to provide enough support for the disc during flexion. The elliptical discs of the cervical and lumbar regions are better suited to withstand flexion-extension, but are weaker during torsion. The disc of the thoracic spine is also thinner than in the cervical or lumbar regions, and there are shorter fibres in the annulus fibrosus; these features increase the amount of strain in the fibres during flexion-extension and torsion. The longer fibre lengths in thicker discs provide better support against disc prolapse. The authors also state that the range of motion during flexion-extension and torsion in the thoracic spine is much more restricted than in the cervical or lumbar spine (Pooni et al. 1986). The combination of these features in the thoracic intervertebral disc, along with the increased compression and physical function of this region, may be one factor influencing an increase in disc herniation in the lower thoracic spine compared to upper spinal regions. However, the next more commonly affected region for transverse or vertical herniations is the lumbar, making the relationship between disc morphology and herniation unclear because these features differ in the lumbar spine compared to the thoracic.

There is also a complex relationship between the morphology of the vertebrae themselves and the intervertebral disc (Adams et al. 2006; Fields et al. 2010; Brown et al. 2008). Adams et al. (2006) found that degenerative changes of the intervertebral disc caused the neural arch to withstand more of the compressive force on the vertebrae

during upright posture. Harrington et al. (2001) found a relationship between the size and form (shape with size) of the vertebral endplate with intervertebral disc herniation. Larger vertebral endplates in males, and more circular endplates (based on measured dimensions) in both males and females, were correlated with disc herniation in the lower lumbar vertebrae. The authors explain that this relationship may be related to LaPlace's law. LaPlaces's law states that the radius of a fluid-filled tube directly relates to the amount of tension the tube can withstand (Letić 2012). The intervertebral disc is a fluid-filled tube, and a larger radius, as seen in both the larger and more circular endplates, could cause higher tension in the disc during compression (Harrington et al. 2001).

**Aetiology:**

The aetiology of intervertebral disc herniation and Schmorl's nodes is poorly understood in both clinical and palaeopathological contexts. The prevalence rates of the lesion are similar in both archaeological and living populations, suggesting that the aetiology is not associated with lifestyle (palaeopathology literature: Novak & Šlaus 2011; Robb et al. 2001; Üstündağ 2009; Caffell & Holst 2010; Kraus et al. 2009; Robb 1994; Saluja et al 1986; Sandness & Reinhard 1992; Šlaus 2000; clinical literature: Schmorl & Junghans 1971; Pfirrmann & Resnick 2001; Dar et al. 2009; Mok et al. 2010). The lesions are commonly seen in the lower thoracic and upper lumbar spine (Pfirrmann & Resnick 2001; Dar et al. 2010), likely resulting from the biomechanical stress on these vertebrae due to the transmission of compressive and shearing forces from the upper body to the lower body in movement during daily activities (Cholewicki & McGill 1996). Humans display Schmorl's nodes in a much higher frequency than do other animals (dogs 5.3% (Gendron et al 2011), chimpanzees 2.0%, and orang-utan

2.2% (Lovell 1990)). This could suggest that the high prevalence of the lesion in humans is a result of stress on the spine due to bipedal locomotion (Dar et al. 2010). Biomechanical studies have indicated that herniations often occur during flexion, extension, and torsion with moderate to heavy loading (Callaghan & McGill 2001; Wilder et al. 1988; Goto et al. 2002). When these events do not result in immediate herniation, they may still affect the integrity of the annulus fibrosus, which could increase the chance of herniation in the future (Wilder et al. 1988).

Modern clinical literature identifies other possible aetiological factors contributing to the development of Schmorl's nodes. Metabolic deficiencies, such as osteoporosis or hyperparathyroidism, can cause weakening of the vertebral endplate which may increase the susceptibility of an individual to develop Schmorl's nodes (Resnick & Niwayama 1978; Dar et al. 2010). Saluja et al (1986) suggested that the lesions are a result of a weakened endplate due to incomplete regression of the notochord during foetal development. Resnick & Niwayama (1995: 1822) discuss how Schmorl's nodes develop as a result of a weakened disc or subchondral bone due to problems during development, such as gaps in ossification, regression of the chorda dorsali, and/or the presence of vascular channels. Studies have also found evidence suggesting a strong genetic predisposition for Schmorl's nodes (Zhang et al. 2010; Williams et al. 2007). The developmental abnormalities suggested by Saluja et al. (1986) and Resnick & Niwayama (1995) may be a result of genetic factors influencing Schmorl's nodes development (Resnick & Niwayama 1995:1822). For example, Williams et al. (2007) performed a twin study on 516 British female volunteers and found that the contribution of heritance in the occurrence of Schmorl's nodes in both the

lumbar and thoracic spines is high, with estimates of heritability at 72% for the thoracic spine and 80% for the lumbar. Their results suggest that the aetiology of Schmorl's nodes is strongly genetically influenced, while also associated with lumbar disc disease (Williams et al. 2007). Schmorl's Nodes also occur in different frequencies in different ethnic groups, although reported prevalence rates are also likely affected by the use of different diagnostic criteria and imaging techniques (Dar et al. 2009; Mok et al. 2010).

Clinically, herniation of the intervertebral disc shows little correlation with patient age (Pfrirrmann & Resnick 2001; Burke 2012; Hamanishi et al. 1994; Dar et al. 2009), but discs with Schmorl's nodes can display degenerative changes earlier in a person's life than those without (Adams et al. 2000). The limited palaeopathological studies also find no correlation between age at death and Schmorl's nodes (Üstündağ 2009; Novak & Šlaus 2011; Klaus et al. 2009; Šlaus 2000). In a study on modern skeletons from the 20$^{th}$ century American Hamann-Todd Skeletal Collection, Cleveland Museum of Natural History, Ohio, USA, Dar et al. (2009) performed an analysis of Schmorl's nodes on 240 adult skeletons. This collection is unique in that it has biographical documentation that accompanies the skeletal remains. They found that 48.3% of individuals had at least one node present in the spine. Schmorl's nodes were more common in males than females (54.2% of 120 males vs. 43.0% of 120 females) with males on average also showing a higher number of lesions (69.3% vs. 30.4% of 511 lesions present). Ethnic origin had a positive correlation, with Schmorl's nodes being more frequent in European than African Americans (60.3% of 120 European-American individuals vs. 36.7% of 120 African-American individuals). The authors comment that the high prevalence of Schmorl's nodes in human populations indicates

that situation specific aetiologies, such as trauma or metabolic deficiencies (e.g. osteoporosis, hyperparathyroidism), can have a major influence on the lesions. Their results appear to suggest a genetic or developmental aetiology, with ethnicity and sex being the main factors affecting the development of Schmorl's nodes (Dar et al. 2009, 2010). It could be suggested that the difference in prevalence between males and females in this sample could be due to variation in physical activities; however, the literature discussed above indicates that spinal development, anatomy, and physiology likely play a substantial role in this difference (Zhang et al. 2010; Williams et al. 2007; Harrington et al. 2001).

Schmorl's nodes have been found in association with moderate disc degeneration, although the association remains unclear (Adams et al. 2002; Mok et al. 2010; Pfirrmann & Resnick 2001; Williams et al. 2007). Has the herniation initiated disc degeneration, or has the degeneration in the disc weakened the disc integrity to the point of herniation? Rannou et al. (2001) comment that disc herniations can occur as a result of a marked stress on the disc, or as a result of a normal stress on a disc which has been altered and/or weakened due to degeneration or disease. Mechanical stress may alter the cellular and molecular mechanisms of disc metabolism, which would contribute to disc degeneration and herniation (Rannou et al. 2001). The annular fibres provide resistance to axial rotation and damage to the annulus, and subsequent disc degeneration may be influenced by the combination of axial stress, flexion, and torsional movements (Krismer et al. 1996; Hickey & Hukins 1979; Vernon-Roberts et al. 2007). Dar et al. (2010) suggest that since Schmorl's nodes are so common, normal daily loading and movement must play a vital role in their development. Although other factors such as

trauma, genetic predisposition, and spinal disease, are all likely to contribute to the condition, these alone would not explain the high prevalence of the lesion in both living and archaeological populations.

Pfirrmann and Resnick (2001) studied radiographs of cadaveric thoracic and lumbar spines of 128 adult individuals from the USA, ranging from 43-93 years of age. They found that any degenerative changes of the spine found to be correlated with Schmorl's nodes were moderate in extent, and that there was no evidence of more severe degenerative changes, such as vertebral collapse or sclerosis, associated with Schmorl's nodes (Pfirrmann & Resnick 2001). The authors also suggest a relationship between the development of Schmorl's nodes and the morphology of the vertebral endplate, stating less concave endplates to be more susceptible to developing Schmorl's nodes.

**Prevalence and Clinical Significance of Schmorl's Nodes:**

Prevalence rates for Schmorl's nodes in both archaeological and living populations have been reported to be between 4 and 76% (palaeopathological literature: Üstündağ 2009; Dar et al. 2009; Novak & Slaus 2011; L'Abbe & Steyn 2007; clinical literature: Mok et al. 2010; Pfirrmann & Resnick 2001) (Table 2.1); the differences in reported figures are due to the use of different diagnostic criteria and diagnostic techniques, such as radiographs, CT scanning, or the macroscopic analysis of dry bone. Purported association of back pain with Schmorl's nodes is unclear, with some studies finding a positive association and others finding the condition to be asymptomatic (Hamanishi et al. 1994; Faccia & Williams 2008; Fukuta et al. 2009; Takahashi et al.

1995; Peng et al. 2003; Fahey et al. 1998). Back pain affects a large number of people (Webb et al. 2003; Maniadakis & Gray 2000; Macfarlane et al. 2012) and is one of the most common health problems in living populations, with a global prevalence rate of between 22 and 65% (Hoy et al. 2012; Walker 2000). Therefore, it is of significant clinical importance to fully understand the aetiology of intervertebral disc herniations because back pain may be a consequence of Schmorl's nodes. Furthermore, recognizing them in bioarchaeology provides a means to explore quality of life in the past, as Schmorl's nodes can by symptomatic (Faccia & Williams 2008).

Faccia and Williams (2008) performed a clinical analysis of MRI scans on 291 adult volunteers from Tennessee, USA. The purpose of the study was to use clinical information to help understand the effect Schmorl's Nodes have on quality of life in terms of resulting back pain, and apply this information to bioarchaeological studies. The authors found that a significant positive correlation existed in patients reporting pain and Schmorl's nodes located in the centre of the vertebral body. They suggested this to be due to a concentration of basivertebral nerve endings in this area of the vertebra (Faccia & Williams 2008; Antonnaci et al. 1998; Fras et al. 2003). This study is unique in that it links the occurrence of a skeletal lesion to reported pain in a clinical setting, helping the interpretation of these palaeopathological lesions and their effect on people in the past.

Table 2.1) Summary of example literature from both palaeopathology and clinical research. For palaeopathological literature, the prevalence of Schmorl's nodes, as well as the date and country of the archaeological site is included. All these studies used macroscopic analysis. For clinical literature, the country and method of diagnosis is included. Separate prevalence rates for males and females are included where available.

| Palaeopathological Literature | | | |
|---|---|---|---|
| **Reference** | **Country** | **Date** | **Prevalence** |
| **Üstündağ 2009** | Austria | $16^{th}$-$18^{th}$ C AD | 31.4% |
| **Novak & Slaus 2011** | Croatia (2 sites) | $16^{th}$-$19^{th}$ C AD | 29.4 % Koprivno site |
| | | | 17.6% Sisak site |
| **Slaus 2000** | Croatia | $14^{th}$-$18^{th}$ C AD | 15.6% (21.1% ♂, 8.8% ♀) |
| **Rathbun 1987** | USA | 1840-1870 AD | 39% (54% ♂, 27% ♀) |
| **Bourbou 2003** | Greece (2 sites) | $7^{th}$-$8^{th}$ C AD | 10.4% Eleutherna site |
| | | | 7.8% Messene site |
| **L'Abbe & Steyn 2007** | Africa | 1910-1999 AD | 4% |
| **Klaus et al 2009** | Peru | 1536-1751 AD | 5.9%-20% |

| Clinical Literature | | | |
|---|---|---|---|
| **Reference** | **Country** | **Method** | **Prevalence** |
| **Schmorl & Junghans 1971** | USA | Macroscopic | 38% |
| **Mok et al. 2010** | China | Radiography | 16.4% (40% ♂, 60% ♀) |
| **Pfirrmann & Resnick 2001** | USA | Radiography | 58% |
| **Hamanishi et al. 1994** | Japan | MRI | 19% |
| **Williams et al. 2007** | UK | MRI | 30% |
| **Dar et al. 2009*** | USA | Macroscopic | 48.3% |

* based on documented skeletal collection

**Palaeopathology:**

Schmorl's nodes have been used as activity indicators in palaeopathological research due to their association with spinal trauma and stress, despite their specific aetiology remaining unknown (Burke 2012; Novak & Šlaus 2011; Klaus et al. 2009; Šlaus 2000; Papathanasiou 2005; Coughlan & Holst 2001; Robb et al 2001; Alesan et al. 1999; Sandness & Reinhard 1992; Lai & Lovell 1992; Jimenez-Brobeil et al. 2010; Robb 1994; Merbs 1983). It is accepted that movement of the spine combined with loading can cause herniations (Callaghan & McGill 2001; Wilder et al. 1988; Goto et al. 2002), but it is not the only factor influencing the development of the condition, and therefore the presence of Schmorl's nodes cannot be used to indicate levels of physical activity in the past. Some authors even use the presence of Schmorl's nodes to suggest sexual division of labour in past populations. Novak & Šlaus (2011) go as far as suggesting that the reason males tend to show more Schmorl's nodes than females is due to differences in the type and frequency of physical work carried out. They discuss the conclusions of other studies, where this difference is suggested to be due to a development or a genetic predisposition. However, they still conclude that physical activity is the main cause, citing sources which use the same ideas, such as Robb (1994) and Üstündağ (2009).

In their study of an ancient skeletal population from Pontecagnano, Italy, Robb et al. (2001) used Schmorl's nodes, along with trauma and tibial periostitis, to indicate differing social status in burials in association with different grave goods. Females buried without pottery had significantly more Schmorl's nodes than females with pottery. The authors suggest this differentiation to indicate unequal levels of physical

stress between different social classes of females. Males without grave goods were also found to have higher rates of trauma, periostitis, and Schmorl's nodes (Robb et al 2001). Šlaus' (2000) paper on a late medieval population from Noca Rača, Croatia, also notes that the aetiology of Schmorl's nodes is unknown, and that their presence should not be used to indicate particular activities. However, the author suggests that the higher frequency of Schmorl's nodes and vertebral osteoarthritis in males is a possible indicator of sexual division of labour and differing social status between the sexes (Šlaus 2000).

Üstündağ (2009) analysed a post-medieval skeletal population from Klostermarienberg, Austria, for the occurrence of Schmorl's nodes. She found that the lesion was more common in younger adults and that frequency did not increase with age in the same way as osteoarthritis and vertebral osteophytosis. She also noted that the lower thoracic vertebrae were the most commonly affected, and suggested this was due to the more extensive movement in this spinal region compared to the lumbar spine. Schmorl's nodes were more common in males than females, and this was suggested to be a result of different physical activities. During harvesting, males would use scythes and females would use sickles; Üstündağ argues that the use of scythes by males would be harder work with more rotational movements than using a sickle, which may explain the higher frequency of Schmorl's nodes in the lower thoracic vertebrae in males (Üstündağ 2009). Although Schmorl's nodes have been shown to develop under loaded torsion, flexion, and extension movements of the spine (Callaghan & McGill 2001; Wilder et al. 1988; Goto et al. 2002), there has been no clinical research to date which suggests that subtle differences in physical activity, such as using a scythe over a sickle, can be hypothesised based on their presence.

Jurmain (1999: 264) suggests that Schmorl's nodes are given more attention than they deserve in palaeopathological analyses, and concludes that since their aetiology is unclear in clinical studies, palaeopathologists should not make any attempt at hypothesizing their aetiology in archaeological skeletons. Since the lesion can be asymptomatic, and their association with back-pain is also unknown, he argues further that they mean very little for the overall health of a population. Faccia and Williams (2008) found that specific localities of the lesion on the vertebrae may cause pain in some individuals, indicating that their presence may have had an effect of the quality of life in the past. While it is agreed that Schmorl's nodes should not be considered as an activity indicator in palaeopathological studies, their presence should not be ignored. They do have an impact on modern health and quality of life, with some lesions being symptomatic (Takahashi et al. 1995; Peng et al.2003; Faccia and Williams 2008), and thus should be considered in the past.

Palaeopathological research has the opportunity to study skeletal remains from a range of human populations, with a wide temporal and geographical scope, without the need of imaging technology or the ethical issues associated with clinical research. The continued analyses of all skeletal remains in palaeopathology can greatly add to the overall understanding of the impact of disease on people's lives in the past. Furthermore, in situations where clinical research has not reached a conclusion on the aetiology of a pathological condition that affects the skeleton, palaeopathological studies may provide beneficial information on epidemiological factors leading to specific lesions such as Schmorl's Nodes in large archaeological samples. Schmorl's nodes and intervertebral disc herniation clearly have a complex multi-factorial aetiology and it is

likely that the lesions can develop in a variety of situations. However, palaeopathologists should be cautious of interpreting the presence of Schmorl's nodes as indicating physical activity affecting the spine, as it is clear that developmental and genetic factors are influencing the presence of the condition. Comparatively increased frequency rates for Schmorl's nodes in a skeletal population cannot be simply taken to indicate increased physical work.

**Conclusion:**

The aetiology of intervertebral disc herniation and Schmorl's nodes remains unclear, with many studies indicating a multi-factorial aetiology. Following a comprehensive analysis of both the clinical and palaeopathological literature, it seems likely that disc herniation occurs when physical strain during loaded flexion-extension and torsional movements affect a spine that may have a genetic or congenital predisposition to the condition. This predisposition may be related to the biochemical composition and/or morphology of the disc itself. The morphology of the vertebrae may also influence the biomechanics of the spine and the development of Schmorl's nodes, and this hypothesis is address in Manuscripts 2 and 3 of this thesis.

## 2.2) Osteoarthritis

Osteoarthritis receives a great deal of attention in both palaeopathological and clinical studies due to its high frequency in human populations (clinical literature: McGonagle et al. 2010; Zhai et al. 2007; Dominick & Baker 2004; palaeopathological literature: Cushnaghan & Dieppe 1991; Van Sasse et al. 1989; Bridges 1991; Jurmain 1999; Weiss & Jurmain 2007; Waldron 1991). Joint disease is one of the most commonly observed conditions in palaeopathology (Waldron 2009; Jurmain & Kilgore 1995), with osteoarthritis being the most prevalent of the joint diseases in clinical medicine (Wolf 2002). The aetiology of osteoarthritis continues to elude researchers. There are many theories explaining possible aetiologies for the development of the disease, all with supporting evidence and convincing arguments. The main theories to date are biomechanical breakdown of the joint due to physical stress, age degeneration, a genetic predisposition, and sex hormones. It is now generally accepted that osteoarthritis is a multifactorial disease, with multiple aetiological factors contributing to the overall degeneration or break-down of the joint structure (Molnar et al. 2009; Felson et al. 2000; Herrero-Beaumont et al. 2009; Spector & MacGregor 2004). This section will provide a brief overview of osteoarthritis, with a focus on aetiology, symptoms, prevalence, and skeletal manifestations.

### Synovial Joints:

As osteoarthritis is a disease affecting the integrity and health of synovial joints, it is important to understand their underlying structure. Synovial joints are the most common type of joint in the human skeleton, and are the only joints which are affected

by osteoarthritic changes. Figure 2.3 displays the synovial joints of the human skeleton, which are composed of the articular surfaces of two individual bones which are linked via a capsule of fibrous tissue at the periosteum; ligaments and tendons lie over the capsule, stabilizing the attachment. Inside the joint capsule there is a synovial membrane, nerves, and lymph and blood vessels; a layer of hyaline cartilage overlies the articular surfaces of the bones, the thickness of which varies between joints depending on size and function (Figure 2.4) (Waldron 2009; Pritzker 1998). This layer of cartilage is only about 1 – 6 mm in depth and provides a smooth surface between the adjacent bones which allows for near-frictionless movement (Herzog & Federico 2007). The friction generated between two bones of a synovial joint has been found to be less than the friction produced between ice skates on ice (Jurmain 1999). The articular surface of bone under the cartilage is called the subchondral bone; it is thinner than the compact bone of the diaphysis, although it has the same histological composition (Jurmain 1999; Waldron 2009).

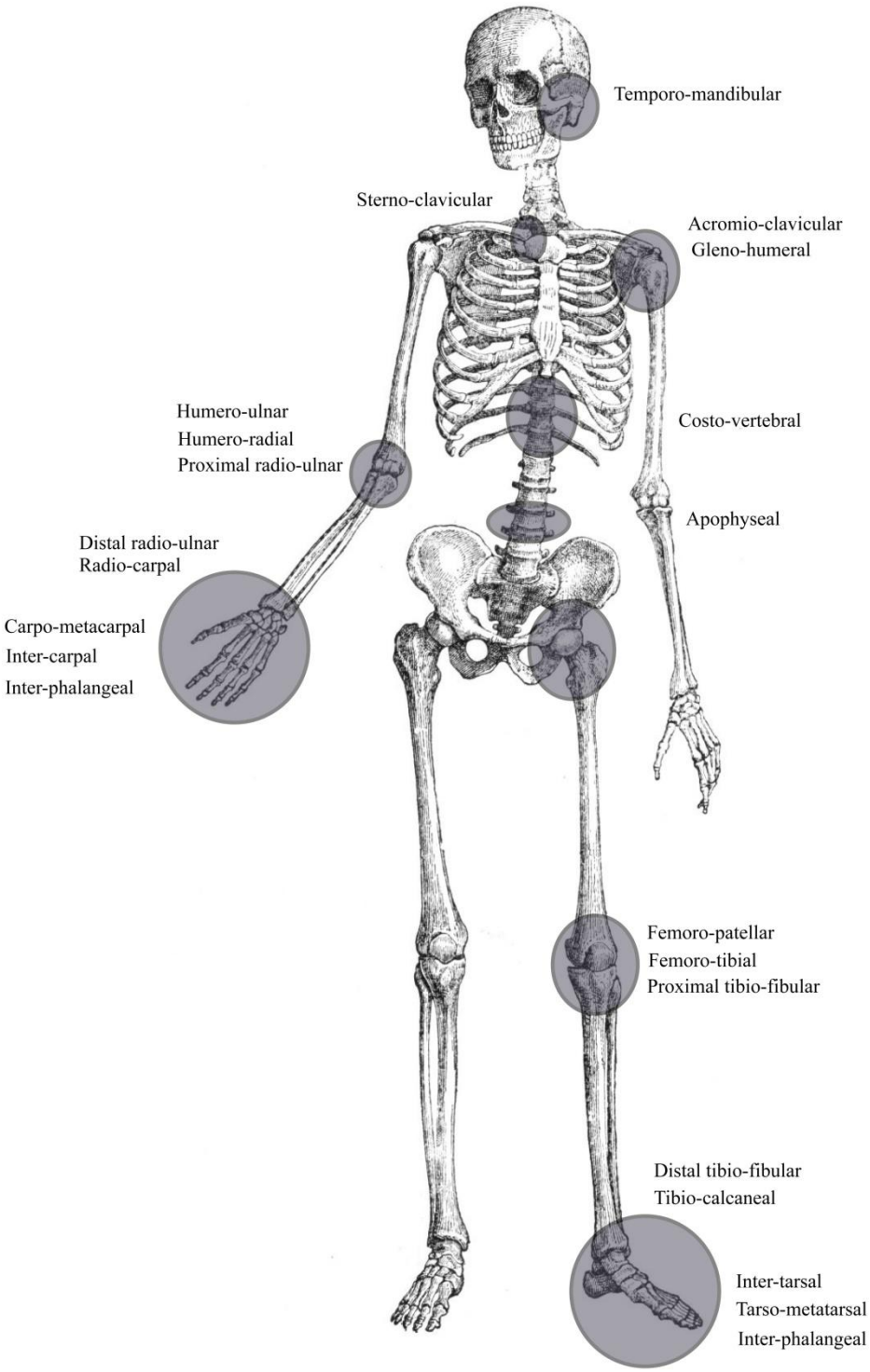


Figure 2.3) Synovial joints of the human body.
Image adapted from http://www.arthursclipart.org/skeletons/skeletons.htm. Accessed July 2012.

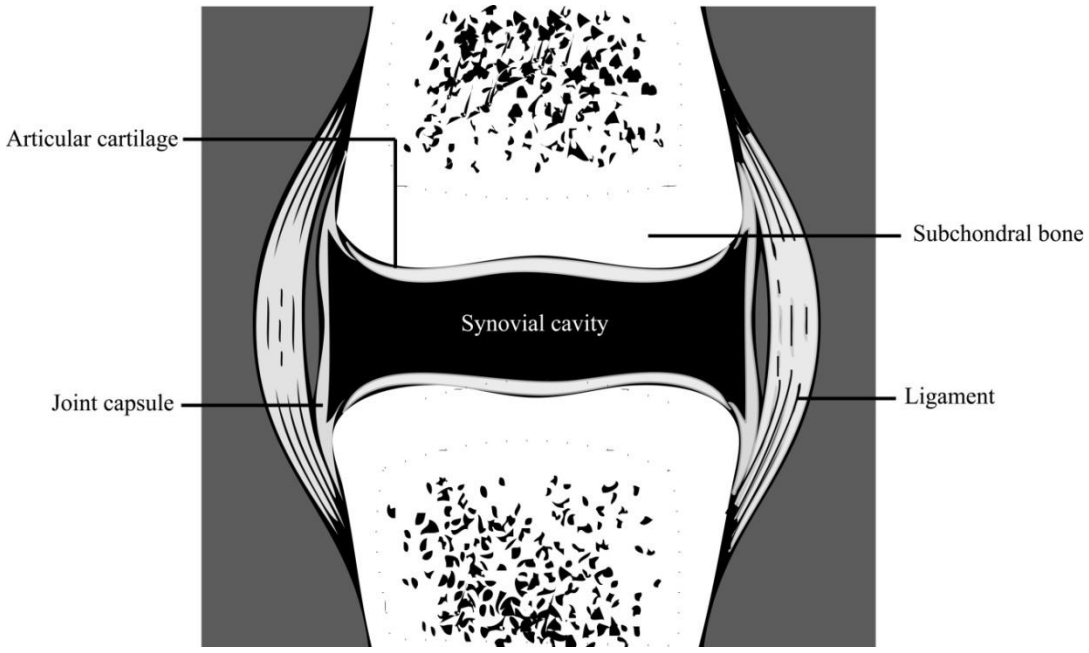


Figure 2.4) Basic anatomy of a synovial joint.
Image adapted from http://www.becomehealthynow.com/popups/joint_healthy_bh.htm, Accessed July 2012.

Articular cartilage of synovial joints is composed of water, collagen fibers, proteoglycan ground substance and chondrocyte cells (Jurmain 1999b; Martin et al. 1998). It is divided into three layers, all of which compose a cartilage layer which is avascular, alymphatic and aneural (Figure 2.5)(Herzog & Federico 2007; Mandelbaum et al. 1998). The main function of articular cartilage is to decrease the friction between two bones and to transmit and distribute any mechanical forces across the joint surface (Herzog & Federico 2007). In order to function properly, articular cartilage must be flexible when under mechanical pressure, such as compressive, tensile, and shear forces; the cartilage will deform under loading, and its elastic qualities will enable it to cope

with heavy loads by releasing water. This loss of water condenses the cartilage by up to 40% of its original depth (Jurmain 1999).

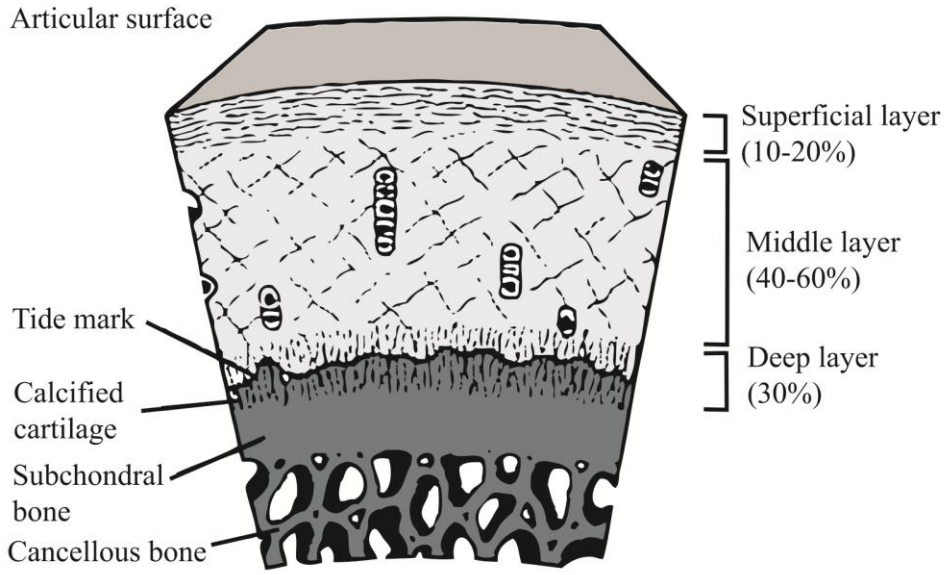


Figure 2.5) Anatomy of articular cartilage, with three layers and underlying subchondral and cancellous bone indicated. Image adapted from Mandelbaum et al. (1998:854).

Osteoarthritis is considered to be the result of a breakdown of one or more joint components; the main indicator of osteoarthritis is the loss of articular cartilage, leading to loss of joint space in patients that is visible on a radiograph. It remains unclear as to whether the damage and loss of the cartilage is the initiator for osteoarthritis, or if the

osteoarthritic changes to the subchondral bone (new bone formation/osteophytes) or other joint components (ligament laxation) precedes cartilage loss (Aspden 2008).

**Aetiology:**

Variation in how the human skeleton responds to aging and stress causes a wide variety of skeletal changes, making their interpretation difficult. It is accepted that the aetiology of osteoarthritis is multifactorial with a variety of factors contributing to the overall degeneration or break-down of the joint structure; the main theories to date are biomechanical breakdown of the joint due to physical stress, increased age, a genetic predisposition, and sex hormones (Molnar et al. 2009; Felson et al. 2000; Herrero-Beaumont et al. 2009; Spector & MacGregor 2004; Weiss 2006). Herrero-Beaumont et al. (2009) performed a literature review of clinical studies of osteoarthritis from 1952 to 2008, and suggest that the main factors contributing to osteoarthritis in living populations is aging, genetics, and sex hormones which stimulate the development of preliminary osteoarthritic changes. They also found that conditions such as underlying obesity and injury may increase the severity of the condition in terms of symptoms and disability.

There is a strong correlation between aging and osteoarthritis (clinical literature: Herrero-Beaumont et al. 2009; Wright et al. 2009; van der Kaan & van der Berg 2008; Van Sasse et al. 1989; Mankin et al. 1986; Prescher 1998; palaeopathological literature: Rando & Waldron 2012; Weiss & Jurmain 2007; Weiss 2005; Maat et al. 1995; Waldron 1992; Hodges 1991). During aging, the ligaments and tendons of the joint structure weaken, and the articular cartilage becomes increasingly susceptible to

breakdown and damage. These changes could cause the development of osteoarthritis due to the transformation of the joint structure (Mankin et al. 1986; Prescher 1998). Aging affects the proteoglycans and the Type II collagen of the extra-cellular matrix, as well as the chondrocytes of the cartilage; the result is weaker cartilage with reduced water content (Herrero-Beaumont et al. 2009). Muscles, ligaments and tendons of joints also undergo changes due to aging; the accumulation of these changes on the joint results in loss of flexibility and increased stiffness due to the reduction of repair capability (Herrero-Beaumont et al. 2009). Whether this correlation with age and osteoarthritis is directly due to the normal degeneration of the joint structure or if it is a result of multiple aetiological factors accumulating during an individual's life, is unknown (Mankin et al. 1986; Wright et al. 2009). Despite the clear relationship between aging and osteoarthritis, there remain situations where young adults display severe osteoarthritis and old adults have healthy joints, indicating that there are factors aside from aging influencing the development of the disease.

Aspden (2008) claims that clinical research on the aetiology of osteoarthritis has focused too much on the articular cartilage itself, as it is generally assumed that the main cause of osteoarthritis is the breakdown of cartilage in the joint. Aspden (2008) suggests that the evidence seen in osteoarthritic research points to a highly complex aetiology which affects the entire musculoskeletal system and not just the articular cartilage. There are many clinical situations where a patient displays other joint changes, such as osteophyte formation radiographically before joint space narrowing, indicating that loss of cartilage is not the sole initiator in development of the disease. The author suggests

that osteoarthritis is a systematic metabolic disease, with biomechanical factors influencing physical manifestation on the specific joints (Aspden 2008).

Repetitive biomechanical strain on a joint surface can damage the articular cartilage and other joint components, and thus physical activity is considered to be one of the major aetiological factors of osteoarthritis (Molnar et al. 2009; Felson et al. 2000; Herrero-Beaumont et al. 2009; Weiss 2006). Clinical studies have also attempted to find a correlation with physical activity and osteoarthritis (Solovieva et al. 2005, Cooper et al. 1994; McAlindon et al. 1999). Solovieva et al. (2005) studied hand osteoarthritis in female dentists and teachers, with the intention of identifying different prevalence patterns of the disease between the two professions with differing mechanical pressures on the hand. The authors found a higher prevalence of hand osteoarthritis in teachers, which was the profession considered to have less mechanical strain on the hand joints. This result, along with the finding that osteoarthritis was significantly more prevalent in the non-dominant hand than the dominant, suggests that mechanical use is not the main aetiological factor behind osteoarthritis of the hand (Solovieva et al. 2005).

Researchers have also investigated the relationship between damage to the anterior cruciate ligament and osteoarthritis of the knee. Lohmander & Felson (2004) found that 50% of 26-40 year old female soccer players who had sustained trauma to their anterior cruciate ligaments displayed radiographic evidence related to osteoarthritis 12 years after the damage occurred; 42% had symptoms related to knee osteoarthritis. A similar study found that 41% of 30-56 year old male soccer players displayed osteoarthritis 14 years after sustaining anterior cruciate ligament damage (von Porat et al. 2004). The prevalence of osteoarthritis in middle aged adults suggest that the damage

to the ligament may be a causative factor in the development of knee osteoarthritis (Frobell et al. 2009); this is also supported by Shepstone et al.'s (1999, 2001) studies which found the main shape difference between healthy and osteoarthritic distal femora focused on the intercondylar notch region, where the anterior cruciate ligament inserts. Medical researchers have used magnetic resonance imaging (MRI) scans to analyze joints, and have found that there are changes to the ligaments before the onset of skeletal changes of osteoarthritis (McGonagle et al. 2010). It has also been suggested that the damage to the ligament was a result of the particular shape of the joint being predisposed to osteoarthritis (Aspden 2008; Shepstone et al. 1999, 2001).

Many researchers in bioarchaeology have focused on studying the relationship between physical activity and osteoarthritis in multiple populations, hoping to find a direct correlation with mechanical stress and even particular physical activities (Watkins 2012; Lieverse et al. 2007; Merbs & Euler 1985; Lai & Lovell 1992; Steen & Lane 1998; Lovell 1994; Merbs 1983; Ortner 1968). Although many clinical studies do find correlations, others find little or no link between physical activity and osteoarthritis. It is now generally accepted that osteoarthritis cannot be used as an indicator of physical "activities" in the past, and attempts to do so are generally carried out with caution (Shrader 2012; Molnar et al. 2011; Molnar et al. 2009; Weiss & Jurmain 2007, Jurmain 1999; Jurmain & Kilgore 1995; Waldron 1994). There is undoubtedly a relationship between osteoarthritis and physical stress on the joint; this relationship, however, is much more complex than was first assumed. It is understandable that physical stress or damage would affect the joint components, and strain on the joint could cause a premature breakdown of the joint's integrity. However, the ability of a joint to withstand

physical strain or to breakdown may be influenced by age, underlying genetics, hormones, body structure, or perhaps the overall shape of the joint.

There can be a high frequency of osteoarthritis in family groups, suggesting that underlying genetic makeup may be a major aetiological factor with individuals being genetically susceptible to the development of osteoarthritis (Spector & MacGregor 2004; Zhai et al. 2007; Bijkerk et al. 1999; Doherty et al. 2000). Genetic disorders such as chondropathies, and mutations affecting Type II collagen and cartilage matrices, are connected with early development and rapid progression of osteoarthritis (McGonagle et al. 2010; Li et al. 2007). As with both aging and physical stress, genetic makeup appears to have a strong influence on the development and progression of osteoarthritis, but this relationship is complex and full understanding of the mechanics of the genetic influence on joints remains elusive (Zhai et al. 2007). As Moskowitz (2004: 16) states: "OA may be the result of abnormal forces acting on a normal joint or of normal forces acting on a joint in which the biomaterials, i.e., the articular cartilage or subchondral bone, are abnormal, perhaps on a genetic basis".

The National Institutes of Health held a conference in 2000 entitled "Stepping Away from OA: Prevention of Onset, Progression, and Disability of Osteoarthritis". In the first publication of this conference (Felson et al. 2000), it is suggested that the reason the aetiology of osteoarthritis continues to elude researchers is because it is not a single disease, but is instead multiple diseases of varying aetiologies which produces similar or identical changes on the joints (Felson et al. 2000). The reasons given for this argument are convincing, and include:

> ‘ 1. Osteoarthritis of the knee and hip may be associated with different risk factors, suggesting that we should regard them as unique diseases…
>
> 2. “Generalized osteoarthritis” may be a distinct disease in which systematic (genetic) predisposition is more important than local (mechanical) factors.
>
> 3. One classification divides people with osteoarthritis into those in whom the cause is known (secondary) or those in whom the cause is unknown (primary).
>
> 4. Osteoarthritis of the hip has been divided into hypertrophic and atrophic forms on the basis of a person’s tendency to develop large osteophytes; other joints may respond similarly to the presence of the disease. Hypertrophic osteoarthritis may be associated with pyrophosphate crystal deposition and diffuse idiopathic skeletal hyperostosis, a disease of bony proliferation at ligament and tendon insertion sites; atrophic forms may be associated with the presence of the basic calcium phosphate crystals and osteoporosis.’ (Felson et al. 2000: 636)

If osteoarthritis is not a single disease, but multiple diseases with different aetiologies, this would greatly change the way that it is viewed in palaeopathology. Would the palaeopathologist be able to identify separate osteoarthritic diseases, or will ‘generalized’ or ‘primary’ osteoarthritis remain an umbrella term for any change without an obvious cause, such as trauma to the joint? Van Sasse et al. (1989) compared data on radiographs of people with symptomatic osteoarthritis in 11 populations of different ethnicities, and found that the age at which osteoarthritis develops may vary but, once it does, the rate or progression is similar in all populations. The authors suggest that although there are population differences apparent in osteoarthritis which is likely due to genetic and environmental factors, whatever the aetiological factors are, they are present in all human populations (Van Sasse et al. 1989).

**Symptoms:**

Many individuals over the age of 65 years are affected by osteoarthritis in one or more joints (Dominick & Baker 2004), and it is the most common reason for surgical replacement of the knee or hip joint (Felson et al. 2000). It can be asymptomatic, with little discomfort for the patient, or it can be incredibly painful and cause disability as a result of the affected joints (Somers et al. 2009; Tucker et al. 2009; Peat et al. 2001; Dekker et al. 1992).

The main signs and symptoms of osteoarthritis include pain and swelling in the affected joint, as well as stiffness when moving (Somers et al. 2009; Tucker et al. 2009; Peat et al. 2001; Felson et al. 2000; Dekker et al. 1992). The disease progresses slowly, and usually has minimal effects on an individual's ability to move normally; severe osteoarthritis can develop over time, causing great discomfort, and possibly leading to disability as a result of involvement of specific joints. To date there is no cure, but there are treatments to slow down the process and relieve some of the associated pain and discomfort (Arthritis Research UK http://www.arthritisresearchuk.org, accessed November 2011).

**Prevalence:**

Osteoarthritis is an incredibly common condition, both today and in the past, with 50-68% of adult individuals over the age of 45 affected (Waldron 1992; Rogers et al. 1987; Dominick & Baker 2004). The prevalence rates reported in clinical and palaeopathological literature are difficult to compare due to inconsistencies in

diagnosing osteoarthritis in archaeological and clinical situations (Larsen 1997). Medical diagnoses rely on radiographic evidence, such as joint space narrowing, osteophyte formation and sclerosis of the joint surface, as well as physical symptoms, such as pain reported by the patient (Figure 2.6) (McGonagle et al. 2010; Jacobson et al. 2008). Palaeopathologists rely on the evidence visible on the skeletal remains, including porosity and eburnation, which are not always visible on radiographs. There is also discrepancy within palaeopathology about which joint changes should be used to diagnose osteoarthritis. This lack of standardization in palaeopathological methods makes comparisons of prevalence rates, frequency, and severity of osteoarthritis difficult between different research articles (Jurmain & Kilgore 1995; Bridges 1993; Waldron & Rogers 1991).

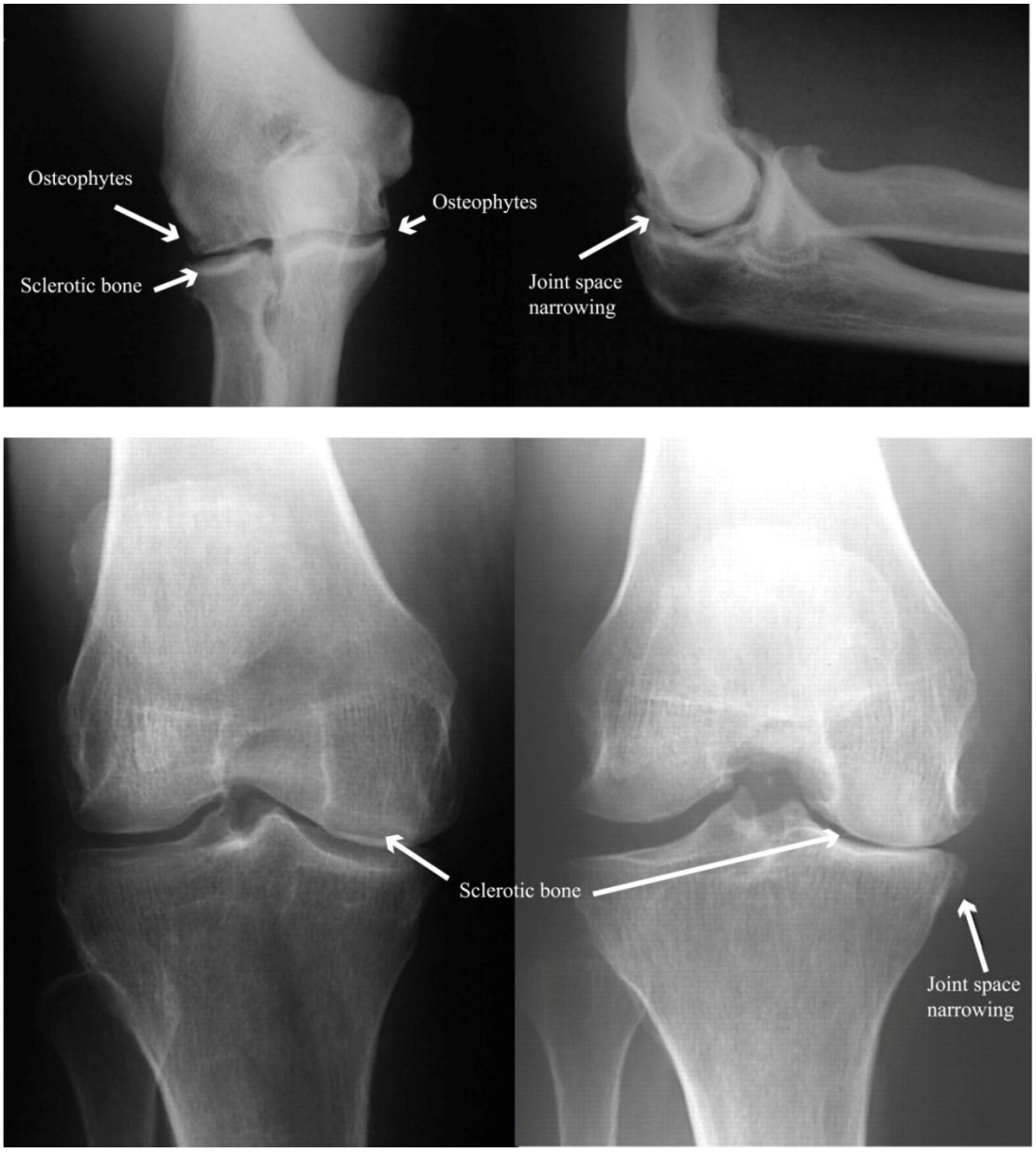


Figure 2.6) Radiographic images of elbow (top) and knee (bottom) osteoarthritis illustrating joint changes identified in clinical situations to diagnose osteoarthritis. Images from Krishnan et al. 2007 (elbow); Mazzuca et al. 2003 (knee).

As adult osteological aging techniques are known to be reliable only to age ranges of 10 or more years (Phenice 1969; Brothwell 1981; Bass 1987; Lovejoy et al. 1985; Işcan et al. 1984; Işcan et al. 1985; Brooks & Suchley 1990; Buikstra & Ubelacker 1994), the lack of accurate ageing methods in adults also hinders comparisons with clinical studies (Rogers & Dieppe 2003). These differences result in discrepancies in prevalence rates reported in palaeopathological studies and medicine, as it is difficult to compare age groups between the estimated age ranges in bioarchaeology and the accurate ages in clinical studies (Petersson 1996; Jurmain & Kilgore 1995; Crubézy et al. 2002).

Dominick and Baker (2004) performed a literature review of medical studies and found high prevalence rates of osteoarthritis, with frequencies of 58% to 68% of individuals older than 65 years in the United States; the criteria for diagnosis varied from radiographic evidence to symptomatic complaints from the patient. In comparison, Waldron (1992) analyzed a skeletal collection from a 14$^{th}$ century Black Death cemetery (Royal Mint) in London, and found that 50% of individuals older than 45 years displayed eburnation, which was used to indicate osteoarthritis. In this example, once the different age categories (65+ vs. 45+) are considered, the prevalence rates found by Dominick and Baker (2004) and Waldron (1992) suggest that the number of individuals afflicted with osteoarthritis were similar in both historical and modern times. This was supported by the study by Crubézy et al. (2002) who compared the prevalence of osteoarthritis in Neolithic, Medieval, and contemporary European populations. The skeletal populations were from two archaeological sites dated from 5700 BC to Medieval times, one in Moravia, Czech Republic, and the other in Nitra-Krskany,

Slovakia. The information from these sites was compared to modern autopsy studies from these regions. The authors found that the prevalence of osteoarthritis and the combinations of joints affected in individuals remains constant over this time frame (Crubézy et al. 2002).

In clinical literature, males under the age of 55 years have a higher prevalence rate of osteoarthritis than females; while females have been found to be more frequently and severely affected by osteoarthritis after the age of 55 years in both the USA and the UK (Roberts & Burch 1966; Felson 1998; Mankin et al. 1986; Hannan 1996). In archaeological investigations, males have been found to have a higher prevalence of osteoarthritis than females (Larsen 1997). Bridges (1991) found that the main difference between the sexes was in severity and not prevalence, with males showing more severe osteoarthritic changes than females. These differences seem to be inconsistent in the literature, with prevalence rates and severity for the sexes changing between populations (Bridges 1991; Bridges 1992). In addition, as mentioned above, the unreliability of osteological adult aging techniques makes it difficult to compare prevalence rates for age groups between living and archaeological populations. The higher prevalence of females over the age of 55 years with severe osteoarthritis today has been suggested to be a result of hormonal changes occurring in post-menopausal women (Felson 1998; Roberts & Burch 1966; Kellergen et al. 1963), while the high prevalence of osteoarthritis in males in historical times has been mainly suggested to be a result of differing physical activities and biomechanical strain (Fahlstrom 1981; Bridges 1991). These diverse explanations for sex differences in prevalence illustrates the inconsistencies in osteoarthritis research; although it is possible that both explanations

are accurate, it becomes obvious after substantial review of both clinical and palaeopathological literature that both explanations are an over-simplification of a very complex disease process.

Individual joints display osteoarthritis with varying frequencies, with the joints of the spine, hands, knees and hips being the most commonly affected (clinical literature: Bijkerk et al. 1999; Petersson 1996; Cushnaghan & Dieppe 1991; palaeopathological literature: Molnar et al. 2009; Lieverse et al. 2007; Waldron 1992). The frequencies of specific joint involvement varies between populations, both in the living and in the past; Bridges (1992) summarizes the findings of 25 studies with different frequencies of specific joint involvement, although all indicate either knee, hip or shoulder as the most affected joints. There are population differences, but the pattern remains that the same joints tend to be commonly or uncommonly affected in all populations, with minor variation between them (Schrader 2012; Watkins 2012; Molnar et al. 2011; Molnar et al. 2009; Lieverse et al. 2007; Van Sasse et al. 1989).

**Palaeopathology:**

The diagnosis of osteoarthritis is well established, in theory, being based on the presence of eburnation, and/or the presence of osteophytes, porosity, or joint contour change (Figure 2.7); however, in practice, it presents a challenge in palaeopathological research (Molnar et al. 2009). Eburnation has been suggested to be the only change pathognomonic of osteoarthritis (Waldron & Rogers 1995, 1991), and intra- and inter-observer error in recording osteoarthritis can be high due to varying experience, skill, and opinions about the skeletal manifestations of osteoarthritis. For example, Miller et

al. (1996) found that only 18% of osteoarthritic joints were correctly identified by palaeopathologists with varying experience.

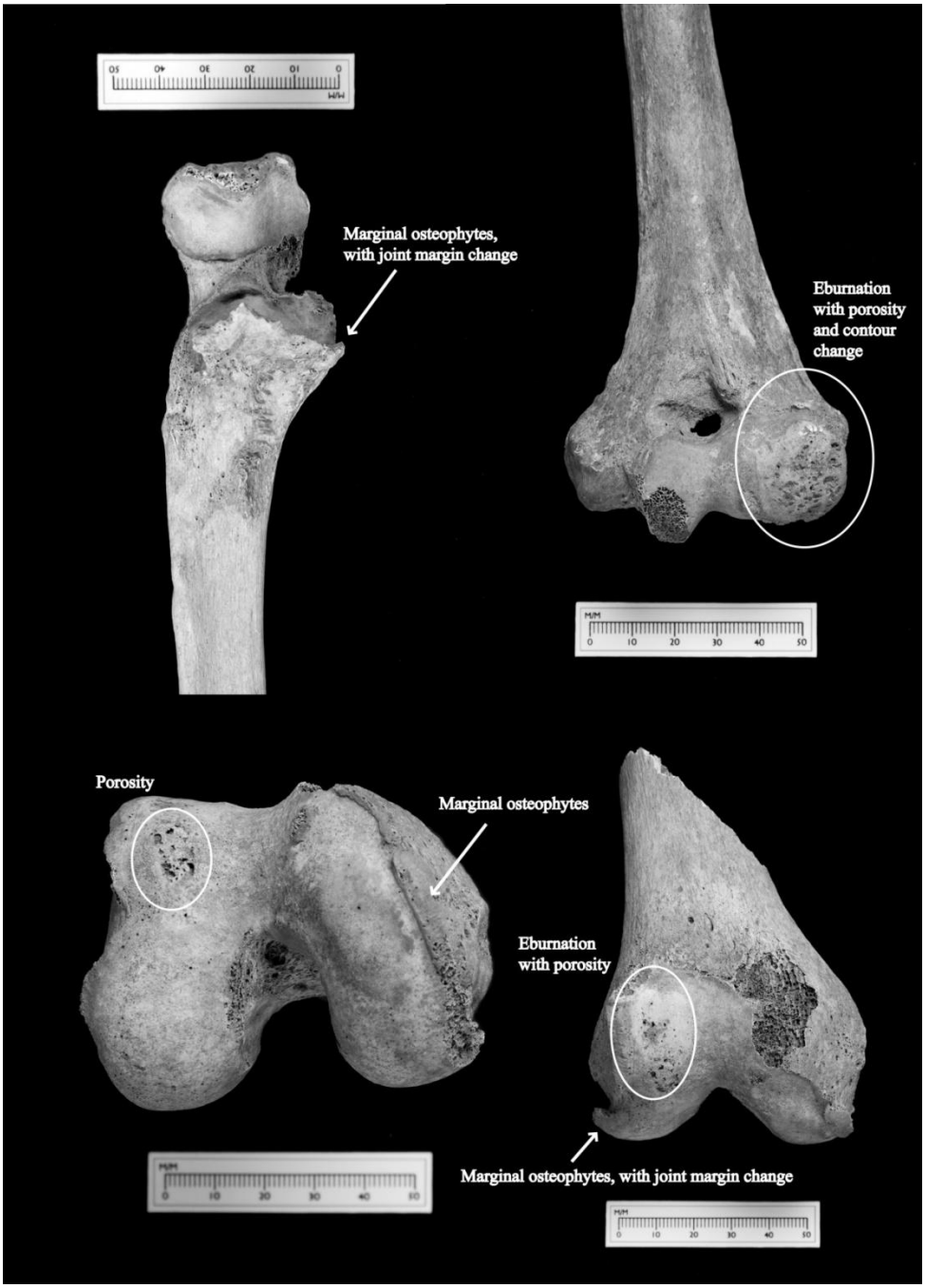


Figure 2.7) Examples of eburnation, osteophytes, and porosity on appendicular joint surfaces from archaeological human remains; top left – right proximal ulna, top right – left distal humerus, bottom left/right – left distal femur. Photos by Jeff Veltch.

Eburnation is caused by the loss of articular cartilage and sclerosis of the subchondral bone causing adjacent joint surfaces to rub together, producing a polished effect (Figure 2.7)(Ortner 2007). For some palaeopathologists, eburnation represents the only circumstance where osteoarthritis can be reliably diagnosed (Waldron & Rogers 1995), but Rothschild (1997) claims that eburnation is merely a result of osteoarthritis, and is not unique to it. Therefore, Rothschild (1997) considers eburnation to be a non-specific change which can only be used to indicate the severity of the disease, but in palaeopathology the presence of eburnation is the only change which indicates a complete loss of articular cartilage at the specific location. However, Rothschild (1997) states that since the American College of Rheumatology do not recognize eburnation as a diagnostic criterion for osteoarthritis, that palaeopathologists should not use it either. Eburnation cannot be recognized on radiographs, which is the main reason it is not used to diagnose osteoarthritis clinically. Although one can sympathize with Rothschild's (1997) argument, as palaeopathology benefits from using clinical literature (i.e. we need to know how diseases affect the skeleton before we can diagnose them in archaeological human remains), it remains an unarguable fact that palaeopathologists must work with what is available.

Osteophytes are bony exotoses which develop on a joint and its margins and are the most common change associated with osteoarthritis (Figure 2.7). These proliferations of new bone can range in size from very small to large spicules of bone (Larsen 1997). Osteophytes can occur without any of the other changes associated with osteoarthritis, indicating that they may not be directly associated with the disease. Many researchers have suggested that they represent degenerative changes, usually associated

with age, and may have more to do with an individual's tendency to form new bone, such as may be seen in enthesophytes, than a disease process affecting the joint (Jurmain 1991; Rogers et al. 1997). Jurmain (1991) states that mechanical stress affects the joint surface, and not the joint margins, and that osteophytes may be a result of aging and not necessarily the result of a breakdown of the joint ultimately resulting in osteoarthritis (Weiss & Jurmain 2007). However, osteophytes continue to be used as indicators of osteoarthritis in both clinical and palaeopathological situations because they accompany other changes, such as eburnation and joint space narrowing (clinical literature: Sumant et al. 2007; Mazzucal et al. 2003; palaeopathological literature: Weiss & Jurmain 2007; Lieverse et al. 2007).

Porosity has been suggested to represent a vascularization of the joint surface during osteoarthritis in order to nourish the stressed joint (Figure 2.7, and Merbs 1983; Woods 1995) and is considered one indicator of osteoarthritis (Waldron & Rogers 1991). Rothschild (1997) performed an analysis of knee joints from 400 skeletons from the Hamman-Todd collection curated at Cleveland Museum of Natural History, Ohio. This collection is composed of documented skeletal material of individuals of both European-American and African-American descent. The diagnosis of osteoarthritis was based on the presence of osteophytes and sclerotic subchondral bone. The author found that only 5% of the individuals displayed both porosity and osteoarthritis together. When these individuals are analyzed, 49% of the individuals who displayed porosity on the joint surface did not have evidence of osteoarthritis, and 97% of the individuals diagnosed with osteoarthritis displayed porosity (Rothschild 1997). Although porosity is used in many palaeopathological studies as an indicator of osteoarthritis when in the

presence of osteophytes or joint contour change, there seems to be very little evidence indicating that this should continue (Waldron & Rogers 1991; Ortner 1968; Bridges 1991; Waldron 1991; Rothschild 1997). Rothschild (1997) makes a final statement in his paper, claiming that "Porosity remains a macroscopic curiosity that has no identifiable clinical correlation and is therefore not a sign of any identifiable rheumatologic disorder. It should be deleted as an identifier of osteoarthritis". Rothschild (1997) makes a convincing argument; however, Wren (2007) found that there was a statistically significant relationship between porosity and the presence of osteoarthritis of the hip in the William M. Bass modern donated skeletal collection. This collection is composed of donated cadaveric skeletons from the USA. It is clear that if porosity is used as an indicator of osteoarthritis, it should be with extreme caution; further research into the relationship between porosity and osteoarthritis is required before a conclusion can be drawn as to its reliability as an indicator of osteoarthritis.

Joint contour changes occur when the subchondral surface of the joint is altered, resulting in deformation of the original joint surface (Figure 2.7), which even becomes unrecognizable in severe cases (Waldron & Rogers 1995). This does not occur on its own, but as a result of osteophytes or sclerosis and eburnation causing remodeling of the joint surface. It can be questioned whether this should be used as an indicator of osteoarthritis when its presence is dependent on other changes; perhaps it should only be mentioned as a result of osteophytes or eburnation, instead of used as a criterion for diagnosis.

Schrader (2012) investigated the prevalence of osteoarthritis in 85 individuals from a skeletal population from New Kingdom Tombos, Nubia. She analyzed

individuals aged young to old adulthood and found no evidence of eburnation on any joint surface. If the diagnostic criteria for osteoarthritis are expanded, 39% of individuals displayed osteophyte formation and porosity (Schrader 2012). The author clearly explained the joint changes identified and how the analyses were considered, but this study provides an excellent example of how different the frequency and prevalence of osteoarthritis can be, depending on the diagnostic criteria used.

As the joint lesions associated with osteoarthritis can also occur as a result of other joint diseases, the pattern of joint involvement throughout the skeleton is vital when considering differential diagnoses (Jurmain & Kilgore 1995). Generalized osteoarthritis can occur on any synovial joint throughout the skeleton, and secondary osteoarthritis generally occurs in bones which have sustained trauma or injury (Ortner 2003; Rogers et al. 2004). Rheumatoid arthritis is generally represented by erosive lesions and follows a distinct symmetric pattern throughout the body, affecting the joints of the hands, wrists, feet, ankles, knees, and the atlanto-axial joint. It can be distinguished from other joint diseases as it usually lacks proliferative bone changes (Arriaza 1993; Rothschild et al. 1990). Psoriatic osteoarthritis is a seronegative spondyloarthropathy which affects the upper and lower limbs asymmetrically (Arriaza 1993; Rothschild & Woods 1991). It mainly affects the hands and feet, distorting the inter-phalangeal joints into a "cup and pencil" appearance (Ortner 2003; Ortner & Utermohle 1981; Arriaza 1993), although it can also affect the knee, elbow, shoulder, sacro-iliac, costovertabral, apophyseal, and sterno-clavicular joints (Arriaza 1993).

One of the main issues with recording and describing osteoarthritis in palaeopathology is the variation in the type of synovial joints found in the human body.

There are six types of synovial joints: hinge, ball and socket, saddle, pivot, condyloid, and gliding, although these are not discrete categories (Calias-Germain 1991). All of these joints are synovial, and all have the ability to develop osteoarthritis. Most palaeopathological studies use the same recording system on every joint, with very little distinction made between the different joint structures. This lack of distinction may cause error in recording, as well as a misunderstanding of the lesions identified; for example, osteophytes 2mm in length appear small and minor on the distal femur, but appear much more severe on the costovertebral joints. It is understandable that osteoarthritis will manifest itself in different ways on different joints and in different areas of the joints, and a simple presence/absence based recording system may not be adequate in palaeopathological research. It is therefore vital to understand the detailed anatomical structure of the skeleton and the joints being analyzed; the cartilage thickness, attaching ligaments, muscles and tendons, as well as the range of movement of the joints will all affect how the joint reacts under stress (physical, genetic or age-related).

Palaeopathological research on osteoarthritis and other joint diseases have greatly benefited clinical understanding of the prevalence, distribution, evolution, and skeletal changes of joint diseases (Dieppe et al. 2006). The field would benefit from a standardization of recording methods and diagnostic criteria used, as continued investigation into skeletal changes related to osteoarthritis may eventually help identify the full aetiology of this disease which has a huge impact on modern life.

**Conclusion:**

Osteoarthritis affects a large proportion of living populations, as well as being highly prevalent in the archaeological record. The aetiology of this common condition remains unclear, although evidence suggests that multiple factors, especially a genetic prediposition, biomechanical stress, and increasing age, influence the development of the condition. The aim of Manuscript 3 is to use geometric morphometrics to try to identify any relationship between joint morphology and osteoarthritis, with the hypothesis that joint morphology may be one factor predisposing individuals to developing the condition.

## 2.3) Leprosy

Leprosy is a chronic infectious disease caused by the *Mycobacterium leprae* that can have severe social implications for both past and present human populations. It has attracted much research interest due its antiquity and the large impact the disease has on the quality of life of its victims. Leprosy has a long history in humans, with the first firm skeletal evidence of the infection dating to 2$^{nd}$ century BC in Egypt (Dzierzykray-Rogalski 1980). It is believed that the *Mycobacterium* was spread from Asia during the reign of Alexander the Great and was brought to Britain by the Romans in the fourth century (Roberts and Manchester 2007; Kjellström 2012). New pathogen ancient DNA analyses indicate that the disease likely originated in East Africa or the Near East and was spread with human migration (Monot et al. 2005). Leprosy is one of few infectious diseases which can leave skeletal evidence on archaeological remains, enabling palaeopathological studies of the palaeoepidemiology, evolution, and impact of the disease in the past. The skeletal manifestations of leprosy will be discussed and described in the following section, with consideration of both the archaeological and clinical impacts of the disease.

Leprosy primarily affects the peripheral nerves and secondarily affects the skin and other tissues of the body, including the eyes, testes, kidneys, bones, blood vessel endothelium, and mucosa of the upper respiratory tract (Lockwood & Reid 2001; Jopling 1982). The infection has an extensive clinical spectrum, with sufferers displaying different symptoms and manifestations of the infection dependent upon their immunological response and resistance to the *Mycobacterium* (Andersen et al. 1994). There are two types of immunologically stable leprosy, tuberculoid and lepromatous

leprosy. Tuberculoid, or paucibacillary leprosy, occurs when the individual has high resistance to the *Mycobacterium*; it mostly affects the post-cranial anatomy, and is characterized by few skin lesions and asymmetrical peripheral nerve damage (Andersen et al. 1994). Lepromatous, or multibacillary leprosy, is more generalized than the tuberculoid form and occurs when the individual has low resistance to the *Mycobacterium*. It is characterized by extensive and symmetrical skin-lesions and peripheral nerve damage (Andersen et al. 1994), as well as deformation of the soft tissues and skeletal elements of the face (Rodrigues and Lockwood 2011). These two different manifestations of leprosy infections are at each end of the immune spectrum, with intermediate 'types' in between (Ridley and Jopling 1966). Leprosy is one of the most varied infectious diseases in terms of physical responses (Ortner 2003), and physiological stress, such as the presence of other infections, can push an intermediate form of leprosy to the lepromatous end of the spectrum (Andersen et al 1994; Jopling & McDougall 1988). Leprosy infections can also have indirect effects on the skeleton, with the infection and resulting soft tissue damage causing destruction and deformation of the underlying skeletal elements; these will be discussed in greater detail below. The differences in targeted areas helps palaeopathologists to try and distinguish between the two types of conditions, as tuberculoid leprosy mainly affects the postcranial bones, and lepromatous leprosy is diagnosed by involvement of the facial bones (Lee and Manchester 2008: 209).

The low temperature of the nasal region provides the optimal environment for the *Mycobacterium*, causing the bacilli to accumulate in this area. *Facies leprosa* refers to the soft tissue changes affecting the face and nasal region described by Vilhelm

Møller-Christensen (1953, 1961, 1965). Rhinomaxillary syndrome is essentially the skeletal manifestation of *facies leprosa*, where the skeletal elements of the face undergo resorption and remodeling. These changes will be described in greater detail in the palaeopathology section below. The upper anterior dentition can be lost ante-mortem and if the infection occurs before adulthood, the normal development of the incisor roots can also be affected causing a dental condition called leprogenic odontodysplasia (Danielsen 1970). These changes can eventually lead to collapse of the central region of the face, which is one of the main physical deformities associated with leprosy and can lead to social and cultural stigmatization (Resnick and Niwayama 1995). The social repercussions of leprosy are discussed in more detail below.

Leprosy also indirectly affects the post-cranial body as the peripheral nervous system, including both the motor and sensory nerves, are damaged from the infection (Brown et al. 1996). The loss of the sensory nerve response, which is responsible for sensation in both deep and cutaneous tissues and joint spatial awareness, can lead to trauma in the limbs and appendages. Individuals who lack sensation in their soft tissues may injure or puncture their bodies, such as the soles of their feet, without knowledge of the trauma due to localized areas of anaesthesia, and thus no pain sensation. Soft-tissue ulcers can become infected, and continued ignorance of the lesion can lead to localized necrosis of the tissue and/or eventual spread of the infection into the blood stream (Lee and Manchester 2008: 215). Concentric diaphyseal remodeling of the pedal phalanges can also be a skeletal indication of leprosy, because of autonomic nerve damage, (Andersen et al. 1992; Andersen and Manchester 1988). Periosteal reactive bone is also a common skeletal lesion associated with leprosy, especially in the lower leg bones,

reflecting inflammation of the soft tissue of the lower legs (and arms) and spread of infection from the feet or hands (Lewis et al. 1994)

Motor neuropathy also occurs as the *Mycobacterium* affects the motor system, resulting in muscular paralysis. Claw-hand deformity occurs due to paralysis of the intrinsic extensor muscles of the hand, and is one physical characteristic of leprosy that is recognized in many countries where the disease prevails (Manchester *pers comm*. March 2008). Drop-foot results from the involvement of the posterior tibial nerve causing the collapse of the longitudinal arch of the foot (Andersen and Manchester 1988; Gilmore 2008). In both hands and feet, characteristic bone changes representing claw hand and drop foot have been identified (Andersen and Manchester 1988; Andersen and Manchester 1987)

**Transmission**:

Leprosy is of low pathogenicity and not highly infectious, with only 10% of people exposed to the *Mycobacterium* actually acquiring the disease (Carmichael 1993). It is generally accepted that *M. leprae* is transmitted via droplets exhaled from the lungs of infected people, and it can take a significant amount of close-contact time within a confined space before transmission of the infection takes place. Generally, only half the individuals exposed to the *Mycobacterium* acquire the disease (Ortner 2003). Although the bacteria tend to remain inside the body's tissue cells (Rodrigues and Lockwood 2011:466), lepromatous leprous sufferers, who are excreting large numbers of bacilli from their nose and skin, can be highly infectious if not treated (Lahiri and Krahenbuhl 2008).

**Clinical Significance and Prevalence:**

Today, leprosy is also referred to as Hansen's disease and mainly occurs in tropical and warm countries where resources are poor (Manchester and Roberts 1989; Britton and Lockwood 2004; Stone et al. 2009). In 1995, antibiotics known as MDT or multidrug therapy, which are used to treat and cure leprosy became freely available. This enabled control over spread of the infection in many countries and subsequently, a drastic decline in 'cases' of leprosy. The infection, however, continues to persist in many countries where access to treatment or education about the infection is deficient. These countries include Angola, Brazil, Central African Republic, Democratic Republic of Congo, India, Madagascar, Mozambique, Nepal, and the United Republic of Tanzania (Figure 2.8) (WHO http://www.who.int/lep/en/ Accessed June 10, 2012; Roberts 2011). Prevalence and frequency figures can be misleading due to under-reporting of the disease, making the exact extent of leprosy infections in the modern world unclear. The most recent reported global prevalence rate for leprosy infections was at the start of 2011, which reports 192,246 cases of affected individuals (WHO http://www.who.int/lep/en/ Accessed June 10, 2012). Leprosy can go undiagnosed despite characteristic signs and symptoms in countries where the infection is rare, including the UK, because clinicians or medical doctors may not always consider the possibility of leprosy, resulting in delayed diagnosis and appropriate medical intervention (Lockwood and Reid 2001).

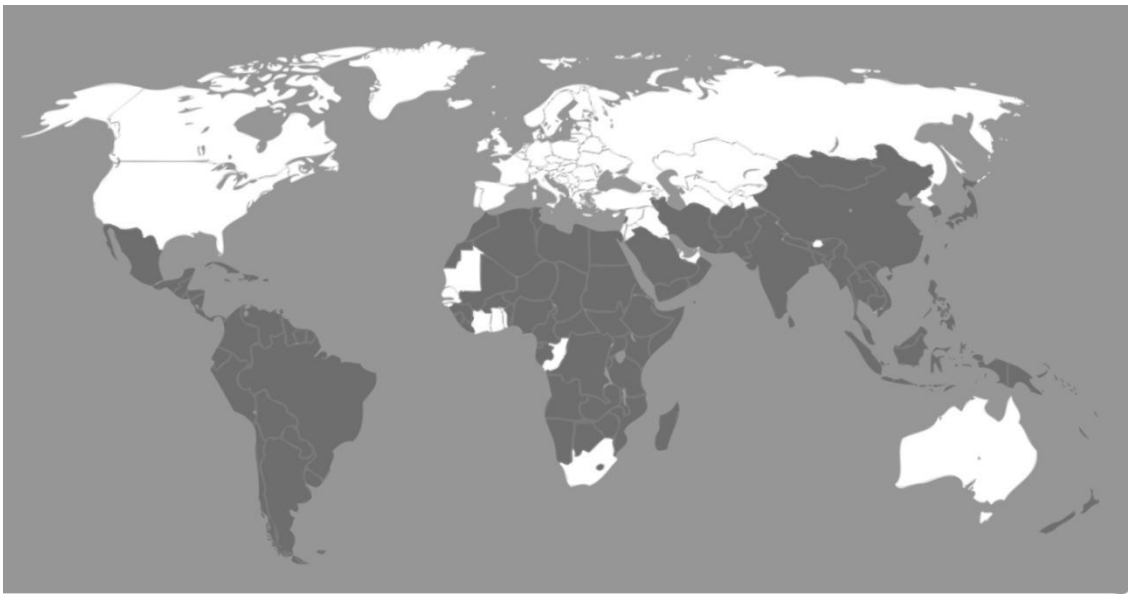

Figure 2.8) Global distribution of leprosy (dark grey) according to the WHO 2011 census of the disease ( http://www.bvgh.org)

Leprosy affects males more often than females, with a 2:1 infection ratio (Ortner 2003). This is due to females having stronger immunological reactions to the *Mycobacterium* than males (Ulrich et al. 1993). The symptoms and signs of a leprosy infection may take up to 20 years to develop before they affect the quality of life of sufferers (Covey 2001). The physical manifestations described above become progressively disfiguring over an individual's life, particularly in the hands, feet and face (Küstner *et al*. 2006; Rodrigues and Lockwood 2011), and many "cured" people still retain disfiguring lesions which can lead to ostracism, both in the past and present. The psychological effects of leprosy must also be considered when the condition is treated, as the social implications associated with stigma and the psychological impact of the physical deformations can have a major impact on an individual's mental health (Behare 1981; Raos et al. 1996).

**Leprosy in Palaeopathology:**

Leprosy reached epidemic level in Medieval England from the 11th-16th centuries A.D., according to historical data, although it started to decline in the 14th century (Rawcliffe 2006; Manchester 1991; Roberts 2011). Our evidence of leprosy in the past comes from historical sources, the opening of hundreds of leprosaria, and skeletal evidence. However, **s**keletal changes develop in only 3-5% of people with leprosy, making any claim about the exact frequency of infected individuals in the past difficult (Roberts 2011; Paterson and Rad 1961; Ortner 2003). Leprosy has held special interest in palaeopathological and historical research because of the identifiable skeletal changes associated with the infection, as well as the social impact the disease had on both the infected and healthy population (Rawcliffe 2006, Richards 1977, Roberts et al. 2002). Furthermore, the occurrence of leprosy in the skeletal remains of past human populations comprises a substantial portion of palaeopathological research and publications, especially in Europe (e.g. Roberts 2002; Belcastro *et al*. 2005; Boldsen and Mollerup 2006; Gilmore 2008; Kjellstrom 2010; Likovsky *et al*. 2006; Lunt 2011; Manchester 1981; Magilton et al 2008; Møller-Christensen 1953; Robbins *et al.* 2009; Stone *et al*. 2009).

Leprosy has also received an appreciable amount of attention in palaeopathological research because it is one of few infectious diseases with which individuals survive for long periods of time. Infections which kill their hosts quickly will not leave evidence on the skeleton. As chronic and prolonged leprosy can leave characteristic skeletal lesions, palaeopathologists have been able to study the palaeoepidemiology of leprosy, as well as how the infection affects the human skeleton.

The skeletal effects of leprosy differs depending on each individual's cellular immune response, as discussed above, the range of which is still not totally known (Scollard *et al.* 2006). This has led to many palaeopathologists qualifying the extent of skeletal changes as early to late lepromatous.

Diagnosis of the infection in human skeletal remains relies on macroscopic description of changes associated with the disease; these changes have been identified and described in detail by Møller-Christensen (1961), and later by Andersen and Manchester (1987, 1988, 1992, Andersen et al. 1992, 1994). Other methods of diagnosis have also been employed in palaeopathology, such as pathogen aDNA analysis (Rubini et al. 2012; Suzuki et al 2010; Taylor et al. 2006, 2010), and histological analysis (Blondiaux et al. 1994). Rhinomaxillary syndrome is suggested to be pathognomonic of lepromatous leprosy (Andersen and Manchester 1992), although Ortner (2003) states that other diseases, such as syphilis, tuberculosis, and cancer can also result in destructive changes in the nasal region of the face, and thus the pattern of lesions throughout the body is vital when considering differential diagnoses (Ortner 2003). Rhinomaxillary syndrome results in erosive, resorptive and proliferative bone changes variously affecting the alveolar and palatine processes of the maxilla, the anterior nasal spine, the intranasal osseous structures, and the margins of the nasal aperture (Figure 2.9) (Andersen and Manchester 1992). Post-cranial changes, such as drop-foot and claw hand deformity, can be considered as possibly related to leprosy, but are not pathognomonic (Andersen et al 1994).

Figure 2.9) Individual displaying skeletal changes indicative of rhinomaxillary syndrome (Skeleton 86, Chichester, West Sussex). White circle indicates resorption of nasal spine, and arrows indicate resorption and rounding of nasal aperture.

The post-cranial lesions identified in palaeopathology are indirectly related to leprosy, mainly as a result of motor and sensory neuropathy and the loss of limb proprioception and nerve sensation, respectively. Claw-hand deformity can be recognized on the skeleton if resulting hyperextension persists long enough to cause distal palmar grooves on the intermediate or proximal phalanges of the hands, called

volar grooves (Andersen and Manchester 1987). The grooves are crescent shaped impressions on the palmar surface of the phalanges resulting from localised atrophy from the continuous pressure of the hyperflexed adjacent phalanx (Figure 2.10) (Lee and Manchester 2008: 213-14). The lower legs can show subperiosteal bone reaction due to non-specific infection from skin ulcers and/or ascending infection from the feet which leads to oedema (fluid build-up in the soft tissues) and swelling in the soft tissue which is seen clinically. The new bone formation can have a 'molten lava' appearance on the tibia and fibula, and the shaft of the fibula can have a swollen appearance (Lee and Manchester 2008: 241; Jopling 1984; Boldsen and Mollerup 2006). The secondary infection, occurring as a result of loss of sensory nerve sensation and subsequent trauma to the foot, can also cause osteomyelitis in the bones of the lower limbs and feet. Compression fractures of the tarsals can indicate drop-foot, and dorsal tarsal bars, exostoses on the superior surface of the tarsals, indicate ligament strain related to collapse of the longitudinal arch (Figure 2.11) (Lee and Manchester 2008: 216). Concentric remodeling can result due to autonomic nerve damage, and ankylosis of the pedal phalanges may occur as a result of septic arthritis from secondary infections originating as a result of foot ulceration (Lee and Manchester 2008: 216-217).

Figure 2.10) Intermediate phalanx displaying crescent shaped groove on distal palmar surface indicating claw-hand deformity.


Figure 2.11) Right and left navicular bones displaying exostoses known as dorsal tarsal bars indicating drop-foot and ligament strain.

Palaeopathological research from all over the globe has been piecing together the epidemiology of leprosy in order to gain insight into the origin, evolution, and spread of the *Mycobacterium*. As stated earlier, the first undisputed osteological evidence of leprosy dates to the 2nd century BC in Egypt (Dzierzykray and Rogalski 1980). However, an individual with lesions suggestive of an infection by *Mycobacterium leprae* has been described from Balathal, India dating to 2000 BC (Robbins et al. 2009),

as well as an individual in Scotland dating to 2300-2000 BC (Roberts 2007). Also, Blau and Yagodin (2005) analysed lesions on an adult female dating to the 1st millennium BC from Ustyurt Plateau, Uzebekistance in Western Cental Asia. This individual represents the earliest evidence for leprosy in Central Asia and adds valuable information to the evolution and dispersion of the infection (Blau and Yagodin 2005). Each new study which identifies evidence of leprosy throughout the globe adds to our overall knowledge of the evolution and spread of the disease in the past. There are few diseases with such characteristic skeletal evidence, the other two being tuberculosis and treponemal diseases, and thus the palaeopathological evidence of leprosy provides a unique opportunity to follow the evolution of a *Mycobacterium* throughout human history.

**Social Significance:**

As discussed above, leprosy can result in severe and obvious physical disfigurement which may lead to associated stigma even today (van Brakel 2003; Cross 2007; Rafferty 2005; Raos et al. 1996), and such social implications, must be considered a possibility in the past. However, in spite of the suggestion that individuals with leprosy have been greatly stigmatized throughout history (Belcastro et al. 2005; Boldsen and Mollerup 2006; Covey 2001), more recent historical and bioarchaeological research suggests that this may not always have been the case (e.g. see Lunt 2011, Rawcliffe 2006, Roberts 2002). Different physical manifestations of the disease makes interpretation of how leprous individuals would have been treated in the past unclear, and likely depends greatly on individual social standing and social perceptions of infection.

During the leprosy epidemic of medieval Europe, many specialized institutions were founded to house and care for individuals suffering from the disease (Rawcliffe 2006; Boldsen 2009; Magilton et al. 2008; Boldsen and Mollerup 2006); this supports the idea that leprosy sufferers were ostracized from the healthy population and many lived outside the city boundaries, in these specialized hospitals. Individuals who died in these institutions were often buried in the associated cemetery, and it is the excavation of theses cemeteries which has provided researchers with many skeletons with leprotic changes, enabling palaeopathologists the opportunity to study the skeletal effects of leprosy (Manchester & Roberts 1989). However, other people, who may have suffered from ailments or diseases other than leprosy, could also have been buried in these cemeteries, making it important to consider different diagnoses when analysing these skeletal remains (Ortner et al 1991). However, most individuals with skeletal evidence of the disease are not actually found in specialized hospital cemeteries, but rather buried with other members of society, suggesting that not all leprous individuals were seen as outsiders from the general public (Roberts 2011).

The aim of the specialized institutions (leprosaria) opened across Europe is thought to have been to segregate the infected, although again there is debate about who was segregated and whether all had leprosy (Likovsky *et al*. 2006; Rawcliffe 2006). Sufferers were expected to live in these institutions and not come into contact with the healthy community; restrictions on daily life were also enforced, but some leprosaria allowed patients to beg and go to markets, even expelling them if they misbehaved (Rubini & Zaio 2009). Sufferers were also expected to carry clappers or bells with them to warn of their presence when in towns and cities (Figure 2.12) (Rawcliffe 2006).

Living in a leprosarium may not, however, have been considered a punishment for individuals suffering from the disease; there is no primary evidence identifying how these people may have felt about their living situations, and having shelter, food, and care may have been a better situation than some other living environments in medieval England.

Figure 2.12) Medieval image of a leprous woman holding a bell to alert others of her presence. (Original image: Museum Ribes Vikinger, Ribe, Denmark. Obtained via: http://www.stanford.edu/class/humbio103/ParaSites2006/Leprosy/Historical.htm, Accessed August 2012)

Historical documents from Medieval Europe suggest that leprosy was considered to be a punishment for sin (Rawcliffe 2006; Cule 2002). The extreme reactions to the

infection by the healthy population in historical evidence stem not only from the associated physical disfigurement, but also from the association of leprosy with the biblical reference to *tsara'ath*, which is now recognized to be referring to skin disease caused by spiritual uncleanliness and not leprosy (Cule 2002; Rubini & Zaio 2009; Brenner 2010). Figure 2.13 is a Medieval illustration of Jesus curing an individual suffering from leprosy; the depiction of the leprous man, covered in lesion, demonstrates the perception of leprosy in Medieval Europe. It is also suggested that leprosy may have been considered to represent a relationship to God, as it was a punishment for sin, and may have given leprous individuals a spiritual significance (Rawcliffe 2006). However, many leprous individuals were not treated differently in death, making this suggestion difficult to qualify (Roberts 2011).

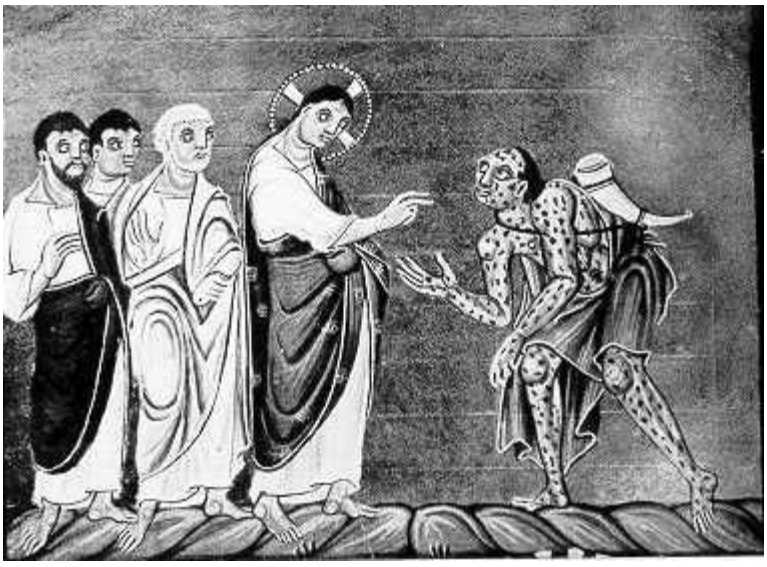

Figure 2.13) Medieval depiction of a leprous man being cured by Jesus. Images like this provide insight into the social importance of the disease, and its association with religious beliefs of the time (http://bonesdontlie.wordpress.com. Accessed August 2012)

The study of leprosy from historical texts and palaeopathology provides insight into the social implications of this infectious disease in the past. Leprosy still has major social significance in society today, making it important to consider the biocultural aspects of the disease when looking at archaeological evidence. The information gained from palaeopathological analysis of leprosy greatly adds to our understanding of the skeletal effects of the disease, as well as provides insight into the impact this socially significant disease had on the quality of life of past peoples.

**Conclusion:**

Leprosy has a major social and physical impact on the lives of its sufferers today, and has gained much attention in palaeopathological research because of its apparent high prevalence in Medieval Europe. Rhinomaxillary syndrome results in a shape deformation of the maxillae and is pathognomonic of lepromatous leprosy. One aim of Manuscript 4 is to use geometric morphometrics to objectively record and describe the shape deformation caused by rhinomaxillary syndrome, as well as use virtual imaging techniques to produce 3D interactive visualisations of the lesions in archaeological human skeletal remains.

## 2.4) Residual Rickets

Rickets is a childhood disease caused by insufficient vitamin D. Vitamin D plays a vital role in maintaining skeletal health in both juveniles and adults. It is an essential component in the mineralization of osseous tissue, as well as in cell growth, immune response, mineral metabolism, and cardiovascular health (Brickley & Ives 2008; Holick 2005). Vitamin D is not a "traditional vitamin" as it has to be synthesized into a metabolically active form before it can be used in the body, and it is therefore more accurately a pro-hormone (Holick 2003). Figure 2.14 illustrates the process by which vitamin D is synthesised and metabolized in the human body. The ultraviolet (UV) light obtained through exposure to the sun triggers synthesis of vitamin D precursors in the skin which undergo several steps of metabolism through the liver and kidneys before becoming a metabolically active form of vitamin D. It is the final product of vitamin D synthesis, 1,25-Dihydroxy vitamin D, which performs the biological functions within the body (Holick 2003). The vitamin is necessary for the absorption of calcium and phosphorus, which mineralizes osteoid. Vitamin D deficiency during adulthood causes osteomalacia, which has similar effects on the body, it is the process of bone remodelling which is affected because skeletal growth and development is complete by adulthood (Holick 2004; Brickley et al. 2005).

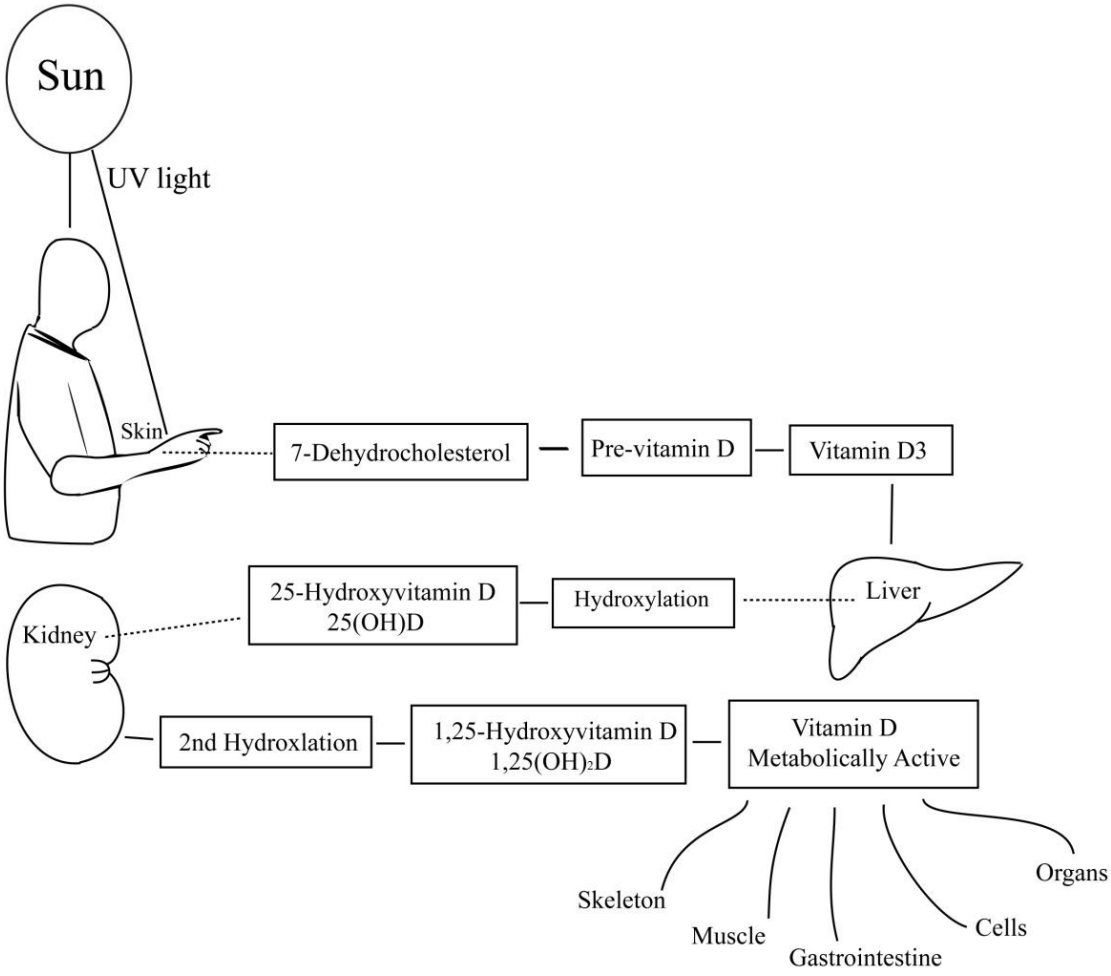


Figure 2.14) Visual description of the synthesis of the metabolically active form of vitamin D. Sunlight triggers the synthesis of the pre-hormone 7-DHC in the skin, which begins the process of synthesize through various pre-vitamin stages in the liver and kidney. Adapted from Brickley and Ives (2008: 79).

Humans, as well as most other vertebrates, obtain the majority of their vitamin D from sunlight (Holick & Chen 2008; Holick 2003). Few foods contain adequate amounts of vitamin D for a healthy balanced diet (Holick 2004; Chen et al. 2007), with dietary sources mainly found in fish oil and fat from aquatic mammals (Wagner & Greer 2008;

Prentice 2008). In some countries today, many foods are fortified with vitamin D in an attempt to provide adequate amounts within a normal diet (Fitzpatrick et al. 2000). Pregnant women who are deficient in vitamin D can increase the risk of their foetus developing infantile rickets (Thandrayen & Pettifor 2010), which also increases the importance of fortifying foods with vitamin D. After birth, infants continue to be at risk of vitamin D deficiency because human milk does not always provide sufficient amounts for a developing infant. In the United States, baby formula and cow's milks are fortified in order to ensure that infants obtain adequate amounts within their diet (Gartner & Greer 2003; Abrams 2002; Fitzpatrick et al. 2000). Children and infants with rickets are often brought back to health when vitamin D and calcium are introduced into their diet, and they are exposed to appropriate amounts of UV light (Fitzpatrick et al. 2000). However, the condition can also be cyclical, with individuals experiencing multiple bouts of the deficiency occurring throughout childhood (Brickley et al. 2010), such as every winter when in some parts of the world UV light availability is low, or during difficult economic period.

Rickets was a major health concern in the early 20$^{th}$ century, and in 1940, it was considered to be the most common childhood illness in the United States (Krieter et al. 2000). However, once the aetiology of the condition was determined and it was recognised that increased sunlight exposure and dietary supplements prevented and cured rickets, the prevalence of the disease decreased, becoming rare by 1960 (Krieter et al. 2000). Rickets is currently re-emerging as a health concern and continues to affect many people globally, even in Western countries such as the USA, the UK, the rest of Europe, Australia, and Canada, where cause and prevention of the condition are well

understood (Holick & Chen 2008; Sparre et al. 2009; Munnus et al. 2012). Krieter et al. (2000) compared the prevalence of reported rickets in two clinics in North Carolina in the 1990's and found that there had been a substantial resurgence of the disease in children. This is a consequence of many factors, including an increase in breast-feeding, as well as the recent fear of skin cancer, as increased awareness of the dangers of exposure of the skin to the sun has resulted in many people staying out of direct sunlight. This has caused many people to keep themselves and their children out of direct sunlight, as well as cover more of their skin with clothing and use strong sunscreen (Holick& Chen 2008; Girish & Subramaniam 2008; Gartner & Greer 2003). This will ultimately help decrease the risk of cancer, but it also leads to an increased risk of vitamin D deficiency (Holick & Chen 2008).

Appropriate exposure to sunlight does not mean excessive exposure. A study performed in Boston found that if adults exposed their face, hands and arms to sunlight for 5 to 30 minutes a day a few times a week, this provided adequate vitamin D to remain healthy (Holick 1986; Fitzpatrick et al. 2000). However, the same exposure during the winter months was found to be less than adequate (Webb et al. 1988). This can be controlled if an individual's diet is nutritionally sufficient, because vitamin $D_3$ can be stored in adipose tissue and released throughout the winter months (Fitzpatrick et al. 2000; Gartner & Greer 2003).

As vitamin D plays a vital role in skeletal development and growth, a deficiency in vitamin D can cause skeletal deformities. These deformities are a result of impairment in osteoblast function which causes subsequent inadequate mineralization of osteoid during bone growth or remodelling (Holick 2003). The exact role vitamin D plays in

bone mineralization is still not fully understood, as it has many different roles involving many proteins and enzymes which all have some effect on osteoblast function (Bikle 2012; Mankin 1974). However, it is understood that vitamin D is required to facilitate the absorption and excretion of calcium and phosphorus in the intestines, both of which are vital components in bone formation. This ensures that there are appropriate amounts of these elements for bone mineralization (Hazell et al. 2012; Brickely & Ives 2008). It is now recognized that the cause of rickets is more complex than inadequate amounts of vitamin D, and that dietary deficits in calcium and phosphorus can also cause rickets in children. For example, calcium deficiency can result in poor mineralization of osteoid which results in rickets, either as a secondary problem exacerbating the condition or as the main cause (Abrams 2002; Kooh et al. 1977; Mankin 1974). A deficiency in phosphorus can also cause rickets, although phosphorus deficiency is less common than that of vitamin D or calcium, except during foetal development (Abrams 2002). Rickets can also be caused by a congenital resistance to vitamin D and not necessarily a dietary insufficiency or lack of sunlight exposure. Instead it can be due to an individual's inability to synthesize or metabolize vitamin D properly (Pitt 1995).

**Clinical Signs and Symptoms:**

An individual is deficient in vitamin D and/or calcium months before clinical signs of the condition are apparent (Gartner & Greer 2003). Clinical investigations into dietary deficiencies can use the amount of 25-hydroxyvitamin D present in the body to indicate if an individual is deficient in vitamin D. 25-hydroxyvitamin D is the metabolite (intermediate form during metabolism) of vitamin D produced by the liver after synthesis of vitamin D in the skin by sunlight or ingested via the diet (Prentice 2008).

Clinical signs of rickets in children can include lethargies, muscle weakness, small stature, and low body weight (Mankin 1974). Impaired motor development and function, along with hypotonia (weak muscle tone) can cause abnormal movement and instability (Hazell et al. 2012; Mankin 1974). Rickets can also impact the child's immune system, making them more susceptible to illness or infection (Wagner & Greer 2008).

The main physical signs of severe and chronic vitamin D deficiency relate to the under-mineralization of osteoid during skeletal development. The cranial bones will become bossed, the long bones and pelvis will deform under body weight, dental development may be delayed, the sternum may become bowed and protrude, and the costochondral junctions of the ribs with the sternum will become enlarged and form nodular protrusions, known as rachitic rosary (Brickley & Ives 2008; Mankin 1974). These skeletal changes are the basis for identification of rickets in palaeopathology.

**Palaeopathology:**

Rickets has been reported in human skeletal remains from as early as the Upper Palaeolithic (Formicola 1995) and the Holocene (Pfeiffer & Crowder 2004), and many palaeopathological studies focus on the presence of rickets in the Medieval Period of Europe (Ortner & Mays 1998; Brickley et al. 2010; Haduch et al. 2009). Rickets, along with other indications of metabolic stress, is of particular interest to many palaeopathologists because of the implications it can have on the quality of life of past societies. One of the main goals of palaeopathological research is to provide insight into the daily lives of peoples and general well-being of societies in the past. Skeletal

evidence indicating metabolic stresses, such as rickets, scurvy, or anaemia, are often used in palaeopathology to indicate periods of strife in populations, especially in transition periods such as to agriculture from hunting and gathering, social differences within societies, and dietary customs (Brickley et al. 2007, 2010; Lewis 2002; Schultz et al. 2007).

Residual rickets is diagnosed when the skeletal evidence (Table 2.2) indicative of childhood rickets persist into adulthood. A lifestyle which results in inadequate vitamin D often would also promote other metabolic and nutritional deficiencies. Individuals can display pathological changes indicative of rickets, scurvy, anaemia, or general ill-health due to poor living conditions (Ortner & Mays 1998). The variety of metabolic diseases which a single skeleton can display can make it difficult for palaeopathologists to diagnose particular conditions in a skeleton, and often the diagnosis is one of 'metabolic stress', as opposed to rickets or scurvy. When diagnosing pathological conditions in palaeopathology, it is of course important to consider the patterns of lesions throughout the skeleton (Ortner & Mays).

Table 2.2) Description of skeletal changes used to diagnose residual rickets in adult skeletal remains (Brickley and Ives (2008: 110).

| Element | Pathological Changes |
|---|---|
| **Long Bones** | - Bowing- medio-lateral and/or antero-posterior deformation<br>- Coxavara – abnormal superior orientation of femoral neck<br>- Abnormal shortening<br>- Medio-lateral widening of proximal femoral diaphysis<br>- Abnormal angulation of knees |
| **Cranium** | - Abnormal bossing on frontal and/or parietal bones<br>- Abnormally large, square cranium<br>- Medially oriented mandibular ramus |
| **Ribs & Sternum** | - Abnormal neck angulation<br>- Diaphysis laterally straightened<br>- 'Pigeon-chest' – protrusion of sternum and sternal ends of ribs |
| **Pelvis & Sacrum** | - Abnormal curvature of ilium<br>- Anterior angulation and ventral orientation of sacrum<br>- Narrowing of pelvis and pelvic inlet<br>- Pubic symphysis 'bulges'<br>- Protusioacetabulae – protrusion of acetabulum into pelvic cavity |
| **Vertebrae** | - Scoliosis or kyphosis - abnormal curvature of spine<br>- Collapse of vertebral bodies |
| **Dentition** | - Abnormalities in enamel formation – enamel hypoplasia<br>- Caries |

As discussed above, children require sufficient nutrition and sunlight exposure in order to sustain normal skeletal development. Insufficient vitamin D, calcium, or phosphorus can lead to poorly mineralized bones which will deform under the child's weight. Mays et al. (2006) analysed infant and juvenile remains from St. Martin's church, Birmingham, and found that 86% of children with rickets displayed leg deformities compared to 31% with arm deformities (Mays et al. 2006; Brickley et al.

2010). Leg deformities are the most likely lesion to persist into adulthood, with 10-25% of affected children displaying leg deformities as adults (Wilkins 1986). As deformation occurs due to weight-bearing, children who suffer from rickets while crawling will often display bowed upper-limbs, and if the child is old enough to walk then the legs will be bowed (Ortner & Mays 1998). Evidence of residual rickets in adult skeletons can provide insight into the possibility that undernourished children survived into adulthood. These individuals would have been the ones who ”survived” their deficiency, either by acquiring a better diet or by increasing their sun exposure (Brickley & Ives 2008). As osteological sexing techniques cannot be used to accurately sex juvenile remains, it is suggested that residual rickets in adults may be used to indicate how males and females were affected differently due to social practices (Lewis 2007).

The occurrence of rickets before the 17$^{th}$ century is relatively rare, and it is not until the Industrial Revolution that the condition became a major health concern (Holick 2006). Industrial Europe saw a large increase in the number of children affected with metabolic disease, including rickets, as environmental conditions worsened due to increases in factories and population size (Lewis 2002). The increase of rickets during the Industral Revolution provides insight into how this social, economic, and environmental change impacted upon the lives of past people. Industrialization changed the way people lived and worked, as even young children worked in factories. Buildings were built close together, coal dust filled the air, and children lived in small dark homes or worked in dark factories (Holick 2004; Roberts & Manchester 2005: 238), thus affecting exposure to UV light.

Haduch et al. (2009) analyzed a single burial from a mid 16th-18th century cemetery in Krosno Odrzańskie, Poland, with severe skeletal deformities. The individual, who could only be tentatively sexed as female, displayed skeletal lesions associated with a severe and chronic vitamin D deficiency, either caused by rickets, osteomalacia, or both. The lower limbs were deformed to a large extent, with approximately 120° medio-lateral angulation of the tibiae and fibulae (Figure 2.15). The skeletal deformities of this individual are so severe that the authors concluded that this likely represents a case of chronic vitamin D deficiency due to renal failure (Haduch et al 2009).


Figure 2.15) Lower limb bones of an individual displaying severe vitamin D deficiency, likely both residual rickets and osteomalacia (Haduch et al 2009: 595).

Recording of long-bone bowing in palaeopathological research is often very subjective, with descriptions such as ‘slight’, ‘marked’, and ‘severe’ used to describe the extent of deformation (Figure 2.16) (Brickley et al. 2010; Haduch et al. 2009). Although diagnosis can also be coupled with radiographic evidence for support, these methods rely heavily on observer experience and interpretation. It has been suggested that much evidence of rickets in the archaeological record goes undiagnosed because it is only the most severely affected individuals who will present visibly deformed bones. Meyers (2010) developed a quantitative method of recognizing rickets in archaeological bone from several London skeletal populations. The author found that by using the ratio of the long bone distal circumference and the diaphyseal length, residual rickets can be accurately identified. The findings of Meyers (2010) suggest that the use of quantitative methods of recording rickets-related bone deformities may benefit palaeopathological studies of metabolic disease. It is one of the aims of Manuscript 4 to determine whether geometric morphometrics can be used to objectively record long-bone deformations due to residual rickets. If these methods are shown to accurately record and describe long-bone deformities, they could offer a means to reliably and objectively record residual rickets in archaeological bone.

Figure 2.16) Examples of bowing in three adult archaeological femora (Chelsea Old Church, London). Note how each femur displays a different degree of bowing and deformation which could be described as slight or moderate, depending on the observers' experience; this illustrates how intra and inter-observer error can be present in describing this condition.

**Conclusion:**

Residual rickets can offer insight into the health and quality of life of past populations, because vitamin D deficiency can indicate social and economic situations which result in inadequate nutrition or lifestyles without adequate exposure to sunlight. Despite this importance, residual rickets has received less attention in palaeopathological literature than many other pathologies, which may be due to the difficulty in diagnosing the condition with confidence. One aim of Manuscript 4 is to use geometric morphometrics to objectively record and describe the deformation of long bone bowing in adults due to vitamin D deficiency during growth. These methods may provide a means of recording the extent of deformation on long bones, enabling palaeopathologists to accurately describe and quantify the severity of the lesion.

# Chapter 3) Materials

## 3.1) Archaeological Context:

This section will provide a brief summary of the archaeological and historic context of each skeletal collection analysed. Figure 3.1 illustrates the location of each site in England. The descriptions of each archaeological collection analysed will be brief, as the hypotheses in this thesis are methodologically based, and the site details are not a major factor in each analysis. Each individual analysed in all manuscripts were chosen either for the presence of a particular pathological lesion or as a healthy control from within the same population.


Figure 3.1) Map of England with locations of the skeletal collections analysed indicated.

**Baldock, Hertfordshire:**

The skeletal remains from Baldock derive from the Roman cemetery in Baldock, Hertfordshire. This cemetery was excavated between 1980 and 1985, with 139 individuals found (Roberts 1984a). The site was occupied from 200-550 AD., with two late Iron Age burials dated from the 1st century also found (Roberts 1984a, 1984b; Burleigh 1984). This collection is curated in the Biological Anthropology Research Centre, School of Archaeological and Environmental Sciences, University of Bradford, West Yorkshire.

**Bowl Hole, Bamburgh, Northumberland:**

The Bowl Hole 7th-8th century AD early medieval skeletal remains were excavated by the Bamburgh Research Project from an early Medieval rural cemetery associated with Bamburgh Castle, Northumberland (Groves 2010; Groves *in press*; http://www.dur.ac.uk/archaeology/research/projects/?mode=project&id=278). The Bowl Hole site produced approximately 100 skeletons and disarticulated bone, was excavated in 1999, 2000, 2002, and 2003 (Groves 2010; Groves *in press;* Groves 2003), and skeletons are curated at Bamburgh Castle.

**Chelsea Old Church, London:**

The skeletal remains from Old Church, Chelsea, London, represent a high-status urban post-Medieval population, dating to the 17th-19th centuries, and consist of 198 individuals. Twenty-five of these individuals had coffin plates which provided biographical information for some people buried there. The site was excavated in 2000

by the Museum of London Archaeological Services (Cowie et al. 2008), and the skeletons are curated at the Centre of Human Bioarchaeology at the Museum of London.

**East Smithfields, London:**

The skeletal collection from the site of East Smithfields, London, consists of individuals buried in the East Smithfield's emergency burial ground during the Black Death epidemic from 1348-1350 AD in London. A total of 759 skeletons were excavated in 1986-1988 by the Museum of London Archaeological Services (Grainger et al. 2008; DeWitte & Hughes-Morey 2012; DeWitte 2010; DeWitte 2009). This collection is curated at the Centre of Human Bioarchaeology at the Museum of London.

**Fishergate House, York:**

The skeletons from the Fishergate House site represent a late Medieval urban population consisting of 244 skeletons dated from the late $10^{th}$ to $16^{th}$ centuries A.D. Fishergate House was a suburb of Medieval York, and there were four churches in the area (St George, St Helen-on-the-Walls, St Andrews and All Saints), but it is unclear to which of these the cemetery belonged (Holst 2005). This collection is curated by the Department of Archaeology at Durham University (http://www.dur.ac.uk/archaeology/facilities_services/fhol/).

**Hereford Cathedral, Hereford, Herefordshire:**

The skeletons excavated at Hereford Cathedral represent an urban Medieval population dating from the $7^{th}$ to the $15^{th}$ centuries (Stone & Appleton-Fox 1996). There were two mass graves found associated with an epidemic infection of the Black Death; other

inhumations conform to the customary Christian burial practices of the time. A total of 1,129 skeletons were excavated, 189 of them from the mass burials collection (Weston *et al, in prep*; Stone & Appleton-Fox 1996). The collection is curated at the Biological Anthropology Research Centre, School of Archaeological and Environmental Sciences, University of Bradford, West Yorkshire.

**Hickleton, South Yorkshire:**

The Hickleton site represents a rural population buried at St. Wilfrid's church, South Yorkshire, dating to both the late Medieval and post-Medieval periods, from the 11$^{th}$ to the 19$^{th}$centuries AD (Sydes 1984; Stroud *unpublished)*. There were 28 individuals in total excavated and they are curated at the Biological Anthropology Research Centre, School of Archaeological and Environmental Sciences, University of Bradford, West Yorkshire.

**St. James and St. Mary Magdalene Cemetery, Chichester, West Sussex:**

The skeletal remains from St. James and St. Mary Magdalene represent those buried in an urban Medieval leprosarium cemetery. The hospital was founded in the 12$^{th}$ century as a leprosarium, to house and care for sufferers of leprosy. After the prevalence of leprosy decreased in England, the hospital became an almshouse for the sick and poor until the late 17$^{th}$ century. Three hundred and eighty-four skeletons were excavated from 1986-87 and 1993 (Magilton 1986, 1993; Magilton et al. 2008). The collection is curated at the Biological Anthropology Research Centre, School of Archaeological and Environmental Sciences, University of Bradford, West Yorkshire.

**St. Mary Graces, East Smithfields, London:**

The skeletal collection from the Cistercian Abbey of St. Mary Graces is dated from 1350-1540 AD, derives from the abbey cemetery and consists of individuals of varying socioeconomic class from the surrounding area of London (Grainger & Phillpotts 2011). The site was excavated in the 1980's by the Museum of London Archaeological Services and is curated at the Centre of Human Bioarchaeology, Museum of London.

## 3.2) Selection of the sites

This thesis comprises a compilation of focused individual research projects which have included the analysis of archaeological skeletons from many English sites. Tables 3.1 through 3.7 (a-c) summarize and describe the composition and details of the skeletal collections used in each individual study.

**Project 1: Schmorl's nodes:**

The collections from London and York were chosen for analysis of vertebrae with Schmorl's nodes (section 2.1) in Manuscripts 1 and 2 because they contain a large number of well-preserved adult skeletons (Crowie et al. 2008, Grainger et al. 2008, Grainger and Phillpotts 2011; Holst 2005). The analysis of lumbar vertebrae included only individuals from Fishergate House, York (Holst 2005), because the results presented in Manuscript 1 indicated that additional analysis would be beneficial to obtain thorough insight into the relationship between the presence of Schmorl's nodes and vertebral morphology in the lower spine. Individuals with Schmorl's nodes were included in the analyses, as well as individuals without the lesion in order to provide a comparative healthy control sample. Sample size was dependent on preservation of vertebrae, and all vertebrae from T10 to L5 were included for each individual when available. Tables 3.1a through 3.1d provide a summary of the sample analysed.

Table 3.1a) Number of individuals included in the analysis of vertebrae with Schmorl's nodes in Manuscript 1, with number of males and females, and number of vertebrae of each vertebral segment summarized. All vertebrae from T10 to T12 were analysed for each individual when available.

| | Sex | | Age | | | | | Health | | | Total |
|---|---|---|---|---|---|---|---|---|---|---|---|
| | ♀ | ♂ | **U** | **YA** | **MA** | **OA** | **U** | **Healthy** | **Stage 1** | **Stage 2** | |
| T10 | 31 | 56 | 6 | 7 | 43 | 39 | 5 | 67 | 16 | 11 | **93** |
| T11 | 37 | 70 | 8 | 8 | 52 | 48 | 7 | 81 | 15 | 19 | **115** |
| T12 | 67 | 41 | 5 | 9 | 51 | 49 | 4 | 53 | 32 | 28 | **113** |
| **Total** | **135** | **167** | **23** | **24** | **146** | **136** | **16** | **201** | **63** | **58** | **322** |

Table 3.1b) Number of vertebrae included in the analysis of vertebrae with Schmorl's nodes in Manuscript 1. Vertebrae are summarized by sex, age and severity of Schmorl's nodes. Age groups are: young adults (YA 18-25 years), middle adults (MA 26-45years), and old adults (OA 46+years). The "Health" of vertebrae is scored according to Knüsel et al. (1997).

| Site | Period | ♀ | ♂ | U | T10 | T11 | T12 | Inds |
|---|---|---|---|---|---|---|---|---|
| **Chelsea Old Church, London** | Post-Medieval (1712-1842 AD) | 34 | 45 | 5 | 69 | 78 | 73 | **84** |
| **East Smithfields Black Death, London** | Medieval (1348-1350 AD) | 1 | 20 | 0 | 15 | 20 | 17 | **21** |
| **St. Mary Graces, London** | Medieval (1350-1540 AD) | 3 | 7 | 2 | 11 | 10 | 9 | **12** |
| **Fishergate House, York, Yorkshire** | Medieval ($12^{th}$-$16^{th}$ C AD) | 7 | 11 | 0 | 0 | 13 | 14 | **18** |
| | **Total** | **45** | **83** | **7** | **95** | **121** | **113** | **135** |

Table 3.1c) Number of individuals included in the analysis of vertebrae with Schmorl's nodes in Manuscript 2, with number of males and females. All vertebrae from T12 to L5 were analysed for each individual when available.

| Site | Period | ♀ | ♂ | U | YA | MA | OA | UN | Inds |
|---|---|---|---|---|---|---|---|---|---|
| Fishergate House, York, Yorkshire | Medieval ($12^{th}$-$16^{th}$ C AD) | 23 | 33 | 3 | 13 | 25 | 19 | 2 | 59 |

Table 3.1d) Number of vertebrae included in the analysis of vertebrae with Schmorl's nodes in Manuscript 2. Vertebrae are summarized by sex, age and severity of Schmorl's nodes. Age groups are: young adults (YA 18-25 years), middle adults (MA 26-45years), and old adults (OA 46+years). The "Health" of vertebrae is scored according to Knüsel et al. (1997).

| | Sex | | Age | | | | | Health | | |
|---|---|---|---|---|---|---|---|---|---|---|
| | ♀ | ♂ | **U** | **YA** | **MA** | **OA** | **U** | **Healthy** | **Affected** | **Total** |
| T12 | 18 | 22 | 2 | 9 | 16 | 15 | 1 | 16 | 26 | **42** |
| L1 | 19 | 22 | 3 | 9 | 19 | 14 | 2 | 22 | 22 | **44** |
| L2 | 19 | 19 | 3 | 9 | 20 | 11 | 1 | 16 | 25 | **41** |
| L3 | 19 | 20 | 4 | 9 | 21 | 10 | 3 | 17 | 26 | **43** |
| L4 | 16 | 17 | 2 | 7 | 20 | 8 | 1 | 25 | 11 | **36** |
| L5 | 15 | 21 | 4 | 8 | 17 | 12 | 3 | 35 | 5 | **40** |

**Project 2: Osteoarthritis:**

The collections from the University of Bradford were chosen for analysis of osteoarthritis of the proximal ulna, distal humerus, and distal femur in Manuscript 3 because they have a large number of adult skeletons (Weston et al. *in prep*; Roberts 1984a, 1984b; Sydes 1984; Stroud *unpublished*). Individuals with osteoarthritis and degenerative changes (section 2.2) were included in analyses, as well as healthy individuals for comparative controls (Tables 3.2a &b). Sample size was dependent on preservation of joint surface, and both sides were included when available.

Table 3.2a) Number of individuals included in analysis of osteoarthritis in Manuscript 3, with number of males and females, and age groups summarized. All joints from right and left sides were analysed for each individual when available.

| Site | Context | Period | YA | MA | OA | Total |
|---|---|---|---|---|---|---|
| **Hereford Cathedral, Cathedral Close, Hereford, Herefordshire** | Urban | Late medieval ($7^{th}$-$15^{th}$ C) | 26 | 10 | 20 | **56** |
| **St James and St Mary Magdalene, Chichester, Sussex** | Leprosarium Almshouse | Late medieval ($12^{th}$-$16^{th}$ C) | 20 | 17 | 29 | **66** |
| **Baldock, Hertfordshire** | Urban | Romano-British ($4^{th}$ C) | 9 | 4 | 5 | **18** |
| **Hickleton, South Yorkshire** | Rural | Late/ Post-medieval ($11^{th}$ -$19^{th}$ C) | 4 | 1 | 2 | **7** |
| | | **Total** | **59** | **32** | **56** | **147** |

Table 3.2b) Number of affected and healthy joints for both males and females, according to side included in the analysis of osteoarthritis in Manuscript 3.

| | | Osteoarthritis | | Osteophytes | | Healthy | | | |
|---|---|---|---|---|---|---|---|---|---|
| | | ♀ | ♂ | ♀ | ♂ | ♀ | ♂ | **Total** | |
| **Ulnae** | Left | 2 | 8 | 6 | 8 | 20 | 31 | **75** | |
| | Right | 0 | 11 | 7 | 14 | 20 | 28 | **80** | **155** |
| **Humeri** | Left | 2 | 6 | 3 | 9 | 32 | 46 | **98** | |
| | Right | 3 | 8 | 7 | 13 | 27 | 44 | **102** | **200** |
| **Femora** | Left | 0 | 2 | 4 | 9 | 17 | 21 | **53** | |
| | Right | 3 | 3 | 4 | 11 | 12 | 19 | **52** | **105** |

**Project 3: Leprosy:**

The skeletal collection of St. James and St. Mary Magdalene Cemetery, Chichester, West Sussex, was chosen for analysis in Manuscript 4 because the collection is composed of individuals buried in the leprosarium hospital (Magilton 1986, 1993, Magilton et al 2008). As the pathological lesion under investigation was rhinomaxillary syndrome of leprosy (section 2.3), this collection was ideal. Individuals were chosen based on the presence of characteristic lesions of leprosy, as well as healthy individuals as comparative controls. The sample size depended on preservation of the facial bones, as this is where the lesion manifests. For example, a total of 66 individuals were digitised during the study on rhinomaxillary syndrome, but as the facial bones are delicate and are often damaged, a subset of those individuals with appropriate landmark preservation was included in Manuscript 4 (Table 3.3a and 3.3b).

Table 3.3a) Number of individuals included in analysis of rhinomaxillary syndrome in Manuscript 4, with number of healthy and affected summarized.

| Collection | Time | ♀ | ♂ | U | YA | MA | OA | U | Total |
|---|---|---|---|---|---|---|---|---|---|
| Chichester, West Sussex | Late Medieval ($12^{th}$-$16^{th}$ C AD) | 12 | 26 | 1 | 7 | 15 | 15 | 1 | 38 |

Table 3.3b) Number of individuals included in analysis of rhinomaxillary syndrome in Manuscript 4, with number of healthy and affected summarized. The collection is curated at the Biological Anthropology Research Centre at the University of Bradford.

| Collection | Time | Healthy | Affected | Total |
|---|---|---|---|---|
| Chichester, West Sussex | Late Medieval ($12^{th}$-$16^{th}$ C AD) | 26 | 14 | 40 |

**Project 4: Residual Rickets:**

The skeletal collection of Chelsea Old Church, London, was chosen for analysis of femoral deformation due to residual rickets in Manuscript 4 because it has a large number of well-preserved individuals, both healthy and with pathological characteristics of residual rickets (section 2.4) (Cowie *et al.* 2008). Eight individuals with femoral deformation were used to analyse shape deformation, and 91 healthy individuals were used as comparative healthy controls. The sample size was dependent on preservation of femora. Tables 3.4a and 3.4b provide a summary of the sample analysed.

Table 3.4a) Individuals included in the analysis of femoral deformation due to residual rickets

| Collection | Time | ♀ | ♂ | U | YA | MA | OA | U | Total |
|---|---|---|---|---|---|---|---|---|---|
| Chelsea Old Church, London | Post-Medieval (1712-1842 AD) | 40 | 45 | 14 | 15 | 28 | 42 | 14 | 99 |

Table 3.4b) Number of individuals included in analysis of femoral deformation due to residual rickets in Manuscript 4, with number of healthy and affected individuals and femora summarized. Both right and left femora were analysed for each individual where available.

| Collection | Time | Healthy | Affected | Total |
|---|---|---|---|---|
| Chelsea Old Church, London | Post-Medieval (1712-1842 AD) | 91 (136 femora) | 8 (14 femora) | 150 |

# Chatper 4) Methods:

## 4.1) Osteological Methods:

Information on age and sex for each skeleton was taken from the original site reports for each skeletal collection (Cowie et al. 2008; Grainger et al.2008; Grainger & Phillpotts 2011; Holst 2005; Groves 2010; Roberts 1984a, 1984b; Stroud *unpublished*; Weston *et al, in prep*). These reports used standard osteological methods to estimate age at death and determine sex of all adult individuals, and these results were verified during analysis. If preservation limited the confidence of age estimation or sex determination, the individual was scored as 'unknown' and excluded from any sex or age specific analyses. Tables 4.1a and 4.1b describe the osteological methods employed with the relevant sources cited. Unknown individuals were included in analyses only if sexual dimorphism and age were found to not contribute to the overall shape variance of the sample. Age categories were as follows: young adult (20-34 years), middle adult (35-49 years) and old adult (50+ years) (Buikstra & Ubelaker 1994).

Table 4.1a) Osteological methods used to determine sex of adults in the archaeological skeletal collections used in analyses for this thesis.

| Reference | Method |
|---|---|
| **Milner 1992** | Preauricular sulcus of oscoxae |
| **Phenice 1969** | Sexual dimorphism of the oscoxae |
| **Bass 1987** | Sexual dimorphism of the oscoxae |
| **Acsadi & Nemeskeri 1970** | Sexual dimorphism of cranium and mandible |
| **Buikstra & Ubelaker 1994** | Sexual dimorphism greater sciatic notch |

Table 4.1.b) Osteological methods used to estimate age of adults in the archaeological skeletal collections used in analyses for this thesis.

| Reference | Method |
|---|---|
| **Brooks &Suchey 1990** | Degeneration of pubic symphysis |
| **Lovejoy et al. 1985** | Degeneration of auricular surface |
| **Işcan et al. 1984** | Degeneration of male sternal rib ends |
| **Işcan et al. 1985** | Degeneration of female sternal rib ends |
| **Brothwell 1981** | Dental wear (prehistoric to Medieval only) |
| **Scheuer& Black 2000** | Late fusing epiphyses |

## 4.2) Palaeopathological Methods:

As discussed in the Introduction, the pathological lesions included for analysis in this thesis were chosen because they either result in a deformation of the bones, which can be quantified with shape analysis techniques, or they have undetermined aetiologies which may be influenced by skeletal morphology. Palaeopathological lesions were identified and diagnosed on archaeological skeletal remains based on traditional macroscopic analysis of pathological bone changes. The diagnosis of each condition analysed in Manuscripts 1-4 of this thesis is described below.

### 4.2.1) Schmorl's nodes - joint disease:

Schmorl's nodes are depressions on the vertebral body caused by herniation of the nucleus pulposus of the intervertebral disc into the vertebral body (section 2.1) (Schmorl 1927; Schmorl & Junghans 1971). These lesions are the focus of Manuscripts 1 and 2. Schmorl's nodes were macroscopically recorded and analysed on both the inferior and superior surfaces of the vertebral bodies and were scored into three

categories based on characteristics described in Knüsel et al. (1997) (Table 4.2). Figure 4.1 illustrates examples of stage 1 and stage 2 lesions.

Table 4.2) Description of Schmorl's nodes according to stage, as defined by Knüsel et al. (1997).

| **Stage** | Depth | Coverage |
|---|---|---|
| **0** | Absent | Absent |
| **1** | < 2 mm | < ½ the equivalent antero-posterior length of the body |
| **2** | >/= 2 mm | > ½ the equivalent antero-posterior length of the body |

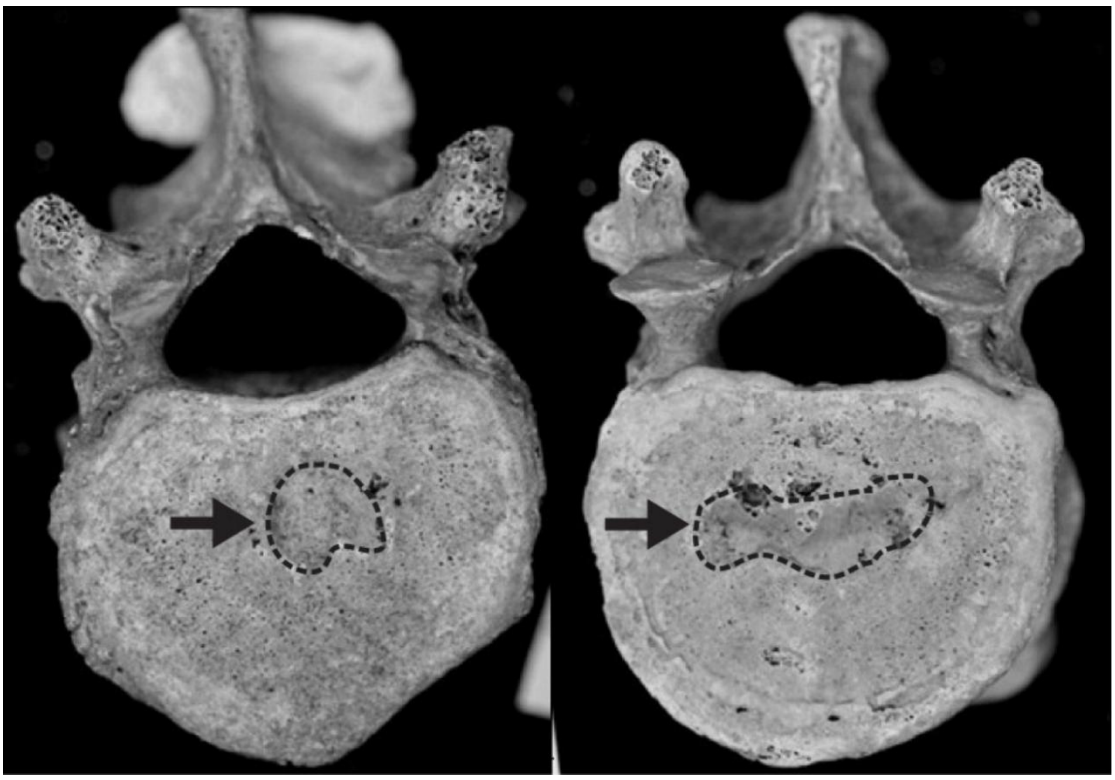

Figure 4.1) Left: Stage 1 Schmorl's node on T12 (Skeleton 532, Chelsea Old Church, London). Right: Stage 2 Schmorl's node on T12 (Skeleton 11703, East Smithfields, London).

**4.2.2) Osteoarthritis - joint disease:**

Osteoarthritis was diagnosed based on the presence of eburnation, which some researchers believe to be the only change pathognomonic of osteoarthritis, because it indicates a complete loss of articular cartilage (Ortner 2007; Weiss & Jurmain 2007). Table 4.3 describes the changes recorded for analysis of osteoarthritic changes. The location of the eburnation was recorded in order to identify the different joint areas or joint compartments affected (e.g. femoro-patellar or femoro-tibial joint compartments). The percentage of the joint affected was recorded to provide information on the extent of the lesion. Degenerative changes, such as osteophyte formation and porosity, were also recorded, although there is disagreement in palaeopathology as to whether these changes should be used to diagnose osteoarthritis, as discussed above (Rothschild 1997; Waldron & Rogers 1995; Weiss & Jurmain 2007); has been discussed in greater detail in section 2.2. Figure 4.2 illustrates joint changes recorded for analysis of osteoarthritis. Osteophytes were recorded in terms of their size (length from original joint margin), as well as location and percentage of joint margin affected. Porosity was recorded in terms of pore size (microscopic vs. macroscopic) and location and percentage of joint covered. These changes were recorded in this manner in order to provide information on what area of the joint was affected, as well as extent and potential severity of changes. As the diagnosis and recording of osteoarthritis in palaeopathology varies between researchers, all changes were recorded in detail in order to have all necessary information available (Waldron & Rogers 1995; Wiess & Jurmain 2007; Miller *et al*. 1996).The analysis of osteoarthritis in Manuscript 3 focused on the joint changes affecting the proximal ulna, distal humerus and distal femur, as these joints are commonly affected in both living

and archaeological populations (clinical literature: Bijkerk et al. 1999; Petersson 1996; Cushnaghan & Dieppe 1991; palaeopathological literature: Molnar et al. 2009; Lieverse et al. 2006; Waldron 1992).

Table 4.3) Description of joint changes recorded for analysis of osteoarthritis on the distal femoral joint in Manuscript 3. Detail on the method of recording, as well as possible differential diagnoses are included.

| Change | Description | Recording | Differential Diagnosis |
|---|---|---|---|
| **Eburnation** | Polishing of sub-chondral bone on joint surface as a result of bone rubbing on bone. | Location and percentage of surface coverage was described and recorded. | Rheumatoid Arthritis |
| **Osteophytes** | Abnormal bony outgrowths on joint margin or joint surface. | Quantified as less than or exceeding 2mm in length from original joint margin. Measurements were taken from original joint margin to outer edge of the osteophyte with a measuring tape. | Degenerative Joint Disease<br>Age related changes<br>Bone former |
| **Porosity** | Abnormal vascularisation of sub-chondral joint surface resulting in pores exposing trabecular bone below sub-chondral compact bone. | Recorded as microporosity, and considered to be a pore smaller than 2mm in diameter, or macroporosity, which is a pore equal to or exceeding 2mm in diameter. | Osteoporosis |

Figure 4.2) Examples of osteoarthritis on joint surfaces. Left: Distal joint of right femur displaying marginal osteophytes (>2mm) - arrow), a large area of eburnation with macroporosity on the lateral condyle (circled). Right: Distal joint of left humerus displaying large area of eburnation and macroporosity on capitulum (circled), and minor osteophytes (<2mm) along anterior joint margin.

**4.2.3) Leprosy - Infectious Disease:**

Leprosy was diagnosed based on skeletal changes in the facial bones (section 2.3). These changes indicate lepromatous leprosy infection and are referred to as "rhinomaxillary syndrome" (Figure 4.3) (Møller-Christensen 1978; Andersen & Manchester 1992; Rodrigues and Lockwood 2011; Britton and Lockwood 2004; Stone et al. 2010). These changes are generally considered to be pathognomonic of lepromatous leprosy; however, other diseases may cause similar lesions (Ortner 2003). Macroscopic analysis of the facial elements of adult crania was performed in order to

identify the presence of rhinomaxillary changes; the infection can cause a range of changes which are divided into 3 groups described in Table 4.3. The analysis of facial bone changes due to rhinomaxillary syndrome is one focus of Manuscript 4.

Table 4.4) Description of macroscopically visible pathological changes in the nasal region, with possible differential diagnoses (Møller-Christensen 1978; Andersen & Manchester 1992; Ortner 2003). Individuals were classified into one of three groups (healthy, early rhinomaxillary syndrome- EMS, & rhinomaxillary syndrome- RMS), depending on the presence and characteristics of lesions.

| Pathological Classification | Description of Lesion | Differential Diagnoses |
|---|---|---|
| **Healthy** | No pathological changes present in the facial bones | |
| **Early Rhinomaxillary Syndrome (EMS)** | - Minor resorption of nasal aperture, possibly with porosity and new bone formation<br>- Porosity on anterior nasal spine as resorption begins<br>- Minor porosity on palate | Treponemal infections |
| **Rhinomaxillary Syndrome (RMS)** | - Resorption of nasal aperture with new bone formation producing rounded remodeled edges.<br>- Resorption of anterior nasal spine<br>- Porosity on palate<br>- Resorption of anterior maxillary alveolus. | - Treponemal infections<br>- Wegener's disease<br>- Periodontal disease<br>- Tuberculosis |

Figure 4.3) Top – healthy individual, Chichester 142: notice the sharp edges of the nasal aperture; the nasal spine has not been resorbed and any loss is due to taphonomic damage. Bottom –Individual with rhinomaxillary syndrome: notice the widening and rounded edges of the nasal aperture and resorption of the anterior nasal spine.

### 4.2.4) Residual Rickets - Metabolic Disease:

Vitamin D deficiency during growth will affect effective mineralization of osseous tissue because of malabsorption of calcium and phosphorus, and these changes can last until adulthood (Brickley& Ives 2008). The skeletal changes visible in adults acquired during growth are known as residual rickets (Haduch et al. 2009; Brickley et al 2010), and it is these changes which are diagnosed and analysed in Manuscript 4. Diagnosis was based on macroscopic changes described in Table 4.5; the abnormality that is the focus of study is the bowing of the femora (Figure 4.4), which occurs due to weight-bearing on inadequately mineralized bone. Osteomalacia can also occur when adults experience vitamin D deficiency, and the skeletal changes can be very similar to residual rickets. The original site report of the Chelsea Old Church skeletal collection (Cowie *et al.* 2008) was referred to locate affected individuals, and macroscopic analysis of bone changes was performed to verify diagnosis before analysis.

Table 4.5) Summary of skeletal changes which can be attributed to residual rickets, with differential diagnoses indicated. Individuals were diagnosed based on the presence of some or all these changes. Table is adapted from Brickley& Ives (2008: 110-111).

| Element | Pathological Changes | Differential Diagnoses |
|---|---|---|
| **Long Bones** | ■ Bowing- medio-lateral and/or antero-posterior deformation. | osteomalacia, Paget's disease, mechanical adaptation to habitual activity |
| | ■ Coxavara – abnormal superior orientation of femoral neck. | |
| | ■ Abnormal shortening | other metabolic conditions, trauma |
| | ■ Medio-lateral widening of proximal femoral diaphysis | osteomalacia |

| | | |
|---|---|---|
| | ■ Abnormal angulation of knees | trauma, infection, Paget's disease |
| **Cranium** | ■ Abnormal bossing on frontal and/or parietals. | congenital abnormality, normal variation, premature birth |
| | ■ Abnormally large, square cranium. | intentional modification, congenital abnormality |
| | ■ Medially oriented mandibular ramus | normal variation of sexual dimorphism |
| **Ribs & Sternum** | ■ Abnormal neck angulation | Osteomalacia |
| | ■ Diaphysis laterally straightened | |
| | ■ 'Pigeon-chest' – protrusion of sternum and sternal ends of ribs | |
| **Pelvis & Sacrum** | ■ Abnormal curvature of ilium | Osteomalacia |
| | ■ Anterior angulation and ventral orientation of sacrum | osteomalacia |
| | ■ Narrowing of pelvis and pelvic inlet | osteomalacia |
| | ■ Pubic symphysis 'bulges' | osteomalacia |
| | ■ Protusioacetabulae – protrusion of acetabulum into pelvic cavity | |
| **Vertebrae** | ■ Scoliosis or kyphosis - abnormal curvature of spine | osteomalacia, congenital |
| | ■ Collapse of vertebral body | osteoporosis, osteomalacia |
| **Dentition** | ■ Abnormalities in enamel formation – enamel hypoplasia | metabolic conditions, nutritional deficiencies, physiological stress during development |
| | ■ Caries | diet, dental hygiene |

Figure 4.4) Left: Healthy adult femur (Skeleton 258, Chelsea Old Church, London). Right: Adult femur displaying bowing due to residual rickets (Skeleton 957, Chelsea Old Church, London).

## 4.3) Geometric Morphometric Methods

Geometric morphometrics is a suite of shape analysis techniques which make up the main analytical methods used in this thesis. The methods rely on analyses of two- or three-dimensional coordinates placed on known anatomical homologous points (landmarks) to identify subtle differences in shape between multiple objects or organisms (Bookstein 1991; Slice 2007; O'Higgins & Jones 1998). These methods can capture even small-scale intra-specific morphological variation, such as that between closely related modern human populations (Viðarsdóttir et al. 2002; Hennessy & Stringer 2002; Cobb & O'Higgins 2007; Franklin et al. 2007), and thus may be able to quantify pathological conditions examined in this thesis, which are often too subtle to identify with more traditional morphometric methods (Perez et al. 2007). Geometric morphometrics encompasses techniques and methods of data acquisition and subsequent analyses of shape variables which do not result in a loss of any geometric information contained within the data (Slice 2005). Since all geometric information is retained, the results of high-dimensional multivariate analyses can be mapped in shape space in order to illustrate and visualize shape variance within the data (Slice 2005).

In geometric morphometrics, the distinction between size and shape is crucial. Shape in this context is independent of size, location, and orientation (Slice 2005), whereas the term 'form' is used for the combination of shape and size (Mitteroecker & Gunz 2009). Shape is also not dissected into individual measurements as independent variables; instead the methods analyse the variation of the entire set of coefficients representing the whole landmark configuration. Thus, geometric morphometrics analyse shape in terms of sets of landmarks, not individual measurements.

### 4.3.1) Landmarks:

Landmarks are anatomical loci which are quantified based on their distance from a set of mutually perpendicular axes, thus producing Cartesian coordinates (Slice 2005). Landmarks should be homologous, easily and repeatedly identified on every specimen studied, as well as being significant in function, development, evolution, or structure of the specimen (Bookstein 1991; Rolf & Marcus 1993; Adams et al. 2004; Stevens & Strand Viðarsdóttir 2008; Mantini & Ripani 2009). Bookstein (1991) originally identified that there are landmark types of varying homology which can be used in geometric morphometrics, and these are the definitions used in this thesis (Table 4.6). However, additional landmark types have been described in Weber and Bookstein (2011). These landmark types differ in terms of their homology, with Type I having strong homology, down to Type III/VI which lack homology. After acquisition, the landmark data are inherently incomparable between individual objects, as each set of axes for the measurements are dependent on individual axes for each object, and include information on orientation and location (Slice 2005). This information must be removed by superimposition (see section 4.3.3) in order to obtain the true shape of the objects under study.

Semi-landmarks, which are Type III, are placed evenly on a curve or outline, and the number of landmarks will depend on the shape information being targeted (Gunz et al. 2005). In order to minimize the shape differences related to landmark spacing, the semi-landmarks are slid on the tangent plane, minimizing the bending energy of the deformation of the thin-plate spline (section 4.3.8) to a reference shape (Bookstein 1997a,b; Mitteroecker & Gunz 2009; Gunz et al. 2005; Gunz 2012; Perez et al. 2006).

Table 4.6) Description and examples of different landmark types for geometric morphometric studies (Stevens & Strand Viðarsdóttir 2008; Bookstein 1991).

| | Description | Example |
|---|---|---|
| Type I | Strong homology, easily located. | Intersection of sutures, tubercle, foramen |
| Type II | Mathematically or geometrically defined, | Highest point of curve |
| Type III | Weak or lacking homology, relative position on an object | Outline, intersection of a curve, |

### 4.3.2) Data Acquisition:

The Cartesian coordinates of three dimensional landmarks are captured using a Microscribe 3DX (error <0.1270 mm) digitizing system (Immersion Corporation, San Jose, CA). The Cartesian coordinates of two dimensional landmarks are captured from digital images using TPS© software (Rohlf 2004).

This thesis has been divided into three separate topics all related to the quantification of pathological lesions. Each analysis has a unique set of landmarks used to capture shape information on the intended skeletal element and these landmark sets are identified and discussed in this section.

**Schmorl's Nodes:**

Two dimensional landmarks were identified and digitised on digital images of healthy and affected lower thoracic and lumbar vertebrae in order to identify possible vertebral morphological associations with Schmorl's nodes (section 2.1). The landmarks were chosen to cover the vertebral body and its pedicles, and to avoid areas which are often damaged taphonomically, such as the spinous and transverse processes. The landmarks are illustrated and described in Figure 4.5 and described in Table 4.7 there are four Type I (1-4), four Type II (5-8), and eight Type III (9-17) landmarks. These landmarks were used in analyses for Manuscripts 1 and 2.

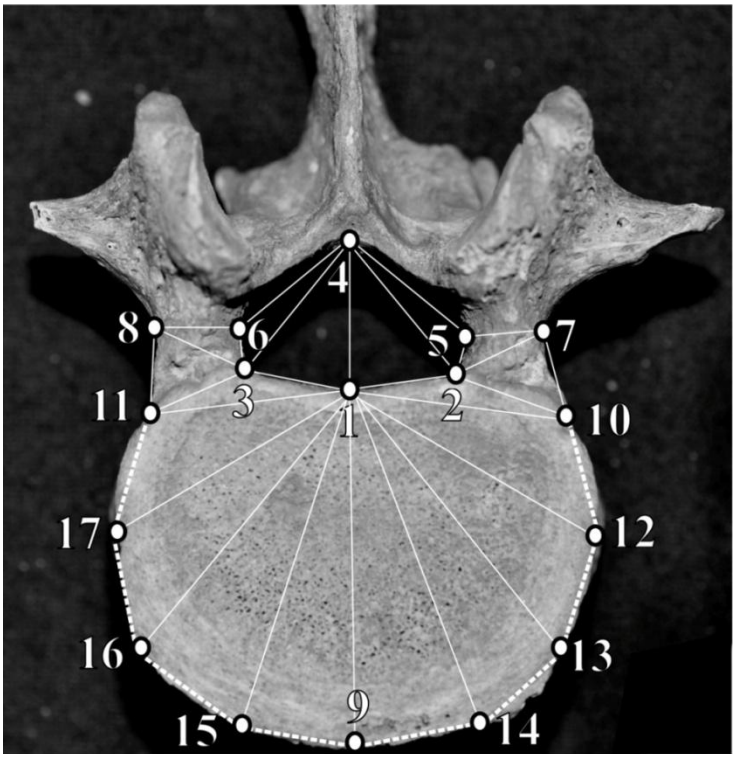


Figure 4.5) 2D landmarks (four Type I, four Type II, and eight Type III) used in analysis of vertebral morphology in vertebrae with Schmorl's nodes. Dashed white line represents sliding range of semi-landmarks. Locations are described Table 4.7.

Table 4.7) Description of 2D landmarks used in Manuscripts 2 and 3 for analysis of vertebrae with Schmorl's nodes.

| Number | Description | Type |
|---|---|---|
| **1** | Central point of the posterior margin of vertebral body | **II** |
| **2** | Left pedicle meets body | **I** |
| **3** | Right pedicle meets body | **I** |
| **4** | Posterior aspect of neural foramen | **II** |
| **5** | Left: widest point of neural foramen | **II** |
| **6** | Right: widest point of neural foramen | **II** |
| **7** | Left: external point of pedicle width | **II** |
| **8** | Right: external point of pedicle width | **II** |
| **9-17)** | Coverage of superior margin of vertebral body | **III** |

**Osteoarthritis:**

Twenty-one 3D landmarks were digitised to cover the proximal ulnar joint surface and margins in order to quantify the shape of osteoarthritic joints. The landmarks were chosen in order to provide adequate coverage of the joint surface and margin, as well as avoid areas that are commonly affected by osteophyte formation (see Section 2.2). The landmarks are illustrated and described in Figure 4.6 and described in Table 4.8; there are two Type II (1, 3), and 19 Type III (2, 4-21) landmarks. These landmarks were used in analyses in Manuscript 3.

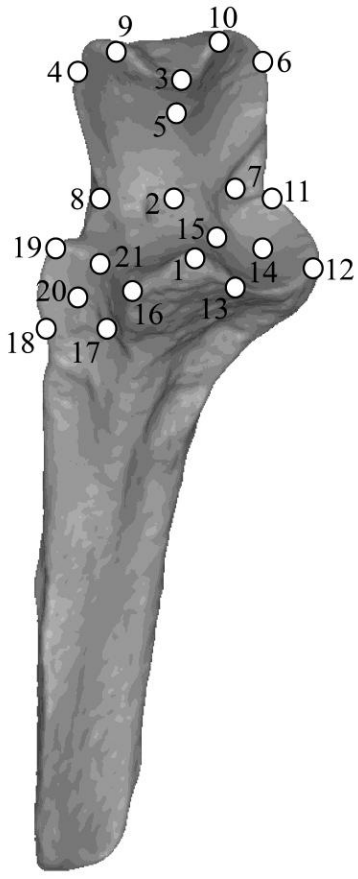


Figure 4.6) 3D landmarks used in analysis of osteoarthritis on the proximal ulna. Locations aredescribed in Table 4.8.

Table 4.8) Description of 3D landmarks used in Manuscript 3 for analysis of osteoarthritis on the proximal ulna.

| Number | Description | Type |
|---|---|---|
| **1** | Anterior most tip of coronoid process | II |
| **2** | Centre of fold in middle of trochlear notch | III |
| **3** | Anterior most tip of olecranon process | II |
| **4** | Lateral end of guiding ridge | III |
| **5** | Middle of guiding ridge | III |
| **6** | Medial end of guiding ridge | III |
| **7** | Medial end of fold in trochlear notch (where joint surface starts) | III |
| **8** | Lateral end of fold in trochlear notch (where joint surface starts) | III |
| **9** | Lateral corner where olecranon process meets joint surface | III |
| **10** | Medial corner where olecranon process meets joint surface | III |
| **11** | Posterior most point on medial ridge of trochlear notch. | III |
| **12** | Medial most point on medial ridge of trochlear notch. | III |
| **13** | Centre of depressed area of medial aspect of trochlear notch (ridge area). | III |
| **14** | Centre of ridge between depressed area of ridge and rest of joint surface. | III |
| **15** | Point on medial side of coronoid process before tip. | III |
| **16** | Point on lateral side of coronoid process before tip. | III |
| **17** | Anterior most point of radial notch | III |
| **18** | Inferior most point on radial notch (centred) | III |

| | | |
|---|---|---|
| **19** | Posterior most point on radial notch. | III |
| **20** | Centre of radial notch (in depression). | III |
| **21** | Centre of ridge separating radial notch with trochlear notch. | III |

Fifteen 3D landmarks were digitised to cover the distal humeral joint surface and margins in order to quantify the shape of osteoarthritic joints. The landmarks were chosen in order to provide adequate coverage of the joint surface and margin, as well as avoid areas that are commonly affected by osteophyte formation (section 2.2). The landmarks are illustrated and described in Figure 4.7 and described in Table 4.9; there are three Type II (13-15), and 12 Type III (1-12) landmarks. These landmarks were used in analyses in Manuscript 3.

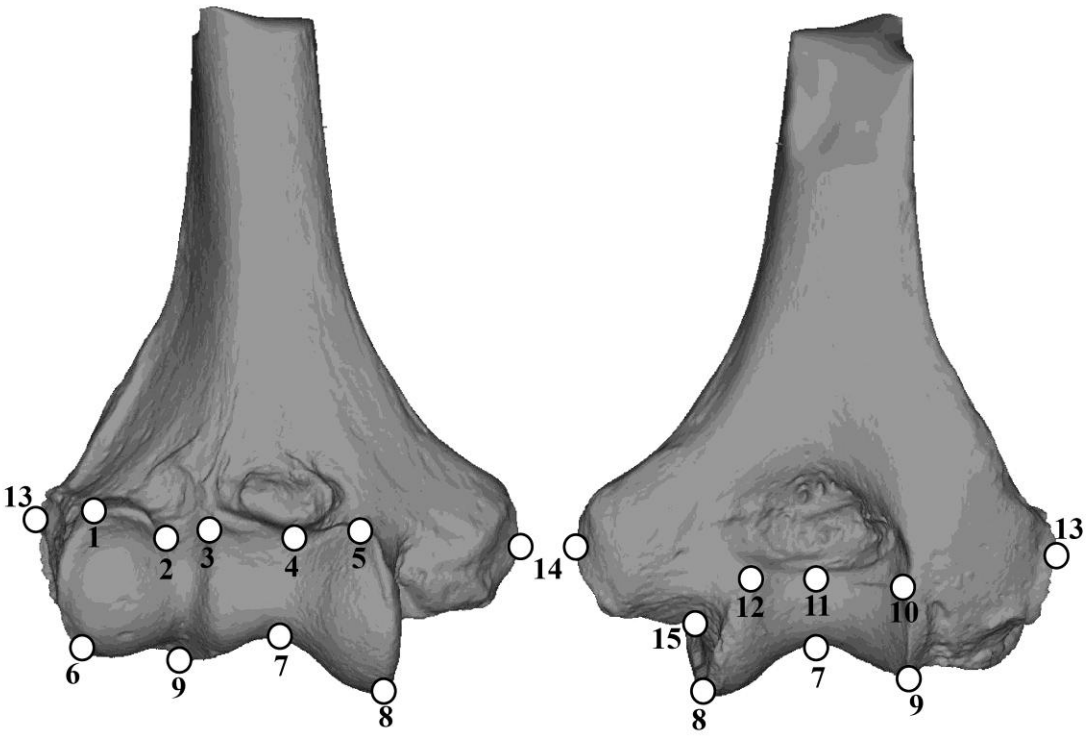


Figure 4.7) 3D landmarks used in analysis of osteoarthritis on the distal humerus. Locations described in Table 4.9.

Table 4.9) Description of 3D landmarks used in Manuscript 1 for analysis of osteoarthritis on the distal humerus.

| Number | Description | Type |
|---|---|---|
| **1** | Proximal most lateral corner of anterior capitular margin. | III |
| **2** | Proximal most medial corner of anterior capitular margin. | III |
| **3** | Proximal most lateral corner of anterior trochlear margin. | III |
| **4** | Proximal most center of anterior trochlear margin. | III |
| **5** | Proximal most medial corner of anterior trochlear margin. | III |
| **6** | Distal most point of lateral capitular margin. | III |
| **7** | Deepest central point of distal trochlea. | III |
| **8** | Distal most medial point of trochlear margin. | III |
| **9** | Distal most lateral point of trochlear margin. | III |
| **10** | Proximal most lateral corner of posterior trochlear margin. | III |
| **11** | Proximal most central point on posterior trochlear margin. | III |
| **12** | Proximal most medial corner of posterior trochlear margin. | III |
| **13** | Lateral most point on lateral epicondyle. | II |
| **14** | Medial most point on medial epicondyle. | II |
| **15** | Deepest central point of articulation between trochlea and medial epicondyle. | II |

Twenty-six 3D landmarks were digitised to cover the distal femoral joint surface and margins in order to quantify the shape of osteoarthritic joints. The landmarks were chosen in order to provide adequate coverage of the joint surface and margin, as well as avoid areas that

are commonly affected by osteophyte formation (section 2.2) The landmarks are illustrated and described in Figure 4.8 and described in Table 4.10; there are 18 Type II (1, 2, 4, 5, 7-9, 12-18, 20-23), and eight Type III (3, 6, 10, 11, 19, 24-26) landmarks. These landmarks were used in analyses in Manuscript 3.

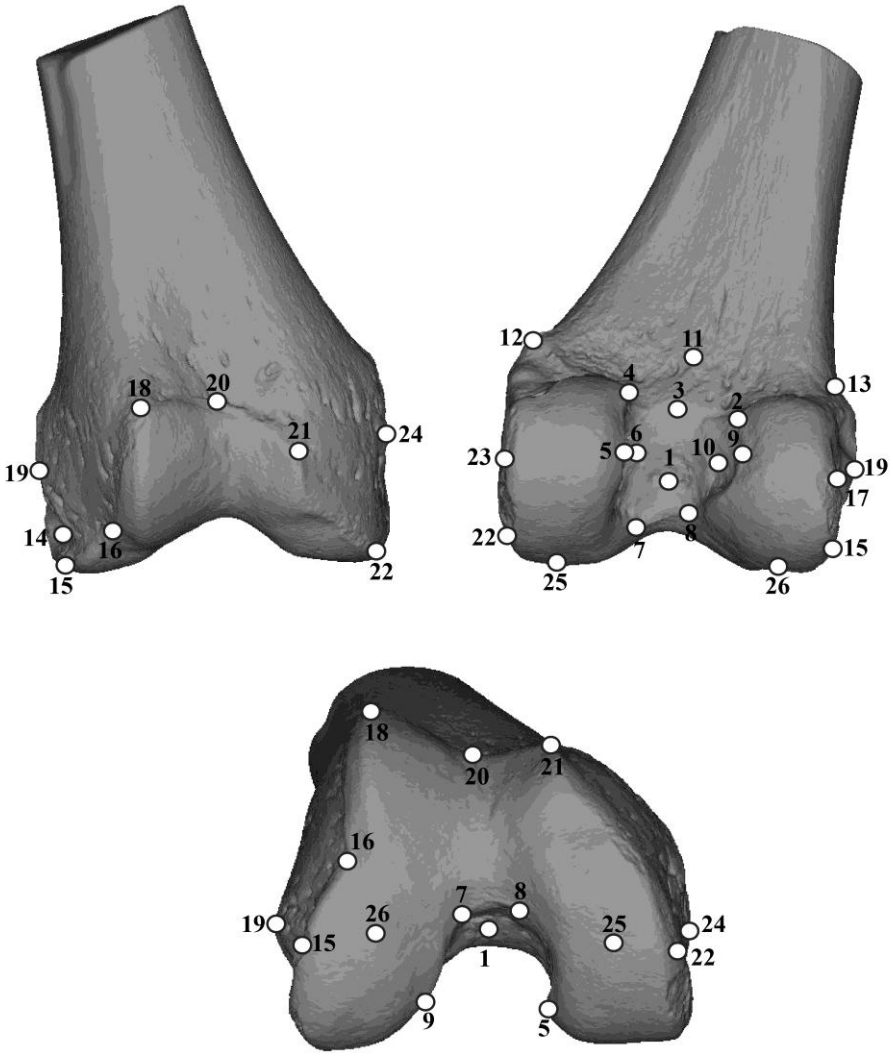


Figure 4.8) 3D landmarks used in analysis of osteoarthritis on the distal femur. Locations described in Table 4.10.

Table 4.10) Description of 3D landmarks used in Manuscript 1 for analysis of osteoarthritis on the distal femur.

| Number | Description | Type |
|---|---|---|
| **1** | Middle of the intercondylar fossa at the deepest point | **II** |
| **2** | Lateral most point on the posterior intercondylar ridge, where line meets lateral condyle | **II** |
| **3** | Central point on the posterior intercondylar ridge | **III** |
| **4** | Medial most point on the posterior intercondylar ridge, where line meets medial condyle | **II** |
| **5** | Central highest point on lateral surface of medial condyle, on edge where condylar surface meets intercondylar fossa | **II** |
| **6** | Central point on medial aspect of intercondylar fossa | **III** |
| **7** | Medial corner of articular surface of anterior patellar surface | **II** |
| **8** | Lateral corner of articular surface of anterior patellar surface | **II** |
| **9** | Central highest point on medial surface of lateral condyle, on edge where condylar surface meets intercondylar fossa | **II** |
| **10** | Central point on lateral aspect of intercondylar fossa | **III** |
| **11** | Point on popliteal surface central between condyles | **III** |
| **12** | Highest central point on abductor tubercle | **II** |
| **13** | Point on lateral aspect of lateral condyle which corresponds with location of abductor tubercle | **II** |
| **14** | Deepest central point of depression posterior to lateral epicondyle | **II** |
| **15** | Highest point on lateral aspect of lateral condyle where articular surface meets epicondylar edge | **II** |
| **16** | Central point of indented area of lateral aspect of lateral condyle | **II** |
| **17** | Point on lateral aspect of lateral condyle where condyle is widest | **II** |
| **18** | Lateral point where anterior patellar surface meets shaft | **II** |

| | | |
|---|---|---|
| **19** | Point of maximum convexity of lateral epicondyle | **III** |
| **20** | Central point where anterior patellar surface meets shaft | **II** |
| **21** | Medial point where anterior patellar surface meets shaft | **II** |
| **22** | Highest point on lateral aspect of medial condyle above medial epicondyle | **II** |
| **23** | Point on medial aspect of medial condyle where medial condyle is widest | **II** |
| **24** | Point of maximum convexity of medial epicondyle | **III** |
| **25** | Highest point on inferior aspect of medial condyle | **III** |
| **26** | Highest point on inferior aspect of lateral condyle | **III** |

**Leprosy:**

Landmarks were identified and digitised in 3D to cover the face of both healthy and lepromatous individuals in order to quantify the shape changes associated with rhinomaxillary syndrome (section 2.3). Adequate preservation of landmark loci was a limitation in this study, as the facial region can be taphonomically damaged; in order to maximise sample size, eight landmarks were used for further analyses. The landmarks are illustrated and described in Figure 4.9 and described in Table 4.11; there are four Type I (1, 4, 6, 7), and four Type II (2, 3, 5, 8) landmarks.

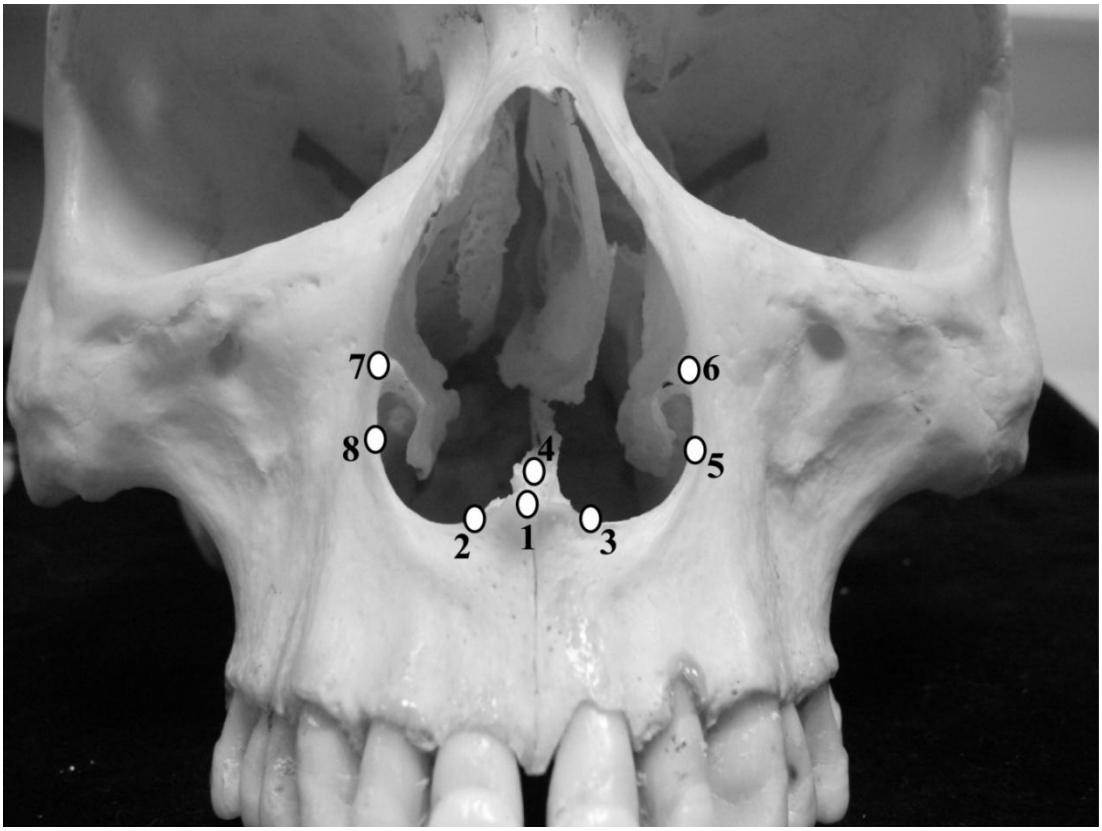


Figure 4.9) 3D landmarks (4 Type I and 4 Type II) used in analysis of rhinomaxillary syndrome. Locations are described in Table 4.11.

Table 4.11) Description of 3D landmarks used in Manuscript 4 for analysis of rhinomaxillary syndrome.

| Number | Description | Type |
|---|---|---|
| **1** | Nasopinale - tip of nasal spine | **I** |
| **2** | Left nariale - inferior aspect of nasal spine | **II** |
| **3** | Right nariale - inferior aspect of nasal spine | **II** |
| **4** | Posterior margin of nasal spine | **II** |
| **5** | Left alare - point where aperture ridge meets aperture margin | **II** |
| **6** | Anterior articulation of left nasal concha with aperture margin | **I** |
| **7** | Anterior articulation of right nasal concha with aperture margin | **I** |
| **8** | Right alare - point where aperture ridge meets aperture margin | **II** |

**Residual Rickets:**

Thirty 2D landmarks were digitised on the anterior aspect of adult femora. The landmarks were chosen to capture the morphology of the femoral diaphysis, head, neck, and distal condyles in order to analyze shape deformity attributed to residual rickets (section 2.4). The landmarks are illustrated and described in Figure 4.10 and described in Table 4.12; there is one Type I (1), nine Type II (2-10) and 19 Type III (11-30) landmarks. These landmarks were used in analyses for Manuscript 4.

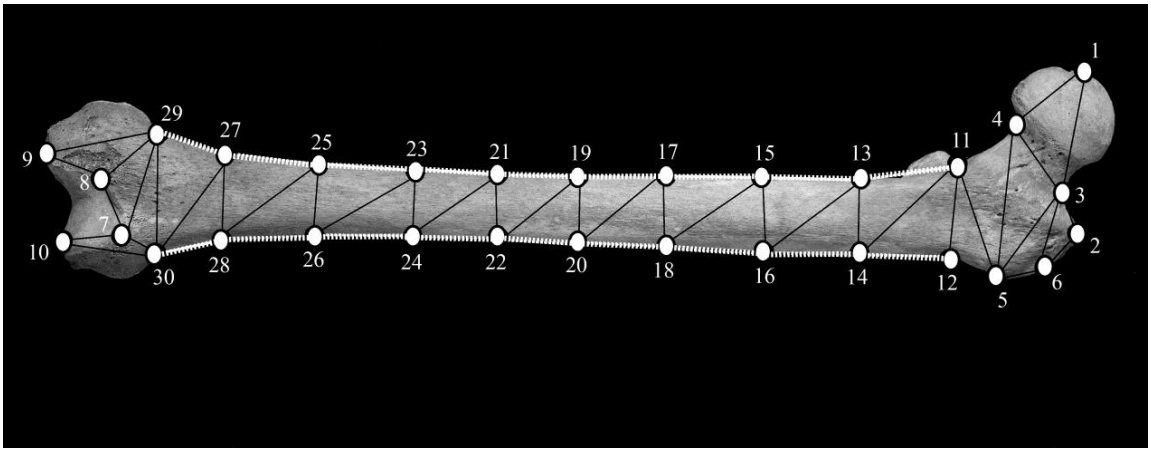


Figure 4.10) 2D landmarks (one Type I, nine Type II, and 19 Type III) used in analysis of femora with residual rickets. Dashed white line along the outer edge of the shaft represents sliding range of semi-landmarks. Locations are described in Table 4.12.

Table 4.12) Description of 2D landmarks used in Manuscript 4 for analysis of femora with residual rickets.

| Number | Description | Type |
|---|---|---|
| **1** | Medial most point of femoral head, at fovea capitis | **I** |
| **2** | Superior most tip of greater trochanter | **II** |
| **3** | Deepest point of superior femoral neck | **II** |
| **4** | Junction between femoral head and inferior aspect of neck | **II** |
| **5** | Lateral most point of greater trochanter | **II** |
| **6** | Central point of greater trochanter | **II** |
| **7** | Superior most point of lateral distal joint margin | **II** |
| **8** | Superior most point of medial distal joint margin | **II** |
| **9** | Inferior most point of medial distal condyle | **II** |
| **10** | Inferior most point of lateral distal condyle | **II** |
| **11-30** | Semi-landmarks covering outer margin of shaft | **III** |

### 4.3.3) Generalized Procrustes Superimposition:

As stated in section 4.3.1, landmark coordinates retain information on size, location, and rotation of the object. In order to obtain the true shape, this information needs to be removed by superimposition. The method of landmark superimposition commonly used in geometric morphometrics is a partial least squares algorithm called Generalized Procrustes Analysis (GPA) (Slice 2007; Dryden & Mardia 1998; Rohlf 2003; Goodall 1991; Bookstein 1997a; Rohlf & Slice 1990). GPA standardises the size of the landmark configurations and removes rotational and translational variation, leaving only the true shape of the object to be analysed. This is accomplished by fixing one object and minimizing the sum of the squared distances between corresponding landmarks of all the other objects in the sample; this is repeated until there is no further reduction in the sum of the Procrustes distances (Gower 1975; Goodall 1991; Slice 2007; Dryden & Mardia 1998; Bookstein 1997a; Rolf & Slice 1990). The Procrustes distance is defined as the square root of the sum of squared differences of corresponding landmark coordinates in two (partial) Procrustes superimposed figures (Slice 2005).

GPA does not result in any loss of shape information and gives equal weight to all landmarks, minimizing any bias on individual areas of the shape (O'Higgins et al. 2001; Rolf 2000; Strand Viðarsdóttir et al. 2002).After superimposition, shape can be analysed as the differences between corresponding landmark coordinates and the average shape of the sample is calculated; this data can be further analysed with multivariate tests to determine the shape variance and any significant patterns within the data (section 4.3.6). GPA was performed in Morphologika© (O'Higgins & Jones 2006) or MorphoJ© (Klingenberg 2008) in all manuscripts within this thesis

GPA results in a loss of several dimensions; the number of dimensions, or degrees of freedom, needed to represent shape is calculated with the following equation:

$$pk-k-k(k-1)/2-1$$

where p is the number of landmarks and k is the dimensions. The dimensionality of shapes in two dimensions is calculated as:

$$2p-2-2-1 = 2p-4$$

and in three dimensions it is:

$$3p-3-3-1 = 3p-7$$

The triangle is often used as an example to explain modern morphometric analyses, as it is the simplest geometric structure to include shape. For a triangle in two dimensions, p would equal 3 and k would equal 2, making 2 degrees of freedom (Slice 2005). This geometric information produces a shape space where shapes are differentiated by distance between corresponding landmark coordinates; GPA can be described as moving the data from a pre-shape space to a shape space (section 4.3.4)

**4.3.4) Kendall's Shape Space:**

Kendall's (1977, 1984) shape space is a geometric structure containing all geometric information after GPA has removed size, rotation, and translation from the data. Within this shape space, shapes are represented by points and the distance between each point is equal to the Procrustes distance (Kendall 1984, 1985; Slice 2005; O'Higgins & Jones 1998; Slice 2001; Baab et al. 2012). Kendall's shape space is spherical for 2D triangles, but more complex for shapes with more than 3 landmarks; this shape space is also non-Euclidean, or non-linear

(Slice 2005; O'Higgins & Strand Viðarsdóttir 1999). After GPA, the shape space for triangles is hemispherical because the shapes have been superimposed to the mean, and only the distance from each shape to this mean is the Procrustes distance (Figure 4.11)(Slice 2001, 2005). Each object or shape is represented by a single point in this shape space (Strand Viðarsdóttir et al. 2002).

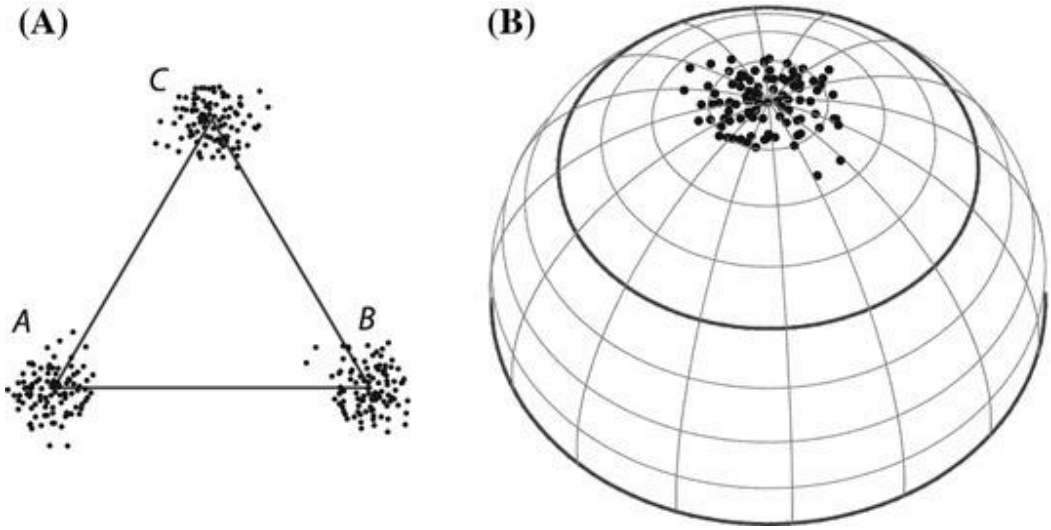


Figure 4.11) Visualization of Kendall's shape space for triangles after GPA (from Mitteroecker & Gunz 2009).(A) Variance of 100 triangle landmarks with outline of mean shape. (B) Isotropic distribution of triangles in shape space, which is (hemi) spherical.

In order to perform inferential statistics which require data to be linear, the data must be transformed into Euclidean (linear) data; this is achieved by taking a tangent of Kendall's shape space at the mean shape (Bookstein 1996b; Stevens & Strand Viðarsdóttir 2008). O'Higgins & Jones (1998) present an excellent explanation of this process by equating the sphere of Kendall's space shape to a globe and the tangent space as a map; the points on the sphere are projected onto the tangent space in order to obtain linear data. The distances

between shapes are preserved from Kendall's shape space to the tangent space (Bookstein 1996b). All analyses in this thesis were performed with Euclidean data in tangent space.

If landmarks have an isotropic distribution, i.e. their distribution is invariant in any direction, the distribution of points within the shape space will also be isotropic (Figure 4.11). However, it is non-isotropic distributions which are biologically interesting in morphometric studies, as it is the shape corresponding to this distribution which can provide insight into shape variation relevant in biological studies, such as variation due to sex, age, pathology, etc. (O'Higgins 2000).

### 4.3.5) Size

Size is retained after scaling during GPA as an independent variable and can be reintroduced into analyses when necessary. The unit of size measurement generally used in geometric morphometric analyses is centroid size which is defined as the square root of the sum of squared distances of the landmarks in a configuration to their average location (Slice 2007). Centroid size is a biologically significant measurement of overall scale of the landmark configuration (Strand Viðarsdóttir et al. 2002).

### 4.3.6) Principal Components Analysis:

The main aim of geometric morphometric studies is to analyse the variation of shape within the sample under study and identify any patterns within this variance which may be biologically interesting. Principal components analysis (PCA) is a multivariate statistical technique applied to landmark data after superimposition (Slice 2007; Reyment 1985; Somers 1986; O'Higgins & Jones 1998; Stevens & Strand Viðarsdóttir 2008; Mitteroeker & Gunz

2009). PCA was performed in Morphologika© (O'Higgins & Jones 2006) and used in all manuscripts within this thesis. PCA calculates the principal axes of shape variation in the Procrustes tangent space in order to illustrate the shape variance in the sample and highlight any patterns occurring within the data (Slice 2007; O'Higgins & Jones 1998; Dryden &Mardia 1998).

The overall shape of the object is separated into uncorrelated shape variables called principal components (PCs), which are orthonormal eigenvectors of the covariance matrix (Jolliffe 2002; Dryden &Mardia 1998). PCA is a descriptive technique which identifies the covariance of shapes from the average. Combining PCA results with 3D or 2D imaging technology enables ready interpretation of patterns of shape variance which may arise in the data (Slice 2007). Each principal component (PC) describes one aspect of the overall shape variance and the majority of shape variance is normally described by the first few PCs (Jolliffe 2002). If the distribution of shape variance is an ellipsoid, PC1 is the axis which goes through the greatest dimensions of the shape concentration, therefore, PC1 describes the largest amount of variance (Legendre & Legendre 1998); the PCs are orthogonal to each other making them statistically independent, and each describes the next greatest dimensionality of the ellipsoid. Therefore, PC2 describes the second largest amount of variance, and so forth (Legendre & Legendre 1998; O'Higgins & Cobb 2007).

### 4.3.7) Canonical Variates Analysis:

Canonical variates analysis (CVA) has similar uses as PCA in morphometrics, as it describes shape variance among groups defined by categorically shared features, such as sex, age, species, and so forth. The canonical variates (CVs) are uncorrelated and describe the

maximum distance between each group mean; the variance between groups is maximized in relation to the within-group variance (Klingenberg & Monteiro 2005; Albretch 1992; Owen & Chmielewski 1985). A CVA plot illustrates the groups' centroid and the variance of shape scattered around the group means. As with PCA, CVA does not determine statistical significance of group differences; in order to obtain a p-value, a multivariate analysis of variance (MANOVA) is performed on the Procrustes distances between the group means (Zelditch et al. 2004; Klingenberg & Monteiro 2005). CVA is performed in MorphoJ© (Klingenberg 2008).

**4.3.8) Visualization of Shape:**

Shape variance within a sample is illustrated on a PCA chart. Wireframes on warp grids in Morphologika© (O'Higgins & Jones 2006), R (R Development Core Team 2010), or TPSRelW© (Rolf 2004) provide visual representation of shape differences in the sample at any point on the PC plots.

The thin-plate spline is a metaphorical thin steel plate, in which the shape differences can be visualized using deformation grids. Deformation grids illustrate the amount of deformation required to change a reference shape, such as a mean of one group, to a target shape, or the mean of another group. The bending energy is the amount of energy required to deform an infinitely thin steel plate from the reference shape to a target shape (Bookstein 1997a, b). Figure 4.12 illustrates a thin-plate spline warp grid showing the bending energy required to deform a reference shape to a target shape.

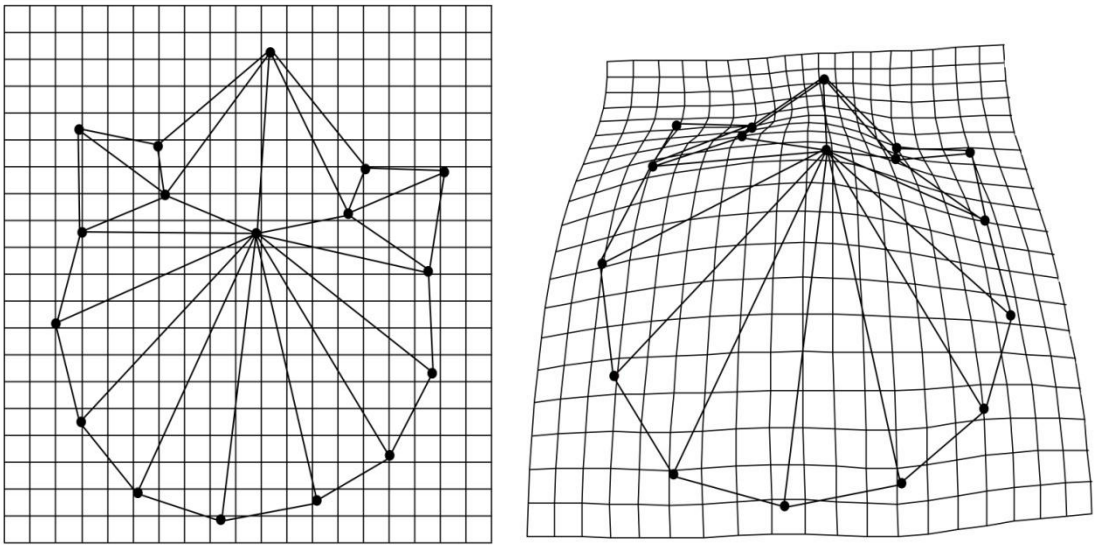

Figure 4.12) Thin-plate spine illustrating bending energy required to deform the reference shape, a healthy T12, to the target shape, a T12 vertebra with a Schmorl's node.

**4.3.9) Discriminant Function Analysis:**

A cross-validated discriminant function analysis (DFA) predicts group membership based on shape variables and the distance between the groups means (Klingenberg 2011; White & Ruttenberg 2007).A greater distance between the means will result in a higher accuracy of correctly classifying individual objects into groups based on shape variables. Once shape variables have been identified, cross-validation analysis determines how accurate and reliable the shape variables are at distinguishing between groups by using repeated random leave-one-out validation (Cardini et al. 2009; Kimmerle et al. 2008).The repeated tests are called permutations, with a number of tests (100+) performed on the data to identify the accuracy of the distinguishing variables. In other words, permutation tests randomly select a single sample, recalculate, and place it back into the dataset to determine the accuracy of

classifying the sample into the correct group. In order to identify the accuracy of cross-validated DFA scores and ensure that they are not a result of over-fitting, DFAs are run on random groups within the dataset (Kovarovic et al. 2011).This randomization of data was performed independent of the leave-one-out cross-validated DFAs during analysis and the results of these randomizations will identify the percentage resulting from chance groupings within the data. For example, if a dataset is randomly divided into two groups and a cross-validated DFA finds an accuracy of 47.5%, this would be considered the percentage related to chance groupings, and results with the targeted groups would need to be higher than this number to be considered viable groupings (Kovarovic et al. 2011).

**4.3.10) Regression Analysis:**

Regression analyses explore the relationship between an independent variable and a dependent variable. There must be an assumption of a causal relationship between the variables (VanPool & Leonard 2011), and a significant regression analysis can provide a basis to argue for a causal relationship between the two variables. In geometric morphometrics, regression analyses can explore shape variables which may be attributable to allometry, age, and size differences (Zelditch et al. 2004). Procrustes data can be regressed on log centroid size and the residuals can be used in further analyses in order to explore shape independent of allometry, as in Manuscript 3 (Sidlauskas et al. 2011).

**4.3.11) Correlation Analysis:**

Correlation analysis explores the relationship between two dependent variables to determine if one variable is correlated, negatively or positively, with the other variable. A causal relationship is not assumed, however, there should be a reason to suspect that the two

dependent variables may correlate, such as both variables being at least partially controlled by the same independent variables (e.g. environment, diet, genetic predisposition) (Van Pool & Leonard 2011). Correlation analyses were performed on interlandmark distances in Manuscript 1.

**4.3.12) Inferential Statistics:**

Inferential statistics can be performed on the linear data, such as PC scores or centroid size, obtained from the tangent of Kendall's shape space. These tests will determine statistical significance of group difference within the samples. The confidence level for all tests run in this study is at the 95% level, where a p-value of less than 0.05 is considered to be statistically significant. The following statistical tests were performed in SPSS© (Microsoft Corporation) and were used in all Manuscripts.

Hotelling's $T^2$ tests analyses the differences between the means of two groups, for example, the difference in centroid size for males and females of a sample. The test assumes the data is normally distributed and has homogenous variance (Dytham 2003). The Hotelling's $T^2$ test is a multivariate generalization of the student *t* test (Hotelling 1931) and determines the probability of the difference between group means being a factor of random sampling or a statistically significant difference (Legendre and Legendre 1998).

ANOVAs (*analysis of variance*) compare the within-group variance compared to the variance between groups, and can be used to test the difference in variation between multiple groups (Legendre and Legendre 1998). ANOVAs were performed when the difference in a variable, such as centroid size, was analysed between three or more groups. The test used in ANOVA is the *F* test, which determines the probability of the *F*-ratio (experimental variation

divided by variation due to error) between groups being due to random variation or that there is a statistically significant difference (Legendre and Legendre 1998).

MANOVAs (*multivariate analysis of variance*) were performed to compare the difference of multivariate data, such as shape, between groups. The Wilks-Lambda (λ) is the statistical test commonly used in MANOVA which determines the probability of the between group differences in multivariate data being due to random sampling or that it is a statistically significant difference (Legendre and Legendre 1998).

### 4.3.13) Intra-Observer Error:

In all four manuscripts, intra-observer error was calculated by comparing the largest Procrustes distance between repeated observations with the smallest Procrustes distance between the other observations. If the largest distance between repeated observations were two to three times smaller than the smallest Procrustes distance between other observations, the amount of error would not affect group classification or statistical analyses (Neubauer et al 2009; Neubauer et al 2010; Lieberman et al 2007; Bienvenu 2011).

### 4.3.14) Microscribe Error:

Two different Microscribe digitisers were used to collect data for the analysis of osteoarthritis (Manuscript 3). There are three different Microscribes in the bioinformatics laboratory at Durham University and for simplicity they will be labeled as such: M1 – large fixed Microscribe, M2- medium portable Microscribe, M3- small portable Microscribe. M1 was used to digitize the collections at Durham University, and M2 was used at the University of Bradford. During analysis of the data, it was recognized that the main shape variance along

PC1 for all three joints analyzed (distal femora, distal humerus, proximal ulna) separated the populations digitised at Durham University and the University of Bradford. The distribution of joints along PC1 was normally distributed and appears to represent possible population differences within the data (Figure 4.13). The data collection for the Durham samples occurred over two different time periods separated by the trip to Bradford. This fact suggested that the shape differences along PC1 were biologically valid, as intra-observer error would have been associated with the time periods of data collection (i.e. the second collection session at Durham University would have overlapped with the collection from University of Bradford). However, the strength of the distinction between these genetically close populations, with a cross-validated DFA result ranging from 91-96% accuracy of correctly classifying joints from Durham or Bradford, was suspicious and an error test to determine the reliability of this finding was undertaken.

The skeletal collection of Fishergate House, York, is curated in the Department of Archaeology at Durham University and was originally digitised with M1. Eight distal femora from this collection were re-digitised with the three Microscribes available in the Durham morphometrics lab, including the original Microscribe (M1), and the one used during the Bradford data collection (M2). When these repeated observations are included in the original dataset, they all group with the femora from the Bradford collections and not with the Fishergate individuals originally digitised (Figure 4.13). These data indicate that the variance along PC1 is an artefact of error and does not represent a biological difference between the skeletal populations.

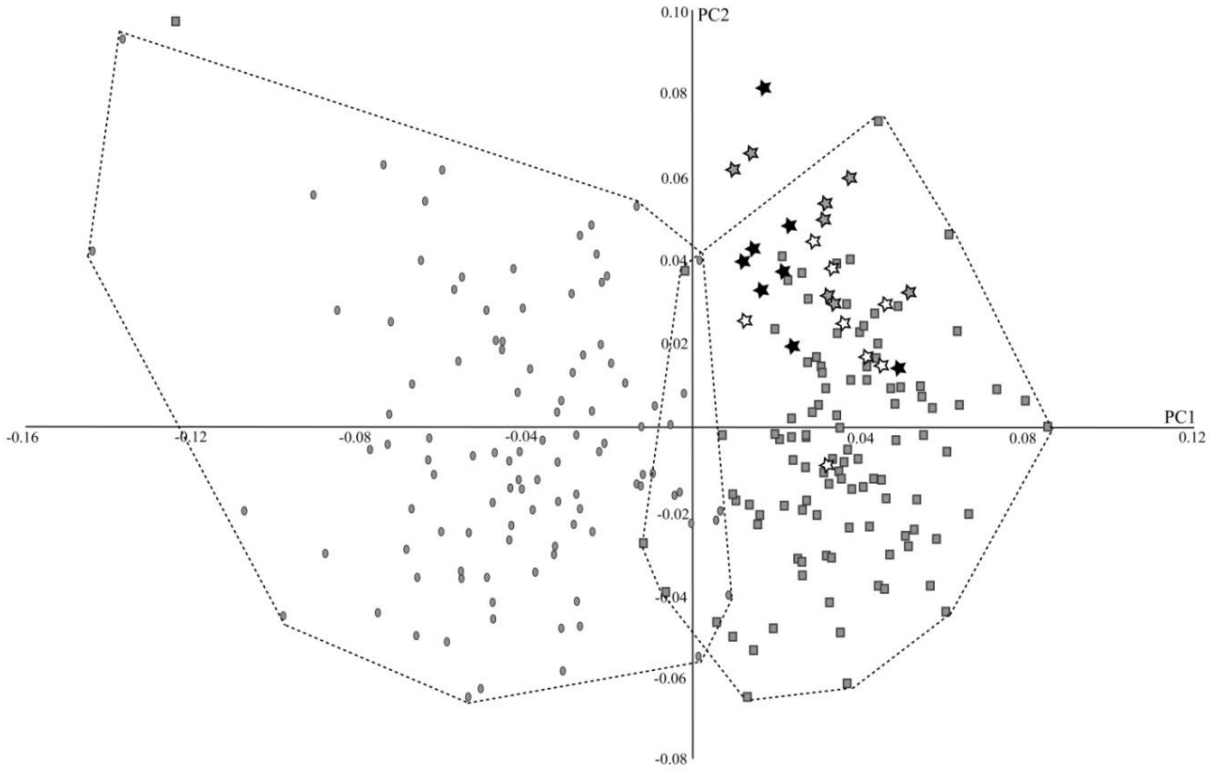


Figure 4.13) PCA chart illustrating variance in the distal femoral joint of all skeletal populations. A similar pattern was apparent for the distal humerus and proximal ulna. The grey circles on the left of PC1 represent those individuals digitised at Durham University with M1 and the squares on the right represent those digitised at the University of Bradford with M2. The stars represent the repeated digitization of the Fishergate House femora with all three Microscribes. Note how they overlap within the variation of the femora digitised with M2 and not with the other Fishergate individuals originally digitised with M1.

After careful consideration of the data, it is concluded that the most likely explanation for this error is related to an internal calibration error between Microscribes. The variance produced by this error is systematic and normally distributed, and intra-observer error would be unlikely to repeatedly produce systematic shape variance, especially over two different time periods. Unfortunately, the error test was unable to reproduce this artefact which suggests that the calibration error is not persistent. This would be a fortunate finding in that M1 is still able to accurately obtain data, but it also indicates that any future data collected with M1 should be scrutinized throughout collection, as this error could occur without being obvious. This finding resulted in a substantial decrease in the sample size available for analysis in Manuscript 3. Regression analyses were considered to remove the error from the data, however, it was decided that the data would be more reliable if only the landmarks from M2 were used.

Figure 4.14 illustrates the PCA chart of the eight femora repeats. The main shape variance is explained by individual variation. PC2 appears to be explained by error, likely by intra-observer error but also Microscribe error. The clear squares, representing those joints digitised with M1, all score more negatively on PC2 than the same joint digitised with the other two Microscribes. This indicates that the error which is attributable to the M1 is systematic, as it results in similar shape differences along PC2. The circles, representing M2 and M3, appear to have overlap and do not always separate in the same pattern, with clear circles sometimes sitting higher on PC2 than filled, and vice versa.

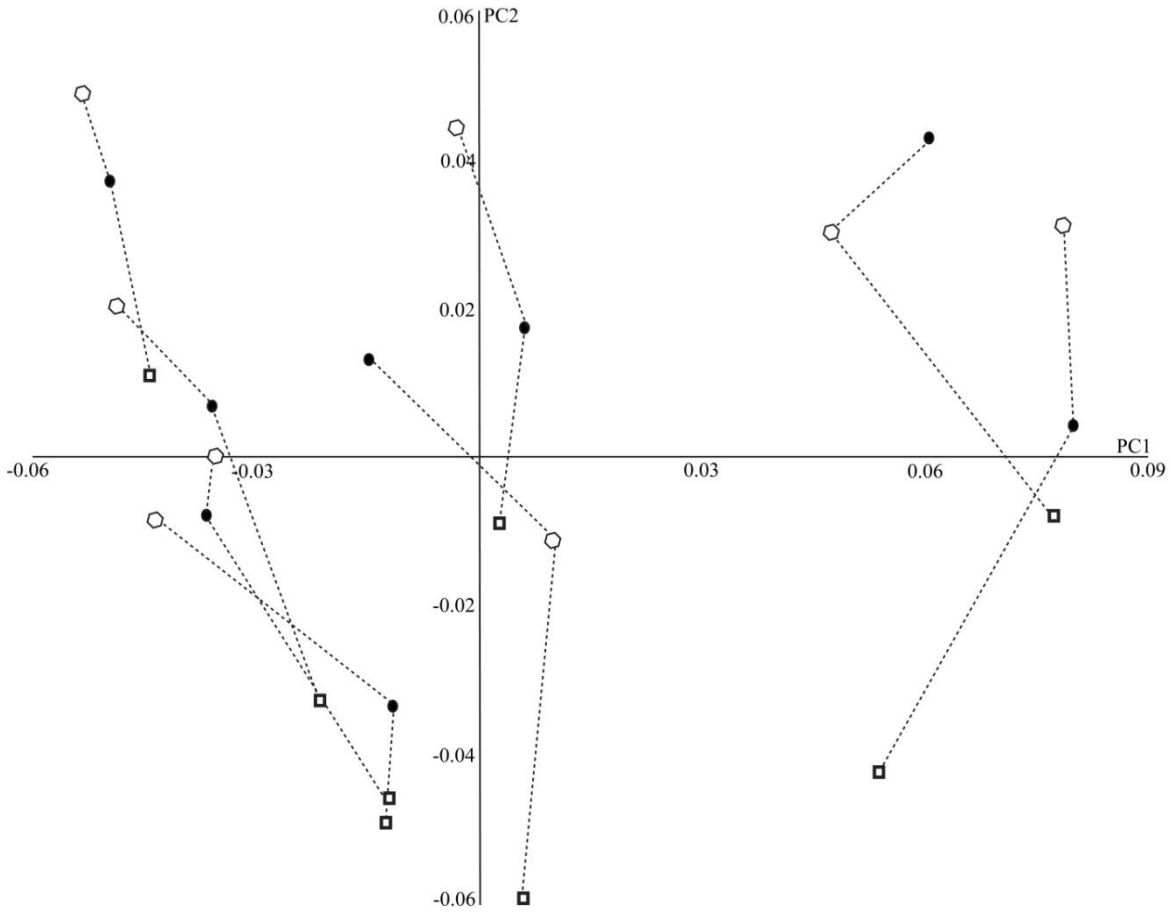


Figure 4.14) PCA chart illustrating the shape variance of eight repeatededly analysed femora with three different Microscribes. The clear squares represent the femora digitised with M1; the clear circles represent the femora digitised with M2, and the filled circles, M3. Note how the clear squares all sit below the circles for each femoral group, indicating that there is a systematic difference is shape related to use of M1.

A single femur was also digitised 10 times with all three Microscribes in order to determine the extent of the difference between each Microscribe. Figure 4.15 illustrates the variance in these data, which indicates that M1 (open squares) separates from the other two Microscribes on PC1. M2 and M3 have some overlap on PC1, but M3 is fully separated.

Although it is expected that there would be some difference between Microscribes when a single joint is digitised 10 times, the variance illustrated indicates that Microscribe error is a stronger factor influencing the data than intra-observer error. These data were taken after the internal calibration error was rectified, and this amount of error would be unlikely to be identified in a larger sample of individuals.

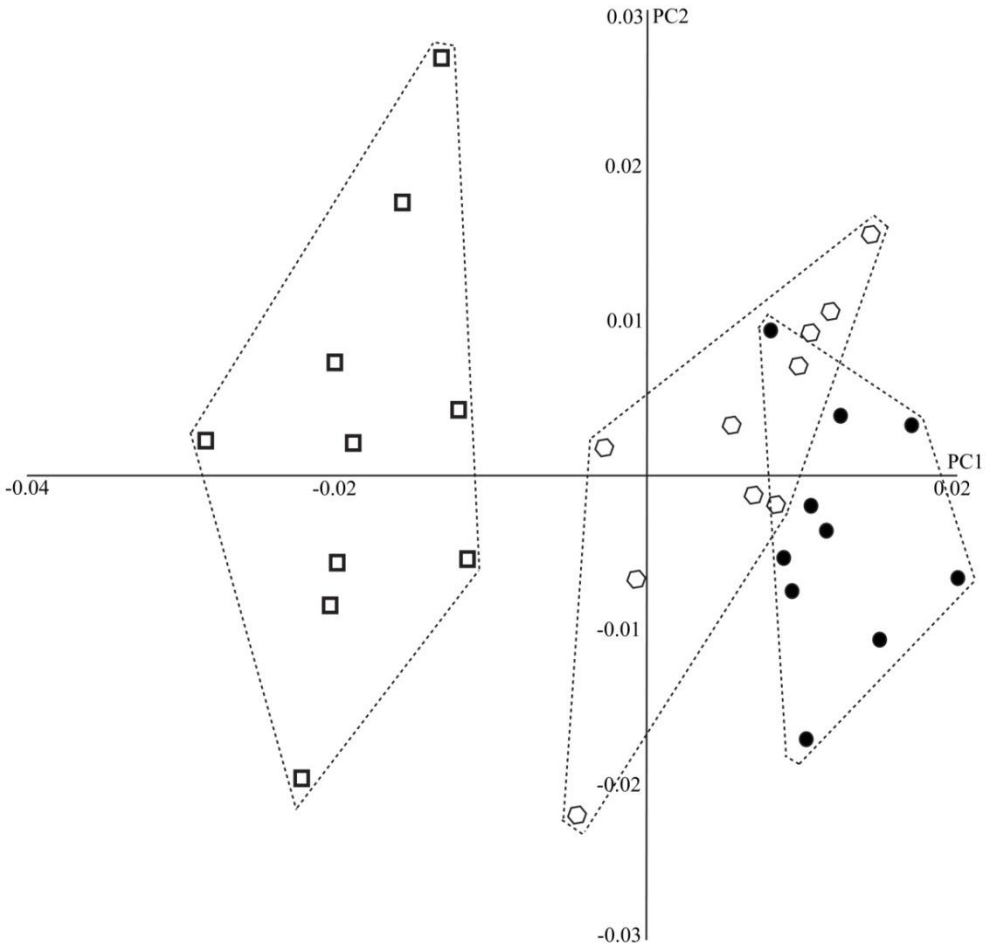


Figure 4.15) PCA chart illustrating the shape variance of a single femur measured 10 times with each Microscribe (M1, M2, and M3). The clear squares represent the femur digitised with M1; the clear circles represent the femur digitised with M2, and the filled circles, M3. Note how the group associated with M1 separate on PC1 from the other two groups.

As the distal femoral joint includes many Type II and Type III landmarks, the Microscribe error was further investigated with more reliable and homologous Type I facial landmarks (section 4.3.2, Figure 4.9, and Table 4.11). Figure 4.16 illustrates the shape variance of ten individuals, indicated by dashed outlines. The main shape variance is related to individual variation and Microscribe error does not appear to affect the data. This suggests that when Type I landmarks are used, the data is reliable and accurate, whereas when the dataset includes many Type II and Type III landmarks, both intra-observer error and mircoscribe error may be exacerbated.

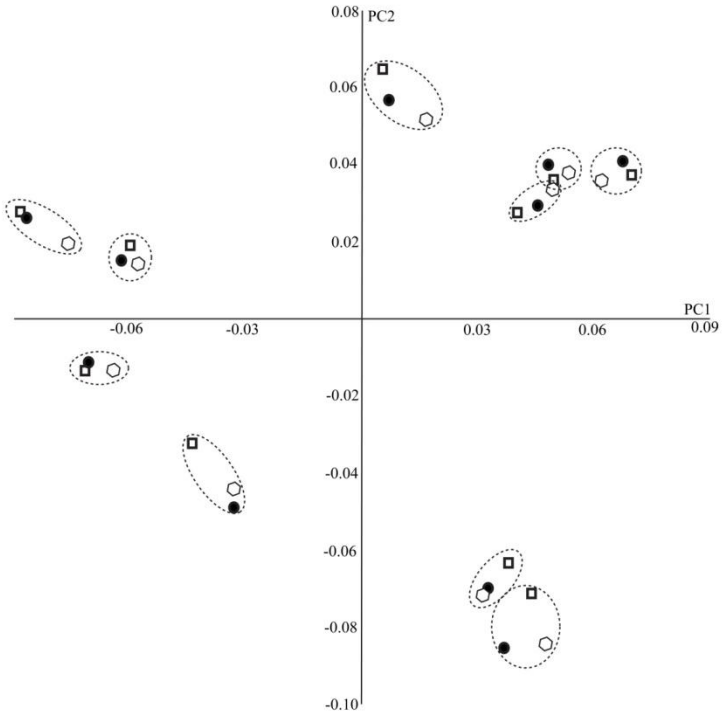


Figure 4.16) PCA chart illustrating the shape variance of Type I facial landmarks for 10 individuals with three Microscribes. The clear squares represent the femora digitised with M1; the clear circles represent the femora digitised with M2, and the filled circles, M3. Each individual is represented by a clear square, clear circle and a filled circle outlined with dashed line.

The following chapters, 5 through 8, are individual manuscripts as outlined above, each of which is intended for publication in peer-reviewed research journals. Therefore, each manuscript is organized to have its own introduction, materials and methods, and discussion within the manuscript. Final discussion and conclusion chapters are also included at the end of the thesis in order to review the main points and overall findings of the research project, and exemplify how each manuscript contributes to the thesis title of ‘Quantifying Palaeopathology Using Geometric Morphometrics”.

# Chapter 5) Manuscript 1

American Journal of Physical Anthropology 2012 129(4): 572-582

## Vertebral Morphology Influences the Development of Schmorl's Nodes in the Lower Thoracic Vertebrae

K.A.Plomp[1,2*]

C.A. Roberts[2]

U. Strand Viðarsdóttir[1]

1) Evolutionary Anthropology Research Group, Department of Anthropology, Durham University, Dawson Building, South Road, Durham DH1 3LE, England
2) Department of Archaeology, Durham University, Dawson Building, South Road, Durham DH1 3LE, England

*** Corresponding author**: **k.a.plomp@durham.ac.uk ph: (44) 7532140689**

Schmorl's nodes are the result of herniations of the nucleus pulposus into the adjacent vertebral body and are commonly identified in both clinical and archaeological contexts. The current study aims to identify aspects of vertebral shape that correlate with Schmorl's nodes. Two-dimensional statistical shape analysis was performed on digital images of the lower thoracic spine (T10–T12) of adult skeletons from the late medieval skeletal assemblages from Fishergate House, York, St. Mary Graces and East Smithfield Black Death cemeteries, London, and postmedieval Chelsea Old Church, London. Schmorl's nodes were scored on the basis of their location, depth, and size. Results indicate that there is a correlation between the shape of the posterior margin of the vertebral body and pedicles and the presence of Schmorl's nodes in the lower thoracic spine. The size of the vertebral body in males was also found to correlate with the lesions. Vertebral shape differences associated with the macroscopic characteristics of Schmorl's nodes, indicating severity of the lesion, were also analyzed. The shape of the pedicles and the posterior margin of the vertebral body, along with a larger vertebral body size in males, have a strong association with both the presence and severity of Schmorl's nodes. This suggests that shape and/or size of these vertebral components are predisposing to, or resulting in, vertically directed disc herniation. Am J Phys Anthropol 149(4): 572-582. 2012 Wiley Periodicals, Inc.

**Keywords:** Disc herniation, Spinal disease, Palaeopathology, Shape Analysis, Neural foramen, Pedicles, Vertebral body

**Introduction:**

Schmorl's nodes are depressions on the inferior and/or superior surface of the vertebral body caused by vertical herniation of the nucleus pulposus through a weakened annulus fibrosus (Figure 1) (Schmorl & Junghans 1971; Faccia & Williams 2008). The lesions are commonly seen in the lower thoracic and lumbar spine, possibly resulting from biomechanical strain on these vertebrae when transmitting compressive and shearing forces from the upper to the lower body during daily activities (Cholewicki & McGill 1996). Other factors suggested to be aetiologically significant to Schmorl's nodes in the clinical literature are metabolic deficiencies, increased body weight, and a genetic predisposition (Williams et al. 2007; Zhang et al. 2010; Dar et al. 2010). The association of back pain with Schmorl's nodes is unclear, with some studies finding a positive association and others finding the condition to be asymptomatic (Faccia & Williams 2008; Hamanishi et al. 1994; Fukuta et al. 2009; Takahashi et al. 1995; Peng et al. 2003; Fahey et al. 1998).

Variability in the size and form (shape + size) of the spinal canal, or neural foramen, and the vertebral body has been the subject of many clinical and palaeopathological studies, as it has been associated with conditions such as acquired and developmental spinal stenosis, scoliosis, and spondylolysis (clinical literature: Inufusa et al. 1996; Masharawi 2012; Masharawi et al. 2008; Meijer et al. 2010; Abbas et al. 2010; Harrington et al. 2001; palaeopathological literature: Watts 2010; Clark et al. 1986). Schmorl's nodes are a relatively common spinal pathology in both clinical and archaeological contexts (clinical literature: Dar et al. 2009; Overvliet et al. 2009; Jang et al. 2010; palaeopathological literature: Üstündağ 2009; Klaus et al. 2009; Slaus 2000). Clinically, herniation of the intervertebral disc shows little correlation with a patient's age, but discs with adjacent Schmorl's nodes can display degenerative changes earlier than those without (Adams et al. 2000). Palaeopathological

studies also find no correlation between age at death and Schmorl's nodes (Üstündağ 2009; Klaus et al. 2009; Slaus 2000). However, the nucleus pulposus becomes increasingly dehydrated with age, decreasing the amount of hydrostatic pressure within the disc (Dar et al. 2009; Ferguson & Steffen 2003; Vernon-Roberts 1989). This suggests that disc herniation is more likely to occur during spinal maturation when the disc is fully hydrated (Dar et al. 2009; Vernon-Roberts 1989).

Dar et al. (2009) performed an analysis of Schmorl's nodes in the spines of 240 adult skeletons from the documented Hamann-Todd Skeletal Collection, Cleveland Museum of Natural History, Ohio, USA and found a prevalence rate of 48.3% of individuals with at least one node present in the spine. They found no strong correlation with trauma, physical stress or metabolic deficiencies, but Schmorl's nodes were more common in males than females (54.2% vs. 43.0%), with males on average also showing a higher number of lesions (69.3% vs. 30.4%). Ethnic origin also appeared to influence the frequency of the lesion, with Schmorl's nodes being more frequent in European than African Americans (60.3% vs. 36.7%). The results suggest a genetic or environmental aetiology, with ethnicity and sex being the main factors affecting the development of Schmorl's nodes (Dar et al. 2009).

Prevalence rates for Schmorl's nodes in both archaeological and living populations have been reported to be between 5-76%, based on the presence of at least one node on the spine (clinical literature: Dar et al. 2009; Pfirrmann & Resnick 2001; Mok et al. 2010; palaeopathological literature: Üstündağ 2009; Novak & Slaus 2011). The variation in reported prevalence rates likely represents differing recording and diagnostic techniques employed, and criteria used to define a Schmorl's node in both clinical and archaeological contexts (e.g. diagnoses based on plain film radiography, computed tomography scans, and magnetic

resonance imaging in clinical diagnosis and, macroscopic diagnosis in dry bone - Silberstein et al. 1999).

The aetiology of intervertebral disc herniation resulting in Schmorl's nodes is poorly understood in both clinical and archaeological situations. Schmorl's nodes have often been used, with varying confidence, to indicate levels of physical stress and activity in palaeopathological studies (Novak & Slaus 2011; Klaus et al. 2009; Slaus 2000; Papathanasiou 2005; Robb et al 2001; Alesan et al. 1999). Although intervertebral disc herniations have been associated with flexion and extension of the spine during loading (Callaghan & McGill 2001; Goto et al. 2002), there are also suggestions of a genetic or congenital component in the development of Schmorl's nodes (Dar et al. 2009; Williams et al. 2007). This paper aims to identify correlations between vertebral shape and the presence of Schmorl's nodes, as vertebral morphology may be a developmental factor influencing the condition. While it has been shown that the size and form (shape + size) of the lower lumbar vertebral body correlates with disc herniation (Harrington et al. 2001), this study aims to determine if the shape and size of the vertebral body and neural foramen, and the shape of the superior articular facets and pedicles correlates with the presence and apparent severity of Schmorl's nodes in the lower thoracic spine. The null hypothesis is that there is no correlation between specific parameters for these features of the lower thoracic vertebrae and herniation of the intervertebral disc into the vertebral body; if this hypothesis is rejected, the results could indicate a specific vertebral shape and size which can predispose an individual to Schmorl's nodes in the lower thoracic spine.

**Materials:**

The skeletal sample analyzed derives from four English skeletal populations. The tenth, eleventh, and twelfth thoracic vertebrae from 135 adult individuals were the subject of analysis (Table 1), or a total of 322 vertebrae (Table 2). The lower three thoracic vertebrae (T10-T12) were chosen because Schmorl's nodes are commonly seen in this spinal segment (Dar et al. 2010; Faccia & Williams 2008). Vertebrae with and without Schmorl's nodes were analyzed so that differences between the shape and/or size of the body, pedicles, superior articular facets and neural foramen could be objectively compared. The skeletons from three sites are dated to the late medieval period ($12^{th}$- $16^{th}$ C AD), while one is post-medieval ($16^{th}$–$19^{th}$ C AD). Of these sites, three were from London and one was from York, England. As all the individuals were from England, the influence of ancestry on spinal morphology was minimized. The skeletal assemblages were chosen to provide a varied sample of individuals of both sexes and all adult age ranges from more than one population to allow a comprehensive analysis of factors which could contribute to vertebral shape. Age and sex information was accessed from site reports (Cowie et al. 2008; Grainger et al.2008; Grainger & Phillpotts 2011; Holst 2005) which had all employed standard osteological methods for sexing and ageing adult skeletons (Phenice 1969; Brothwell 1981; Bass 1987; Lovejoy et al. 1985; Işcan et al. 1984,1985; Brooks & Suchley 1990; Buikstra & Ubelaker 1994).

Table 1) Number of individuals analyzed for each skeletal collection, with number of males and females (U=unkown), and number of vertebrae of each vertebral segment summarized.

| Collection | Period | Reference | ♀ | ♂ | U | T10 | T11 | T12 | Individuals |
|---|---|---|---|---|---|---|---|---|---|
| **Chelsea Old Church, London** | Post-Medieval (1712-1842 AD) | Cowie *et al.* 2008 | 34 | 45 | 5 | 69 | 78 | 73 | 84 |
| **East Smithfields Black Death, London** | Medieval (1348-1350 AD) | Grainger *et al.* 2008 | 1 | 20 | 0 | 15 | 20 | 17 | 21 |
| **St. Mary Graces, London** | Medieval (1350-1540 AD) | Grainger & Phillpotts 2011 | 3 | 7 | 2 | 11 | 10 | 9 | 12 |
| **Fishergate House, York** | Medieval ($12^{th}$-$16^{th}$ C AD) | Holst 2005 | 7 | 11 | 0 | 0 | 13 | 14 | 18 |

Table 2) Number of vertebrae analyzed by sex, age and severity of Schmorl's nodes. Age groups are: young adults (18-25 years), middle adults (26-45years), and old adults (46+years) (U=unknown). The "Health" of vertebrae is scored according to Knüsel et al. (1997).

| | Sex | | | Age | | | | Health | | | Total |
|---|---|---|---|---|---|---|---|---|---|---|---|
| | ♀ | ♂ | U | Young | Middle | Old | U | Healthy | Stage 1 | Stage 2 | Vertebrae |
| **T10** | 31 | 56 | 6 | 7 | 43 | 39 | 5 | 67 | 16 | 11 | 93 |
| **T11** | 37 | 70 | 8 | 8 | 52 | 48 | 7 | 81 | 15 | 19 | 115 |
| **T12** | 67 | 41 | 5 | 9 | 51 | 49 | 4 | 53 | 32 | 28 | 113 |
| **Total** | 135 | 167 | 23 | 24 | 146 | 136 | 16 | 201 | 63 | 58 | 322 |

## Methods:

Schmorl's nodes were recorded on both the inferior and superior surfaces of the vertebral bodies and macroscopically scored based on Knüsel et al. (1997) into three groups: healthy vertebrae have no sign of Schmorl's nodes, Stage 1 lesions are less than 2mm in depth and cover less than half of the antero-posterior length of the body, and Stage 2 lesions are equal to or exceed these parameters in depth or length. Vertebrae were included in the pathological group based on the most severe lesion present. Figure 1 illustrates examples of stage 1 and stage 2 lesions. Intra-observer error was determined by KAP with 11 vertebrae scored 3 times and was found to be minimal (kappa 0.83).

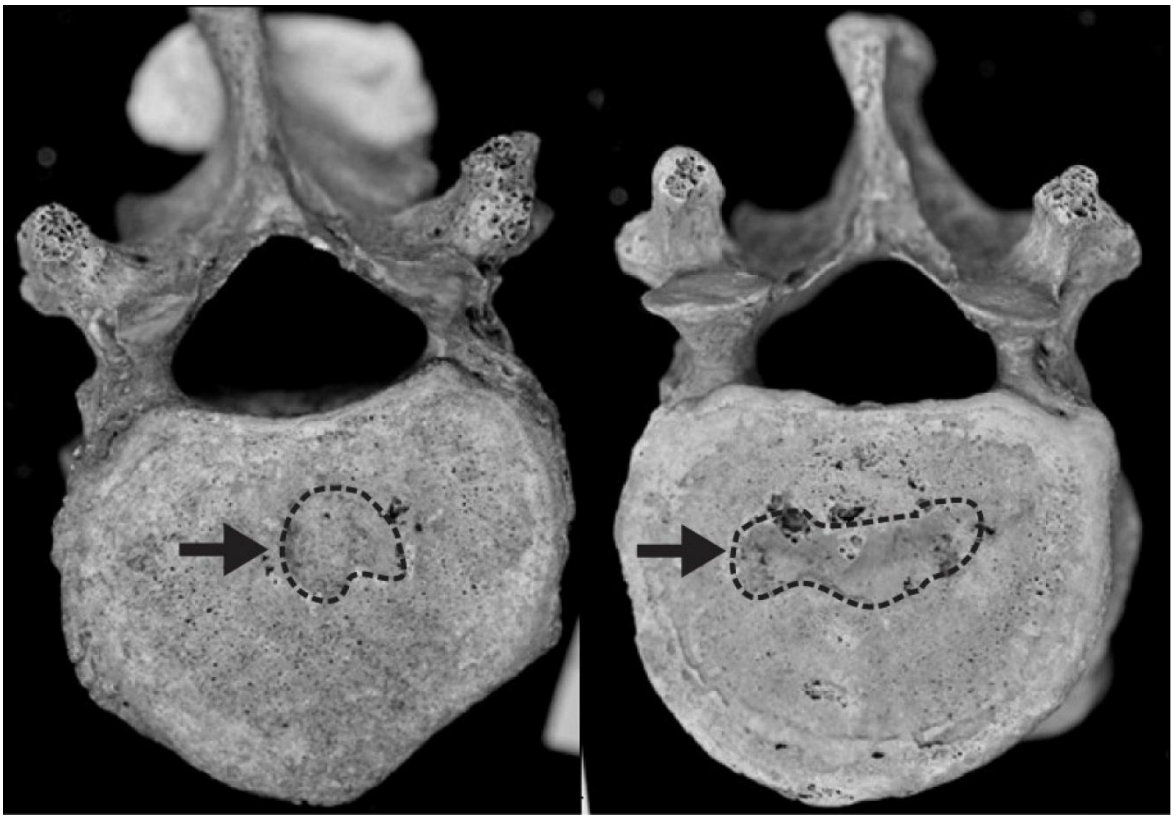

Figure 1) Left: Stage 1 Schmorl's node on T12. Right: Stage 2 Schmorl's node on T12.

The study used geometric morphometrics to quantify and compare vertebral shape and size (O'Higgins 2000). Digital images were taken of each vertebra and landmarks digitized on the superior aspect using TPSdig© software (Rohlf 2004). Twenty-one landmarks were chosen to cover the margin of the vertebral body, the neural canal, pedicles, and superior articular facets (Figure 2). Sliding semi-landmarks, which lack homology, were placed evenly along the margin of the vertebral body (Bookstein 1997). Variations in these landmark groupings were analyzed to find any correlation between vertebral shape and the presence and severity of Schmorl's nodes. The sample size varies with each landmark grouping depending

on archaeological preservation of individual vertebrae and the subsequent presence of landmarks.

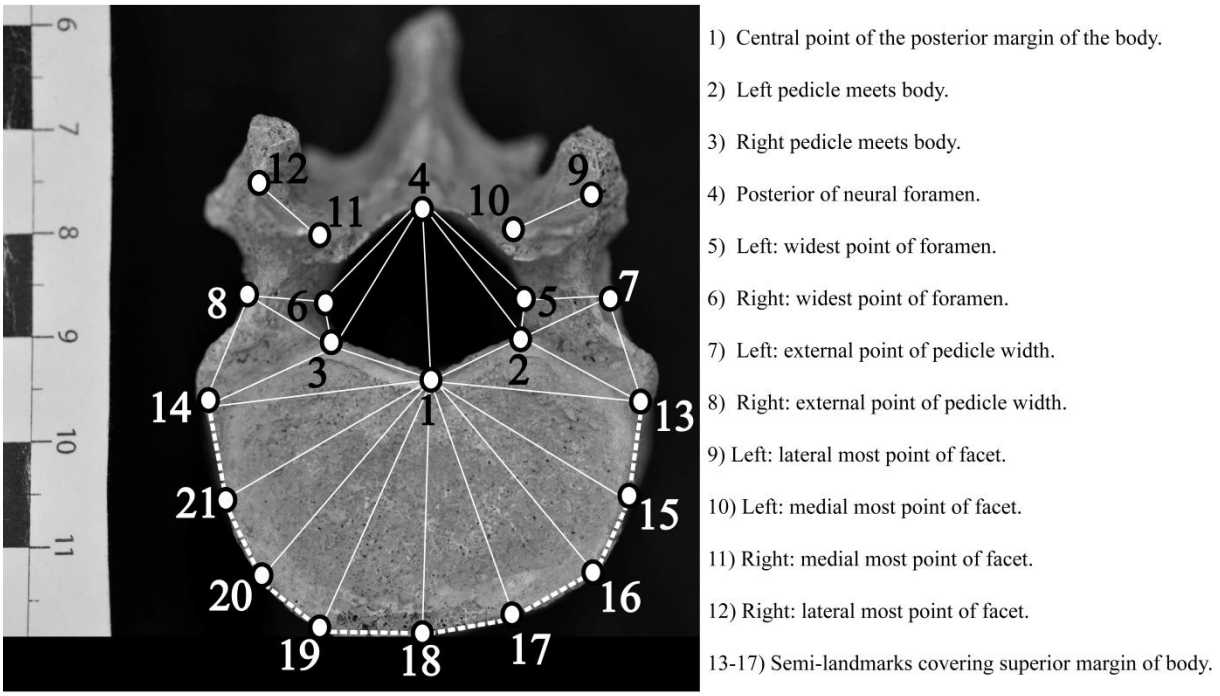


Figure 2) Location and description of the 21 landmarks digitized on the body and posterior elements of the T10, T11 and T12 vertebrae.

Statistical analyses were run in Morphologika© (O'Higgins & Jones 2006), R (R Development Core Team 2010), and SPSS® 16.0 (Inc., Chicago IL). Generalized procrustes analysis (GPA) was performed to standardise the size of the landmark configurations and remove rotational and translational variation. Semi-landmarks were slid along the tangent plane to minimize bending energy of deformation in order to minimize the shape differences related to spacing of landmarks on a curve (Bookstein 1997). Subsequent analysis was performed on these superimposed data (Slice 2007; Rohlf 2003; Goodall 1991; Bookstein

1997; Rohlf & Slice 1990). Principal components analysis (PCA) was used to explore the shape variation occurring in the sample. In order to reduce noise on higher principal components, only those representing more than five percent of the total shape variance were subject to further statistical analyses (Zelditch et al. 2004; O'Higgins & Jones 1998; Stevens & Strand Viðarsdóttir 2008; Mitteroeker & Gunz 2009). Discriminant function analysis with cross-validation (DFA) was used to determine the accuracy of discrimination between groups within the sample based on shape variables, and validated with 100 permutations (Klingenberg 2011; White & Ruttenberg 2007; Cardini et al. 2009; Kimmerle et al. 2008). MANOVAs, ANOVAs, and Hotelling $T^2$ tests were used to determine statistical significance of group differences, with the level of significance at $p=0.05$. Centroid size, the square root of the sum of the squared distances of each landmark from the centroid of the landmark configuration, was used as the measure of size, as it is mathematically defined and does not introduce bias into the analysis (Zelditch et al. 2004). Inter-landmark distances were measured and analyzed for metrical differences between groups. Intra-observer error was assessed following the example by Neubauer et al (2009) by comparing the greatest Procrustes distance between 10 repeated observations and the smallest distance between other vertebrae; the smallest distance between different vertebrae was close to twice the greatest distance between the repeated observations, indicating that intra-observer error was unlikely to affect group classification (Neubauer et al 2009; Neubauer et al 2010; Lieberman et al 2007; Bienvenu 2011).

**Results:**

Initially, all 21 landmarks were analyzed for each vertebral segment. The shape of the superior intervertebral articular facets (landmarks 9-12) was highly variable and was not associated with the presence of Schmorl's nodes; these landmarks were therefore removed

from the dataset during further analysis to reduce the amount of noise caused by shape variation unrelated to the lesions. Non-pathological factors affecting vertebral shape were analyzed to determine shape variance of the sample. Age was found to not be correlated with vertebral morphology. There was little difference in the frequency of Schmorl's nodes between skeletal samples, with late medieval Fishergate House, York, having a frequency of 58.8% individuals affected, the two late medieval London populations 62.9%, and the post-medieval London population (Chelsea Old Church) having a frequency of 55.8%. As mentioned above, Schmorl's nodes were recorded on both the inferior and superior surfaces of the vertebral body, and vertebrae were included in the pathological group based on the most severe lesion present. Stage 2 vertebrae had lesions more frequently on both surfaces than did Stage 1. There was no distinction between vertebral shapes, based on the 17 remaining landmarks, associated with different lesion location, except the shape associated with the severity of the lesions discussed below. Males showed a higher frequency of Schmorl's nodes, with 70.1% of males and 34.1% of females displaying at least one lesion.

Sexual dimorphism influences the size of the vertebral body, with males showing a significantly larger centroid size for the body than females ($p<.001$). On average, vertebrae with Schmorl's nodes had larger vertebral bodies than healthy vertebrae in both males and females, although the difference was only statistically significant in males ($p<0.01$); it is possible that these results could be influenced by the smaller sample of affected vertebrae in females. In both males and females, the average centroid size of the body for vertebrae with Stage 2 Schmorl's nodes was larger than those with Stage 1 lesions, and Stage 1 lesion vertebrae were, on average, larger than healthy vertebrae, but again the only significant difference in centroid size of the vertebral body was recorded between pathological and

healthy vertebrae in males. Variability in shape (17 landmarks) was examined using GPA, PCA and DFA, with cross-validated DFA distinguishing the sexes at 75.9% accuracy based on shape variables for the first 5 PCs. Males and females were analyzed separately and the results of MANOVAs on all 3 groups are summarized in Table 3. Males show significant differences on both T10 ($\lambda$ 0.515, $p<0.05$) and T11 ($\lambda$ 0.517, $p<0.01$) between affected and healthy vertebrae on PC1 ($p<0.01$), but for T12 the only significant difference is on PC3. For females, the significant differences occur on high PCs; this could be due to the small sample size of affected vertebrae in females, or it could indicate that there is a large amount of shape variability occurring in this landmark configuration unrelated to the lesions. The shape differences in vertebrae from both sexes associated with the presence and severity of Schmorl's nodes were concentrated in the morphology of the neural foramina and pedicles.

Males and females show similar shape differences between groups (Figure S1 & S2), and therefore, affected and healthy vertebrae, and all three stages, were compared with the sexes pooled. The cross-validated DFA scores for the first 5 PCs summarized in Table 4. The main shape difference on the vertebral body between healthy and affected vertebrae is a relative posterior translation of the posterior margin of the vertebral body. The bodies of affected vertebrae had a relatively more circular shape while the healthy bodies had an almost heart shape appearance; this was most apparent in T12 (Figure 4). Figures 3a-c display PCA charts distinguishing the healthy and the two pathological groups (Stage 1 and Stage 2) for each vertebra with sexes pooled.

Table 3) Summary of statistical values for comparisons of healthy, Stage 1, and Stage 2 vertebrae for both sexes. MANOVAs were performed for comparisons of shape, with Wilks' lambda (λ), F ratio, and p-value reported. ANOVAs were performed for comparisons of centroid size, with both F ratio and p-value reported. Significance level was set at p=0.05.

*indicates significant value

| | 17 Landmarks | | Neural Foramen and Pedicles | |
|---|---|---|---|---|
| | **Shape** | **Centroid Size** | **Shape** | **Centroid Size** |
| **Males** | | | | |
| T10 | λ 0.363, F=2.374, p=0.028* PC1 p=0.001* | F=3.556, p=0.049* | λ 0.776, F=1.083, p=0.385 PC2 p=0.008* | F=1.025, p=0.365 |
| T11 | λ 0.355, F=3.396, p=0.002* PC1 p=0.006* | F=3.691, p=0.043* | λ 0.436, F=5.256, p<0.001* PC1 p=0.005*, PC2 p<0.001* | F=0.106, p=0.900 |
| T12 | λ 0.573, F=1.669, p=0.113 PC3 p=0.015* | F=6.492, p=0.005* | λ 0.488, F=3.718, p<0.001* PC2 p<0.001* | F=0.335, p=0.717 |
| **Females** | | | | |
| T10 | λ 0.643, F=0.791, p=0.637 | F=0.776, p=0.388 | λ ,0.542 F=2.081, p=0.041* PC1 p=0.001* | F=0.874, p=0.431 |
| T11 | λ 0.731, F=0.680, p=0.736 | F=2.035, p=0.156 | λ 0.539, F=1.956, p=0.057 PC1 p=0.035* | F=0.418, p=0.660 |
| T12 | λ 0.525 F=1.767, p=0.232 PC5 p=0.045* | F=2.195, p=0.136 | λ 0.457 F=2.105, p=0.044* PC1 p=0.011* | F=0.091, p=0.913 |

Table 4) Percentage of vertebrae (sexes pooled) correctly classified on the basis of a discriminant function analysis with cross-validation, carried out on the first 5 PCs (> 75% of the total shape variation) from analyses of 17 landmarks. The first column includes all three groups – Stage 1, Stage 2, and healthy vertebrae; the second column shows the results of a pair-wise analysis of Stage 2 and healthy vertebrae.

| | All 3 Groups | | | | Stage 2 vs. Healthy | | |
|---|---|---|---|---|---|---|---|
| | **Stage 1** | **Stage 2** | **Healthy** | **Average** | **Stage 2** | **Healthy** | **Average** |
| **T10** | 72.7 % | 38.9 % | 55.6 % | 53.6 % | 81.8 % | 70.4 % | 73.6 % |
| **T11** | 52.5 % | 52.4 % | 55.9 % | 54.5 % | 63.6 % | 85.3 % | 80.0 % |
| **T12** | 61.5 % | 28.6 % | 51.8 % | 45.9 % | 76.9 % | 74.1 % | 75.0 % |

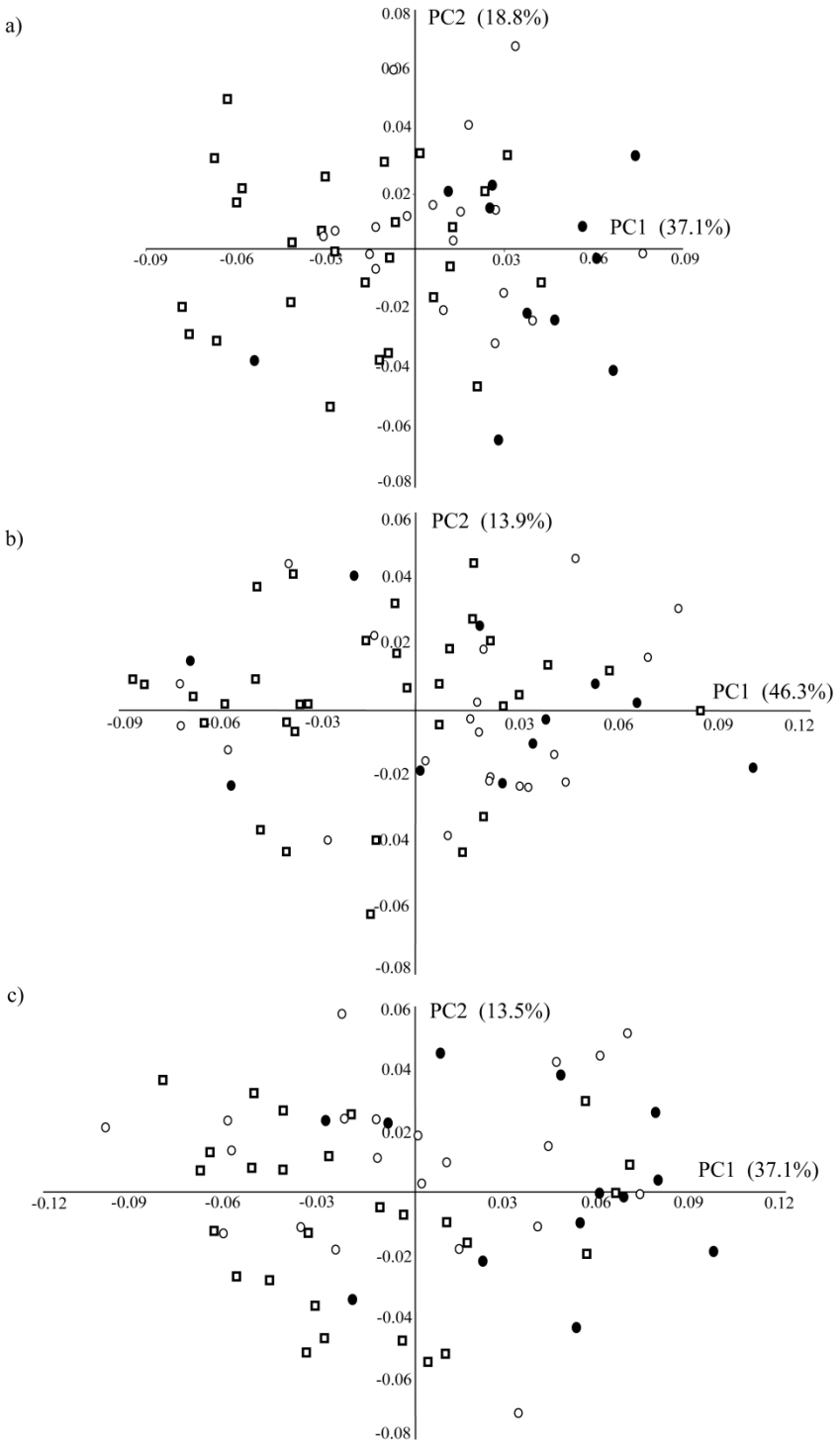


Figure 3) PCA charts showing the pattern of shape variance of 17 landmarks within both sexes on PC1 (x-axis) and PC2 (y-axis) for: (a) T10 (55.9% of the total shape variance), (b) T11 (60.2% of the total shape variance), and (c) T12 (50.6% of the total shape variance). Clear squares represent healthy vertebrae, clear circles are stage 1, and filled circles are stage 2.

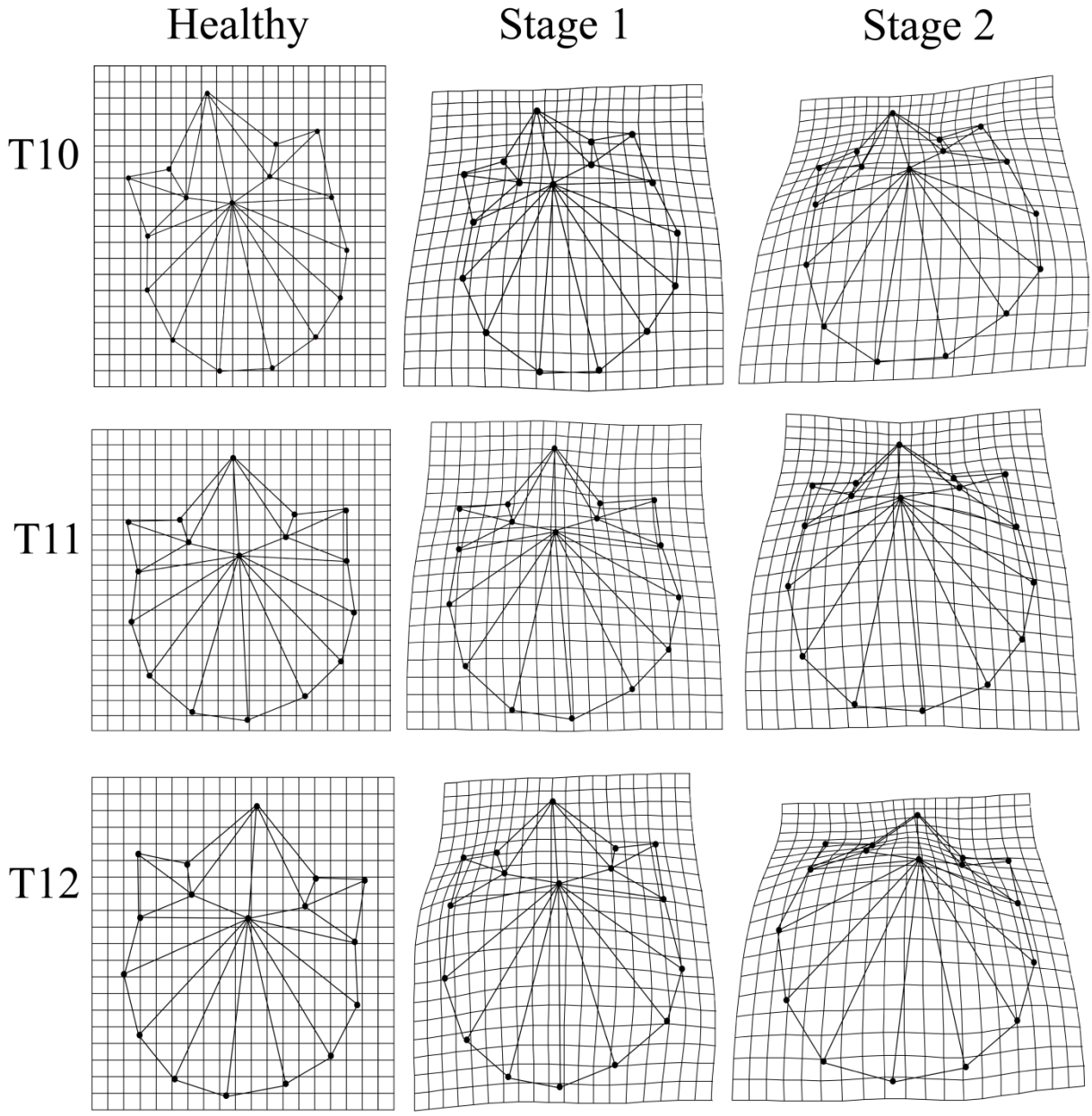


Figure 4) Deformation grids with wireframe illustrations of the mean landmark configuration morphed to represent the shape associated with each pathological group. Deformation grids have been magnified 2x to aid interpretation of shape differences.

The shape of the posterior margin of the vertebral body and pedicles is the most distinguishing feature for the three groups in all vertebrae of both males and females. Males and females show similar shape differences between groups (Figure S3 & S4), therefore the sexes were pooled for the cross-validated DFA scores in Table 5. Figures 5a-c display PCA charts for each vertebra of both males and females, illustrating the shape variance along the first two PCs. With pooled sex, the first 4 PCs gave the greatest discrimination in T12 with an accuracy of correct classification of Stage 2 vertebrae of 91.3% and 93.9% for healthy vertebrae in a pair-wise DFA with cross-validation. When males and females are analyzed together, the shape variables represented by the first 5 PCs are significantly different for all three groups ($p<0.01$), as well as for affected vs. healthy. Pair-wise analysis of the groups found all comparisons to be statistically significant based on the first 5 PCs, except for Stage 1 vs. healthy in T10 vertebrae. Figure 6 illustrates the shape associated with the variance along the first two PCs for all three vertebrae of both males and females. The sexual dimorphism in these 8 landmarks is less than the full 17 landmarks, with a cross-validated DFA finding an accuracy of 65.4% for distinguishing the sexes with the first 5 PCs. When males and females were analyzed separately, the results were significant between affected and healthy vertebrae on PC1. Stage 2 and healthy, in both males and females, were significantly different on PC1 in T11 and T12 ($p<0.01$), but only on PC2 in T10. MANOVAs were also performed on the 3 groups for both sexes, and the results are summarized in Table 3.

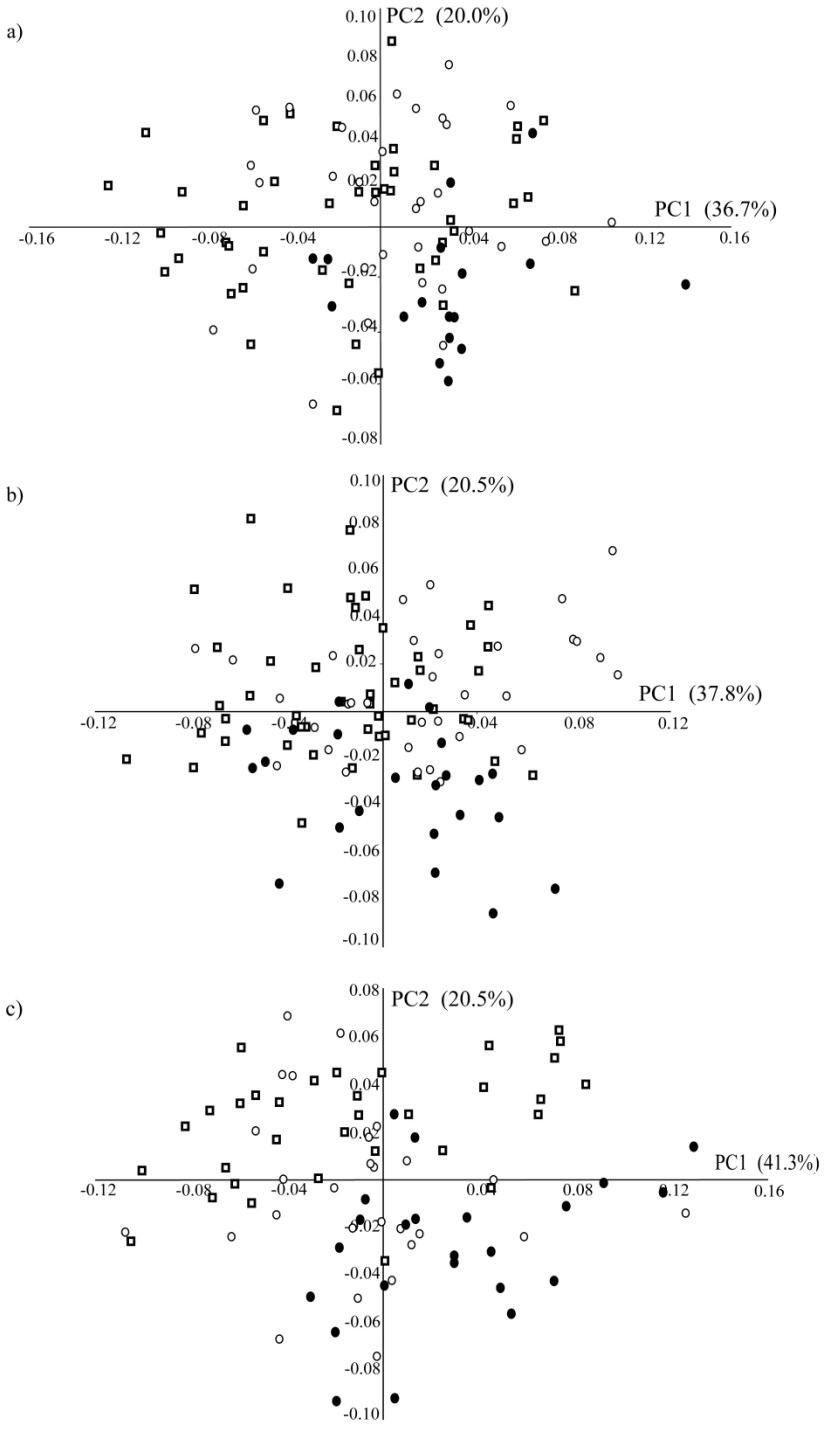


Figure 5) PCA charts showing the pattern of shape variance of 8 landmarks on the neural canal and pedicles within both sexes on PC1 (x-axis) and PC2 (y-axis) for: (a) T10 (56.7% of the total shape variance), (b) T11 (58.3% of the total shape variance), and (c) T12 (61.8% of the total shape variance). Clear squares represent healthy vertebrae, clear circles are stage 1, and filled circles are stage 2.

Table 5) Percentage of vertebrae of pooled sexes correctly classified on the basis of a discriminant function analysis with cross-validation, carried out on the first 5 PCs (> 80% of the total shape variation) from analyses of 8 landmarks on the neural foramen and pedicles. The first column includes all three groups – Stage 1, Stage 2, and healthy vertebrae; the second column shows the results of a pair-wise analysis of Stage 2 and healthy vertebrae.

| | **Stage 1** | **Stage 2** | **Healthy** | **Average** | **Stage 2** | **Healthy** | **Average** |
|---|---|---|---|---|---|---|---|
| **T10** | 37.5 % | 70.6 % | 40.9 % | 45.2 % | 70.6 % | 70.4 % | 70.5 % |
| **T11** | 51.5 % | 69.6 % | 57.4 % | 58.3 % | 73.9 % | 80.8 % | 78.6 % |
| **T12** | 18.5 % | 78.3 % | 75.8 % | 57.8 % | 87.0 % | 93.9 % | 91.1 % |

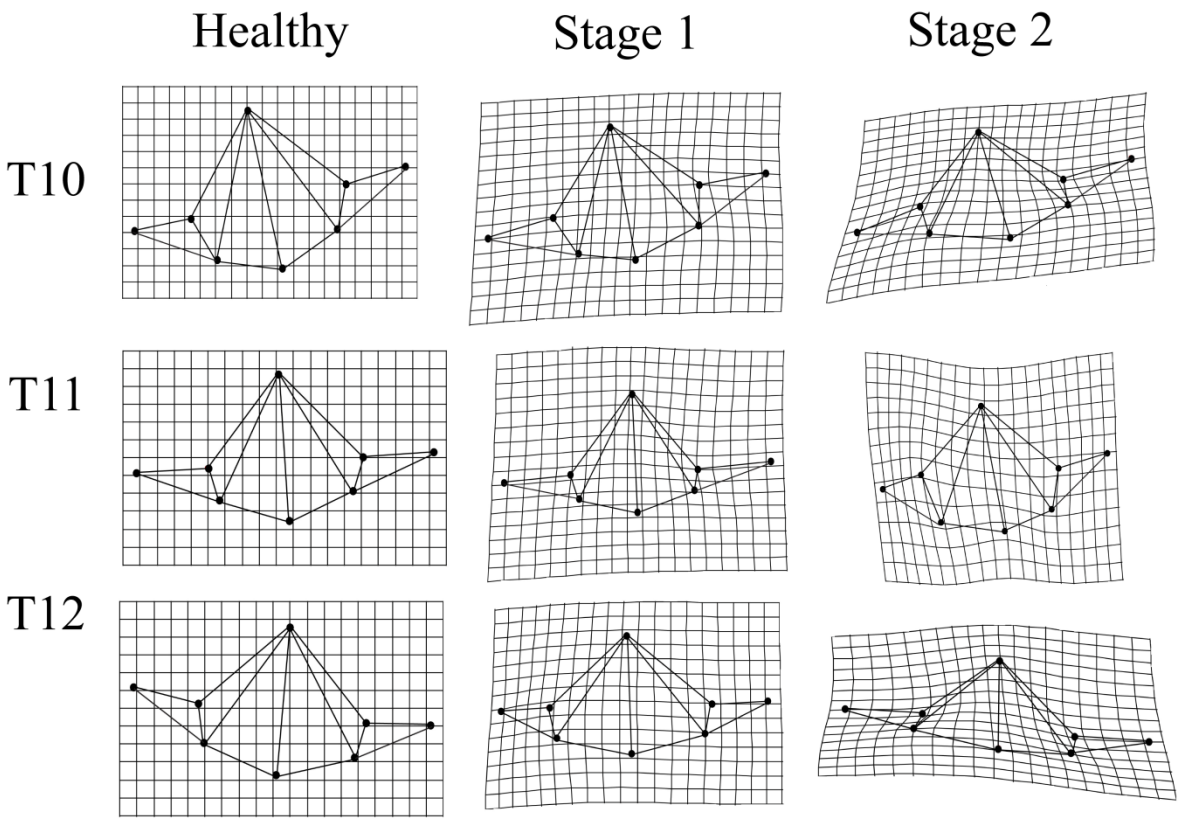


Figure 6) Deformation grids with wireframe illustrations of the mean landmark configuration for neural foramen and pedicles, morphed to represent the shape associated with each group. Deformation grids have been magnified 2x to aid interpretation of shape differences.

In both sexes, the centroid size of the neural foramen was not statistically different between groups; it is the shape of the neural foramen and pedicles which differs between affected and healthy vertebrae. The average inter-landmark distances of the neural foramen identifies a greater sagittal width in healthy vertebrae; this distance is significant in both T11 and T12, but not T10. The average distance in the anterior coronal length is greater in affected vertebrae, again with statistically significant differences seen only in T11 and T12. The widest coronal point of the foramen is greater, on average, in vertebrae with Schmorl's nodes, with T11 showing the only significant difference. The widest point is located closer to the vertebral body on both sides of T12 vertebrae with Schmorl's nodes ($p<0.001$); T11 showed a significant difference only on the right side, and T10 did not show significant differences. A correlation analysis found the distance between the widest point of the neural foramen and the vertebral body to be negatively correlated with the size of the vertebral body in T12; this was only significant on the right side of T10, and not significant on T11. As a general trend, healthy vertebrae have thicker pedicles than those with Schmorl's nodes although inter-landmark distances for pedicle width were not statistically significant between pathological groups or affected vs. healthy vertebrae, and uncorrelated with vertebral body size.

The main differences between healthy and pathological vertebrae are found in the shape of the neural foramen and pedicles, not size, in both males and females. The shape differences when the sexes are pooled are illustrated in Figure 6, with deformation grids exaggerated at 2x magnification to ease interpretation. There is a relatively greater coronal width in the neural foramen of affected vertebrae, and the widest point of the foramen is located closer to the vertebral body with shorter thinner pedicles in relation to the body. Affected vertebrae also have relatively shorter sagittal lengths. This is influenced by the

posterior margin of the body being level with the anterior portion of the pedicles, as opposed to a healthy morphology where the margin is anteriorly positioned with respect to the pedicles.

**Discussion:**

The presence of Schmorl's nodes is strongly associated with specific vertebral shapes, with a 91.1% accuracy of identifying Stage 2 vertebrae from healthy T12 vertebrae based solely on the shape of the neural foramen and pedicles. The shape of the neural foramen, influenced by the posterior margin of the vertebral body, and pedicles has a stronger correlation with the presence of Stage 2 Schmorl's nodes in T12 vertebrae than in T10 or T11. However, the morphological differences represented by the first 5 PCs are statistically significant in all three vertebral segments. The shape differences between affected and healthy vertebrae are most apparent in T11 and T12 (Figure 6). The lesions are also associated with large vertebral bodies in males, and a more circular body shape, influenced by the shape of the posterior vertebral margin, in both sexes. As the main shape differences are similar in both males and females, pooling the sexes for the DFA scores provide a clear and concise way to determine the accuracy of using these shape variables to distinguish healthy vertebrae and those with Schmorl's nodes, regardless of sex. The fact that these DFA scores are high, even with sexual dimorphism included, indicate the strength of the correlation between shape and Schmorl's nodes.The aims of this study have been fulfilled and the null hypothesis is rejected. These data indicate that there is a correlation between vertebral morphology and Schmorl's nodes in the lower thoracic spine.

There is a clear association of a particular vertebral morphology with the presence and severity of Schmorl's nodes, and this raises the question as to whether the data illustrate a

morphological difference which influences the condition, or a morphological change resulting from the condition. Johnson et al. (1988) analyzed the spinal canal of the upper thoracic vertebrae of mice and found that bone remodelling does not cause post-developmental shape change in the neural foramen, suggesting that the shape of the spinal canal likely remains constant throughout an individual's life in the absence of ligament ossification or trauma. This is supported by the clinical study of Masharawi & Salame (2011) and the current study, with both studies showing no correlation between neural foramen shape and age. As the neural foramen is fully formed by six years of age, the shape identified as contributing to the formation of Schmorl's nodes is acquired during vertebral development and likely influences the development of Schmorl's nodes, as opposed to resulting from the condition (Scheuer & Black 2000: 196).

As discussed earlier, Dar et al. (2009) showed that Schmorl's nodes occur at different frequencies dependent on sex and ethnic background. They concluded that there may be a congenital factor in the aetiology of Schmorl's nodes, and that they likely develop during spinal maturation (Dar et al. 2009). When considering the results presented in the current study alongside the findings of Dar et al. (2009), it can be suggested that the shape of the lower thoracic vertebrae may represent a developmental factor influencing the formation of the lesions.

Vertebrae with Stage 1 Schmorl's nodes were the least accurately classified based on DFA scores; however, the group was statistically different from vertebrae with Stage 2 Schmorl's nodes for all three vertebrae, and healthy T11 and T12 vertebrae. These results may validate the practice of scoring the lesions into two groups based on severity, as these groupings are statistically viable based on vertebral morphology.

Harrington et al. (2001) found that larger vertebral endplates in males, and more circular endplates (based on measured dimensions) in both males and females, were correlated with disc herniation in the lower lumbar vertebrae. The authors suggest that this could be related to LaPlace's law, where the radius of a fluid-filled tube directly relates to the amount of tension the tube can withstand. Harrington and co-workers propose that the intervertebral disc can be considered to be a fluid-filled tube, and that a larger radius, as seen in both the larger and more circular endplates, causes higher tension in the disc during compression (Harrington et al. 2001). The main shape difference in the current study was that affected vertebral bodies were more circular, as opposed to more heart shaped in healthy vertebrae, due to the translation of the posterior margin of the vertebral body posteriorly. The affected vertebrae were also larger than healthy vertebrae in males, which is similar to the findings of Harrington et al. (2001); this could provide one explanation as to why males are more commonly affected by Schmorl's nodes than females (Dar et al. 2009). Although the biomechanical function of lower thoracic and lower lumbar vertebrae differ, LaPlace's law would still affect the tension in the intervertebral discs of the thoracic vertebrae.

There is a complex relationship between the posterior vertebral elements and vertebral stability (Adams et al. 2006; Fields et al. 2010; Brown et al. 2008). Adams et al. (2006) found that degenerative changes of the intervertebral disc caused the neural arch to withstand more of the compressive force on the vertebrae during upright posture. Whyne et al. (1998) tested the role of the posterior arch and pedicles in providing vertebral strength at the thoracolumbar junction; they found that the pedicles act as a buttress during compressive forces, with the posterior arch and pedicles providing structural support to the posterior wall of the vertebral body. The shape of the posterior margin of the vertebral body and pedicles in both sexes, and

the size of the vertebral body in males, are the main morphological differences between healthy and affected vertebrae in the present study. Biomechanical experiments which include vertebrae and their associated soft tissue would have to be conducted to fully investigate the relationship between pedicle morphology and intervertebral disc herniation. However, as the current data suggest there may be a complex relationship between pedicle morphology and Schmorl's nodes, this research provides a preliminary basis for further research into the influence of vertebral morphology on spinal biomechanics. T12 showed the strongest distinction between foramen and pedicle shape in relation to the presence of Schmorl's nodes, and this could be a result of the biomechanical importance of vertebral morphology at this junction between the different vertebral segments. The 12th thoracic vertebra is transitional between the thoracic and lumbar spine, and the transitional nature is reflected in the orientation of the articular facets and the curve of the spinal column (kyphotic in the thoracic region and lordotic in the lumbar region) (Masharawi et al. 2004; Masharawi et al. 2005; Masharawi et al. 2008). This may contribute to the occurrence of Schmorl's nodes in this vertebra because it is intermediate between two functionally and morphologically different spinal regions (Qui *et al.* 2006).

Palaeopathologists often use Schmorl's nodes as activity indicators for populations in the past (Novak & Slaus 2011; Klaus et al. 2009; Slaus 2000; Papathanasiou 2005; Robb et al 2001; Alesan et al. 1999). However, the current study supports the hypothesis discussed by Dar et al. (2009), that Schmorl's nodes are likely to be a result of developmental or congenital factors. There is an association of Schmorl's nodes with activity, as vertebrae transmit compressive and shearing forces from the upper to the lower body during daily activities (Cholewicki & McGill 1996), and Schmorl's nodes have been associated with flexion and

extension of the spine during loading (Callaghan & McGill 2001). However, it is clear that their aetiology is more complicated than can be explained by physical activity alone and it is recommended that the lesions should not be used as activity indicators in archaeological skeletal populations in future research. The vertebral shape described may play a vital role in spinal stability and the ability of the vertebral elements to withstand the daily physical stress of loaded flexion and extension (Whyne et al. 1998; Masharawi et al. 2010), which may in turn affect the biomechanics of the intervertebral disc. The complex relationship between vertebral morphology, especially of the posterior elements, and the intervertebral disc warrants further investigation.

**Conclusion:**

The results of this study indicate that palaeopathological research should be cautious of using Schmorl's nodes to indicate spinal trauma or physical stress, and hence "activity", as other factors also appear to influence the development of the lesions. The presence of Schmorl's nodes is strongly correlated with the shape of the pedicles and the posterior margin of the vertebral body in both sexes, in particular T12, and the vertebral body size in males. The reason for this correlation remains unclear. However, the circular body shape associated with Stage 2 vertebrae may influence the amount of tension in the disc, and with the illustrated pedicle shape, may influence an individual's susceptibility to vertical herniation under compressive forces. The vertebral morphology related to Schmorl's nodes may be due to normal human variation, with the correlation with Schmorl's nodes occurring as a result of this particular shape predisposing an individual to biomechanical instability and strain. This, of course, is relevant to clinical medicine.

This study has highlighted a potentially vital factor in the aetiology of Schmorl's nodes not yet recognized - the underlying shape of the posterior vertebral body and pedicles. The aim of the study was to identify any correlation between vertebral morphology and the presence of Schmorl's nodes, and the null hypothesis is rejected based on the findings. This study represents promising groundwork for the analysis of vertebral morphology in relation to Schmorl's nodes, and future research will focus on expanding this study with the analysis of other aspects of vertebral morphology such as the spinous process and costovertebral articular facets. Lumbar vertebrae will also be analyzed, and three dimensional shape analyses will also be performed. The articular facets were not correlated with the presence or severity of Schmorl's nodes, but the use of 3D landmarks may identify three dimensional aspects of facet shape related to the lesions; future research using different landmark techniques would be beneficial. The shape of the vertebral elements in juveniles in relation to different stages of Schmorl's node development will also provide beneficial information on the role of ontogeny and spinal development on the condition.

**Acknowledgments:**

The authors would like to thank the Museum of London for access to the London skeletal samples, and Malin Holst, Mike Griffiths Associates, and Durham University for access to the York sample. Special thanks go to Durham University and the Canadian Centennial Scholarship Fund for financial aid to KAP during this research, to Helgi Pétur Gunnarsson for aid with software, and to Jelena Bekvalac and Rebecca Redfern, Museum of London, Joe Owen and Charlotte King, Durham University, for help and guidance. The authors would also like to thank the reviewers and editors who provided much appreciated advice and suggestions for earlier drafts of this paper.

References:

Abbas J, Hamoud K, May H, Hay O, Medlej B, Masharawi Y, Peled N, Hershkovitz I. 2010. Degenerative lumbar spinal stenosis and lumbar spine configuration. Eur Spine J 19: 1865-1873.

Adams MA, Freeman B, Morrison HP, Nelson IW, Dolan P. 2000.Mechanical initiation of intervertebral disc degeneration. Spine 25(13): 1625-1636.

Adams MA, Pollintine P, Tobias JH, Wakley GK, Donal P. 2006. Intervertebral disc degeneration can predispose to anterior vertebral fractures in the thoracolumbar spine. J Bone Miner Res 21(9): 1409-1416.

Alesan A, Malgosa A, Simó C. 1999. Looking into the demography of an Iron Age population in the Western Mediterranean. I. Mortality. Am J Phys Anthropol 110: 285-301.

Bass WM. 1987 (1971). Human osteology: A laboratory and field manual. Missouri Archaeol Soc Spec Pap 2: Columbia.

Bienvenu T, Guy F, Coudyzer W, Gilissen E, Rouadlès G, Vignaud P, Brunet M. 2011. Assessing endocranial variations in great apes and humans using 3D data from virtual endocasts. Am J Phys Anthropol 145: 231-246.

Bookstein F. 1997. Landmark methods for forms without landmarks: Morphometrics of group differences in outline shape. Med Image Anal 1(3): 225-243.

Brooks ST, Suchey JM. 1990. Skeletal age determination based on the os pubis: Comparison of the Acsádi-Nemeskéri and Suchey-Brooks methods. J Hum Evol 5: 227–38

Brothwell DR. 1981 (1963). Digging up bones: the excavation, treatment and study of human skeletal remains. Cornell University Press: Ithaca, New York.

Brown KR, Pollintine P, Adams M. 2008. Biomechanical implications of degenerative joint disease in the apophyseal joints of human thoracic and lumbar vertebrae. Am J Phys Anthropol 136: 218-326.

Buikstra JE, Ubelaker DH. 1994. Standards for Data Collection from Human Skeletal Remains. Research Series, no. 44. Fayetteville, Arkansas Archaeological Survey.

Callaghan JP, McGill SM. 2001. Intervertebral disc herniation: studies on a porcine model exposed to highly repetitive flexion/extension motion with compressive force. Clin Biomech 16:28-37.

Cardini A, Nagorsen D, O'Higgins P, Polly PD, Thorington Jr. RW, Tongiorgi P. 2009. Detecting biological distinctiveness using geometric morphometrics: An example case from the Vancouver Island Marmot. Ethol Ecol Evol21: 209-223.

Cholewicki J, McGill S. 1996. Mechanical stability of the in vivo lumbar spine: Implications for injury and chronic low back pain. ClinBiomech 11(1): 1-15.

Clark GA, Hall NR, Armelagos GJ, Borkan GA, Panjabi MM, Wetzel FT. 1986. Poor growth prior to early childhood: Decreased healthy and life-span in the adult. Am J Phys Anthropol 70: 145-160.

Cowie R, Bekvalac J, Kausmally T. 2008. Late 17th- to 19th-century burial and earlier occupation at All Saints, Chelsea Old Church, Royal Borough of Kensington and Chelsea. London, Archaeology Studies Series, Museum of London Archaeology Service.

Dar G, Masharawi Y, Peleg S, Steinberg N, May H, Medlej B, Peled N,Hershkovitz I. 2010. Schmorl's nodes distribution in the human spine and its possible etiology.Eur Spine J 19: 670-675.

Dar G, Peleg S, Masharawi Y, Steinberg N, May H, Hershkovitz I.2009. Demographic aspects of Schmorl's nodes. Spine 34(9): E312-E315.

Faccia KJ, Williams RC. 2008. Schmorl's nodes: Clinical significance and implications for the bioarchaeological record. Int J Osteoarchaeol 18(1): 28-44.

Fahey V, Silberstein M, Anderson R, Briggs C. 1998. The pathogenesis of Schmorl's nodes in relation to acute trauma: An autopsy study. Spine 23(21): 2272-2275.

Ferguson SJ, Steffen T. 2003. Biomechanics of the aging spine. Eur Spine J 12:S97-S103.

Fields AJ, Lee GL, Keaveny TM. 2010. Mechanisms of initial endplate failure in the human vertebral body. J Biomech 43: 2126-3131.

Fukuta S, Miyamoto K, Iwata A, Hosoe H, Iwata H, Shirhashi K, Shimizu K. 2009. Unusual back pain caused by intervertebral disc degeneration associated with Schmorl's node at Th11/12 in a young athlete, successfully treated by anterior interbody fusion. Spine 34(5): E195-E198.

Goodall C. 1991. Procrustes methods in the statistical analysis of shape.J Roy Stat Soc. Series B 53(2): 285-339.

Goto K, Tajima N, Chosa E, Totoribe K, Kuroki H, Arizumi Y, Arai Takashi. 2002. Mechanical analysis of the lumbar vertebrae in a three-dimensional finite element method model in which intradiscal pressure in the nucleus pulposus was used to establish the model. J Orthop Sci 7: 243-246.

Grainger I, Phillpotts C. 2011. The Cistercian abbey of St. Mary Graces, East Smithfield, London. London, Archaeology Studies Series, Museum of London Archaeology Service.

Grainger I, Hawkins D, Cowal L, Mikulski R. 2008. The Black Death cemetery of East Smithfield, London. London, Archaeology Studies Series, Museum of London Archaeology Service.

Hamanashi C, Kawabata T, Yosii T, Tanaka S. 1994. Schmorl's nodes on magnetic resonance imaging: their incidence and clinical relevance. Spine 19: 450-453.

Harrington JF, Sungarian A, Rogg J, Makker VJ, Epstein MH. 2001. The relation between vertebral endplates shape and lumbar disc herniations. Spine 26: 2133-2138.

Holst M. 2005. Fishergate House artefacts and environmental evidence: The human bone. Arch Planning Consultancy, UK. Accessed online, July 3, 2010.

Inufusa A, An HS, Lim TH, Hasegawa T, Haughton VM, Nowicki BH. 1996. Anatomical changes of the spinal canal and intervertebral foramen associated with flexion-extension movement. Spine 21(21): 2412-2420.

Işcan MY, Loth SR, Wright RK. 1984. Age estimation from the rib by phase analysis: White males. J Forensic Sci 29: 1094–104.

Işcan MY, Loth SR, Wright RK. 1985. Age estimation from the rib by phase analysis: White females. J Forensic Sci 30: 853–63.

Jang JS, Kwan HK, Lee JJ, Hwang SM, Lim SY. 2010. Rami communicans nerve block for the treatment of symptomatic Schmorl's nodes. Korean J Pain 23(4): 262-265.

Johnson DR, O'Higgins P, McAndrew TJ. 1988. The relationship between age, size and shape in the upper thoracic vertebrae of the mouse. J Anat 161:73-82

Kimmerle EH, Ross A, Slice, D. 2008. Sexual dimorphism in America: Geometric morphometric analysis of the craniofacial region. J Forensic Sci 53(1): 54-57.

Klaus HD, Larsen CS, Tam ME. 2009. Economic intensification and degenerative joint disease: Life and labor on the postcontact north coast of Peru. Am J Phys Anthropol 139: 204-21.

Klingenberg CP. 2011. MorphoJ: An integrated software package for geometric morphometrics. MolEcol Res 11: 353-357.

Knüsel CJ, Göggel S, Lucy D. 1997. Comparative degenerative joint disease of the vertebral column in the medieval monastic cemetery of the Gilbertine Priory of St. Andrew, Fishergate, York, England. Am J Phys Anthropol 103: 481-495.

Lieberman DE, Carlo J, Ponce de León M, Zollikofer CP. 2007. A geometric morphometrics analysis of heterochrony in the cranium of chimpanzees and bonobos. J Human Evol 52: 647-662.

Lovejoy CO, Meindl RS, Pryzbeck TR, Mensforth RP. 1985. Chronological metamorphosis of the auricular surface of the ilium: A new method for the determination of age at death. Am J Phys Anthropol 68: 15–28.

Masharawi Y. 2012. Lumbar shape characterization of the neural arch and vertebral body in spondylolysis: A comparative skeletal study. Clin Anat 25: 224-230.

Masharawi Y, Salame K. 2011. Shape variation of the neural arch in the thoracic and lumbar spine: Characterization and relationship with the vertebral body shape. Clin Anat 24(7): 858-867.

Masharawi Y, Dar G, Peleg S, Steinberg N, Medlej B, May H, Abbas J, Hershkovitz I. 2010. A morphological adaptation of the thoracic and lumbar vertebrae to lumbar hyperlordosis in young and adult females. Eur Spine J 19: 768-773.

Masharawi Y, Salame K, Mirovsky Y, Peleg S, Dar G, Steinberg N, Hershkovitz I. 2008. Vertebral body shape variation in the thoracic and lumbar spine: Characterization of its asymmetry and wedging. Clin Anat 21: 46-54.

Masharawi Y, Rothschild B, Salame K, Dar G, Peleg S, Hershkovitz I. 2005. Facet tropism and interfacet shape in the thoracolumbar vertebrae: Characterizations and biomechanical interpretation. Spine 30(11): E281-E292.

Masharawi Y, Rothschild B, Dar G, Peleg S, Robinson D, Been E, Hershkovitz I. 2004. Facet orientation in the thoracolumbar spine. Spine 29(16): 1755-1763.

Meijer GJM, Homminga J, Hekman EEG, Veldhuizen AG, Verkerke GJ. 2010. The effect of three-dimensional geometrical changes during adolescent growth on the biomechanics of a spinal motion segment. J Biomech 43: 1590-1597.

Mitteroecker P, Gunz P. 2009. Advances in geometric morphometrics. Evol Biol 36: 235-247.

Mok F, Samartzis D, Karppinen J, Luk K, Fong D, Cheung K. 2010. Prevalence, determinants, and association of Schmorl's nodes of the lumbar spine with disc degeneration: A population-based study of 2449 Individuals. Spine 35(21): 1944-1952.

Neubauer S, Gunz P, Hublin JJ. 2010. Endocranial shape changes during growth in chimpanzees and humans: A morphometric analysis of unique and shared aspects. J Human Evol 59:555-566.

Neubauer S, Gunz P, Hublin JJ. 2009. The patterns of endocranial ontogenetic shape changes in humans. J Anat 215: 240-255.

Novak M, Šlaus M.2011.Vertebral pathologies in two early modern period ($16^{th}$-$19^{th}$ Century) populations from Croatia. Am J Phys Anthropol 145: 270-281.

O'Higgins P. 2000. The study of morphological variation in the hominid fossil record: Biology, landmarks and geometry. J Anat 197(1): 103-120.

O'Higgins P, Jones N. 2006. Tools for statistical shape analysis. Hull York Medical School.

O'Higgins P, Jones N. 1998. Facial growth in Cercocebus torquatus: An application of three-dimensional geometric morphometric techniques to the study of morphological variation. J Anat 193: 251-272.

Overvliet GM, Beuls EAM, ter Laak-Poort M, Cornips EMJ. 2009. Two brothers with a symptomatic thoracic disc herniation at T11-T12: Clincial report. ActaNeurochir 151: 393-396.

Papathanasiou A. 2005. Health status of the Neolithic population of Alepotrypa Cave, Greece. Am J Phys Anthropol 126: 377-390.

Peng B, Wu W, Hou S, Shang W, Wang X, Yang Y. 2003. The pathogenesis of Schmorl's nodes. J Bone Joint Surg 85 B: 879-882.

Phenice TW. 1969. A newly developed visual method of sexing the os pubis. Am J Phys Anthropol 30: 297–302

Pfirrmann C, Resnick D. 2001. Schmorl's nodes of the thoracic and lumbar spine: Radiographic-pathologic study of prevalence, characterization, and correlation with degenerative changes of 1,650 spinal levels in 100 cadavers. Radiology 219: 368-374.

Qui TX, Teo EC, Zhang QH. 2006. Comparisons of kinematics between thoracolumbar T11-T12 and T12-L1 functional spinal units. J Eng Med 220: 493-504.

R Development Core Team. 2012. R: A language and environment for statistical computing. R Foundation for Statistical Computing Vienna, Austria. ISBN 3-900051-07-0, URL http://www.R-project.org

Robb J, Bigazzi R, Lazzarini L, Scarsini C, Sonego F. 2001. Social "status" and biological "status": A comparison of grave goods and skeletal indicators from Pontecagnano. Am J Phys Anthropol 115: 213-22.

Rohlf FJ. 2004. TPSDig Version 1.40. Ecology and Evolution, SUNY at Stony Brook.

Rohlf FJ. 2003. Bias and error in estimates of mean shape in geometric morphometrics. J Hum Evol 44: 665-683.

Rohlf FJ, Slice D. 1990. Extensions of the Procrustes method for the optimal superimposition of landmarks. Syst Zool 39(1):40-59.

Scheuer L, Black S. 2000. Developmental juvenile osteology. Academic Press: London, UK.

Schmorl G, Junghans H. 1971. The human spine in health and disease. New York: Grune & Stratton.

Silberstein M, Opeskin K, Fahey V. 1999. Spinal Schmorl's nodes: Sagittal sectional imaging and pathological examination. Australas Radiol 43: 27-30.

Šlaus M. 2000. Biocultural analysis of sex differences in mortality profiles and stress levels in late Medieval populations from Nova Rača, Croatia. Am J Phys Anthropol 111: 193-209.

Slice DE. 2007. Geometric morphometrics. Annu Rev Anthropol 36: 261-281.

SPSS Inc. 2007.SPSS Base 8.0 for Windows User's Guide.SPSS Inc., Chicago IL.

Stevens SD, Strand Viðarsdóttir U. 2008. Morphological changes in the shape of the non-pathological bony knee joint with age: A morphometric analysis of the distal femur and proximal tibia in three populations of known age at death. Int J Osteoarchaeol 18: 352-371.

Takahashi K., Miyazaki T, Ohnari H, Takino T, Tomita K. 1995. Schmorl's nodes and low-back pain. Eur Spinel J 4: 56-59.

Üstündağ H. 2009. Schmorl's nodes in a Post-Medieval skeletal sample from Klostermarienberg, Austria. Int J Osteoarchaeol 19: 695-710.

Vernon-Roberts B. 1989. Pathology of intervertebral discs and apophyseal joints. In: Jayson MIV, editor. The lumbar spine and back pain. Edinburgh: Churchill Livingstone. p 37-55.

Watts R. 2010. Non-specific indicators of stress and their association with age at death in Medieval York: Using stature and vertebral neural canal size to examine the effects of stress occurring during different periods of development. Int J Osteoarchaeol 21(5): 568-576.

White JW, Ruttenberg BI. 2007. Discriminant function analysis in marine ecology: Some oversights and their solutions. Mar Ecol Prog 329: 301-305.

Whyne CM, Hu SS, Klisch S, Lotz J. 1998. Effect of the pedicle and posterior arch on vertebral body strength predictions in finite element modeling. Spine 23(8): 899-907.

Williams FMK, Manek NJ, Sambrook P, Spector TD, MacGregor AJ. 2007. Schmorl's nodes: Common, highly heritable, and related to lumbar disc disease. Arthritis Rheum 57(5): 855-60.

Zelditch ML, Swiderski DL, Sheets HD, Fink. 2004. Geometric morphometrics for biologists: A primer. Elsevier Academic Press: San Diego, CA.

Zhang N, Li F, Huang Y, Teng C, Chen W. 2010. Possible key role of immune system in Schmorl's nodes. Med Hypotheses 74: 552-554.

**Supplementary Figures:**

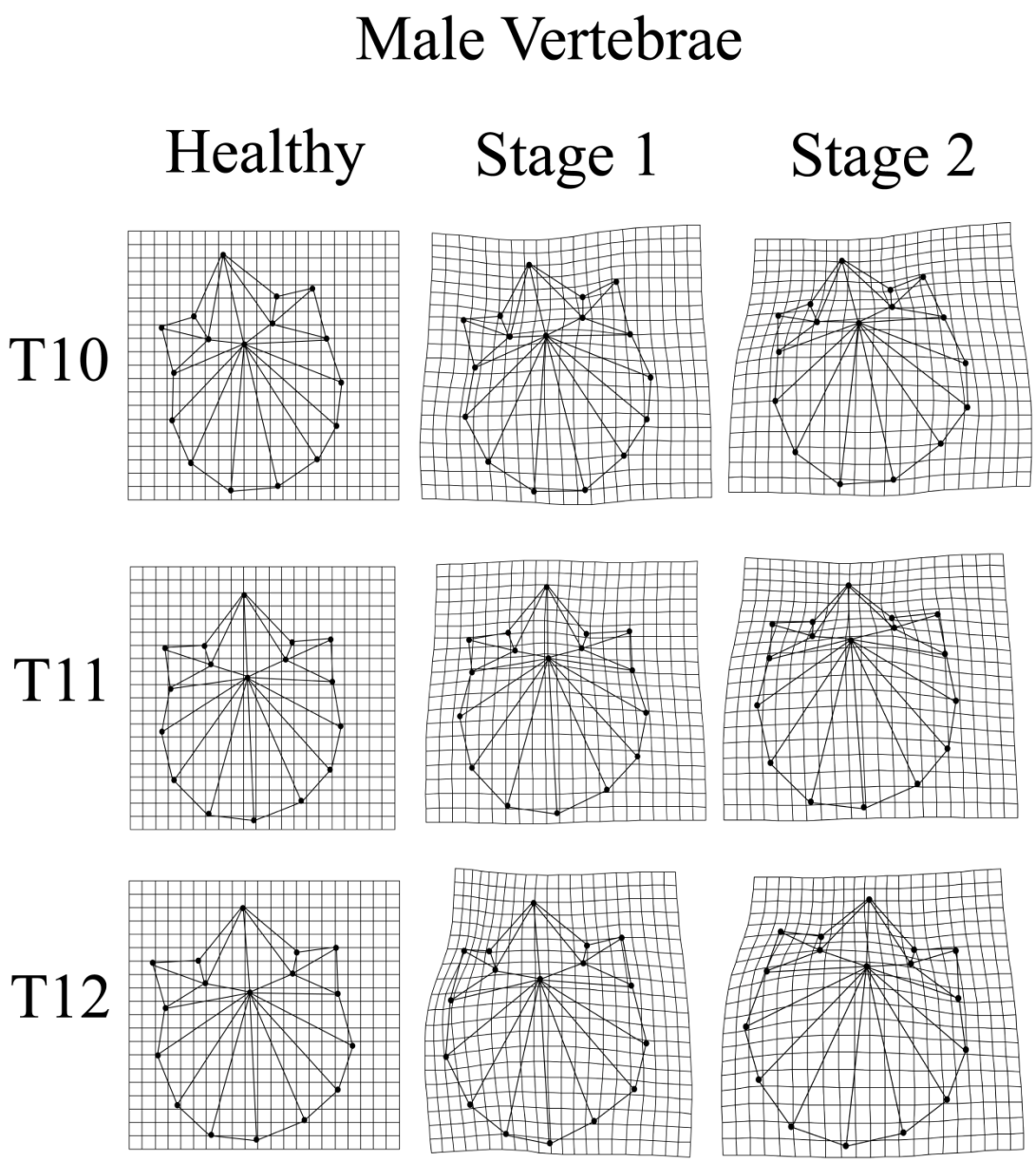


Figure S1) Deformation grids with wireframe illustrations of the mean landmark configuration of males morphed to represent the shape associated with each pathological group. Deformation grids have been magnified 2x to aid interpretation of shape differences

.

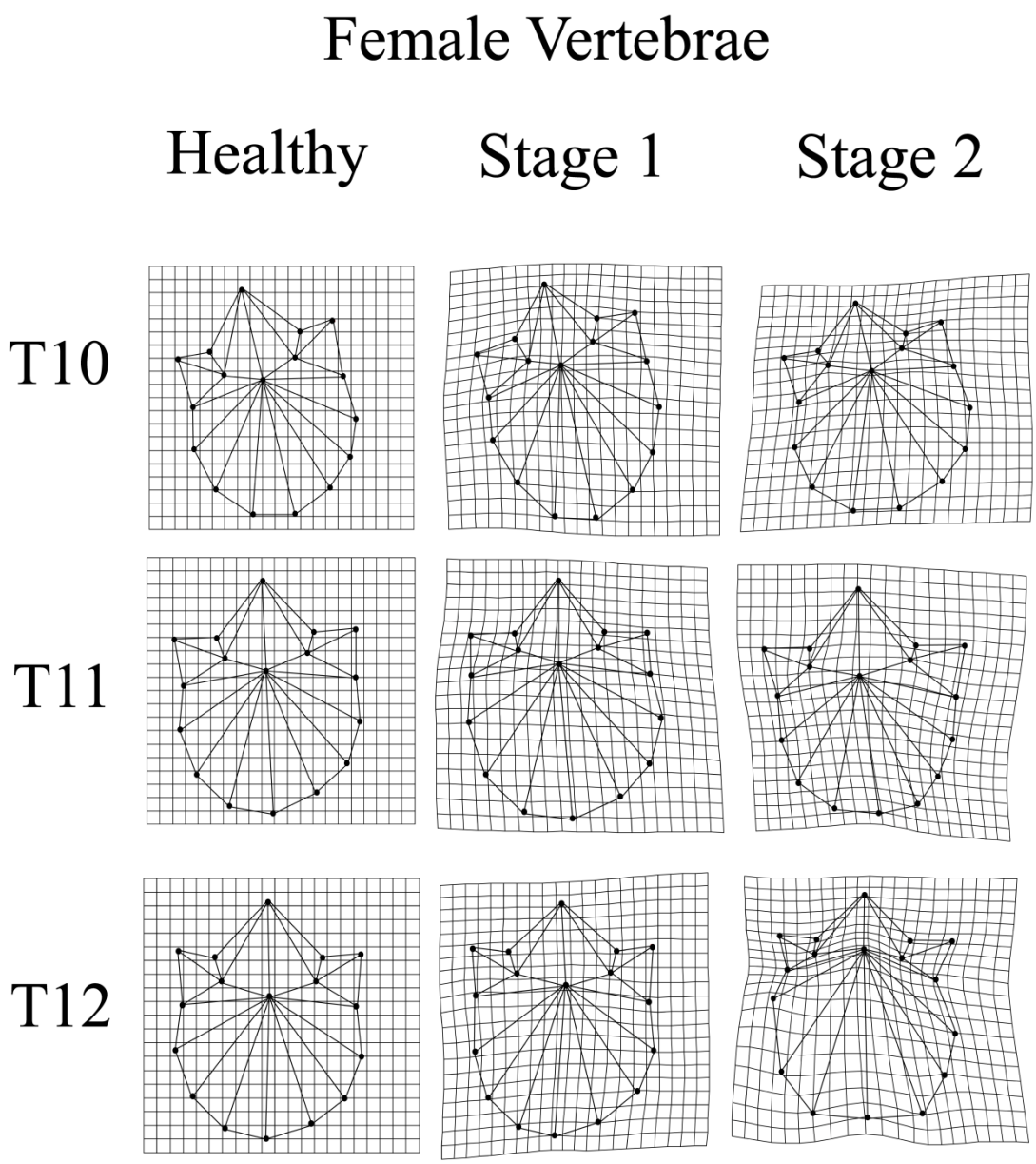


Figure S2) Deformation grids with wireframe illustrations of the mean landmark configuration of females morphed to represent the shape associated with each pathological group. Deformation grids have been magnified 2x to aid interpretation of shape differences.

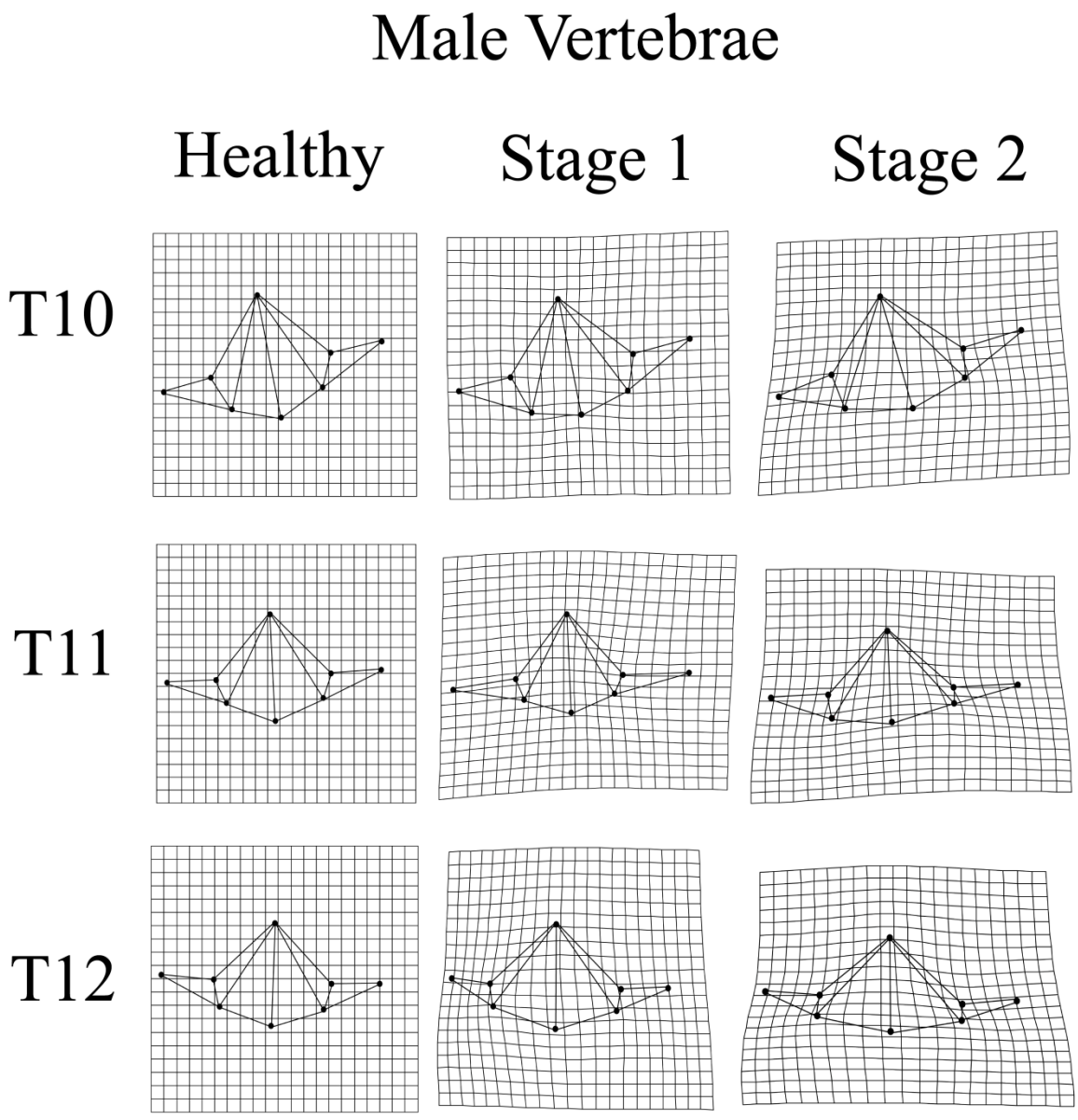


Figure S3) Deformation grids with wireframe illustrations of the mean landmark configuration for neural foramen and pedicles of males, morphed to represent the shape associated with each group. Deformation grids have been magnified 2x to aid interpretation of shape differences.

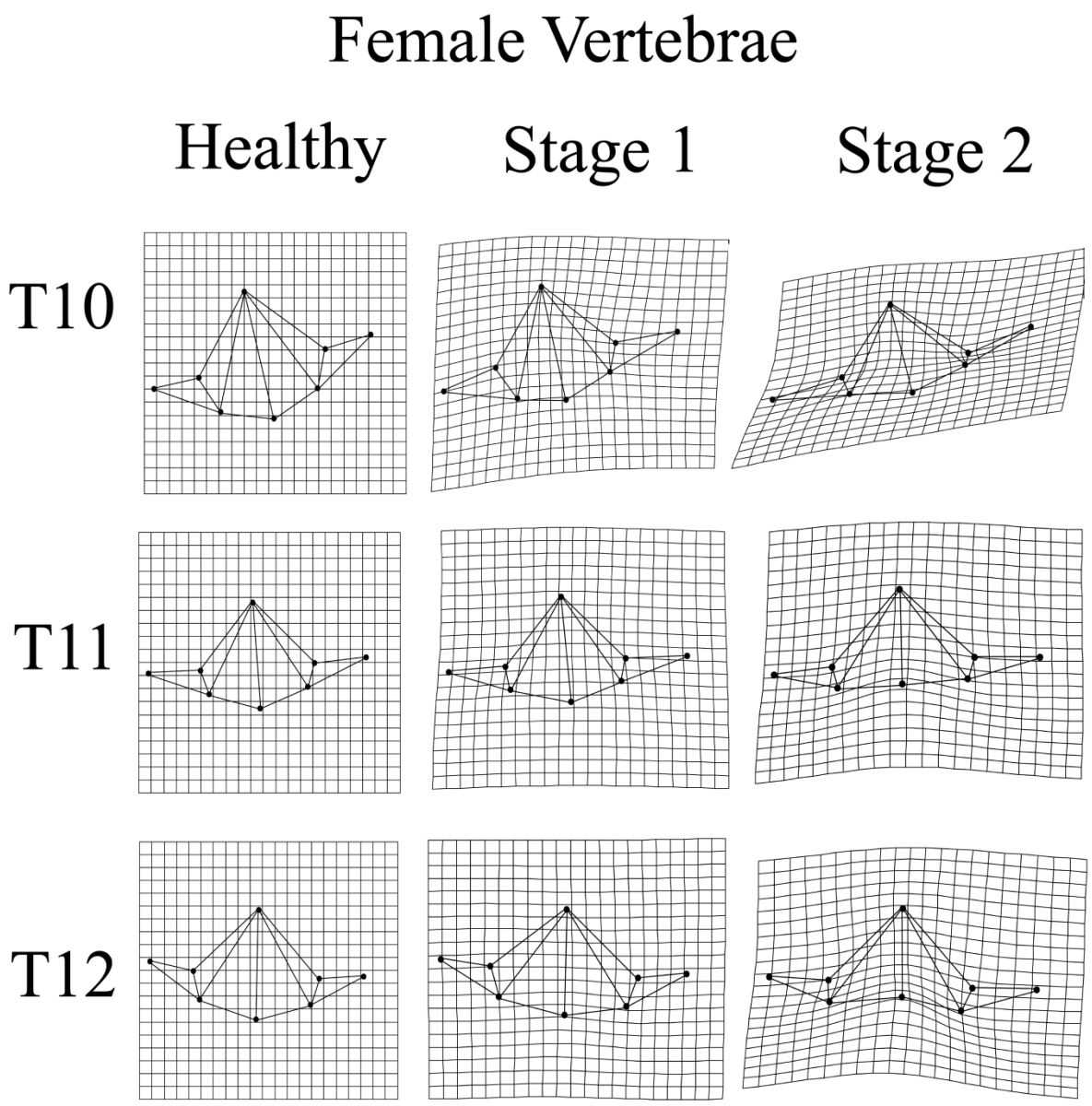


Figure S4) Deformation grids with wireframe illustrations of the mean landmark configuration for neural foramen and pedicles of females, morphed to represent the shape associated with each group. Deformation grids have been magnified 2x to aid interpretation of shape differences.

## Chapter 6) Manuscript 2

# Vertebral Morphology as an Aetiological Factor in the Development of Schmorl's Nodes at the Thoraco-Lumbar Junction and the Lumbar Spine of a Medieval English Population from Fishergate House, York

Kimberly A. Plomp[1,2*] , MSc

Charlotte A. Roberts[2], PhD

Una Strand Viðarsdóttir[1,] , PhD

1) Evolutionary Anthropology Research Group, Department of Anthropology, Durham University, Dawson Building, South Road, Durham DH1 3LE
2) Department of Archaeology, Durham University, Dawson Building, South Road, Durham DH1 3LE

*** Corresponding author:** una.vidarsdottir@durham.ac.uk

**Abstract:**

Schmorl's nodes are depressions on vertebrae due to herniation of the nucleus pulpous into the inferior or superior vertebral body. The aetiology of Schmorl's nodes remains unclear; however, it has been suggested that a genetic or congential predisposition may play a vital role in their occurrence. This study provides a extension of our previous study which analyzed the shape of the lower thoracic spine and found that vertebral morphology is associated with intervertebral disc herniation. Sixty adult individuals from the late medieval archaeological cemetery site of Fishergate House, York, were analysed using 2D geometric morphometric techniques to identify any relationship between vertebral morphology and the development of Schmorl's nodes at the thoraco-lumbar junction and in the lumbar spine. Schmorl's nodes were identified macroscopically in vertebral bodies and recorded based on location, depth, and size. The morphology of the superior aspect of the vertebrae was analysed for possible correlations with the presence of Schmorl's nodes using multivariate statistical techniques. There is a strong correlation between the shape of the neural foramen, pedicles, and vertebral body in vertebrae with Schmorl's nodes in the twelfth thoracic vertebrae and L1-L4 of the lumbar spine. The biomechanical significance of vertebral morphology is not fully understood, but the pedicle shape identified on affected vertebrae may not provide adequate structural support for the vertebral bodies, resulting in disc herniation. The results support the findings of our previous study, and indicate that vertebral morphology may be an important aetiological factor in vertical intervertebral disc herniation and the development of Schmorl's nodes.

**Keywords** Disc herniation, geometric morphometrics, shape analysis, palaeopathology

**Introduction:**

Schmorl's nodes are lytic depressions with sclerotic margins caused by a herniation of the nucleus pulposus of the intervertebral disc into the superior or inferior surface of vertebral bodies (Schmorl & Junghans 1971; Pfirrmann & Resnick 2001). They affect the lower thoracic and lumbar spine most frequently and are common in both living and archaeological populations, with prevalence rates ranging from 5-77% depending on the sample studied and recording protocol used (clinical literature: Pfirrmann & Resnick 2001; Dar et al. 2009; Mok et al. 2010; palaeopathological literature: Novak & Šlaus 2011; Robb et al. 2001; Üstündağ 2009). The exact aetiology of intervertebral disc herniation continues to elude researchers, the general consensus being that their cause is multi-factorial, with physical strain or trauma identified as the main contributory factors influencing their development (Dar et al. 2010; Mok et al. 2010; Baranto et al. 2006; Gordon et al. 1991; Rannou et al. 2001). Many authors, however, also note that other factors are associated with the frequency of the lesion, with genetic predisposition and particular disc composition often cited as contributing to the condition (Williams et al. 2007; Anakwenze et al. 2011; Burke et al. 2012; Overliet et al. 2009). Schmorl's nodes are as common in archaeological populations as in the living, indicating that the aetiological factors influencing their development are not linked to a modern lifestyle (palaeopathology literature: Novak & Šlaus 2011; Robb et al. 2001; Üstündağ 2009; Caffell & Holst 2010; Kraus et al. 2009; Robb 1994; Saluja et al 1986; Sandness & Reinhard 1992; Šlaus 2000; clinical literature: Schmorl & Junghans 1971; Pfirrmann & Resnick 2001; Dar et al. 2009; Mok et al. 2010).

In palaeopathological studies, Schmorl's nodes have been suggested to represent physical stress on the spine and have been used as activity indicators in the past (Novak &

Slaus 2011; Klaus et al. 2009; Slaus 2000; Papathanasiou 2005; Robb et al 2001; Alesan et al. 1999). Although intervertebral disc herniations have been associated with flexion and extension of the spine during loading (Callaghan & McGill 2001; Goto et al. 2002), there are also other aetological factors contributing to the development of Schmorl's nodes (Dar et al. 2009; Williams et al. 2007). Many studies of living populations have found that the likelihood of Schmorl's nodes does not increase with age, but that they are generally more common in males than females (Mok et al. 2010; Faccia & Williams 2008; Harrington et al. 2001). Ethnic background has also been shown to be a determinant in the frequency of the lesion (Dar et al. 2009), and a twin-study performed by Williams et al (2007) found that there could be a strong genetic influence in the development of Schmorl's nodes. Harrington et al.'s (2001) study on the size and form of the lower lumbar spine in relation to transverse disc herniation found that larger lumbar vertebral bodies in males, and vertebral bodies with larger radii in both males and females, were more prone to disc herniation.

In a previous study, a significant correlation was noted between the morphology of the vertebral body, neural canal, and pedicles and the presence of Schmorl's nodes in the lower thoracic spine (T10-T12) (Plomp et al. 2012). It is hypothesised that there will also be a relationship between Schmorl's nodes and lumbar vertebral morphology. The present paper aims to expand upon our previous study of thoracic vertebrae by analyzing the morphology of vertebrae in the thoraco-lumbar junction and lumbar spine in order to investigate if the morphological association found in the lower thoracic spine also exists in the lumbar vertebrae (Plomp et al. 2012). If a relationship is found, it would indicate that vertebral morphology is associated with the development of Schmorl's nodes in the lumbar spine.

**Materials and Methods:**

This study analyses vertebrae from an archaeological collection curated in the Department of Archaeology at Durham University (http://www.dur.ac.uk/archaeology /facilities_services/fhol/, Accessed Oct 2012). The use of archaeological human remains for this type of research enables the analysis of vertebrae without the need for imaging technology, and allows direct examination of the dry bone surfaces of vertebrae. However, differential preservation of the spine in individual skeletons can affect what parts of the spine are observable. The sample studied here is composed of the T12 vertebrae and lumbar spines (L1-L4) of 60 adult individuals (33 male, 23 females, 3 unsexed adults) from the cemetery site of Fishergate House, York, dated to the $12^{th}$-$16^{th}$ centuries AD (Table 1). The sample size of affected L5 vertebrae was too small to be considered for statistical analyses. Analyses included both vertebrae exhibiting Schmorl's nodes and healthy vertebrae. The number of vertebrae in each dataset varies depending on bone preservation and consequently the preserved landmarks available for analysis (Table 2). Standard osteological analyses of the skeletons had previously been performed to determine sex and age at death (Brooks & Suchey 1999; Milner 1992; Işcan et al. 1984, 1985; Lovejoy et al. 1985; Acsádi & Nemeskéri 1970; Phenice 1969) and this information was extracted from the archaeological site report (Holst 2005).

Table 1) Number of individuals, with sex and age indicated (YA = young adult (18-25 years), MA = middle adult (26-45years),, OA = Old adult (46+years), U=Unknown), included in the analysis. Age categories based on Buikstra and Ubelaker (1994).

| Site | Period | Reference | ♀ | ♂ | U | YA | MA | OA | U | Inds |
|---|---|---|---|---|---|---|---|---|---|---|
| Fishergate House, York, Yorkshire | Medieval ($12^{th}$-$16^{th}$ C AD) | Holst 2005 | 23 | 33 | 3 | 13 | 25 | 19 | 2 | 59 |

Table 2) Summary of data by vertebral segment. Due to differential preservation of landmarks two datasets were analyzed: one with 17 landmarks, and another limited to eight landmarks.

| | 17 Landmarks | | | 8 Landmarks | | |
|---|---|---|---|---|---|---|
| | **Healthy** | **Affected** | **Total** | **Healthy** | **Affected** | **Total** |
| **T12** | 8 | 10 | 18 | 16 | 26 | 42 |
| **L1** | 16 | 12 | 28 | 22 | 22 | 44 |
| **L2** | 6 | 13 | 19 | 16 | 25 | 41 |
| **L3** | 8 | 13 | 21 | 17 | 26 | 43 |
| **L4** | 16 | 6 | 22 | 35 | 17 | 52 |

Schmorl's nodes were recorded on both superior and inferior surfaces, and macroscopically scored as belonging to one of three groups, based on Knüsel et al. (1997). Healthy vertebrae had no evidence of the lesions; stage 1 lesions were less than 2mm in depth and covered less than half the antero-posterior length of the body, and stage 2 lesions exceeded these parameters (Knüsel et al. 1997). Figure 1 provides examples of the lesion stages. The vertebrae were categorized based on the highest score.

Figure 1) Vertebrae displaying Schmorl's nodes; the lesion on the left is stage 1 and the lesion on the right is stage 2.

Geometric morphometrics were used to quantify and compare vertebral shape (O'Higgins 2000). Images were standardized for vertebral orientation, angle, and distance from camera to ensure shape differences were not a result of orientation differences. Eight two-dimensional homologous landmarks and nine semi-landmarks, capturing the superior margin of the vertebrae, were digitized on these standardised images using TPSdig© software (Rohlf 2004) (Figure 2). Statistical analyses were performed in Morphologika© (O'Higgins &

Jones 2006), and R (R Development Core Team). Generalized procrustes analysis (GPA) removed rotational and translational variation, as well as standardising the size of the landmark configurations (Bookstein 1997; Goodall 1991; Rohlf 2003; Rohlf & Slice 1990; Slice 2007). Principal components analyses (PCA) were used to summarise and illustrate the pattern of shape variability within the sample. Discriminant function analysis with leave-one-out cross-validation (DFA) was used to establish the power of discrimination between groups within the sample (Cardini et al. 2009; Kimmerle 2008; White & Ruttenberg 2007). To minimize noise from higher components, the number of PCs included in the cross-validated DFA was reduced using the method proposed by Baylac and Frieβ (2005), and cross-validated scores were tested against over-fitting by randomization, as described by Kovarovic et al. (2011), with only scores above chance reported. Centroid size, the square root of the sum of the squared distances of each landmark from the centroid of the landmark configuration, was used as the measure of size, as it does not introduce bias into the analysis (Zelditch et al. 2004). MANOVA, ANOVA, and Chi-squared ($\chi^2$) tests were used to determine statistical significance of group differences. Intra-observer error was calculated by comparing the greatest Procrustes distance between repeated observations and the smallest distance between other vertebrae. The greatest distance between the repeated observations was half the smallest distance between different vertebrae which indicates that intra-observer error is unlikely to affect the classification of groups within the data (Bienvenu et al. 2011; Lieberman et al. 2007; Neubauer et al. 2009, 2010).

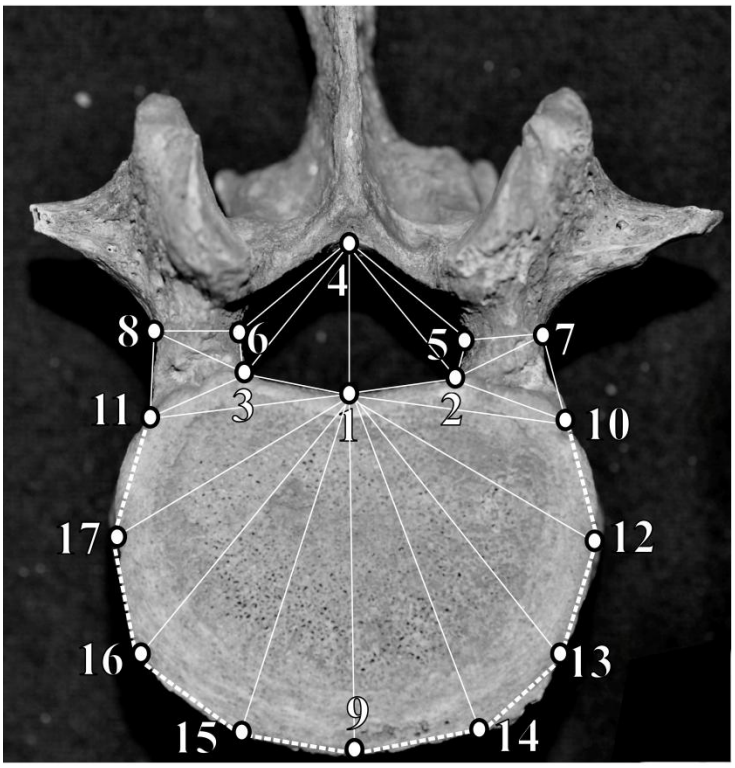


Figure 2) Location of landmarks used for shape analysis. Landmarks 1 through 17 are analyzed in the first dataset, and landmarks 1 through 8, focus on the neural canal and pedicles are included in the second dataset.

**Results:**

On average, affected vertebrae were larger than their healthy counterparts, except for the fourth lumbar, where the average centroid size of healthy vertebrae was larger than those affected. These differences in size were small and failed to reach statistical significance for all vertebrae, even when controlling for sex ($p>0.269$) (figure 3). Males had on average larger centroid sizes than females for all vertebrae although, again, this was not statistically significant ($p>0.084$). Females were affected more often than males, with 65.2% of females and 54.5% of males having a node on at least one vertebra, although this difference was not significant ($\chi^2$ $p=0.425$). However, males had multiple vertebrae affected more often than females, with 77.8% of affected males having lesions on more than one vertebrae compared to

66.7% of affected female; again this was not significant ($\chi^2$ p=0.730). Sexual dimorphism did not have a statistically significant effect on shape in this population so all subsequent analyses was based on pooled sex datasets. There was no significant difference in the occurrence of Schmorl's nodes with age ($\chi^2$ p=0.523), although adults in the middle age range were more often affected (68.0%), and young (53.8%) and old (52.6%) adults showed almost equal prevalence rates.

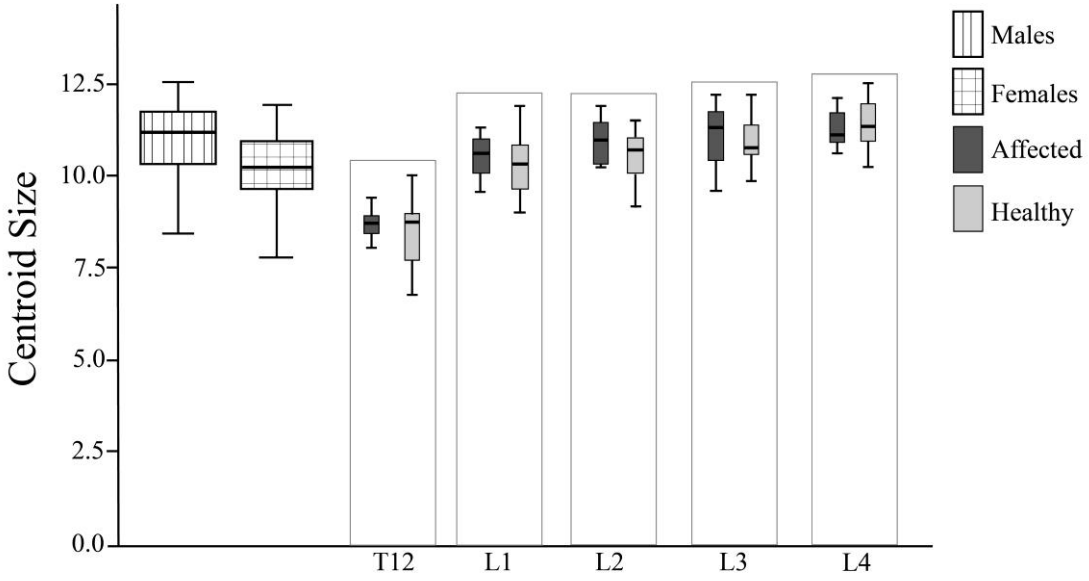


Figure 3) Chart displaying centroid size of male and female vertebrae, as well as the size differences between healthy and affected vertebra.

Table 3 summarises the results of the cross-validated DFA for each vertebra from T12 to L4. The best discrimination between healthy and affected is found in T12, L2, and L3. Table 4 summarizes the results of MANOVAs performed on the PCs included in each DFA (Tables 3 & 5). For 17 landmarks, there are statistical differences for all vertebrae except L1

and L4, but L4 did show a significant value on PC3. When the eight landmarks are analyzed, including a larger sample size, all vertebrae show a statistical difference.

Table 3) Summary of correctly identified vertebrae from the DFA with cross-validation, based on 17 landmarks for each vertebra, with the number of PCs and total variance for each.

| | DFA Scores | | | PCs |
|---|---|---|---|---|
| | **Affected** | **Healthy** | **Total** | **Total Variance** |
| **T12** | 100 % | 100 % | 100 % | 6 PCs = 90.5 % |
| **L1** | 72.7 % | 68.8 % | 70.4 % | 11 PCs = 96.6 % |
| **L2** | 75.0 % | 83.3 % | 77.8 % | 7 PCs = 93.7% |
| **L3** | 100 % | 100 % | 100 % | 20 PCs = 86.1 % |
| **L4** | 66.7 % | 62.5 % | 63.6 % | 3 PCs = 74.7 % |

Table 4) Summary of MANOVA scores (Wilks lambda λ, F-ratio, p-value) of PC values for all vertebrae in both sets of landmarks.

| | 17 landmarks | | | 8 landmarks | | |
|---|---|---|---|---|---|---|
| **T12** | λ 0.151 | F= 13.52 | p = 0.000* | λ 0.537 | F= 6.22 | p = 0.000* |
| **L1** | λ 0.484 | F= 1.26 | p = 0.343 | λ 0.561 | F= 3.53 | p = 0.004* |
| **L2** | λ 0.294 | F= 3.66 | p = 0.025* | λ 0.682 | F= 2.65 | p = 0.032* |
| **L3** | λ 0.003 | F= 52.47 | p = 0.004* | λ 0.735 | F= 2.67 | p = 0.037* |
| **L4** | λ 0.735 | F= 2.17 | p = 0.127<br>PC3 p=0.042* | λ 0.739 | F= 3.25 | p = 0.014* |

* indicates significant value

Figure 4 illustrates the morphological differences between the mean shapes of healthy and affected vertebrae for each vertebra with the deformation illustrated using a thin-plate spline. Affected vertebrae have relatively shorter pedicles than healthy, and the posterior margin of the vertebral body encroaches more into the neural canal, resulting in a relatively more circular vertebral body in affected bones when compared to a more heart-shaped body in

the healthy vertebrae. These changes are most apparent in T12 and L3, although they do occur to a lesser extent in the other vertebrae.

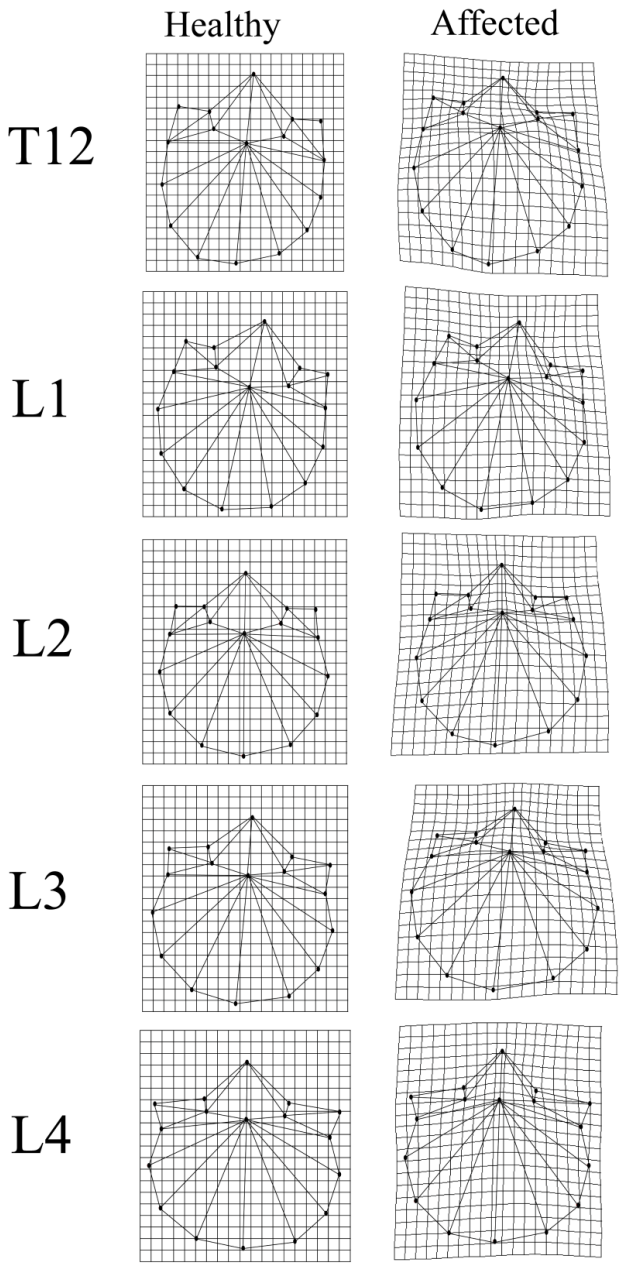


Figure 4) Wireframe images representing the mean morphology of healthy and affected vertebrae. Thin-plate splines illustrate the area of deformation in morphology from the healthy to the affected vertebrae; the deformation of the grids has been multiplied by 2 for ease of interpretation.

Shape differences between the means of all affected and healthy T12-L4 vertebrae are illustrated in figure 5. There is a clear separation of affected and healthy vertebrae on a combination of PC2 and PC3 (28.7% total variance), with wireframe images illustrating the differences between the mean shapes of healthy and affected vertebrae. When all vertebrae are analyzed in a single dataset, a cross-validated DFA found an accuracy of 74.8% (74.1% affected, 75.4% healthy) in classifying affected and healthy vertebrae based on scores on the first 7 PCs (89.8% total variance). The group means for all vertebrae were also analyzed, and a cross-validated DFA found a 90% accuracy of correctly classifying affected (100%) and healthy vertebrae (80%) on the first 6 PCs, representing 99.4% of the total shape variance.

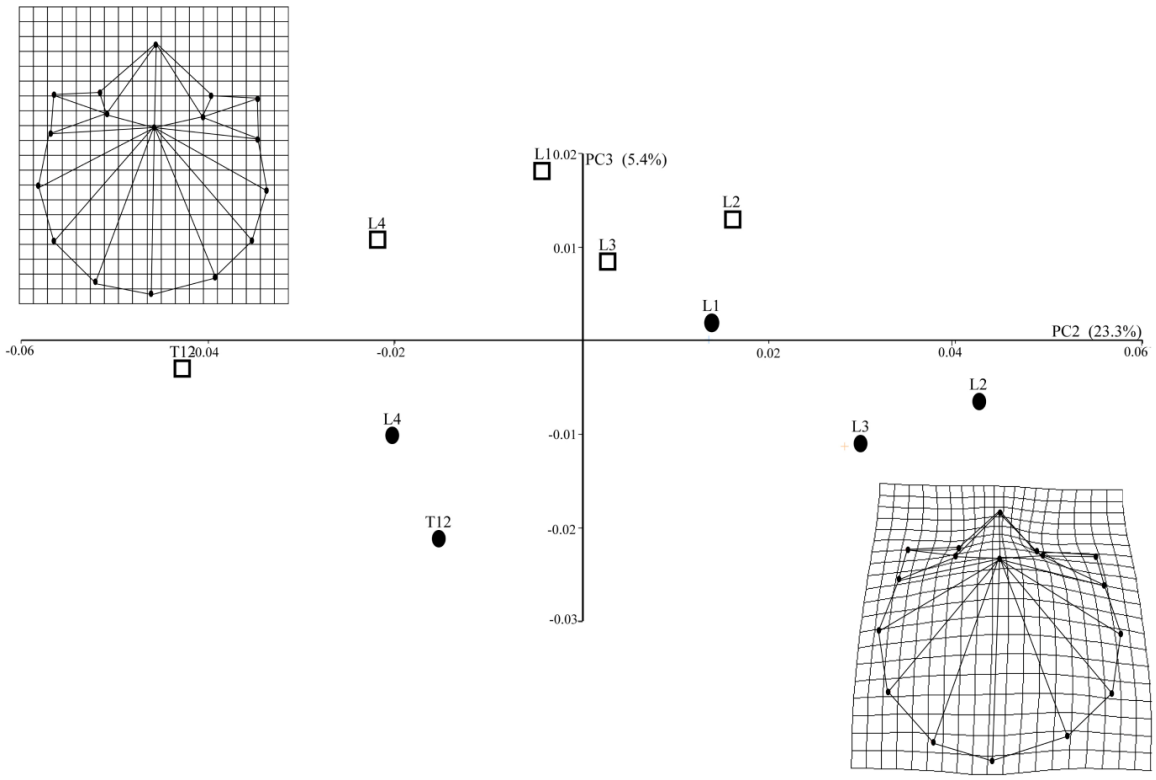


Figure 5) PCA chart illustrating shape variability of sample means on PC2 and PC3, representing 28.7% of the total variance (open squares – healthy, filled circles – affected). Affected and healthy vertebrae separate on a combination of PC2 and PC3. Wireframes illustrate the mean shape of healthy (left) and affected (right) vertebrae, with deformation multiplied by 2 for ease of interpretation.

To increase sample size, analyses were repeated using only the eight landmarks of the neural foramen and pedicles (Table 3), the anatomy of which had been shown to differ between healthy and affected bones in the analyses of the full dataset. Decreasing the number of landmarks generally decreases the power of the discriminant function, with the exception of those bones which already had poor success rate in the initial cross-validation (L1 and L4: table 5). Figure 6 illustrates the shape variance of group means, with affected and healthy vertebrae separating on PC2 and PC3. The DFA of group means had a 90% (100% affected,

80% healthy) accuracy of classifying affected and healthy groups on the first 3 PCs, representing 99.2% of the total variance.

Table 5) Summary of correctly identified vertebrae from the DFA with cross-validation based on eight landmarks of the neural canal and pedicles for each vertebra with the number of PCs included and total variance for each.

| | **DFA Scores** | | | **PCs** |
|---|---|---|---|---|
| | Affected | Healthy | Total | % Total Variance |
| **T12** | 80.8 % | 81.2 % | 81.0 % | 3 PCs = 78.2 % |
| **L1** | 77.3 % | 73.9 % | 75.6 % | 8 PCs = 96.9 % |
| **L2** | 68.0 % | 75.0 % | 70.7 % | 6 PCs = 93.6% |
| **L3** | 65.4 % | 82.4 % | 72.1 % | 5 PCs = 93.2 % |
| **L4** | 64.7 % | 71.4 % | 69.2 % | 5 PCs = 89.4 % |

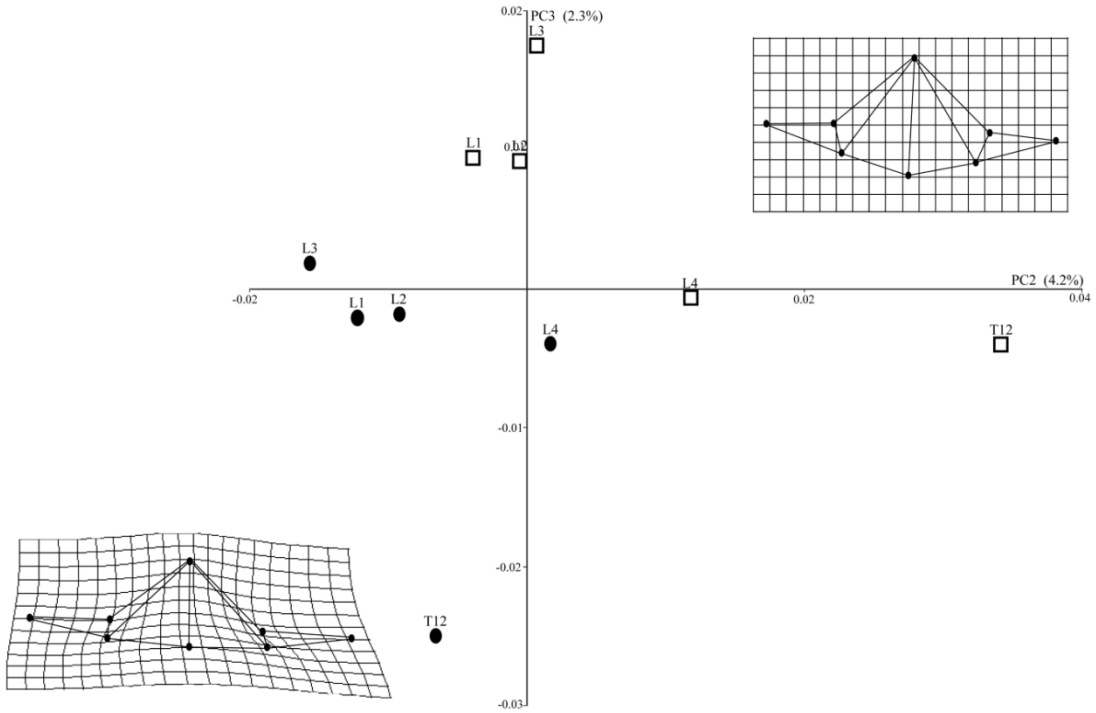


Figure 6) PCA chart illustrating shape variability of group means on PC2 and PC3, representing 6.5% of the total variance (open squares – healthy, filled circles – affected). Wireframes illustrate the mean shape of healthy (right) and affected (left) vertebrae, with deformation multiplied by 2 for ease of interpretation.

**Discussion:**

The results indicate a correlation between vertebral morphology and the presence of Schmorl's nodes at the thoraco-junction and vertebrae L2-4 of the lumbar spine. Affected and healthy T12s were correctly classified with an accuracy of 100% based on vertebral morphology. The morphology of the lumbar spine, with the exception of L1, is also strongly correlated with the presence of Schmorl's nodes, with L2 and L3 having the highest DFA scores (87.5% and 100%) for classifying affected and healthy vertebrae. These results support

the previous findings in the lower thoracic spine and indicate that the shape characteristics identified in affected lumbar vertebrae are similar to those identified in affected T10 to T12 vertebrae (Plomp et al. 2012).

Figures 4 and 5 illustrate how affected and healthy means separate based on shape variables illustrated on PC2 and 3, indicating that the shape differences associated with affected vertebrae are similar in the twelfth thoracic vertebrae and lumbar spine, regardless of spinal region. The group means represent a reduced variance that best discriminates between these groups and the actual variance would show some overlap between the groups. However, our results do suggest that the general morphological trends occurring in affected vertebrae are similar in vertebrae from T12 to L4. The group means of affected and healthy vertebrae with 17 landmarks separate on a combination of PC2 and PC3, which represents 28.7% of the total shape variance. Considering that this sample consists of five morphologically and functionally different vertebrae, the results are of great biological relevance. There was no statistical difference identified with the 17 landmarks on L1, but when the larger sample included in the eight landmark dataset was analysed, there was a significant difference found between healthy and affected L1 vertebrae.

The morphology of affected vertebrae in the lumbar spine is similar to the morphology of affected vertebrae in the lower thoracic spine identified in our previous study (Plomp et al. 2012), with shape differences being most obvious in T12, L2, and L3. Harrington et al. (2001) found that larger vertebral bodies in males and more circular vertebral bodies in males and females in the lower lumbar spine were correlated with disc herniations, as predicted by LaPlace's law. LaPlace's law states that the tensile strength of a fluid filled tube (i.e. the intervertebral disc) under compression is directly related to its radius, with a larger radius

being less able to withstand compressive forces (Letić 2012). The shape of vertebrae with Schmorl's Nodes identified in this study, with the posterior margin of the vertebral body encroaching into the neural foramen, would have a larger antero-posterior radius than healthy vertebrae. This shape could invoke LaPlace's law and cause the intervertebral discs to withstand compressional stress less efficiently than the more heart-shaped healthy vertebrae (Harrington et al. 2001; Plomp et al. 2012). This hypothesis requires clinical experimentation of spines with associated soft-tissue in order to verify the relationship between vertebral body shape and vertical disc herniation. However, the current study, along with the findings of Harrington et al. (2001) and Plomp et al. (2012), indicate that vertebral morphology is strongly associated with the development of Schmorl's nodes.

The strongest distinction between foramen and pedicle shape in relation to the presence of Schmorl's nodes occurs in T12 and L3. The strong association in T12 may indicate the importance of vertebral morphology on biomechanics at this transition from the thoracic to lumbar spine. The thoraco-lumbar junction (T12-L1) represents a change from one functional spinal unit to another, with morphological differences in the articular facets and vertebral bodies between the kyphotic thoracic spine and the lordotic lumbar spine (Masharawi et al. 2004, 2005, 2008; Qui et al. 2006). Dar et al. (2010) have suggested that the amount of torsional movement and the resulting stress of these movements on the different spinal segments (thoracic and lumbar) may also influence the herniation of the disc and subsequent formation of the Schmorl's node. The thoracic spine has facets oriented on the frontal plane which permit axial rotation, whereas the lumbar spine has facets oriented on the sagittal plane that limit axial rotation (Qui et al. 2006). Although, 2D shape analysis of the medial-lateral width and orientation of the articular facets did not find any correlation with the presence of

Schmorl's nodes in the lower thoracic vertebrae (Plomp et al. 2012), it is possible that future analyses of vertebrae in three dimensions will identify important morphological differences occurring in the articular facets. L3 is not a transitional vertebra and it shows similar results as T12, making it difficult to associate the strength of the DFA score with a transitional morphology. These results may indicate an important aspect of lumbar spine biomechanics, as each vertebra displays a different degree of correlation between morphology and Schmorl's nodes which may be related to a difference in biomechanical function and stress along the thoracic and lumbar spine.

The amount of loading, as well as the type and range of movement permitted, varies along the thoracic and lumbar spine (Edmondston & Singer 1997; Frtiz et al. 1998). Spinal and vertebral morphology plays a significant role in biomechanics (Robbins et al. 1994; Noailly et al. 2007), and clinical studies have found that disc herniation occurs when there is repetitive flexion and extension of the spine with moderate to heavy loads (Gordon 1991; Callaghan & McGill 2001). This highlights the importance of considering both different types of spinal movement and vertebral morphology as risk factors in disc herniation. The vertebral morphology identified in the current study may play a vital role in the ability of vertebrae to withstand loaded extension and flexion. Many studies have found a complex relationship between morphology of the posterior vertebral elements and vertebral stability (Adams et al. 2006; Fields et al. 2010; Robson Brown et al. 2008). Whyne *et al*. (1998) found that the pedicles provide a supportive buttress during compressive forces acting on the vertebrae at the thoraco-lumbar junction. The posterior arch and pedicles provide structural support to the posterior wall of the vertebral body and aid in tension resistance (Whyne et al. 1998; El-Khoury & Whitten 1993). Severe degeneration of the intervertebral disc results in a transfer of

loading from the vertebral body to the neural arch, causing the posterior elements to withstand a greater amount of the compressive force during upright posture (Adams 2012, Adams et al. 2006). Schmorl's nodes have been associated with degenerative disc changes in the lumbar spine (Williams et al. 2007). The morphology of the pedicles could affect the structural support these features provide for the more circular vertebral bodies, especially if they were to undergo abnormal loading due to the transfer of weight after disc degeneration. Again, this hypothesis requires biomechanical experiments performed on vertebrae and their associated soft tissue in order to investigate the exact role that these vertebral elements have on spinal stability.

The aetiology of Schmorl's nodes is unclear; however, a genetic predisposition and underlying congenital factors have been suggested to be the key causes, with physical strain influencing their development (Dar et al. 2009, 2010; Williams et al. 2007; Mok et al. 2010). Schmorl's nodes have been found to differentially affect individuals based on sex and ethnic background, and Dar et al (2009) conclude that the aetiology of Schmorl's nodes may be congenital and likely develop during spinal maturation. The present study supports our previous findings (Plomp et al. 2012) in that 2D vertebral shape is correlated with the presence of Schmorl's nodes. It also provides an expansion of the previous findings by indicating that the shape of affected vertebrae identified in the lower thoracic spine are similar throughout the thoraco-lumbar and lumbar spine. The vertebral shape identified may be the result of a developmental factor determining the morphology of the vertebrae and eventually predisposing them to the formation of the lesions due to the influence of spinal morphology on the overall stability and function of the spine.

Although there is a relationship between physical strain on the spine with the occurrence of intervertebral disc herniation (Callaghan & McGill 2001; Goto et al. 2002), it is suggested that palaeopathologists should be cautious when using the presence of Schmorl's nodes to indicate physical activity in the past. The current results pertaining to the twelfth thoracic vertebra and the first to fourth lumbar vertebrae, as well as other studies, indicate that factors other than physical activity are also influencing herniations of the intervertebral disc (Harrington et al. 2001; Williams et al. 2007) and the development of Schmorl's nodes (Dar et al. 2009, 2010; Plomp et al. 2012).

**Conclusion:**

The results support and extend the findings of our previous study and indicate that the relationship between vertebral morphology and Schmorl's nodes is an area which would benefit from further research. A particular morphology of the twelfth thoracic vertebra and the lumbar spine is strongly associated with the presence or absence of Schmorl's nodes. The reason for this relationship remains unclear; however, the shape of the pedicles and posterior aspect of the vertebral body plays a vital role in spinal stability and the ability of the vertebral elements to withstand physical stress. The pedicle morphology identified in this analysis may provide inadequate buttressing for a relatively larger vertebral body, resulting in a decrease of the disc's ability to withstand stress during loaded flexion-extension and torsional movements, causing the intervertebral disc to herniate into the vertebral endplate. This hypothesis requires biomechanical experiments of spines and their associated soft-tissue in order to investigate the exact influence pedicle morphology has on spine stability. The results of such a study could have clinical significance, especially in relation to the need for spinal surgery and pedicle pin placement.

The use of archaeological skeletal remains allows the analysis of vertebrae in their dry state from multiple populations from different time periods and geographic locations, and this study illustrates the benefits of considering a condition seen clinically with a deeper time perspective than is possible in clinical situations. The methods used in this research are transferable to CT scans and radiographs and have potential for predicting the development of Schmorl's nodes in the living. Future research will analyze 3D morphology of both the lower thoracic and lumbar spines to identify shape variation not seen in 2D analysis. It will also focus on complete spines from documented skeletal collections, where information on body mass and lifestyle is available. The current study focuses on the variation in morphology in the thoraco-lumbar spines of one archaeological skeletal population, with variable preservation of vertebrae for each individual. Future research looking at a larger number of skeletal samples, as well as individuals with entire spines preserved will provide further insight into the relationship between vertebral morphology and health in modern human populations.

**Acknowledgments:**

The authors would like to thank Malin Holst, York Osteoarchaeology, Mike Griffiths Associates, and Field Archaeology Specialists, York for the excavation and initial analysis of the Fishergate House skeletons, and to Durham University for access to this now curated site. Special thanks go to Durham University and the Canadian Centennial Scholarship Fund for financial aid to KAP during this research and Helgi Pétur Gunnarsson for help with the analyses.

**References:**


Acsádi, G, Nemeskéri, J. 1970. *History of human life span and mortality*. Akadémiai Kiadó, Budapest.

Adams MA. 2012. Basic science of spinal degeneration. *Surgery* 30(7): 347-350.

Adams MA, Pollintine P, Tobias JH, Wakley GK, Donal P. 2006. Intervertebral disc degeneration can predispose to anterior vertebral fractures in the thoracolumbar spine. *Journal of Bone Mineral Research* 21(9): 1409-1416.

Alesan A, Malgosa A, Simó C. 1999. Looking into the demography of an Iron Age population in the Western Mediterranean. I. Mortality. *American Journal of Physical Anthropology* 110: 285-301.

Anakwenze OA, Kancheria V, Rendon N, Drummond DS. 2011. Adolescent disc dysplasia and back pain. *Journal of Child Orthopaedics* 5: 49-53.

Baranto A, Hellström M, Nyman R et al. 2006. Back pain and degenerative abnormalities in the spine of young elite divers: A 5 years follow-up magnetic resonance imaging study. *Knee Surgery and Sports Traumatology Arthroscopy* 14: 907-14.

Baylac M, Frieβ M. 2005. Fourier descriptors, Procrustes superimposition, and datadimensionality: An example of cranial shape analysis in modern human populations. In: Slice D, ed. *Modern Morphometrics in Physical Anthropology*. New York: Springer 145-62.

Bienvenu T, Guy F, Coudyzer W et al. 2011. Assessing endocranial variations in great apes and humans using 3D data from virtual endocasts. *American Journal of Physical Anthropology* 145: 231-46.

Bookstein F. 1997. Landmark methods for forms without landmarks: Morphometrics of group differences in outline shape. *Medical Image Analysis* 1(3): 225-43.

Brooks ST, Suchey JM. 1999. Skeletal age determination based on the os pubis: Comparison of the Acsádi-Nemeskéri and Suchey-Brooks methods. *Journal of Human Evolution* 5: 227-38.

Buikstra JE, Ubelaker DH. 1994. *Standards for Data Collection from Human Skeletal Remains*. Research Series, no. 44. Fayetteville, Arkansas Archaeological Survey.

Burke KL. 2012. Schmorl's nodes in an American military population: Frequency, Formation, and Etiology. *Journal of Forensic Sciences* 57(3): 571-7.

Caffell A, Holst M. 2010. *The church of St. Michael and St. Lawrence, Fewston, North Yorkshire*. York Osteoarchaeology Ltd

Callaghan JP, McGill SM 2001. Intervertebral disc herniation: studies on a porcine model exposed to highly repetitive flexion/extension motion with compressive force. *Clinical Biomechanics* 16:28-37.

Cardini A, Nagorsen D, O'Higgins P et al. 2009. Detecting biological distinctiveness using geometric morphometrics: An example case from the Vancouver Island Marmot. *Ethology, Ecology & Evolution* 21: 209-23.

Dar G, Masharawi Y, Peleg S et al. 2010. Schmorl's nodes distribution in the human spine and its possible etiology. *European Spine Journal* 19: 670-5.

Dar G, Peleg S, Masharawi Y et al. 2009. Demographic aspects of Schmorl's nodes. *Spine* 34(9): E312-15.

Edmondston SJ, Singer KP. 1997. Thoracic spine: anatomical and biomechanical considerations for manual therapy. *Manual Therapy* 2(3): 132-143.

El-Khoury GY, Whitten CG. 1993. Trauma to the upper thoracic spine: Anatomy, biomechanics, and unique imaging features. *American Journal of Roentgenology* 160(1): 95-102.

Faccia KJ, Williams RC. 2008. Schmorl's nodes: Clinical significance and implications for the bioarchaeological record. *International Journal of Osteoarchaeology* 18(1): 28-44.

Fields AJ, Lee GL, Keaveny TM. 2010. Mechanisms of initial endplate failure in the human vertebral body. *Journal of Biomechanics* 43: 2126-3131.

Fritz JM, Erhard RE, Hagen BF. 1998. Segmental instability of the lumbar spine. *Physical Therapy* 78: 889-896.

Goodall C. 1991. Procrustes methods in the statistical analysis of shape. *Journal of the Royal Statistical Society*. Series B 53(2): 285-339.

Gordon SJ, Yang KH, Mayer PJ et al. 1991. Mechanism of disc rupture: A preliminary report. *Spine* 16(4): 450-6.

Goto K, Tajima N, Chosa E, Totoribe K, Kuroki H, Arizumi Y, Arai Takashi. 2002. Mechanical analysis of the lumbar vertebrae in a three-dimensional finite element method model in which intradiscal pressure in the nucleus pulposus was used to establish the model. *Journal of Orthopaedic Science* 7: 243-246.

Harrington JF, Sungarian A, Rogg J, Makker VJ, Epstein MH. 2001. The relation between vertebral endplates shape and lumbar disc herniations. *Spine* 26: 2133-8.

Holst M. 2005. *Fishergate House artefacts and environmental evidence: The human bone*. Arch Planning Consultancy, UK; Accessed online, July 3, 2010.

Işcan MY, Loth SR, Wright RK. 1984. Age estimation from the rib by phase analysis: White males. *Journal of Forensic Sci*ences 29: 1094–104.

Işcan MY, Loth SR, Wright RK. 1985. Age estimation from the rib by phase analysis: White females. *Journal of Forensic Sci*ences 30: 853–63.

Kimmerle EH, Ross A, Slice, D. 2008. Sexual dimorphism in America: Geometric morphometric analysis of the craniofacial region. *Journal of Forensic Sci*ences 53(1): 54-7.

Knüsel CJ, Göggel S, Lucy D. 1997. Comparative degenerative joint disease of the vertebral column in the medieval monastic cemetery of the Gilbertine Priory of St. Andrew, Fishergate, York, England. *American Journal of Physical Anthropology* 103: 481-95.

Kovarovic K, Aiello LC, Cardini A, Lockwood CA. 2011. Discriminant function analyses in archaeology: are classification rates too good to be true? *Journal of Archaeological Science* 38: 3006-18.

Klaus HD, Larsen CS, Tam ME. 2009. Economic intensification and degenerative joint disease: Life and labor on the postcontact north coast of Peru. *American Journal of Physical Anthropology* 139: 204-21.

Letić M. 2012. Feeling wall tension in an interactive demonstration of Laplace's law. *Advances in Physiology Education* 36(2): 176

Lieberman DE, Carlo J, Ponce de León M, Zollikofer CP. 2007. A geometric morphometrics analysis of heterochrony in the cranium of chimpanzees and bonobos. *Journal of Human Evolution* 52: 647-62.

Lovejoy CO, Meindl RS, Pryzbeck TR, Mensforth RP. 1985. Chronological metamorphosis of the auricular surface of the ilium: A new method for the determination of age at death *American Journal of Physical Anthropology* 68: 15–28.

Masharawi Y, Salame K, Mirovsky Yet al. 2008. Vertebral body shape variation in the thoracic and lumbar spine: Characterization of its asymmetry and wedging. *Clinical Anatomy* 21: 46-54.

Masharawi Y, Rothschild B, Salame K et al. 2005. Facet tropism and interfacet shape in the thoracolumbar vertebrae: Characterizations and biomechanical interpretation. *Spine* 30(11): E281-92.

Masharawi Y, Rothschild B, Dar G et al. 2004. Facet orientation in the thoracolumbar spine. *Spine* 29(16): 1755-63.

Milner GR. 1992. *Determination of skeletal age and sex: A manual prepared for the Dickson Mound reburial team.* Dickson Mound Museum, Lewiston, Illinois.

Mok F, Samartzis D, Karppinen J et al. 2010. Prevalence, determinants, and association of Schmorl's nodes of the lumbar spine with disc degeneration: A population-based study of 2449 Individuals. *Spine* 35(21): 1944-52.

Neubauer S, Gunz P, Hublin JJ. 2010. Endocranial shape changes during growth in chimpanzees and humans: A morphometric analysis of unique and shared aspects. *Journal of Human Evolution* 59:555-66.

Neubauer S, Gunz P, Hublin JJ. 2009. The patterns of endocranial ontogenetic shape changes in humans. *Journal of Anatomy* 215: 240-55.

Noailly J, Wilke HJ, Planell JA, Lacroix D. 2007. How does geometry affect the internal biomechanics of a lumbar spine bi-segment finite element model? Consequences on the validation process. *Journal of Biomechanics* 40: 2414-2425.

Novak M, Šlaus M. 2011. Vertebral pathologies in two early modern period ($16^{th}$-$19^{th}$ Century) populations from Croatia. *American Journal of Physical Anthropology* 145: 270-81.

O'Higgins P. 2000. The study of morphological variation in the hominid fossil record: Biology, landmarks and geometry. *Journal of Anatomy* 197(1): 103-20.

O'Higgins P, Jones N. 2006. *Morphologika: Tools for statistical shape analysis*. Hull York Medical School.

Overvliet GM, Beuls EAM, ter Laak-Poort M, Cornips EMJ. 2009. Two brothers with a symptomatic thoracic disc herniation at T11-T12: Clinical report. *Acta Neurochir* 151: 393-96.

Papathanasiou A. 2005. Health status of the Neolithic population of Alepotrypa Cave, Greece. *American Journal of Physical Anthropology* 126: 377-390.

Phenice TW. 1969. A newly developed visual method of sexing the os pubis. *American Journal of Physical Anthropology* 30: 297–302

Pfirrmann C, Resnick D. 2001. Schmorl's nodes of the thoracic and lumbar spine: Radiographic-pathologic study of prevalence, characterization, and correlation with degenerative changes of 1,650 spinal levels in 100 cadavers. *Radiology* 219: 368-74.

Plomp KA, Roberts CA, Strand Viðarsdóttir U. 2012. Vertebral morphology influences the development of Schmorl's nodes in the lower thoracic vertebrae. *American Journal of Physical Anthropology* 149(4): 572-582.

Qui TX, Teo EC, Zhang QH. 2006. Comparisons of kinematics between thoracolumbar T11-T12 and T12-L1 functional spinal units. *Journal of English Medicine* 220: 493-504.

R Development Core Team. *R: A language and environment for statistical computing*. R Foundation for Statistical Computing Vienna, Austria. ISBN 3-900051-07-0, URL http://www.R-project.org; 2012

Rannou F, Corvol M, Revel M, Poiraudeau S. 2001. Disk degeneration and disk herniation: the contribution of mechanical stress. *Joint Bone Spine* 68: 543-46.

Robb J. 1994. Skeletal signs of activity in the Italian Metal Ages: Methodological and interpretative notes. *Human Evolution* 9(3): 215-29.

Robb J, Bigazzi R, Lazzarini L et al. 2001. Social "status" and biological "status": A comparison of grave goods and skeletal indicators from Pontecagnano. *American Journal of Physical Anthropology* 115: 213-22.

Robbin A, Skalli W, Lavaste F. 1994. Influence of geometrical factors on the behavior of lumbar spine segments: a finite element analysis. *European Spine Journal* 3: 84-90.

Robson Brown K, Pollintine P, Adams M. 2008. Biomechanical implications of degenerative joint disease in the apophyseal joints of human thoracic and lumbar vertebrae. *American Journal of Physical Anthropology* 136: 218-326.

Rohlf FJ. 2004. Version 1.40. *Ecology and Evolution*, SUNY at Stony Brook.

Rohlf FJ. 2003. Bias and error in estimates of mean shape in geometric morphometrics. *Journal of Human Evolution* 44: 665-83.

Rohlf FJ, Slice D. 1990. Extensions of the Procrustes method for the optimal superimposition of landmarks. *Systematic Zoology* 39(1): 40-59.

Saluja G, Fitzpatrick K, Bruce M, Cross J. 1986. Schmorl's nodes (intervertebral herniations of intervertebral disc tissue) in two historic British populations. *Journal of Anatomy* 145: 87-96.

Sandness KL, Reinhard KJ. 1992. Vertebral pathology in prehistoric and historic skeletons from Northeastern Nebraska. *Plains Anthropologist* 37(141): 299-309.

Schmorl G, Junghans H. 1971. *The human spine in health and disease*. New York: Grune & Stratton.

Šlaus M. 2000. Biocultural analysis of sex differences in mortality profiles and stress levels in late Medieval populations from Nova Rača, Croatia. *American Journal of Physical Anthropology* 111: 193-209.

Slice DE. 2007. Geometric morphometrics. *Annual Review of Anthropology* 36: 261-81.

Üstündağ H. 2009. Schmorl's nodes in a Post-Medieval skeletal sample from Klostermarienberg, Austria. *International Journal of Osteoarchaeology* 19: 695-710.

White JW, Ruttenberg BI. 2007. Discriminant function analysis in marine ecology: Some oversights and their solutions. *Marine Ecology Progress Series* 329: 301-5.

Whyne CM, Hu SS, Klisch S, Lotz J. 1998. Effect of the pedicle and posterior arch on vertebral body strength predictions in finite element modeling. *Spine* 23(8): 899-907.

Williams FMK, Manek NJ, Sambrook PN et al. 2007. Schmorl's nodes: Common, highly heritable, and related to lumbar disc disease. *Arthritis & Rheumatism* 57(5): 855-60.

Zelditch ML, Swiderski DL, Sheets HD, Fink. 2004. *Geometric morphometrics for biologists: A primer*. San Diego, CA: Elsevier Academic Press.

## Chapter 7) Manuscript 3

Submitted to: International Journal of Osteoarchaeology

# Morphological characteristics of healthy and osteoarthritic joint surfaces in archaeological skeletons

K.A.Plomp[1,2*]

C.A. Roberts[2]

U. Strand Viðarsdóttir[1]

1) Evolutionary Anthropology Research Group, Department of Anthropology, Durham University, Dawson Building, South Road, Durham DH1 3LE 2) Department of Archaeology, Durham University, Dawson Building, South Road, Durham DH1 3LE

*** Corresponding author: k.a.plomp@durham.ac.uk**

Abstract:

Osteoarthritis is a major health concern in living populations, as well as being one of the most common pathological lesions identified in the archaeological record. The aetiology of the disease remains unclear, with a multi-factorial influence of physical strain, age, genetics, and obesity. Previous studies have identified a relationship between the presence of knee osteoarthritis on the distal femoral joint and the morphology of the intercondylar notch, patellar groove, and medial condyle. The current study expands this research to investigate the relationship between distal femoral, distal humeral, and proximal ulnar joint morphology and osteoarthritis with 3D shape analysis techniques. These methods provide a more detailed analysis of joint morphology in order to determine any relationship between 3D shape and osteoarthritis. The results indicate a complex relationship between joint shape and knee osteoarthritis, with eburnated right femora showing a statistically significant association. The shapes associated with eburnated or affected femoral joints all relate to osteophyte development, and therefore likely represent systematic shape changes and not a particular joint shape predisposing individuals to the condition. There was no identifiable relationship found in the proximal ulna or distal humerus, indicating that joint shape is unlikely to influence the development of the condition in the elbow joint, and that any shape changes produced by osteoarthritis are not systematic or quantifiable. The joints analysed in this study were highly influenced by asymmetry, sexual dimorphism, and allometry, resulting in a small sample size of affected joints in many datasets. Further analyses of large skeletal samples are needed to more thoroughly investigate the possible relationship of distal femoral joint shape and osteoarthritis.

Keywords: geometric morphometrics, eburnation, osteophytes, degenerative joint disease

**Introduction:**

Osteoarthritis receives a great deal of attention in both palaeopathological and clinical studies due to its high frequency in human populations past and present (palaeopathological literature: Bridges 1991; Jurmain 1999; Weiss & Jurmain 2007; Waldron 1991; Lieverse et al. 2006; clinical literature: Cushnaghan & Dieppe 1991; McGonagle et al. 2010; Zhai et al. 2007; Hootman et al. 2003). It has a major impact on modern life, with many individuals over the age of 65 years affected by osteoarthritis in one or more joints (Dominick & Baker 2004). Despite its prevalence, the aetiology of osteoarthritis continues to elude researchers. The main theories to date are biomechanical breakdown of the joint due to physical stress, degeneration associated with increasing age, a genetic predisposition, and sex hormones (Molnar et al. 2009; Felson et al. 2000; Herrero-Beaumont et al. 2009; Spector et al. 1996; Rogers et al. 2004; Weiss 2006). It is now generally accepted that osteoarthritis is a multifactorial disease with multiple aetiological factors contributing to the overall degeneration or break-down of the joint structure (Felson et al. 2000; Spector & MacGregor 2004; Weiss 2006).

The occurrence of osteoarthritis of the knee is very common (Rogers et al. 1990; Bridges 1992; Weiss & Jurmain 2007). Felson et al. (1987) found a prevalence rate of 27% in individuals less than 70 years of age and in 44% of individuals over 80 years of age being affected by knee osteoarthritis in the Framingham Heart Study cohort, USA. In contemporary Western populations knee osteoarthritis is one of the main causes of pain and disability, and often attributed to obesity which causes increased stress on the joint (Manek et al. 2003; Spector et al. 1994; Felson et al. 1988; Cooper et al. 2000; Maly et al. 2008; Spector & Hart 1992). Osteoarthritis of the elbow has been considered uncommon, with clinical prevalence reported at 1.3 – 7% (Dalal et al. 2007; Rettig et al 2008). However, elbow osteoarthritis has

been found to be more prevalent in archaeological samples, with Debono et al. (2004) reporting 27% of individuals affected from a Medieval necropolis in Provence, France. This difference could be due to the condition being under-reported clinically, the use of different diagnostic criteria (radiographs, CT scans, macroscopic analysis of dry bone), or differences in physical activities between living and past populations (Doherty & Preston 1989; Debono et al. 2004).

Although the majority of osteoarthritis research focuses on the articular cartilage, the idea that other joint components, including the ligaments and the subchondral bone, also play an important role in the development and progression of osteoarthritis has been gaining credibility (Karsdal et al. 2008; Tan et al. 2006; Brandt et al. 2006; Hunter et al. 2005; Bailey et al. 2004). Bone morphology is influenced by epigenetic factors, including biomechanical stress during growth or remodeling (Pearson & Lieberman 2004; Ruff 2000). However, subchondral bone has been found to have far less plasticity when it comes to physical influences than the diaphyseal cross-section or trabecular architecture (Ruff & Runestad 1992), suggesting that, in the absence of pathology, the joint geometry developed during childhood is retained throughout adulthood (Frost 1994a,b). There is a complex relationship between genetics and physical stress and the development of osteoarthritis. It is hypothesized that the morphology of the joint itself, influenced by genetics and biomechanical necessity, may influence the development or progression of osteoarthritis by contributing to the overall stability and functionality of the joint compartment (Frost 1994a,b; Wada et al. 1999; Shepstone et al. 1999, 2001; Quasnichka et al. 2005). The current study aims to identify a possible relationship between joint morphology of the knee and/or elbow with osteoarthritis. The specific joints chosen for analysis are the distal femur, distal humerus, and proximal ulna.

These joints were chosen because they undergo different physical stress and strains which would likely impact the importance of morphology on the biomechanics and function of the joints.

Previous research in this area is limited. Rettig et al. (2008) used metric analyses on radiographs of 90 elbows of living patients from Indiana, USA to identify any morphological characteristics of the distal humerus which may predispose individuals to osteoarthritis. However, they found no statistically significant relationships. Shepstone et al. (1999, 2001) performed a 2D shape analysis using geometric morphometrics on the inferior aspect of the distal femoral joint of 101 adult femora from the archaeological skeletal collection of St. Peter's Church, Barton on Humber, UK (Waldron & Rodwell 2007). They were able to identify a relationship between distal femoral shape and osteoarthritis, with the eburnated joints having narrower U shaped intercondylar notches, wider medial condyles, and shallower patellar grooves. The authors suggest that the shape difference of the intercondylar notch may be a risk factor for developing osteoarthritis but suggest further research is needed (Shepstone et al. 2001). Wada et al (1999) performed a traditional morphometric analysis on patients and cadavers, and also found a correlation between narrow intercondylar notches and the progression of osteoarthritis. Their results suggest that osteophyte development in the intercondylar notch occurs to stabilize the anterior cruciate ligament (ACL) in the early stages of osteoarthritis.

This paper expands the previous work by analyzing the full three-dimensional morphology of the distal femur, distal humerus, and proximal ulna from archaeological skeletal populations to identify possible correlations of joint shape with osteoarthritis. The secondary aim of this paper is to investigate the potential of using 3D geometric morphometric

techniques in osteoarthritis studies, as these methods could also be employed in clinical research. These methods will enable a more detailed and accurate investigation of the relationship between joint shape and osteoarthritis than is possible with 2D shape analyses or traditional morphometrics. As Shepstone et al. (1999, 2001) and Wada et al. (1999) have found a correlation between joint morphology and osteoarthritis in the distal femur, it stands to reason that osteoarthritis may also correlate with the morphology of the distal humerus and proximal ulna. The null hypothesis to be tested is one of no relationship between joint morphology and the presence of osteoarthritis. If this is refuted and a relationship exists, it could indicate a joint morphology which in itself influences the development and/or progression of osteoarthritis.

**Materials and Methods:**

One hundred and forty-seven individuals, producing a total of 155 ulnae, 200 humeri, and 105 femora, from four archaeological English populations dating from the $4^{th}$-$19^{th}$ centuries AD were analysed. These populations were chosen based on the large number of well preserved adult skeletons. The number of joints per individual studied was dependent on preservation (Table 1, Table 2). Age and sex of skeletons were determined using standard osteological methods using cranial, mandibular, and pelvic morphology (Phenice 1969; Acsadi & Nemeskeri 1970; Lovejoy et al. 1985; Işcan et al. 1984, 1985; Brooks & Suchey 1990; Milner 1992).

Table 1) Number of individuals analysed for each skeletal collection, with number of males and females summarized.

| Site | Context | Period | Reference | ♀ | ♂ | YA | MA | OA | Total |
|---|---|---|---|---|---|---|---|---|---|
| **Hereford Cathedral, Cathedral Close, Hereford, Herefordshire** | Urban | Late medieval ($7^{th}$-$15^{th}$ C) | Weston *et al, in prep*; | 29 | 27 | 26 | 10 | 20 | **56** |
| **St James and St Mary Magdalene, Chichester, Sussex** | Leprosarium Almshouse | Late medieval ($12^{th}$-$16^{th}$ C) | Magilton et al 2008 | 19 | 47 | 20 | 17 | 29 | **66** |
| **Baldock, Hertfordshire** | Urban | Romano-British ($4^{th}$ C) | Roberts 1984a, 1984b | 7 | 11 | 9 | 4 | 5 | **18** |
| **Hickleton, South Yorkshire** | Rural | Late/ Post-medieval ($11^{th}$ -$19^{th}$ C) | Sydes 1984, Stroud *unpublished* | 3 | 4 | 4 | 1 | 2 | **7** |
| | | | **Total** | **58** | **89** | **59** | **32** | **56** | **147** |

Eburnation describes polishing of the joint surface due to the complete loss of articular cartilage and is considered to be pathognomonic of osteoarthritis in palaeopathology (Waldron 1991; Ortner 2003). Eburnation was recorded as present or absent on the joint surface. The location of eburnation was reported to differentiate between joint compartments affected (e.g. tibio-femoral, femoro-patellar, radio-capitellar, ulno-trochlear). Osteophyte formation, porosity, and joint contour change were also recorded and considered in analyses (Rogers & Waldron 1995) (Figure 1). Osteophytes were recorded according to size (</> 2mm from the original joint margin) and according to the percentage of the joint margin covered. The presence of porosity and the percentage of a joint surface covered were also recorded. Joint contour change was recorded based on location (Rogers & Waldron 1995). As there is disagreement in palaeopathology as to which joint changes should be used to diagnose

osteoarthritis (Weiss & Jurmain 2007; Waldron 1991; Jurmain 1991; Rogers & Waldron 1995; Schrader 2012; Rothschild 1997), joints with pathological changes were divided into two groups for analysis. The first group is comprised of only those joints displaying eburnation with osteophytes, porosity, and/or joint contour change and this group is compared with healthy joints. The second group is comprised of joints displaying eburnation, or two or more of osteophytes, porosity, and joint contour change (based on Rogers & Waldron 1995). For simplicity, the first group is identified as 'eburnated' and the second is termed 'osteoarthritis'. Table 2 summarizes the composition of the data for side, sex, and health of each joint.

Table 2) Number of joints for each side and sex in groups labeled as eburnated, osteoarthritis (including those from the eburnation group), and healthy controls. Number of joints per individual studied was dependent on joint preservation.

| | | Eburnated | | Osteoarthritis | | Healthy | | | |
|---|---|---|---|---|---|---|---|---|---|
| | | ♀ | ♂ | ♀ | ♂ | ♀ | ♂ | **Total** | |
| Ulnae | Left | 2 | 8 | 8 | 16 | 20 | 31 | **75** | |
| | Right | 0 | 11 | 7 | 15 | 20 | 28 | **80** | **155** |
| Humeri | Left | 2 | 6 | 5 | 15 | 32 | 46 | **98** | |
| | Right | 3 | 8 | 10 | 21 | 27 | 44 | **102** | **200** |
| Femora | Left | 0 | 2 | 4 | 11 | 17 | 21 | **53** | |
| | Right | 3 | 3 | 7 | 14 | 12 | 19 | **52** | **105** |

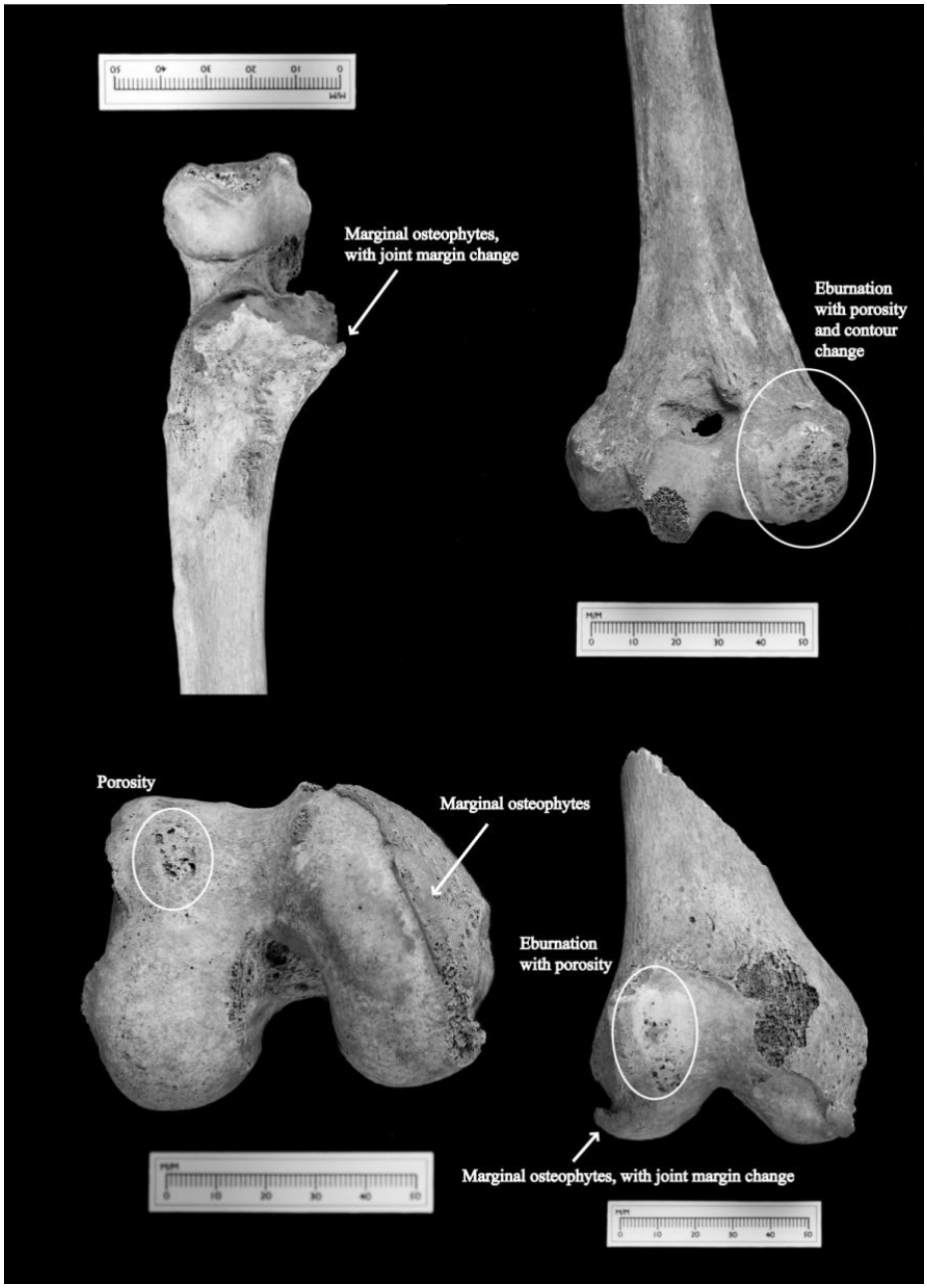


Figure 1) Examples of osteoarthritis with areas of eburnation with porosity circled and arrows indicating osteophyte formation. (Photographs by Jeff Veitch, Department of Archaeology, Durham University)

Three-dimensional Cartesian coordinates of landmarks were digitized on the joint surfaces using a Microscribe® GLS digitizing system (EMicroscribe Inc) (Figures 2 - 4). These landmark data were then superimposed using generalized Procrustes analysis (GPA), which removes all scale and translational variation from the data (Slice 2007; Rohlf 2003; Goodall 1991; Bookstein 1997; Rohlf & Slice 1990); size information in the form of centroid size, was retained as an independent variable. Centroid size is the square root of the sum of the squared distances of each landmark from the centroid of the landmark configuration (Slice 2007). Principal components analysis (PCA) is used to examine patterns of shape variance (O'Higgins & Jones 1998; Stevens & Strand Viðarsdóttir 2008; Mitteroeker & Gunz 2009). To obtain optimal discrimination between groups and reduce noise on higher principal components (PC), the number of PCs included in the cross-validated DFA was reduced using the method proposed by Baylac and Frieβ (2005) and analyses were run on PCs representing five percent or more of the total shape variance (Zelditch et al. 2004; O'Higgins & Jones 1998; Stevens & Strand Viðarsdóttir 2008; Mitteroeker & Gunz 2009). Cross-validated discriminant function analysis (DFA) was used to determine the power of discrimination between healthy joints and those with osteoarthritic changes (White & Ruttenberg 2007; Cardini et al. 2009; Kimmerle et al. 2008). Regression analysis was performed to assess the influence of allometry, age, and sexual dimorphism on the morphology of the joints, and statistical analyses were run on the regression residuals to analyze shape with and without these effects (Slice 2007; Sidlauskas et al. 2011). MANOVAs and ANOVAs were performed to determine statistical significance of group differences, with level of significance set at $p<0.05$. Analyses were run in Morphologika© (O'Higgins & Jones 2006), MorphoJ (Klingenberg 2008), the EVAN toolbox, R (R Development Core Team 2010), and SPSS©

(SPSS Inc.). Intra-observer error was tested with 6 repeated observations of each joint type, and the smallest distance between different joints was equal to or less than 1.5 times the greatest distance between the repeated observations, indicating that intra-observer error was unlikely to affect group classification (Neubauer et al 2009; Neubauer et al 2010; Lieberman et al 2007; Bienvenu 2011).

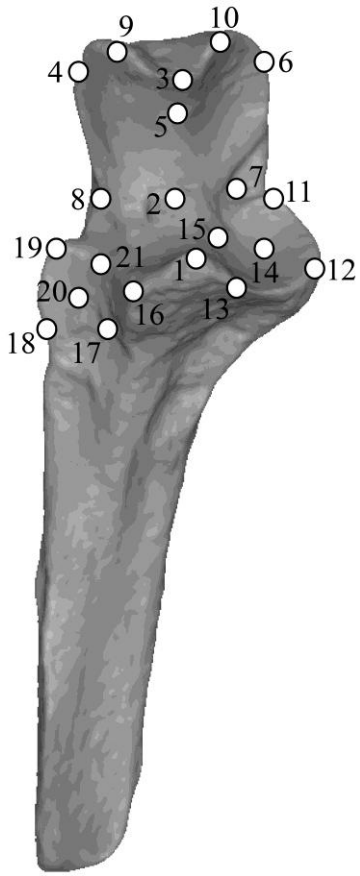


Figure 2) Locations of 21 landmarks digitized on the proximal ulnar joint.

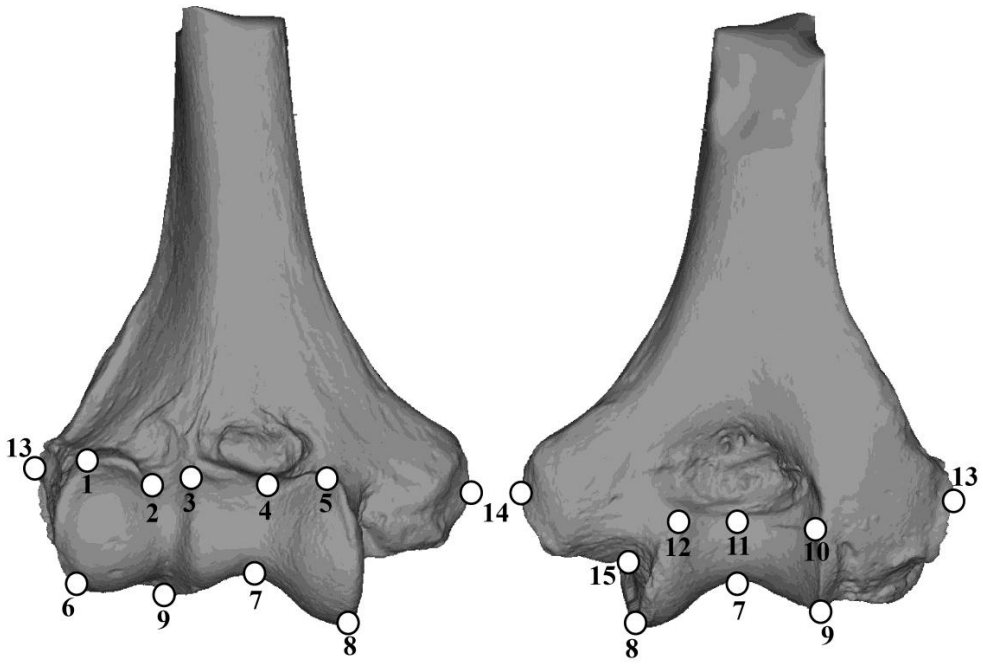


Figure 3) Locations of 15 landmarks digitized on the distal humeral joint.

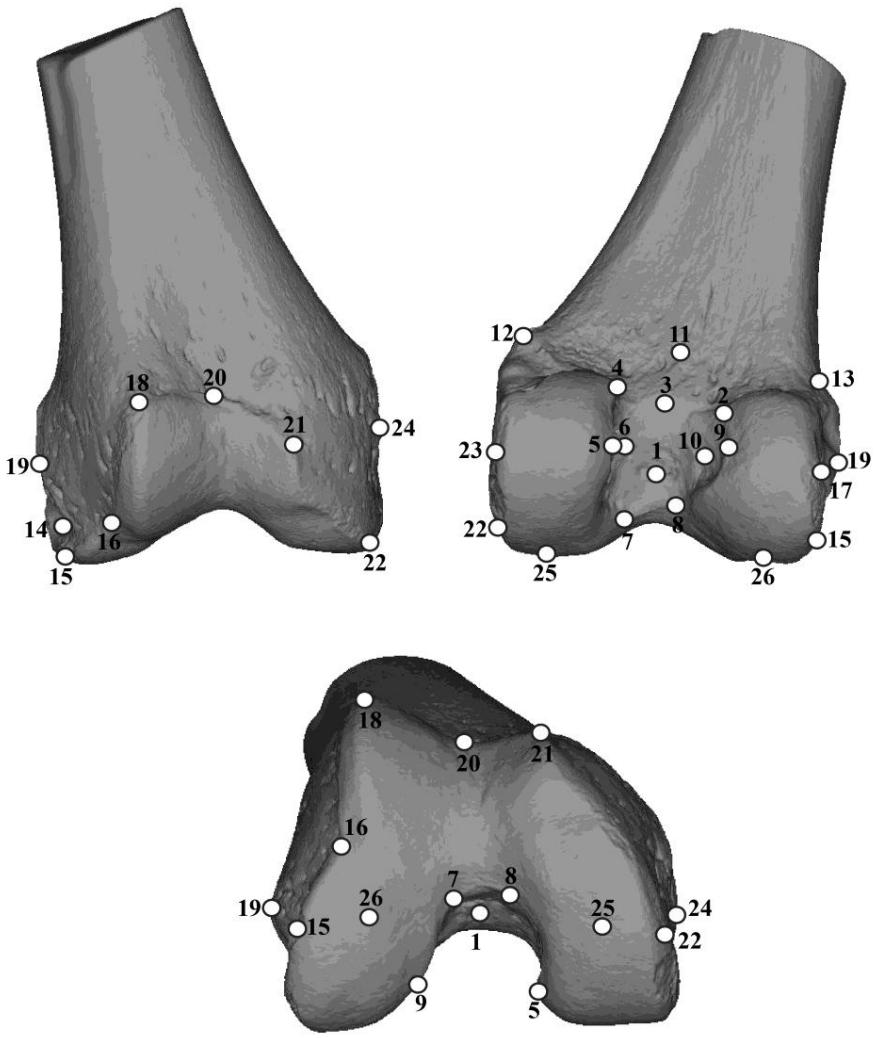


Figure 4) Locations of 26 landmarks digitized on the distal femoral joint.

**Results:**

Non-pathological influences of shape:

Table 3 summarizes the DFA scores associated with non-pathological influences of shape for healthy controls of all three joints analysed. Asymmetry was found to be a major contributor to shape in all joints. An ANOVA on centroid size found that males have significantly larger joints than females ($p<0.001$) and regression analyses revealed a linear relationship between shape and log centroid size in all joints, which was explained by sexual dimorphism. This indicates that the main shape differences between male and female joints are allometric. There were no age-related joint shape changes identifiable in any of the three joints.

Table 3) Summary of cross-validated DFA scores for non-pathological influences on shape on all three joints analysed. The DFA score indicates the percentage of joints accurately classified based on side, sex, and age.

| | Asymmetry | Sexual Dimorphism | | Age |
|---|---|---|---|---|
| | | Left | Right | |
| Ulnae | 80.4% | 70.8% | 49.2% | 39.8% |
| Humeri | 73.9% | 70.0% | 73.9% | 38.3% |
| Femora | 89.9% | 74.5% | 72.9% | 30.4% |

Osteoarthritis:

Males displayed substantially more eburnation and osteoarthritis than females in both the knee and the elbow (table 4). There was a pattern of increasing prevalence of eburnation and osteoarthritic joint changes with increasing age (table 4). Table 5 summarizes the prevalence of affected joints. The elbow is more often affected by eburnation than is the knee and the proximal ulna is more often affected by any pathological change than are the other two joints.

Table 4) Crude prevalence rates (in percentage) of individuals with eburnated joints and/or joints with osteoarthritis. Crude prevalence rate represents the number of individuals affected with the appropriate bones preserved.

| | ♀ | ♂ | YA | MA | OA |
|---|---|---|---|---|---|
| Eburnated | 25.8% | 12.1% | 10.7% | 21.9% | 27.1% |
| Osteoarthritis | 42.7% | 37.9% | 28.6% | 34.4% | 59.2% |

Table 5) Crude prevalence rates (in percentage) of joints displaying eburnation and/or osteoarthritis for each joint analysed. Crude prevalence rate represents the number of individuals affected with the appropriate bones preserved.

| | Eburnated | Osteoarthritis |
|---|---|---|
| Ulnae | 15.5% | 41.8% |
| Humeri | 12.2% | 27.5% |
| Femora | 9.7% | 34.7% |

Any relationship between joint morphology and pathological changes are minimal compared to asymmetry or sexual dimorphism for all three joints, even after regression analyses are performed. Attempts were made to cancel out the effect of these influences by removing the shape variables associated with asymmetry and sexual dimorphism. This was done by splitting the data into groups (side and sex) and scaling each individual joint to the mean shape of its associated group (sex or side), and then scaling those means to the overall mean of the sample. The results obtained through this method did not produce better discrimination of pathological joints, likely indicating how small the shape differences are compared to the impact of sexual dimorphism and asymmetry on joint shape. Therefore, in order to minimise the effect of these non-pathological influences on the results, the data were divided into individual datasets for sex and side. Unfortunately, this division of the data resulted in small sample sizes of affected joints in many datasets.

Regression analyses identified allometry as a contributing factor to joint shape even after sub-division of data, and as osteophyte development would affect the size of the joint, all data were regressed on log centroid size. Table 6 summarizes the results of the cross-validated DFA scores of the regression residuals for all eburnated joints compared with healthy controls. Table 7 summarizes the cross-validated DFA scores of the regression residual for all osteoarthritic (including eburnated) joints compared with healthy controls. The scores for all analyses in these tables are based on PCs representing five percent or greater of the total shape variance. The results for the female left humerus, male femora, and female right femora are the most accuractely classified when comparing eburnated and healthy joints. When the osteoarthritic grouping is considered, only the female left humerus and the female femora display accurate results.

Table 6) Cross-validated DFA scores of joints with eburnation compared to healthy joints for all three joints separated by side and sex. Scores are based on PCs which represent more than five percent of the total shape variance (up to PC8) and indicate the percentage of joints accurately classified as healthy or pathological.

| | | Male | | Female | |
|---|---|---|---|---|---|
| | | Left | Right | Left | Right |
| Ulnae | Eburnated | 12.5% | 36.4% | 50.0% | - |
| | Healthy | 61.3% | 71.4% | 90.0% | - |
| | Total | 51.3% | 61.5% | 86.4% | - |
| Humeri | Eburnated | 33.3% | 50.0% | 100.0% | 33.3% |
| | Healthy | 47.8% | 72.7% | 87.5% | 77.8% |
| | Total | 46.1% | 69.2% | 88.2% | 73.3% |
| Femora | Eburnated | 70.0% | 100.0% | - | 100.0% |
| | Healthy | 90.5% | 94.7% | - | 100.0% |
| | Total | 82.6% | 95.5% | - | 100.0% |

Table 7) Cross-validated DFA scores of log centroid regressed variables of all joints with osteoarthritis (including eburnation) and healthy joints for all three joints separated by side and sex. Scores are based on PCs which represent more than five percent of the total shape variance (up to PC8) and indicate the percentage of joints accurately classified as healthy or pathological.

| | | Male | | Female | |
|---|---|---|---|---|---|
| | | Left | Right | Left | Right |
| Ulnae | Osteoarthritic | 33.3.% | 40.0% | 37.5% | 42.8% |
| | Healthy | 41.4% | 46.4% | 70.0% | 80.0% |
| | Total | 38.3% | 43.4% | 60.7% | 70.4% |
| Humeri | Osteoarthritic | 66.7% | 40.9% | 80.0% | 33.3% |
| | Healthy | 82.6% | 55.8% | 71.8% | 64.3% |
| | Total | 78.7% | 50.8% | 72.9% | 56.7% |
| Femora | Osteoarthritic | 54.5% | 64.3% | 75.0% | 71.4% |
| | Healthy | 80.9% | 78.9% | 100.0% | 75.0% |
| | Total | 80.9% | 72.7% | 95.2% | 73.7% |

Affected ulnae were not accurately classified based on the shape variables. Of the distal humeri, only the female left joints were accurately classified. However, MANOVAs found the difference between the groups to be non-significant and the affected joints do not group from healthy on the initial PCs (figure 5). This indicates that the affected joints do not represent an identifiable group based on shape variables.

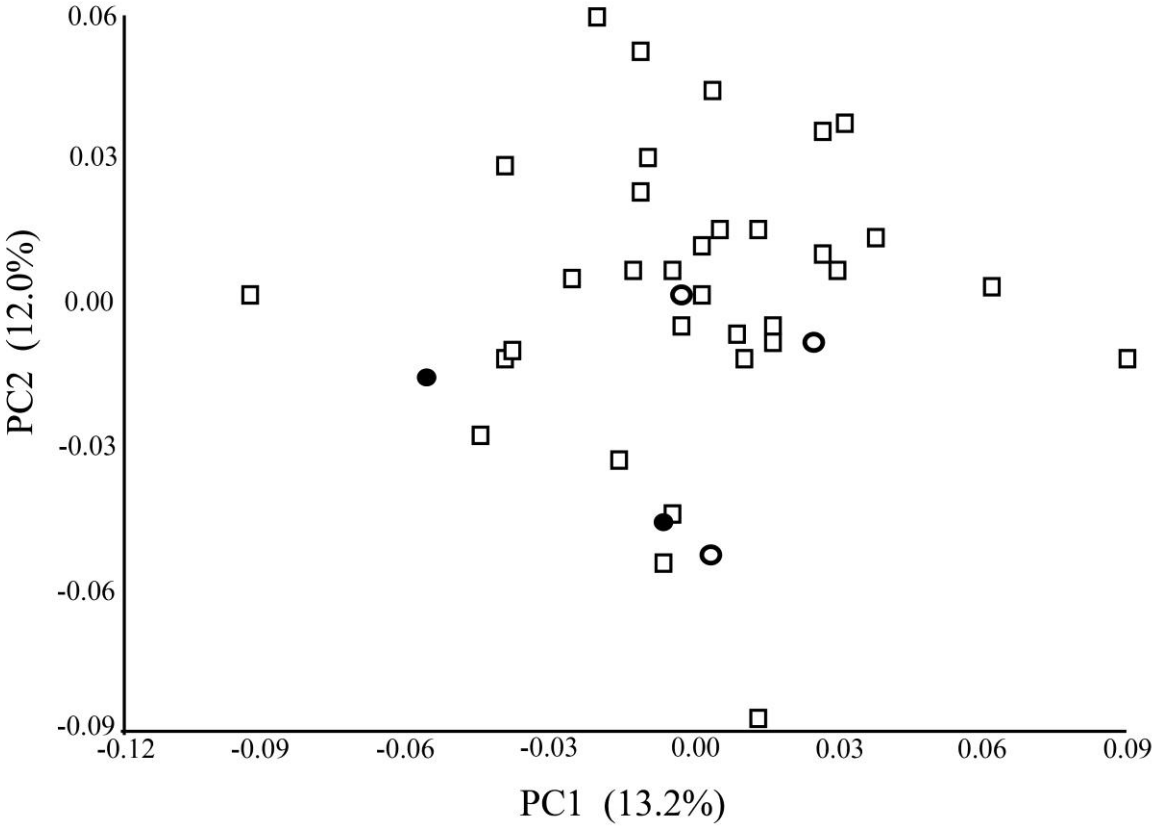


Figure 5) PCA chart displaying shape variance of female left distal humeri on PC1 and PC2,, representing 25.2% of the total shape variance. Open squares represent healthy joints, open circles are osteoarthritic joints, and filled circles are eburnated joints.

The distal femur shows the strongest separation of both eburnated and osteoarthritic joints. Affected male and female right femora were accurately classified and found to be statistically different ($p<0.022$) for both pathological groupings. There were no female left femora with eburnation, but the joints with osteoarthritis (no eburnation) were statistically different from healthy joints ($p=0.006$) and tend to group at the positive end of PC5 and PC6 (figure 7). Eburnated male left femora were accurately identified with the cross-validated DFA, but a MANOVA did not find a statistically significant difference from healthy joints. This could be a result of the small sample size of eburnated joints, and a larger sample size may produce a significant result.

The wireframes illustrated in figures 6 and 7 demonstrate the mean shapes of eburnated or osteoarthritic and healthy distal femoral joints. The main shape differences associated with affected femora relate to the intercondylar notch, with eburnated right and osteoarthritic left female femora showing a relative narrowing of the notch compared to healthy joints (arrow 1). This is especially evident in the male right femora. Eburnated male right and osteoarthritic female left femora appear to have wider condyles than do healthy bones (arrow 2), although this difference is not apparent in female right femora. Eburnated right femora, both male and female, also display relatively deeper patellar grooves than healthy joints (arrow 3).

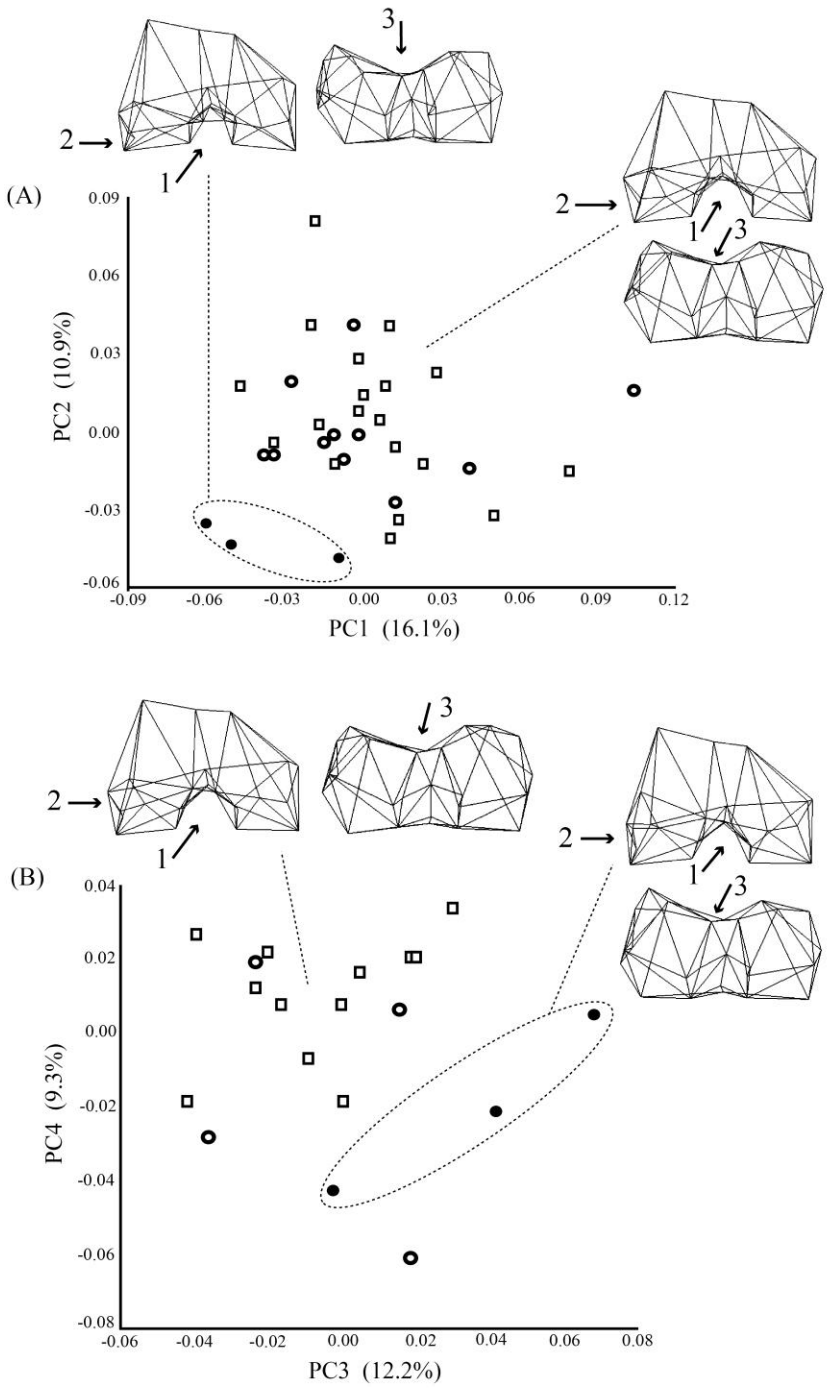


Figure 6) PCA charts illustrating shape variability of (a) male right distal femora on PC1 and PC2, representing 27% total shape variance and (b) female right distal femora on PC3 and PC4, representing 21.5% total shape variance. Open squares represent healthy joints, open circles represent osteoarthritic joints (no eburnation), and filled circles represent eburnated joints. Wireframes illustrate the shape of mean healthy and eburnated joints.

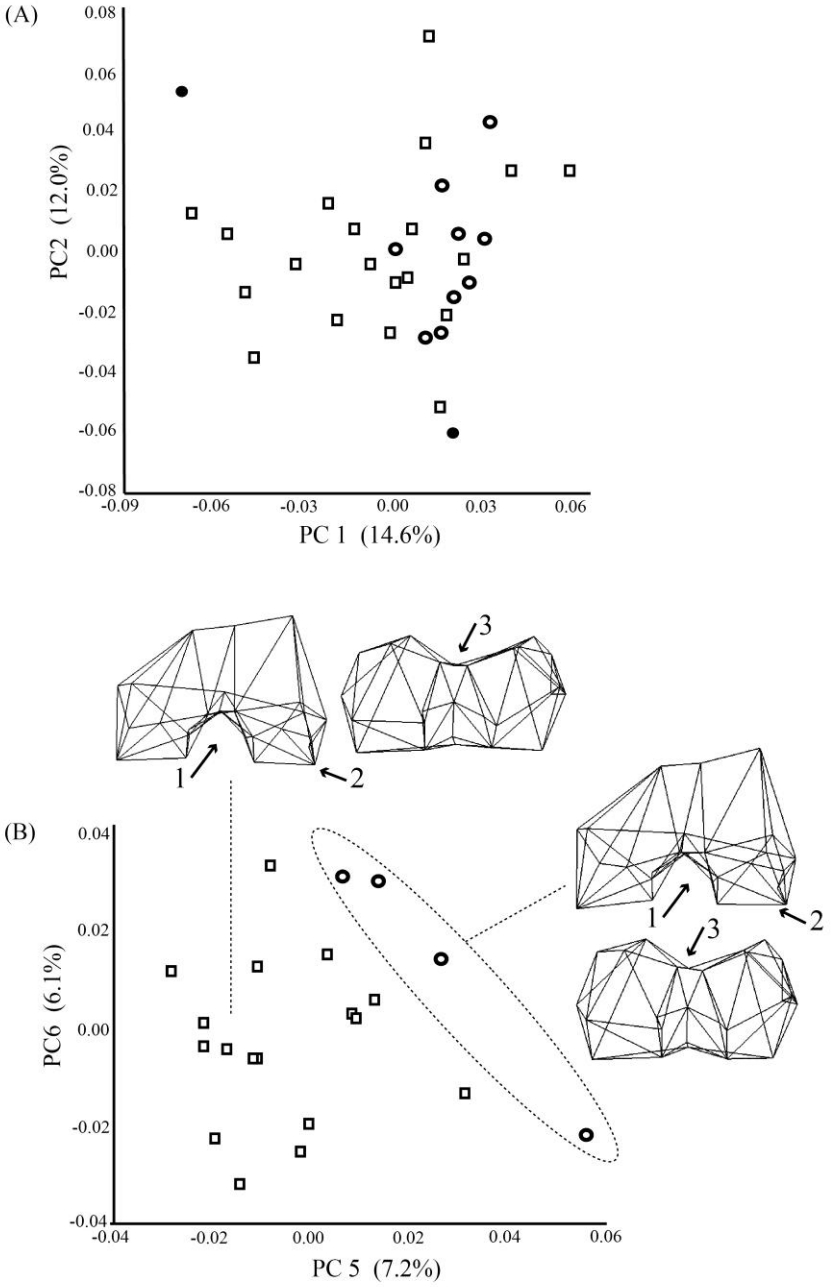


Figure 7) PCA charts illustrating shape variability of (a) male left distal femora on PC1 and PC2, representing 26.6% total shape variance and (b) female left distal femora on PC5 and PC6, representing 13.3% total shape variance. Open squares represent healthy joints, open circles represent osteoarthritic joints (no eburnation), and filled circles represent eburnated joints. Wireframes illustrate the shape of mean healthy and osteoarthritic (no eburnation) female left joints.

There is no pattern in the distal humeral data related to differences in morphology associated with humero-ulnar osteoarthritis and radio-humeral osteoarthritis. The sample size of affected femoral joints was too small to identify the presence of any pattern associated with femoro-patellar or femoro-tibial osteoarthritis, as only two joints (one male left and one female right) displayed femoro-patellar osteoarthritis, and the others displayed femoro-tibial osteoarthritis. Of the male right joints, two had eburnation on the medial condyle, while one had eburnation on the lateral condyle.

**Discussion:**

The results indicate a tentative relationship between distal femoral joint shape and osteoarthritis, with the right femora showing statistically significant shape differences between eburnated and healthy joints. There was also a significant difference between female left osteoarthritic joints (without eburnation) and healthy joints. However, there was no relationship identified in the male left femora or the affected right joints without eburnation. The proximal ulnae and distal humeri also showed no identifiable relationship between a specific morphology and osteoarthritis. The null hypothesis, therefore, is supported for the elbow joints, but can be neither supported nor refuted for the distal femur.

The prevalence of knee osteoarthritis in this population was low and the affected sample size is too small to make any strong conclusions. The results, however, do suggest that the use of 3D shape analyses have the potential to identify a relationship between femoral joint morphology and osteoarthritis. Shepstone et al. (1999) and Wada et al. (1999) analysed all femora (side, sex) in a single dataset. As the current study identified asymmetry, sexual dimorphism, and allometry as major contributors to joint morphology, the relationship

between distal femoral joint morphology and eburnation may be more complex than previously identified. The shape differences identified in the current study are similar to those reported by Shepstone et al. (1999) and Wada et al. (1999), as both male and female right eburnated femora, as well as female left osteoarthritic (no eburnation) joints, had narrower intercondylar notches, although the inverted 'U' shaped notch described by Shepstone et al. (2001) was not apparent in these data. Eburnated male right and osteoarthritic female left femora also have wider medial condyles than do healthy femora. However, Shepstone et al. (1999) found that eburnated femora had shallower patellar grooves, while the current study identified the groove as relatively deeper in eburnated right femora when compared with healthy joints.

Many studies have identified a relationship between a smaller or narrower intercondylar notch and damage to the ACL (LaPrade et al. 1994; Good et al. 1991; Souryal et al. 1988; Anderson et al. 1987) and Tan et al. (2006) found that ligaments may be one of the first joint components affected by the onset of osteoarthritis. Quasnichka et al. (2005) found that laxer ACLs were correlated with joint instability in guinea pigs, and suggest that this predisposed the animals to osteoarthritis. They also found that the intercondylar notch underwent remodeling, becoming narrower, in response to the lax ACL. The narrow intercondylar notch identified in the current study could be a result of osteophyte development, as found by Wada et al. (1999), and may provide stabilization for the ACL. The findings of Quasnichka et al. (2005) suggest the possibility that the osteoarthritis in these joints was initiated by a lax ACL (Amele & Young 2006). However, this shape difference was not found in the male left femora and, with the exception of the female left femora, joints which displayed osteophytes without eburnation do not represent identifiable groups on the

PCA charts. The joints showing systematic shape differences associated with the presence of eburnation could represent a difference in disease progression. The osteoarthritic joints lacking eburnation may represent an earlier stage of the disease and may therefore not have developed the shape changes identified with the eburnated right femoral joints. As Quasnichka et al. (2005) found that osteophytes can form in the notch to stabilize a lax ACL, the joints with narrow notches identified here may represent a later stage of the disease whereby the joint has needed to respond with stabilization techniques. The present data are insufficient to answer these questions, but do indicate a possible avenue for future research.

The wider medial condyles identified in the male right eburnated and female left osteoarthritic joints may also represent a stabilization technique, as suggested by Shepstone et al. (1999). Individuals with knee osteoarthritis display different femoral alignments and ranges of leg movements than healthy controls, especially in flexion, extension, and adduction (Sharma et al. 2001; Shiozaki et al. 1999; Baliunas et al. 2002; Hunter et al. 2005; Childs et al. 2004; Kaufman et al. 2001). These biomechanical differences in osteoarthritic knees could initiate adaptive remodeling in the subchondral bone as a response to the physical stress (Eckstein et al. 1999; Dedrick et al. 1993; Goldring & Goldring 2010; Day et al. 2004). The medial condyle generally bears more weight than the lateral condyle (Lewek et al. 2004; Ruff 1988) and has been shown to undergo more deformation during loaded flexion (Nambu et al. 1991). Therefore, it is possible that the wider medial condyles represent a functional adaptation to stabilize the joints during degeneration (Ruff et al. 2006; Dedrick et al 1993). However, the eburnated female right joints do not show the same difference in medial condylar width. This may be an issue with sample size and the inclusion of more eburnated femora could provide better insight into how the joint responds to osteoarthritis.

There are some morphological similarities between affected femoral joints, but these are not consistent throughout the data, and therefore this does not support the hypothesis that joint morphology may be one factor predisposing individuals to osteoarthritis. The narrow intercondylar notch and wider medial condyles are likely influenced by new bone formation on the joint margins (osteophytes) as an adaptive response to stabilize the affected joint (Quasnichka et al. 2005; Wada et al. 1999; Shepstone et al. 1999). The present data suggest that eburnation is the osteoarthritic change most likely to influence femoral joint shape change or be influenced by a specific morphological type. Right femoral joints with eburnation are more accurately identified when analyzed without other osteoarthritic joints. As the joints described as 'osteoarthritic' based on wider diagnostic criteria are not represented as identifiable groups, with the exception of the female left femora, this may indicate that there are different factors influencing the variation in osteoarthritic joint changes. This could suggest that palaeopathologists should differentiate between eburnated and non-eburnated osteoarthritic joints when analyzing archaeological skeletons.

The results of this study support the findings of Rettig et al. (2008) in that there are no morphological characteristics of the joint associated with osteoarthritis on the distal humerus. This study also found no relationship between proximal ulnar morphology and osteoarthritis. Osteoarthritic elbow joints do not represent an identifiable sub-group within this skeletal population, indicating that joint morphology is unlikely to influence the development of osteoarthritis. Additionally, any joint changes such as osteophyte development or sclerotic subchondral bone do not result in a progressive or systematic alteration or deformation of the joint morphology.

It is unclear why the distal femur would show a relationship between joint morphology and eburnation while the distal humerus and proximal ulna do not. It could be related to the different biomechanical functions of the two, as the knee is a weight-bearing joint and the elbow is not. In the absence of trauma or injury, the elbow joint is one of the most stable joints in the body due to the ulnar collateral ligament, medial collateral ligament, anterior capsule, and its interlocking articular morphology (Morrey & An 1983, 2005; King et al. 1993; Schwab et al. 1980). Perhaps osteoarthritis does not result in a systematic shape change in the elbow because of its physiological stability, and therefore the joint does not undergo stabilizing remodeling to the same extent as the weight-bearing distal femur. Eckstein et al. (1993, 1994, 1995) used Finite Element analysis to determine the influence of joint morphology on stress distribution and found that the incongruity of the humero-ulnar joint, due to the deep trochlear notch, permits equal and bicentric distribution of stress in the joint (Merz et al. 1997). This indicates that, unlike the distal femoral joint, the humero-ulnar joint is not predominantly affected by loading or stress in one area of the joint (such as the medial condyle of the femur) and, therefore, any functionally adaptive changes to the subchondral bone would not result in a focused morphological change in one joint region. The lack of patterning in the data does not indicate that the shape of elbow joints are not changed by osteoarthritis; instead, the results indicate that these changes are not systematic and do not affect each joint in a predictable or quantifiable manner.

The main limitation in this research relates to sample size. Joint shape is strongly influenced by factors unrelated to osteoarthritis, such as asymmetry and sexual dimorphism, and for best results the sample had to be divided by side and sex for separate analyses. The data from the distal femur indicate that these methods could possibly be used to quantify joint

shape related to osteoarthritis. This study provides a preliminary indication that 3D geometric morphometrics analysis of the knee joint related to osteoarthritis will benefit from further analysis. However, future research would need to include a substantially larger sample in order to ensure that the number of joints for each side and sex are sufficient for statistical analysis.

**Conclusion:**

The current study was unable to identify specific distal humeral or proximal ulnar joint shapes which may predispose individuals to developing osteoarthritis. In addition, there was no trend or pattern in the data associated with osteoarthritis, indicating that the condition does not alter the shape of these joints in a systematic manner. There was a tentative relationship between eburnation and distal femoral morphology, but it remains unclear whether the shapes identified predispose individuals to osteoarthritis or if osteoarthritis systematically alters the joint morphology. The shapes associated with eburnation on the distal femur can be explained by functional adaptive responses to stress and therefore, likely do not represent a shape influencing the break-down of the joint components. The results indicate that further analysis with larger sample size may identify an important relationship between distal femoral joint morphology and osteoarthritis. As these methods can be used in clinical situations to quantify shape on radiographs or CT images, future investigation into the relationship between distal femoral morphology and osteoarthritis could have clinical significance.

Future research should focus on larger sample sizes of pathological joints. Longitudinal clinical studies on living patients may indicate if the joint morphology is altered by osteoarthritis and how this relates to the progression of the disease. Associated

physiological information, such as body mass and height, would also greatly expand the outcomes of this research. These data could also be combined with finite element methods analyses to identify load distributions in relation to joint morphology.

**Acknowledgements:**

The authors would like to thank Dr. Jo Buckberry and the Biological Anthropology Research Centre at the University of Bradford for access to the skeletal collections. Special thanks go to Durham University and the Canadian Centennial Scholarship Fund for financial aid to KAP during this research. Thanks to Helgi Pétur Gunnarsson for aid with software and Jeff Veltch for photographs.

**References:**

Acsádi, G, Nemeskéri, J. 1970. *History of human life span and mortality*. Akadémiai Kiadó, Budapest.

Ameye L.G., Young M.F. 2006. Animal models of osteoarthritis: lessons learned while seeking the 'Holy Grail'. *Current Opinion in Rheumatology* 18: 537-547.

Anderson, A.F, Lipscomb A.B. Luidahi K.J., Addelstone, R.B. 1987. Analysis of the intercondylar notch by computed tomography. *American Journal of Sports Medicine* 15: 547-552.

Bailey, A.J., Mansell J.P., Sims T.J., Banse X. 2004. Biochemical and mechanical properties of subchondral bone in osteoarthritis. *Biorheology* 41: 349-358.

Baliunas, A.J., D.E. Hurwitz, A.B. Ryals, A. Karrar, J.P. Case, J.A. Block, & T.P. Andriachhi. 2002. Increased knee joint loads during walking are present in subjects with knee osteoarthritis. *Osteoarthritis and Cartilage* 10: 573-579.

Baylac, M., Friess, M. 2005. Fourier descriptors, Procrustes superimposition, and datadimensionality: An example of cranial shape analysis in moden human populations. In Modern *Morphometrics in Physical Anthropology*, Part 1 Theory and Methods, Slice D. (ed), Kluwer.

Bienvenu T, Guy F, Coudyzer W, Gilissen E, Rouadlès G, Vignaud P, Brunet M. 2011. Assessing endocranial variations in great apes and humans using 3D data from virtual endocasts. *American Journal of Physical Anthropology* 145: 231-246.

Bookstein, F. 1997. Landmark Methods for Forms Without Landmarks: Morphometrics of Group Differences in Outline Shape. *Medical Image Analysis* 1(3): 225-243.

Brandt, K.D., Radin E.L, Dieppe P.A., van de Putte L. 2006. Yet more evidence that osteoarthritis is not a cartilage disease. *Annals of Rheumatic Diseases* 65: 1261-1264.

Bridges, P.S. 1991. Degenerative Joint Disease in Hunter-Gatherers and Agriculturalists From the Southeastern United States. *American Journal of Physical Anthropology* 85: 379-391.

Brooks ST, Suchey JM. 1990. Skeletal age determination based on the os pubis: Comparison of the Acsádi-Nemeskéri and Suchey-Brooks methods. *Journal of Human Evolution* 5: 227–38.

Burleigh, G. 1984.Excavations at Baldock 1980–81: An interim report. *Hertfordshire's Past* 12:3–17.

Cardini, A., Nagorsen, D.,O'Higgins, P., Polly, P.D. , Thorington Jr., R.W. , Tongiorgi, P. 2009. Detecting biological Distinctiveness Using Geometric Morphometrics: An Example Case From the Vancouver Island Marmot. *Ethology Ecology & Evolution* 21: 209-223.

Childs, J.D., P.J. Sparto, G.K. Fitzgerald, M. Bizzini, & J.J. Irrgang. 2004. Altertations in lower extremity movement and muscle activation patterns in individuals with knee osteoarthritis. *Clinical Biomechanics* 19: 44-49.

Cooper, C., S. Snow, T.E. McAlindon, S. Kellingray, B. Stuart, D. Coggon, & P. Dieppe. 2000. Risk factors for the incidence and progression of radiographic knee osteoarthritis. *Arthritis & Rheumatism* 43(5): 995-1000.

Cushnaghan, J. & P. Dieppe. 1991. Study of 500 patients with limb joint osteoarthritis. I. Analysis by age, sex, and distribution of symptomatic joint sites. *Annals of Rheumatic Diseases* 50: 8-13.

Dalal, S., Bull M., Stanley D. 2007. Radiographic changes at the elbow in primary osteoarthritis: A comparison with normal aging of the elbow joint. *Journal of Shoulder and Elbow Surgery* 16(3): 358-361.

Day, J.S., van der Linden J.C., Bank, R.A., Ding, M., Hvid I., Sumner D.R., Weinans H. 2004. Adaptation of subchondral bone in osteoarthritis. *Biorheology* 41(3): 359-368.

Debono L., Mafart B., Jeusel E., Guipert G. 2004. Is the incidence of elbow osteoarthritis underestimated? Insights from palaeopathology. *Joint Bone Spine* 71(5): 397-400.

Dedrick D.K., Goldstein S.A., Brandt K.D. O'Connor B.L., Goulet R.W., Albrecht M. 1993. A longitudinal study of subchondral plate and trabecular bone in cruciate-deficient dogs with osteoarthritis followed up for 54 months. *Arthritis & Rheumatism* 36: 1460-1467.

Doherty M., Preston B., 1989. Primary osteoarthritis of the elbow. *Annuals of Rheumatic Dieases* 48: 743-747.

Dominick, K.L., T.A. Baker. 2004. Racial and ethnic differences in osteoarthritis: Prevalence, outcomes, and medical care. *Ethnicity and Disease* 14(4): 558-566.

Eckstein, F., Lohe F., Schulte E., Muller-Gerbl M., Milz S., Putz R. 1993. Physiological incongruity of the humero-ulnar joint: a functional principal of optimized stress distribution acting upon articulating surfaces? *Anatomy & Embryology* 188: 449-455.

Eckstein F., Merz, B., Schmid P., Putz R. 1994. The influence of geometry on the stress distribution in joints – a finite element analysis. *Anatomy & Embryology* 189: 545-552.

Eckstein F., Merz B., Schon M., Jacobs C.R., Putz R. 1999. Tension and bending, but not compression alone determine the functional adaptation of subchondral bone in incongruous joints. *Anatomy & Embryology* 199: 85-97.

Felson, D.T., Naimark A., Anderson J., Kazis L., Castelli W., Meenan R.F., 1987. The prevalence of knee osteoarthritis in the elderly. The Framingham osteoarthritis study. *Arthritis & Rheumatism* 30(8): 914-918.

Felson D.T., J.J. Anderson, A. Naimark, A.M. Walker, R.F. Meenan. 1988. Obesity and knee osteoarthritis. *Annals of Internal Medicine* 109: 18–24.

Felson, D.T. 2000. Osteoarthritis: New insights – Part 1: The disease and its risk factors. National Institute of Health Conference. *Annals of Internal Medicine* 133: 635-646.

Frost H.M. 1994a. Perspectives: A vital biomechanical model of synovial joint design. *The Anatomical Record* 240: 1-18.

Frost H.M. 1994b. Perspectives: A biomechanical model of the pathogenesis of arthrosis. *The Anatomical Record* 240: 19-31.

Goldring M.B., Goldring S.R. 2010. Articular cartilage and subchondral bone in the pathogenesis of osteoarthritis. *Annals of the New York Academy of Sciences* 1192: 230-237.

Good L., Odensten M., Gillquist J. 1991. Intercondylar notch measurements with special reference to anterior cruciate ligament surgery. *Clinical Orthopaedics* 263: 185-189.

Goodall, C. 1991.Procrustes Methods in the Statistical Analysis of Shape. *Journal of the Royal Statistical Society*. Series B 53(2): 285-339.

Herrero-Beaumont, G., J.A. Roman-Blas, S. Castañeda, & S.A. Jimenez. 2009. Primary Osteoarthritis no longer primary: Three subsets with distinct etiological, clinical, and therapeutic characteristics. *Seminars in Arthritis and Rheumatism* 39: 71-80.

Hootman, J.M., C.A. Macera, C.G. Helmick, & S.N. Blair. 2003. Influence of physical activity-related joint stress on the risk of self-reported hip/knee osteoarthritis: A new method to quantify physical activity. *Preventive Medicine* 36:636-644.

Hunter D.J., Zhang Y., Sokolove J., Niu J. 2005. Trapeziometacarpal subluxation predisposes to incident trapeziometacarpal osteoarthritis: the Framingham study. *Osteoarthritis & Cartilage* 13: 953-957.

Işcan MY, Loth SR, Wright RK. 1984. Age estimation from the rib by phase analysis: White males. *Journal of Forensic Science* 29: 1094–104.

Işcan MY, Loth SR, Wright RK. 1985. Age estimation from the rib by phase analysis: White females. *Journal of Forensic Science* 30: 853–63.

Jurmain, R.D. 1999. *Stories From the Skeleton*. Amsterdam: Gordon & Breach Publishers.

Karsdal, M.A., Leeming, D.J., Dam E.B., Henriksen K., Alexandersen P., Pastoureau P., Altman R.D., Christiansen C. 2008. Should subchondral bone turnover be targeted when treating osteoarthritis? *Osteoarthritis and Cartilage* 16: 638-646.

Kaufman, K.R., C. Hughes, B.F. Morrey, M. Morrey, & K. An. 2001. Gait characteristics of patients with knee osteoarthritis. *Journal of Biomechanics* 34: 907-915.

Kimmerle, E.H., Ross, A., Slice, D. 2008.Sexual Dimorphism in America: Geometric Morphometric Analysis of the Craniofacial Region. *Journal of Forensic Sciences* 53(1): 54-57.

King, G.J.W., Morrey B.F., An, K. 1993. Stabilizers of the elbow. *Journal of Shoulder and Elbow Surgery* 2: 165-174.

Klingenberg, C.P. 2008. MorphoJ: An Integrated Software Package for Geometric Morphometrics. *Molecular Ecology Resources* 11: 353-357.

LaPrade, R.F., Burnett Q.M. 1994. Femoral intercondylar notch stenosis and correlation to anterior cruciate ligament injuries. *The American Journal of Sports Medicine* 22(2): 198- 203.

Lewek M.D., Rudolph K.S, Snyder-Mackler L. 2004. Control of frontal knee laxity during gait in patients with medial compartment knee osteoarthritis. *Osteoarthritis & Cartilage* 12:745-751.

Lieberman DE, Carlo J, Ponce de León M, Zollikofer CP. 2007. A geometric morphometrics analysis of heterochrony in the cranium of chimpanzees and bonobos. *Journal of Human Evolution* 52: 647-662.

Lieverse, A.R., A.W. Weber, V.I. Bazaliiskiy, O.I. Goriunova, & N.A. Savel'ev. 2006. Osteoarthritis in Siberia's Cis-Baikal: Skeletal indicators of Hunter-Gatherer Adaptation and Cultural Change. *American Journal of Physical Anthropology* 132: 1-16.

Lovejoy CO, Meindl RS, Pryzbeck TR, Mensforth RP. 1985. Chronological metamorphosis of the auricular surface of the ilium: A new method for the determination of age at death. *American Journal of Physical Anthropology* 68: 15–28.

Magilton, J., Kenny, J., Boylston, A., & Council for British Archaeology 2008. *Lepers outside the gate: excavations at the cemetery of the hospital of St James and St Mary Magdalene, Chichester, 1986-87 and 1993*. York: Council for British Archaeology.

Maly, M.R., P.A. Costigan, S.J. Olney. 2008. Mechanical factors relate to pain in knee osteoarthritis. *Clinical Biomechanics* 23: 796-805.

Manek, N.J., D. Hart, T.D. Spector, & A. J. MacGregor. 2003. The association of body mass index and osteoarthritis of the knee joint. *Arthritis and Rheumatism* 48(4): 1024-1029.

McGonagle, D., A.L. Tan, J. Carey, & M. Benjamin. 2010. The anatomical basis for a novel classification of osteoarthritis and allied disorders. *Journal of Anatomy* 216: 279-291.

Merz, B., Eckstein, F., Hillebrand, S., Putz, R. 1997. Mechanical implications of humero-ulnar incongruity- finite element analysis and experiment. *Journal of Biomechanics* 30(7): 713-721.

Milner GR. 1992. *Determination of skeletal age and sex: A manual prepared for the Dickson Mound reburial team.* Dickson Mound Museum, Lewiston, Illinois.

Mitteroecker, P., Gunz, P.2009.Advances in Geometric Morphometrics. *Evolutionary Biology* 36: 235-247.

Molnar, P., T.P. Ahlstrom, & I. Leden. 2009. Osteoarthritis and activity – An analysis of the relationship between ebunarion, musculoskeletal stress markers (MSM) and age in two Neolithci hunter-gatherer populations from Gotland, Sweden. *International Journal Osteoarchaeology* 21(3): 283-291.

Morrey, B.F., An, K. 1983. Articular and ligamentous contributions to the stability of the elbow joint. *The American Journal of Sports Medicine* 11(5): 315- 319.

Morrey B.F., An, K. 2005. Stability of the elbow: Osseous constraints. *Journal of Shoulder and Elbow Surgery* 14(1): S174-S178.

Nambu T., Gasser B., Schneider E., Bandi W., Perren S.M. 1991. Deformation of the distal femur: A contribution towards the pathogenesis of osteochondrosis dissecans in the knee joint. *Journal of Biomechanics* 24(6): 421-423, 425-433.

Neubauer S, Gunz P, Hublin JJ. 2010. Endocranial shape changes during growth in chimpanzees and humans: A morphometric analysis of unique and shared aspects. *Journal of Human Evolution* 59:555-566.

Neubauer S, Gunz P, Hublin JJ. 2009. The patterns of endocranial ontogenetic shape changes in humans. *Journal of Anatomy* 215: 240-255.

O'Higgins, P., Jones, N. 1998.Facial Growth in *Cercocebus torquatus*: An application of three-dimensional geometric morphometric techniques to the study of morphological variation. *Journal of Anatomy* 193: 251-272.

O'Higgins P, Jones N. 2006. *Tools for statistical shape analysis*. Hull York Medical School.

Ortner D. 2007 (2003). *Identification of pathological conditions in human skeletal remains*. 2nd Ed. London: Academic Press.

Pearson O.M., Lieberman D.E. 2004. The aging of Wolff's "Law": Ontogeny and responses to mechanical loading in cortical bone. *Yearbook of Physical Anthropology* 47: 63-99.

Phenice TW. 1969. A newly developed visual method of sexing the os pubis. *American Journal of Physical Anthropology* 30: 297–302

Quasnichka H.L., Anderson-MacKenzie J.M., Tarlton J.F. Sims T.J., Billingham M.E. Bailey A.J. 2005. Cruciate ligament laxity and femoral intercondylar notch narrowing in early-stage knee osteoarthritis. *Arthritis & Rheumatism* 52(10): 3100-3109.

R Development Core Team. 2012. R: *A language and environment for statistical computing. R* Foundation for Statistical Computing Vienna, Austria. ISBN 3-900051-07-0, URL http://www.R-project.org

Rettig L.A., Hastings H., Feinberg J.R. 2008. Primary osteoarthritis of the elbow: Lack of radiographic evidence for morphological predisposition, results of operative debridement at intermediate follow-up, and basis for a new radiographic classification system. *Journal of Shoulder and Elbow Surgery* 17: 97-105.

Roberts, C.A. 1984a. *The human skeletal report from Baldock, Hertfordshire*. Unpublished. Bradford, Calvin Wells laboratory, University of Bradford, North Hertfordshire District Council Archaeology Services.

Roberts, C.A. 1984b. *The Barratt inhumation cemetery, Baldock, Hertfordshire (A11/BAL 11), Human skeletal material*. Unpublished. Bradford, Calvin Wells laboratory, University of Bradford, North Hertfordshire District Council Archaeology Services.

Rohlf FJ. 2003. Bias and error in estimates of mean shape in geometric morphometrics. *Journal of Human Evolution* 44: 665-683.

Rohlf, F. J. and Slice, D. 1990. Extensions of the Procrustes Method for the Optimal Superimposition of Landmarks. *Systematic Zoology*, 39(1):40-59.

Rogers, J. & T. Waldron. 1995. *A field guide to joint disease in archaeology*. Chichester; New York: J. Wiley.

Rogers, J. Watt, I, Dieppe P. 1990. Comparison of visual and radiographic detection of bony changes at the knee joint. *British Medical Journal* 300(6721): 367-368.

Rogers, J., L. Shepstone, & P. Dieppe. 2004. Is osteoarthritis a systematic disorder of bone? *Arthritis and Rheumatism* 50(2): 452-457.

Rothschild, B.M. 1997. Porosity: A curiosity without diagnostic significance. *American Journal of Physical Anthropology* 104(4): 529-533.

Ruff , C.B. 1988. Hindlimb articular surface allometry in hominoidea and Macaca, with comparisons to diaphyseal scaling. *Journal of Human Evolution* 17 (7):687-714

Ruff C.B. 2000. Body size, body shape and long bone strength in modern humans. *Journal of Human Evolution* 38: 269-290.

Ruff C.B., Runestad J.A. 1992. Primate limb bone structural adaptations. *Annual Review of Anthropology* 21: 407-433.

Ruff, C.B., Holt B., Trinkaus E. 2006. Who's afraid of the big bad Wolff?: "Wolff's Law" and bone functional adaptation. *American Journal of Physical Anthropology* 129(4): 484-498.

Schrader SA. 2012. Activity patterns in New Kingdom Nubia: An examination of enthseal remodeling and osteoarthritis at Tombos. *American Journal of Physical Anthropology* 149: 60-70.

Schwab, G.H., Bennett J.B., Woods G.W., 1980. Biomechanics of elbow instability: the role of the medial collateral ligament. *Clinical Orthopaedics* 146: 42-52.

Sharma, L., J. Song, D.T. Felson, S. Cahue, E. Shamiyeh, & D.D. Dunlop. 2001. The role of knee alignment in disease progression and functional decline in knee osteoarthritis. *The Journal of the American Medical Association* 286(2): 188-195.

Shepstone, L., J. Rogers, J. Kirwan, & B. Silverman. 1999. The Shape of the Distal Femur: A Palaeopathological Comparison of Eburnated and Non-Eburnated Femora. *Annals of Rheumatic Diseases* 58: 72-78.

Shepstone, L., J. Rogers, J.R. Kirwan, & B.W. Silverman. 2001. Shape of the Intercondylar Notch of the Human Femur: A Comparison of Osteoarthritic and Non-Osteoarthritic bones from a Skeletal Sample. *Annals of Rheumatic Diseases* 60: 968-973.

Shiozaki, H., Y. Koga, G. Omori, G. Yamamoto, & H.E. Takahashi. 1999. Epidemiology of osteoarthritis of knee in a rural Japanese population. *The Knee* 6:183-188.

Sidlauskas, B.L, Mol J.H., Vari R.P. 2011. Dealing with allometry in linear and geometric morphometrics: A taxonomic case study in the Leporinus cylindrformis groups (Characiformes: Antostomidae) with description of a new species from Suriname. *Zoological Journal of the Linnean Society* 162: 103-130.

Slice, D. E. 2007. Geometric Morphometrics. *Annual Review of Anthropology* 36: 261-281.Somers, K.M. 1986. Multivariate allometry and removal of size with principal components analysis. *Systematic Zoology* 35(3): 359-368.

Spector T.D., Hart D.J. Doyle D.V. 1994. Incidence and progression of osteoarthritis in women with unilateral knee disease in the general population: the effect of obesity. *Annals of the Rheumatic Diseases* 53: 565-568.

Spector T.D., Cicuttini F., Baker J., Loughlin J., Hart D. 1996. Genetic influences on osteoarthritis in women: a twin study. *British Medical Journal* 312: 940-944.

Spector, T.D., & Hart, D.J. 1992. How serious is knee osteoarthritis? *Annals of the Rheumatic Diseases* 51: 1105-1106.

Spector, T.D. & A.J. MacGregor. 2004. Risk Factors for Osteoarthritis: Genetics. *Osteoarthritis and Cartilage* 12: S39-S44.

SPSS Inc. 2007. *SPSS Base 8.0 for Windows User's Guide*. SPSS Inc., Chicago IL.

Souryal T.O., Moore H.A., Evans J.P. 1988. Bilaterality in anterior cruciate ligament injuries: Associated intercondylar notch stenosis. *American Journal of Sports Medicine* 16: 449-454.

Stevens, S. D., Strand Viðarsdóttir, U. 2008. Morphological Changes in the Shape of the Non-Pathological Bony Knee Joint with Age: A Morphometric Analysis of the Distal Femur and Proximal Tibia in Three Populations of Known Age at Death. *International Journal of Osteoarchaeology* 18: 352-371.

Stroud, G.(no year) *The human skeletal remains from Hickleton, South Yorkshire*. Unpublished skeletal report, held at the Biological Anthropology Research Centre, Archaeological Sciences, University of Bradford.

Sydes B. 1984. *The excavation of St. Wilfrid's church, Hickleton: an intrim report, September 1984*. Unpublished report. Shefflied: South Yorkshire County Council Archaoloigy

Tan, A.L., Toumi H., Benjamin M., Grainger A.J., Tanner S.F., Emery P., McGonagle D. 2006. Combined high-resolution magnetic resonance imaging and histological examination to explore the role of ligaments and tendons in the phenotypic expression of early hand osteoarthritis. *Annals of Rheumatic Diseases* 65: 1267-1272.

Wada M, Tatsuo H., Baba H., Asamoto K., Nojyo Y. 1999. Femoral intercondylar notch measurements in osteoarthritic knees. *Rheumatology* 38(6): 554-558.

Waldron, T. 1991. The Prevalence of, and the Relationship Between Some Spinal Diseases in a Human Skeletal Population from London. *International Journal of Osteoarchaeology* 1: 103-110.

Waldron T., Rodwell W. 2007. *St. Peter's Barton-upon-Humber, Lincolnshire: A Parish church and its community*. Oxford: Oxbow Publishing.

Weston, D., Boylston, A., Ogden, A.R. (in prep) *The Mappa Mundi Excavation at Hereford Cathedral in 1993: Report on the Human Skeletal Remains*. Unpublished.

Weiss, E. 2006. Osteoarthritis and body mass. *Journal of Archaeological Science* 33: 690-695.

Weiss, E. & R. Jurmain. 2007. Osteoarthritis Revisited: A Contemporary Review of Aetiology. *International Journal of Osteoarchaeology* 17(5): 437-450,

White JW, Ruttenberg BI. 2007. Discriminant function analysis in marine ecology: Some oversights and their solutions. *Marine Ecology Progress Series* 329: 301-305.

Zhai, G., D.J. Hart, B.S. Kato, A. MacGregor, & T.D. Spector. 2007. Genetic influence on the progression of radiographic knee osteoarthritis: A longitudinal twin study. *Osteoarthritis and Cartilage* 15: 222-225.

## Chapter 8) Manuscript 4

# Virtual Palaeopathology: Using 3D Shape Analysis and Imaging Technology to Objectively Record and Describe Disease Processes Affecting Archaeological Skeletal Remains

K.A.Plomp[1,2*]

C.A. Roberts[2]

U. Strand Viðarsdóttir[1,3]

1) Evolutionary Anthropology Research Group, Department of Anthropology, Durham University, Dawson Building, South Road, Durham DH1 3LE
2) Department of Archaeology, Durham University, Dawson Building, South Road, Durham DH1 3LE

*** Corresponding author: k.a.plomp@durham.ac.uk**

Abstract:

Virtual technologies are becoming increasingly available and accessible for many research institutions and universities throughout the world. These technologies have been used to reconstruct and visualize hominin fossil material, analyze species specific morphologies, and investigate human population variation. Virtual methods of analysis and visualization have been widely used in palaeoanthropology and physical anthropology, but their potential for use with archaeological skeletal remains is only beginning to be explored. This paper provides examples of such applications in a bioarchaeological context. Human variation in both healthy and diseased skeletal remains are recorded and described objectively, and the shape changes resulting from pathological conditions are visualized and illustrated in interactive ways. This paper applies virtual techniques to skeletons showing evidence of leprosy and residual rickets, and highlights the benefits of incorporating quantitative data and visual methods in recording and visualizing palaeopathological lesions. Many learning environments, such as universities, schools, and museums, do not have ready access to comparative skeletal collections for teaching and research, especially skeletons displaying pathological lesions, making the dissemination of virtual data a revolutionary step in palaeopathology in particular. The pathological bones which were the focus of this project could be statistically discriminated from healthy bones, and the changes in shape due to disease illustrated with both 3D and 2D imaging techniques.

Keywords: geometric morphometrics, rickets, leprosy, rhinomaxillary, learning environment, bioarchaeology

**Introduction:**

Virtual Anthropology (VA) can be described as a multidisciplinary approach to anthropological research using digital data and 3D imaging, and is becoming increasingly popular in biological- and palaeoanthropology (Weber et al. 2001, 2011; Recheis et al. 1999; Elton & Cardini 2008; Kullmer 2008). VA techniques have been used to reconstruct hominin fossil material, analyze species specific morphologies, as well as investigate morphological variation in modern human populations (Strand Viðarsdóttir et al. 2002; Hennessy & Stringer 2002; Cobb & O'Higgins 2007; Franklin et al. 2007; Weber & Bookstein 2011). Geometric morphometrics are a suite of shape analysis techniques used in VA to obtain and analyse digital information describing the morphology of biological material. Traditional recording methods in palaeopathology rely heavily on macroscopic descriptions and can be highly subjective and dependent on observer experience (Waldron & Rogers 1991; Miller et al. 1996). Geometric morphometric techniques provide the potential of new objective and transparent methods for recording pathological lesions (Mitteroeker et al. 2004; Perez 2007) as well as comparative digital data. These data can then be combined with imaging technology, such as 3D surface laser scanning or 2D deformation grids, to produce detailed images of disease progression on human bones and teeth to use as an instructional and/or descriptive visual tool.

Our paper will illustrate the use of geometric morphometrics with two palaeopathological case studies. These methods can be applied to virtual scans or physical specimens and combined with 3D and 2D visualization of the pathological lesions to produce interactive visualizations of disease processes, as well as objectively record the lesions. In this paper we combine 3D landmark data from original bones with high resolution 3D images to

record, analyse and describe one of the palaeopathological lesions attributable to leprosy, rhinomaxillary syndrome - RMS (Case Study 1). The use of 3D virtual imaging is becoming popular in bioarchaeology (Kuzminsky and Gardiner 2012; Marfart et al. 2007), with an increase in the practice of using 3D laser scanning to document palaeoanthropological and archaeological skeletal material (see e.g. Smithsonian Institution http://humanorigins.si.edu/evidence/3d-collection; University of Bradford http://www.barc.brad.ac.uk/FromCemeterytoClinic/index.php; Swiss Mummy Project http://www.research-projects.uzh.ch/p2282.htm; British Museum Mummy project thttp://www.britishmuseum.org/explore/highlights/highlight_objects/aes/m/mummy_of _nesperennub.aspx. Accessed July 2012). These databases have been designed to provide access to 3D images for researchers, students, and the general public. With this in mind, our first case study (leprosy) intends to illustrate the potential of using quantifiable methods of recording pathological lesions which can be incorporated with virtual images for visualization and interpretation of pathological shape changes.

As many institutions and researchers may not have access to 3D shape analysis equipment, the second case study will illustrate how standardized 2D digital photographs can also be used to explore pathological variation in skeletal shape with considerable accuracy. Case study 2 focuses on using 2D landmark data to objectively record the deformation of femora related to long bone bowing due to vitamin D deficiency. The examples presented in this paper illustrate the benefits of using quantitative methods to record and describe palaeopathological lesions and demonstrate the advantages of using digital data for visualization of pathological conditions in archaeological remains.

**Disease processes studied**

The pathological conditions illustrated in this paper are rhinomaxillary syndrome caused by leprosy and the femoral deformation of residual rickets due to vitamin D deficiency. These lesions were chosen as they change the shape of the affected bones, and display morphological variation related to the severity of the conditions. The progressive nature of the lesions in rhinomaxillary syndrome and residual rickets makes them perfect palaeopathological entities to highlight the possibilities of using geometric morphometrics in palaeopathology and bioarchaeology.

*Leprosy:*

Leprosy is a chronic infectious disease caused by *Mycobacterium leprae* which affects the peripheral nerves primarily, and the skin and other tissues of the body secondarily (the eyes, testes, kidneys, bones, blood vessel endothelium, and mucosa of the upper respiratory tract) (Jopling 1982). It can manifest itself as tuberculoid or paucibacillary leprosy, where the infected individual has a high resistance to the *Mycobacterium*, or as lepromatous (multibacillary) leprosy, where the infected individual has low resistance (Rodrigues and Lockwood 2011). The different manifestations of leprosy are at each end of the immune spectrum, with several "types" in between (Ridley and Jopling 1966). The low temperature of the nasal region provides the optimal environment for the *Mycobacterium*, causing the bacilli to accumulate in this area. In bioarchaeology, tuberculoid leprosy mainly affects the postcranial bones, whereas lepromatous leprosy is diagnosed by involvement of the facial bones (Manchester & Lee 2008). *Facies leprosa* (Møller-Christensen 1978) or rhinomaxillary syndrome (Andersen and Manchester 1992) describes manifestations of lepromatous leprosy

in the facial skeleton, which result in erosive, resorptive and proliferative bone changes variously affecting the alveolar and palatine processes of the maxilla, the anterior nasal spine, the intranasal osseous structures, and the margins of the nasal aperture. The upper anterior dentition can be lost antemortem and the normal development of the incisor roots affected (leprogenic odontodysplasia – Danielsen 1970). These changes can eventually lead to collapse of the central region of the face.

Rhinomaxillary syndrome is generally considered to be pathognomonic of lepromatous leprosy in archaeological skeletal remains and the pathological changes accumulate over decades to become progressively more disfiguring (figure 1) (Andersen and Manchester 1992; Küstner et al. 2006; Rodrigues and Lockwood 2011). This suite of lesions is the focus of the 3D shape analysis illustrated in this paper. Its aim is to quantify the changes in the nasal aperture and nasal spine due to leprosy, and produce 3D images of the shape changes by deforming a healthy (reference) face to a leprous (target) face using virtual imaging technologies. The data and 3D images are used to demonstrate the potential of shape analyses and virtual imaging techniques to illustrate pathological changes on the face related to leprosy.

Figure 1) Left: Healthy individual (Skeleton 142, Chichester, West Sussex). Right: Individual with rhinomaxillary syndrome (Skeleton 86, Chichester, West Sussex), note rounded edges of nasal aperture (arrow) and resorption of the nasal spine (circle).

*Residual Rickets:*

Vitamin D is a fundamental element needed for the mineralization of osseous tissue through enabling the absorption of calcium and phosphorus, as well as contributing to an individual's immune response, cell growth, and cardiovascular health (Brickley & Ives 2008; Holick 2005; Holick 2004; Wang et al. 2008). Deficiency in vitamin D can occur due to genetic, metabolic, or environmental factors (Brickley et al. 2007), and will result in inadequate mineralization of osteoid during bone remodelling in development. The main cause of vitamin D deficiency is lack of appropriate exposure to sunlight, which stimulates the formation of vitamin D in the skin (Brickley et al 2005; Holick 2003). Vitamin D deficiency during growth results in rickets and the most obvious skeletal manifestations are bowing of the weight-bearing long bones (figure 2) and ribs due to inadequately mineralized ("soft") bone. The skeletal changes acquired during growth can persist into adulthood, a condition known as residual rickets (Haduch et al. 2009; Brickley et al 2010; Ivanhoe 1994) which forms the focus

of the 2D shape analysis illustrated in this paper. The aim was to quantify and record the medio-lateral deformation of adult femora attributed to residual rickets and the data are used to demonstrate the benefits of 2D shape analysis techniques in illustrating and recording pathological deformation of the femora from vitamin D deficiency.

Figure 2) Left: healthy femur (Skeleton 258, Chelsea Old Church, London). Right: Femur displaying medio-lateral bowing of the diaphysis and coxa vara of the femoral head and neck (Skeleton 957, Chelsea Old Church, London).

**Materials and Methods:**

The skeletons analysed in the case study on leprosy were derived from the late Medieval skeletal collection of Sts. James and Mary Magdalene, Chichester, West Sussex, England (Magilton et al. 2008), curated at the Biological Anthropology Research Centre, School of Archaeological and Environmental Sciences, University of Bradford, England (http://www.barc.brad.ac.uk/Chichester.php, Accessed July 2012). Eight facial landmarks were digitized from forty adult individuals with (14) and without (26) RMS bone changes. Due to the wide variation in the preservation of the nasal region for these individuals, a limited number of landmarks on the inferior aspect of the nasal aperture was chosen in order to allow a large enough sample of pathological individuals and healthy controls to produce statistically relevant results (Table 1).

The femora for the second case study on rickets were derived from 99 adult skeletons from the post-Medieval skeletal collection of Chelsea Old Church, London, curated at the Centre for Human Bioarchaeology, Museum of London (Table 1) (http://www.museumoflondon.org.uk/Collections-Research/LAARC/Centre-for-Human-Bioarchaeology/Database/Post-medieval+cemeteries/Chelsea.htm, Accessed August 2012). The sample comprises 91 healthy and eight affected individuals. The femur is a robust bone, and generally well preserved in archaeological situations, but preservation of right and left femora varied, with some individuals having only one femur appropriately preserved for study. Preservation of bone in archaeological contexts depends on many taphonomic factors such as soil acidity, temperature, water content, as well as damage from animal and insect behaviour, plant destruction, and microbial attack (Roberts 2009:39-72; Jans et al. 2004).

Robust bones such as the femur are more likely to survive these conditions than more fragile bones, such as those of the face.

Table 1) Samples of healthy and affected individuals analyzed in each illustrative study, with collection, time period, and reference included.

| Case Study | Collection | Time | Reference | Healthy | Affected | Total |
|---|---|---|---|---|---|---|
| Leprosy | Chichester, West Sussex | Late Medieval ($12^{th}$-$16^{th}$ C AD) | Magilton *et al.* 2008 | 26 | 14 | 40 |
| Residual Rickets | Chelsea Old Church, London | Post-Medieval (1712-1842 AD) | Cowie *et al.* 2008 | 91 | 8 | 150 |
| | | | | (136 femora) | (14 femora) | |

Case study 1: 3D mensuration (Leprosy)

For the leprosy study, three-dimensional Cartesian coordinates of eight landmarks were digitized on the inferior aspect of the nasal aperture and nasal spine using a Microscribe® GLS digitizing system (EMicroscribe Inc) (table 2, figure 3). Preservation of the facial region in some skeletons caused problems in locating many anatomical landmarks; the eight landmarks listed here were chosen to represent the shape of the part of the face most prone to be affected in lepromatous leprosy. As rhinomaxillary syndrome can result in a deformation of this region, landmark placement on affected individuals could be problematic; however, error tests indicated that intra-observer error did not affect group classification.

Table 2) Description of eight 3D landmark loci on the nasal aperture and spine.

| Number | Description |
|---|---|
| **1** | Tip of nasal spine |
| **2** | Left inferior aspect of nasal spine |
| **3** | Right inferior aspect of nasal spine |
| **4** | Posterior margin of nasal spine |
| **5** | Left point where aperture ridge meets aperture margin |
| **6** | Anterior articulation of left nasal concha with aperture margin |
| **7** | Anterior articulation of right nasal concha with aperture margin |
| **8** | Right point where aperture ridge meets aperture margin |

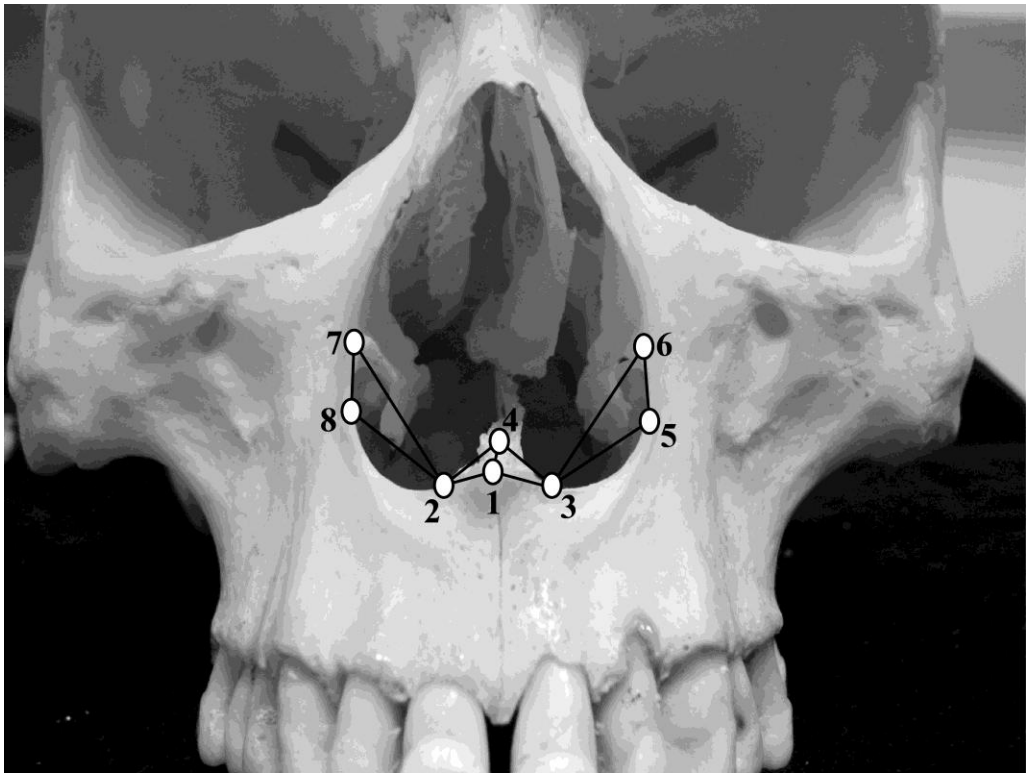


Figure 3) Location of 3D landmarks used for shape analysis of the nasal spine and the inferior margin of the nasal aperture. Numbers refer to the descriptions in table 2. Polygons interlink landmarks to aid in visualization of shape changes.

Case study 2: 2D mensuration (rickets)

In the study of rickets, standardized digital images of the ventral plane of each femora were taken for analysis. Femora were standardized based on angle of femoral neck, orientation, and distance from camera. The images of left femora were mirrored, in the horizontal plane, to standardize the images to the appearance of a right femur, and 30 two-dimensional landmarks covering the ventral exterior margins of adult femora were digitized on the photographs using TPSDig© (Rolf 2004) (table 3, figure 4). Sixteen of these landmarks are classed as semi-landmarks, which lack homology, and were placed evenly along the diaphysis. These landmarks were consequently slid along the tangent plane to reduce the amount of shape variance related to differential landmark spacing (for full description of this method see Bookstein 1997; Baab et al. 2012). The effect of asymmetry on femoral shape was analyzed by comparing left and right sides after being mirrored. Shape variance of 2D objects can be illustrated using the thin-plate spline, which is a metaphorical thin steel plate in which the shape differences can be visualized using deformation grids. The thin-plate spline grid illustrates the amount of deformation required to change a reference shape, such as a mean of one group, to a target shape, or the mean of another group. The bending energy is the amount of energy required to deform an infinitely thin steel plate from the reference shape to a target shape (Bookstein 1997a, b).

Table 3) Description of 30 2D landmarks covering the external margin of the femoral diaphysis and metaphysis for the analysis of femoral deformation due to residual rickets.

| Number | Description |
|---|---|
| **1** | Medial most point of femoral head, at fovea capitis |
| **2** | Superior most tip of greater trochanter |
| **3** | Deepest point of superior femoral neck |
| **4** | Junction between femoral head and inferior aspect of neck |
| **5** | Lateral most point of greater trochanter |
| **6** | Central point of greater trochanter |
| **7** | Superior most point of lateral distal joint margin |
| **8** | Superior most point of medial distal joint margin |
| **9** | Inferior most point of medial distal condyle |
| **10** | Inferior most point of lateral distal condyle |
| **11-30** | Semi-landmarks covering outer margin of shaft |

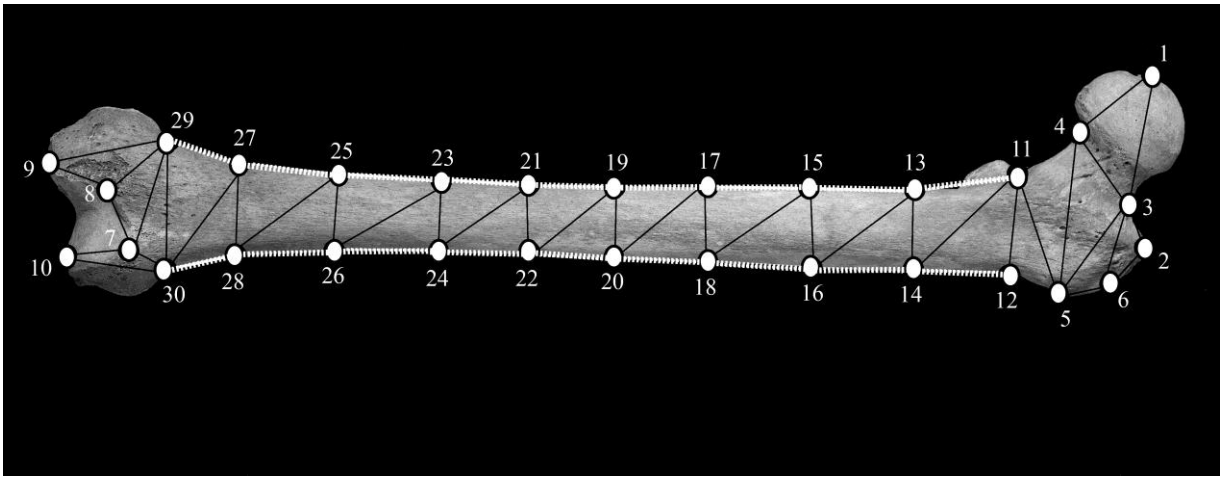


Figure 4) Location 2D landmarks used for shape analysis of femora. Polygons interlink landmarks to aid in visualization of shape changes; white dashed line represents distance between sliding landmarks. Landmark numbers refer to descriptions in table 3.

Statistical Analyses:

Following data acquisition, the statistical procedures do not differ between the two and three dimensional studies; the only difference being the number of dimensions recorded for each coordinate, and subsequently the number of dimensions generated by the statistical analyses. Generalized procrustes analysis (GPA) was performed to remove redundant orientation information (translation and rotation) from the data and partition shape from size (Slice 2007; Rohlf 2003; Goodall 1991; Bookstein 1997; Rohlf & Slice 1990). Principal components analysis (PCA) was used to explore the pattern of shape variation within the sample (O'Higgins & Jones 1998; Stevens & Strand Viðarsdóttir 2008; Mitteroeker & Gunz 2009). Discriminant functions (DFA) were calculated between groups and their strength assessed by leave-one-out cross-validation (Klingenberg 2011; White & Ruttenberg 2007; Cardini et al. 2009; Kimmerle et al. 2008). In order to minimize noise from higher components, the number of PCs included in statistical analyses was reduced using the method described by Baylac and Frieβ (2005). The DFA scores were tested for over-fitting with randomized tests and only those scoring higher than chance are reported here (Kovarovic et al. 2011). Statistical significance of group differences was assessed using MANOVA and ANOVA. Size was calculated as centroid size, which is a mathematically defined measurement of size independent of shape; and is defined as the square root of the sum of the squared distances of each landmark from the centroid of the landmark configuration (Zelditch et al. 2004). Intra-observer error was assessed by comparing the greatest Procrustes distance between repetitions and the smallest distance between other observations; the smallest distance between different observations was close to three times greater than the greatest distance between the repetitions, indicating that intra-observer error is unlikely to affect group

classification (Neubauer et al. 2009; Neubauer et al. 2010; Lieberman et al. 2007; Bienvenu 2011).

Analyses were run in Morphologika© (O'Higgins & Jones 2006), the EVAN toolbox, and R (R Development Core Team 2010). An excellent introduction to all these methods can be found in Baab et al. (2012).

Skeletons with leprosy were identified based on the original site report (Magilton 1986, 1993) and confirmed by macroscopic analysis using the criteria described in Table 4. Although there is a circularity of argument in using facial changes to diagnose the disease and subsequently discriminating based on the same criteria, the analyses are presented here for illustrative purposes of the techniques only, with full awareness of that circularity. Individuals were divided into three groups based on the extent of changes identified in the naso-maxillary region (table 4).

Table 4) Description of macroscopically visible pathological changes in the nasal region. Individuals were classified as healthy or as having rhinomaxillary syndrome depending on the presence and characteristics of the lesions listed (Møller-Christensen 1953, 1961, 1965, 1978; Andersen and Manchester 1992).

| **Pathological Classification** | **Description of Lesion** |
|---|---|
| Healthy | No pathological changes present in the nasal region |
| Rhinomaxillary Syndrome (RMS) | - Resorption of nasal aperture with new bone formation through remodelling producing rounded edges.<br>- Resorption of nasal spine<br>- Porosity on palate<br>- Resorption of anterior maxillary alveolus. |

Vitamin D deficiency is diagnosed based on macroscopic changes characteristic of the condition, such as abnormally square crania with pronounced frontal and/or parietal bossing, medial orientation of the mandibular ramus, abnormal angulation of ribs and protrusion of the sternum, deformation of sacrum and pelvis, and abnormal curvature of long bones (Cowie et al. 2008; Brickley & Ives 2008). The original site report of the Chelsea Old Church skeletal collection (Cowie et al. 2008) was referred to in order to identify skeletons with rickets, and macroscopic analysis of the long bones verified deformation. The deformation of the femoral diaphysis and femoral neck is the focus of this illustrative example.

**Results:**

Leprosy:

Statistical analyses of the landmark coordinates found individuals with rhinomaxillary changes to be correctly classified with an accuracy of 85.4% (affected 75.0%; healthy 88.5%) based on the first 5 PCs, representing 80.4% of the total shape variance in the sample. A MANOVA found the shape differences between the two groups to be significantly different ($\lambda$ 0.526, p=0.001). The wireframes in figure 5 illustrate the shape differences between a healthy individual and a lepromatous individual. These same shape differences are also further illustrated in figure 6, which displays a 3D scan of the healthy reference human cranium on the left and the image on the right is the same scan after being warped to fit the landmark configuration of the target individual with rhinomaxillary syndrome. The shape changes associated with the lesion are visible in the warped scan, with a widening of the nasal aperture and resorption of the anterior nasal spine.

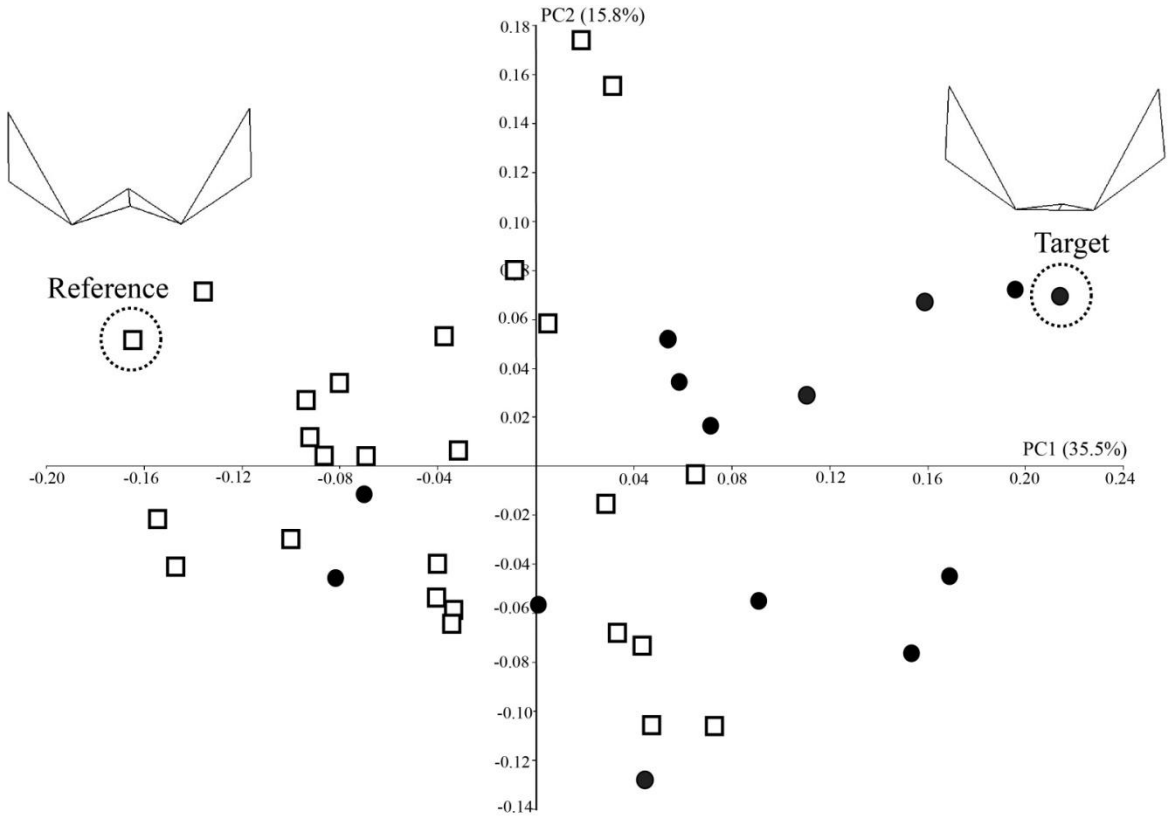


Figure 5) PCA chart illustrating shape variance in the nasal region in all three groups on PC1 and PC2 which together explain over 50% of the total shape variation; open squares are healthy individuals, and filled circles are individuals with rhinomaxillary syndrome. Note that affected individuals tend to sit on the positive end of PC1, representing 35.5% of the total shape variance, although there is overlap between all groups. The shape differences between the healthy reference individual and the lepromatous target individual are illustrated in the wireframes.

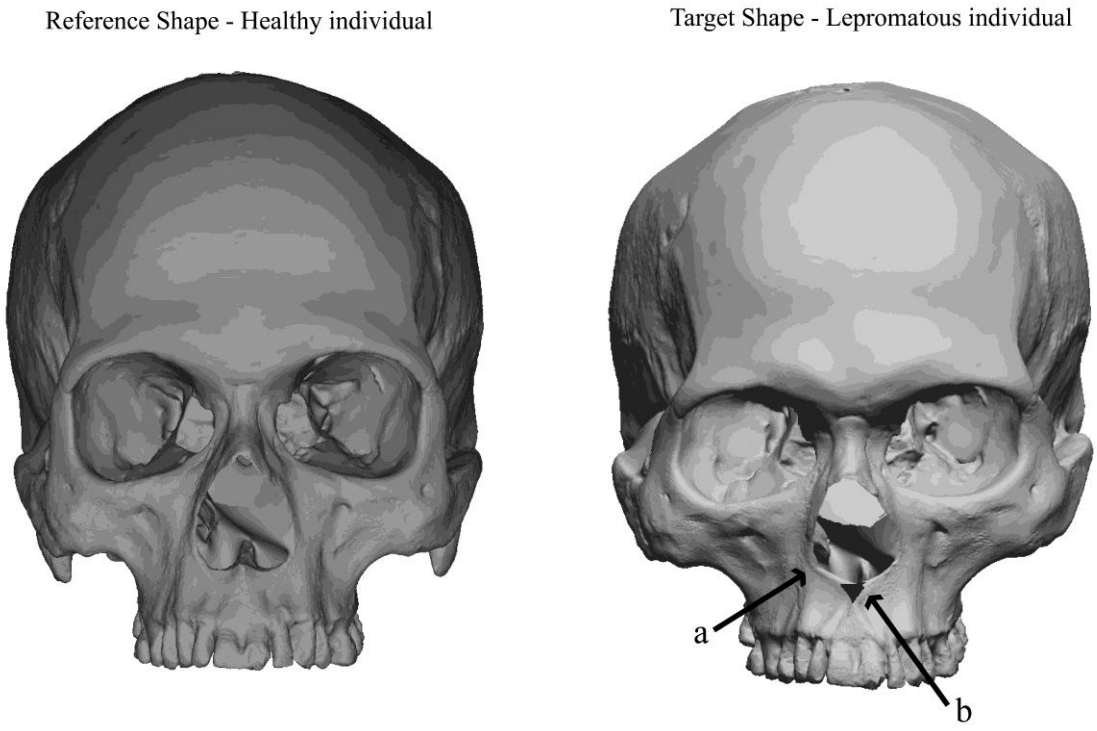


Figure 6) The image on the left is a 3D laser scan of a healthy adult cranium; the image on the right is the same cranium after being warped to fit the landmark configuration of an individual with rhinomaxillary syndrome. Note the characteristic changes due to the RMS lesions, with a widening of the nasal aperture (a) and loss of the nasal spine (b) in the cranium on the right.

Residual Rickets:

Asymmetry is a major influence on healthy femoral shape. When both left and right bones are superimposed and analyzed together, left and right femora can be discriminated with 84.6% (right 87.9 %, left 81.4%) accuracy on the basis of those aspects of shape variance contained on the first 16 PCs, representing 94.5% of the total shape variance. Therefore, left and right femora will be analyzed for shape differences related to residual rickets both together and separately. Table 5 summarizes the statistical results for distinguishing healthy and affected femora with pooled and separate sides.

Table 5) Summary of statistical results for healthy vs. affected femora, with both sides analysed separately. The DFA scores represent the percentage of femora accurately classified as healthy or affected based on the number of PCs indicated, with the total percentage of shape variance represented by those PCs stated. MANOVA (Wilks lambda λ, p-value) results indicate the statistical significance of the shape differences between the two groups.

| | | DFA scores | | | MANOVA results |
|---|---|---|---|---|---|
| | | Accuracy | PCs | Variance | |
| Right femora | Affected | 83.3% | 3 PCs | 69.2% | λ 0.761, p=0.002* |
| | Healthy | 84.3% | | | |
| | Total | 84.2% | | | |
| Left femora | Affected | 100.0% | 7 PCs | 86.2% | λ 0.639, p=0.000* |
| | Healthy | 95.4% | | | |
| | Total | 95.8% | | | |

* indicates significant value

Figure 7 shows PCA charts illustrating the separation of groups for both left and right femora, and Figure 8 illustrates the shape differences between healthy and affected bones using deformation grids which aid interpretation of the shape change from healthy to affected femora. The main shape changes of affected femora include a relative inferior orientation of the femoral head and neck (figure 8-a), a medio-lateral curvature affecting the proximal (top) half of the diaphysis (figure 8-b), and a relative thickening of the shaft (figure 8-c). The orientation of the distal condyles also differs, with the medial condyle being relatively more anteriorly oriented, while the lateral condyle is relatively more posteriorly oriented (figure 8-d). There also appears to be a superiorly directed extension of the distal joint surface, which could be a result of the change in condyle orientation (figure 8-e).

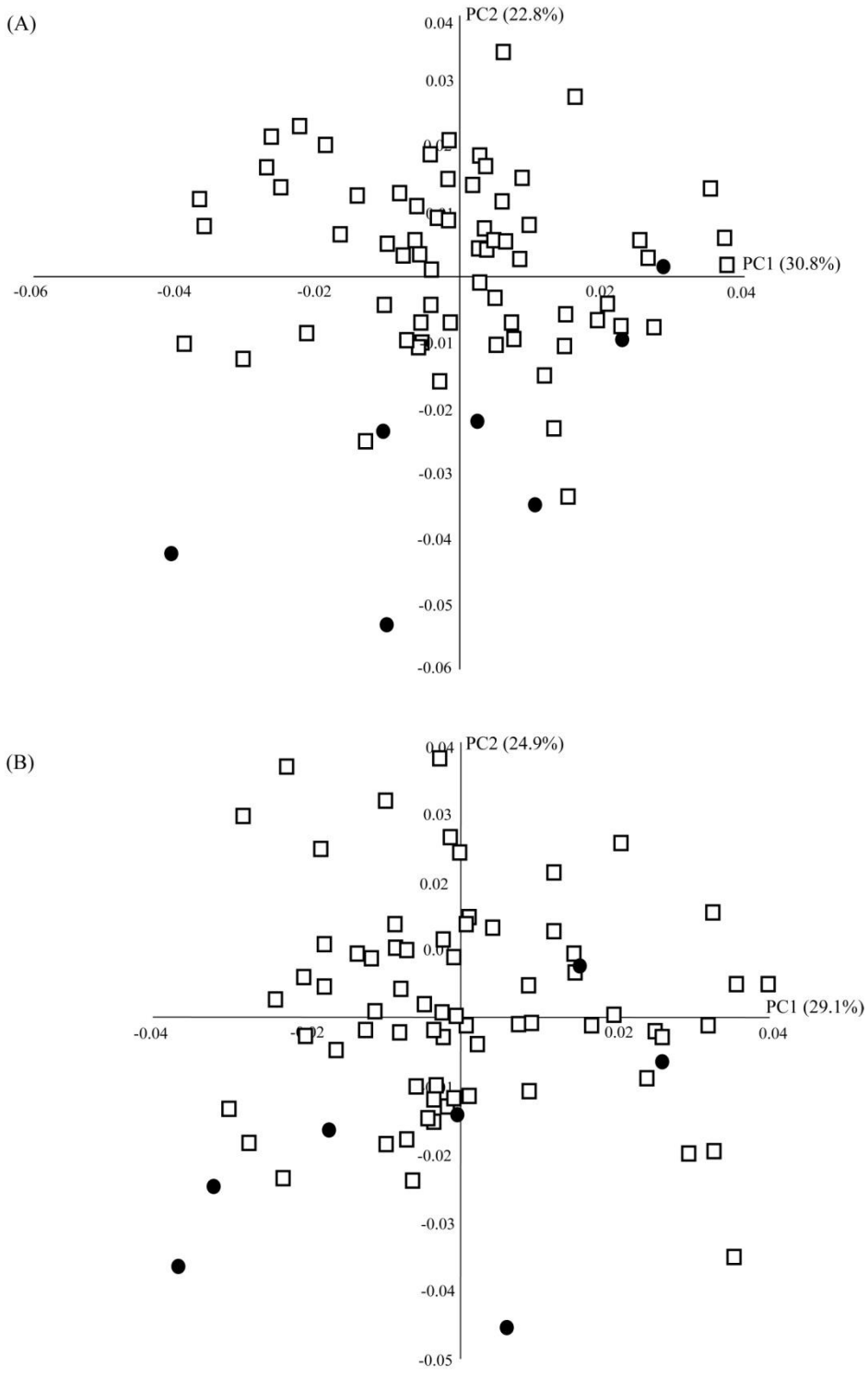


Figure 7) PCA charts for left (A) and right (B) femora displaying the pattern of shape variability on PC1 and PC2 which together explain more than half the total variance within the samples; open squares are healthy and filled circles are affected femora. Both left and right affected femora tend to be on the negative end of PC2, but there is substantial overlap.

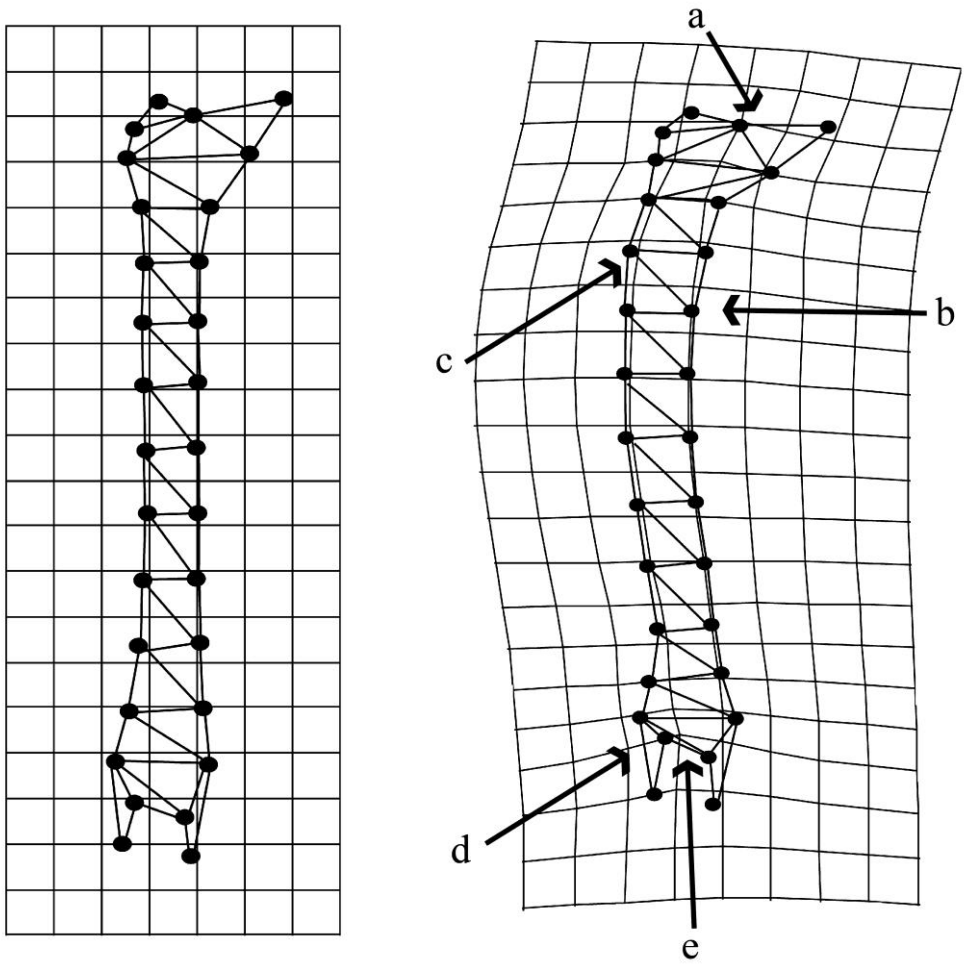


Figure 8) Thin Plate Spline grids warped to illustrate the change in mean shape from healthy to affected left femora (Figure 7a). Deformation has been magnified by 2x for ease of interpretation. Shape differences described in text (a-e) are indicated with arrows.

**Discussion:**

These case studies illustrate that skeletal lesions associated with rhinomaxillary syndrome (leprosy) and vitamin D deficiency can be readily quantified with geometric morphometrics. Using 3D and 2D imaging techniques, the changes in morphology associated with these lesions can be reliably illustrated and the process of deformation visualized. As this is an illustrative study, the results only provide a quantification of macroscopically visible

shape deformation without attempting interpretation of the aetiology or pathogenesis of the conditions. The aim is simply to demonstrate the potential of using VA techniques to illustrate pathological shape changes and how geometric morphometric methods can be integrated with palaeopathological research to objectively record pathological shape deformation.

*Case study: Leprosy*

The shape deformation of the nasal region can be easily quantified using geometric morphometrics, as a statistical difference was found between the facial shapes of healthy and affected individuals. The landmark data obtained by 3D digitization was used to morph a virtual 3D image to illustrate the shape deformation attributed to rhinomaxillary syndrome. Landmark data were obtained by digitizing the actual skeletal elements, but the same methods could also be applied directly to 3D scans. The combination of these methods with virtual imaging technology can produce interactive demonstrations of disease processes affecting archaeological skeletons, as well as opening up the possibility of diagnostic tools to be used by workers with little experience of leprotic changes, or on samples displaying early stages of the disease.

Unfortunately, the preservation of the fragile facial elements decreased the number of landmarks available for analysis. The ideal situation would have been to include an analysis of the entire face or maxilla, however, preservation made this impossible and the resulting datasets could only quantify shape changes related to the nasal aperture. Despite the limitations of the case study, it illustrates the potential of using VA techniques in palaeopathology. As the use of virtual databases to preserve and visualize bioarchaeological and particularly palaeopathological collections becomes common practice (Smithsonian

Institute http://humanorigins.si.edu/evidence/3d-collection; University of Bradford http://www.barc.brad.ac.uk/FromCemeterytoClinic/index.php, Accessed July 2012), the adoption of geometric morphometrics as a recording method in palaeopathology will increase the potential of such virtual databases. This particular case study provides a simple demonstration of the potential applications of VA techniques to palaeopathological research. The same techniques and digital images can also be used to supplement teaching materials in palaeopathology and will enable the use of interactive learning environments online or in schools, universities, and museums that lack access to the original archaeological material or casts.

*Case study 2: Rickets*

The results indicate that geometric morphometrics on two dimensional landmarks can be used to record and describe deformations of long bones related to residual rickets, and that the shape changes resulting from inadequate mineralization are statistically distinguishable from the morphology of healthy femora. Traditional recording and description of long-bone deformation often rely on qualitative descriptors, such as 'slight', 'marked', and 'severe' (Brickley et al. 2010). The combination of geometric morphometrics shape analyses with macroscopic descriptions will greatly strengthen the results of studies analyzing deformation due to rickets by objectifying and quantifying the extent of deformation.

Left femora were more frequently correctly classified, 95.8% compared to 84.2% for the right. Human limb bones are asymmetrical (Auerbach & Ruff 2006; Steele & Mays 1995) and, although the right upper limbs are generally dominant due to handedness, in the lower limb, the left is generally the dominant side and is the dominant weight bearing limb (Macho

1991; Chhibber & Singh 1970; Čuk et al. 2001). The results of our study suggest that the left femur undergoes greater deformation during rickets, possibly as a result of the effect of functional dominance on the inadequately mineralized limb. The link between vitamin D deficiency and long bone curvature may warrant further inquiry in the future. The deformation grids in figure 8 indicate that the lateral diaphyseal margin is curved to a greater extent than the medial aspect. Radiographic characteristics of long bone deformation display a thickening of the cortical bone on the concave surface of the diaphysis (Berry 1952), which is likely represented by the difference in curvature on medial and lateral aspects. This increase in cortical bone results in a straighter diaphyseal edge most likely to stabilize the bone during deformation. This indicates that the changes quantified using geometric morphometrics can be related to both macroscopic and radiographic changes used to diagnose rickets.

*Virtual Methods*:

The case studies presented in this paper demonstrate the possible uses of geometric morphometrics and virtual imaging technology in palaeopathological research. The incorporation of VA techniques with traditional methods will provide new ways to record and analyse pathological lesions, as well as illustrate the effect disease processes have on bone. The first case study illustrated how geometric morphometric data can be used with VA images to produce visualizations of the disease process, and the second case study illustrates how even in the absence of 3D technology, 2D geometric morphometric methods can still be used to describe, record, and analyse pathological deformation. The application of this data to palaeopathological studies and site reports can decrease the subjectivity and observer error inherent in macroscopic description by allowing for objective recording of pathological lesions.

Geometric morphometrics techniques have been used in few bioarchaeological and palaeopathological studies to date. However, when applied they have provided new insights into research questions which would be difficult to answer using traditional methods. Perez (2007) used geometric morphometrics to describe and classify artificial cranial deformation from multiple South American archaeological populations, and found that cranial shape could be classified based on deformation practices related to different populations and social customs. Mitteroeker et al. (2004) used geometric morphometrics to describe the cranial shape changes in an individual with hydrocephaly from the Neolithic. The fact that the main shape differences were an enlargement of the parietal bones indicated that the condition was acquired and not congenital, as the frontal sutures were already fused before the condition developed (Mitteroeker et al. 2004).

A further benefit that virtual methods can offer bioarchaeology is that they are non-destructive and the datasets can be archived and made available digitally to be shared with other researchers and institutions. Elton and Cardini (2008) discuss the benefits of using virtual datasets for sharing and archiving anthropological information, emphasizing that open-access to data facilitates research across the world, without the expense of and time for travel, and preserves valuable skeletal collections from research-related contamination (DNA) and damage through handling (Malmström et al. 2005; Caffell et al. 2001; Roberts & Mays 2011; Bowron 2003). Virtual collections will become especially important as reburial and/or repatriation of human skeletal material from many areas of the world is becoming increasingly more common (Márquez-Grant & Fibiger 2011; Mays 2010; Mays & Smith 2009; Flessas 2008). Once human remains have been reburied, they are lost to future bioarchaeologists. The non-destructive recording of healthy and pathological skeletal variation with geometric

morphometrics and virtual images will help preserve information for future researchers and students.

Virtual methods also have potential beyond research, as virtual environments and 3D imaging have been found to significantly benefit the learning outcomes in anatomical teaching (Petersson et al. 2009; Nicholson et al. 2006). This suggests that VA innovations can greatly benefit teaching in palaeopathology and provide supportive learning materials on pathological lesions. Many countries do not have a large focus on palaeopathological research (Buikstra & Roberts 2012) and many institutions lack access to archaeological skeletons, especially those with the pathological conditions illustrated here. Learning and teaching these topics without access to actual skeletal material or high quality casts means that both students and teachers have to rely on textual descriptions and photographs. The new methods and technologies now available enable the creation of interactive learning environments where pathological lesions and the effect they have on skeletal morphology can be visualized, demonstrated, and interpreted without the need for direct access to the archaeological material. Learning environments can be created through access to geometric morphometric datasets and 3D/2D imaging techniques online or through digital datasets. Virtual images can be used to supplement macroscopic descriptions and photographs, and can be made available either as still-frames or videos which can be used as study aids by students or demonstration aids by teachers.

For the best results using shape analyses in palaeopathology, the disease process under study should result in progressive and/or systematic shape deformations from healthy skeletal morphology. There are two main limitations with using geometric morphometrics on bioarchaeological material. The first is that skeletal elements have to have adequate landmark

preservation for analysis; many archaeological skeletons can be damaged and be missing areas where landmarks were chosen. However, different combinations of landmarks can be used, as in case study 1, to include different sample sizes. The second limitation of using virtual reconstructions and deformation grids for analyzing pathological lesions is the lack of detail on bone changes such as subtle periosteal new bone formation or porosity, which is not adequately displayed on the images. Macroscopic descriptions should therefore always be included with virtual data. The optimal situation will always be hands-on access to the archaeological skeletons. However, where that is impossible or impractical, virtual images and/or data can supplement textual and photographic resources. These resources can be shared digitally and accessed by students, teachers, and researchers on a global scale, especially as more institutions make their digital collections available online. Although there are limitations to teaching with virtual reconstructions when compared to using the original bones or casts, they can provide an ideal addition to teaching that is based on textual descriptions and pictures.

**Conclusion:**

This paper outlines the benefits and potential of incorporating virtual anthropology methods, especially geometric morphometrics, into bioarchaeological, and specifically palaeopathological, research. The case studies presented in this paper are simple demonstrations of how geometric morphometrics can be applied in palaeopathology to quantify and record pathological lesions affecting archaeological skeletal remains. Geometric morphometrics provide a means to objectively record pathological shape changes in bone, and will greatly strengthen many palaeopathological reports and studies. Digital data and the visualization of archaeological human remains, including both healthy (normal) and

pathological (abnormal; palaeopathology) variations, will substantially add to the ability of researchers to share and store their data, as well as enable many universities and museums to provide teaching materials. This can all be accomplished while preserving the integrity of irreplaceable curated archaeological skeletons, as the methods are non-destructive and non-invasive.

Future research will include skeletal elements with deformation resulting from other causes, such as trauma or congenital conditions. The limitations of this research relate mainly to preservation of archaeological human remains; the targeted region, in this case the facial region or femora, must have the landmarks present, well preserved, and identifiable on every skeleton included in a study.

Acknowledgements:

The authors would like to thank the Biological Anthropology Research Centre at the University of Bradford and the Museum of London for access to the skeletal samples. Special thanks go to Durham University and the Canadian Centennial Scholarship Fund for financial aid to KAP during this research, to Helgi Pétur Gunnarsson for aid with software, and to Jo Buckberry, University of Bradford, and Jelena Bekvalac and Rebecca Redfern, Museum of London, for access to the skeletal collections.

References:

Andersen JG, Manchester K. 1992. The rhinomaxillary syndrome in leprosy: A clinical, radiological and palaeopathological study. *International Journal of Osteoarchaeology* 2: 121-129.

Auerbach BM, Ruff CB. 2006. Limb bone bilateral asymmetry: variability and commonality among modern humans. *Journal of Human Evolution* 50(2) 203-218.

Baab KL, McNulty K, Rohlf J. 2012. The shape of human evolution: a geometric morphometrics perspective. *Evolutionary Anthropology* 21: 151-165.

Berry JN. 1952. Radiological signs in rickets and their differential diagnosis. *Indian Journal of Paediatrics* 19(75): 110-114.

Bienvenu T, Guy F, Coudyzer W, Gilissen E, Rouadlès G, Vignaud P, Brunet M. 2011. Assessing endocranial variations in great apes and humans using 3D data from virtual endocasts. *American Journal of Physical Anthropology* 145: 231-246.

Bookstein, F. 1997. Landmark Methods for Forms Without Landmarks: Morphometrics of Group Differences in Outline Shape. *Medical Image Analysis* 1(3): 225-243.

Bowron EL. 2003. A new approach to the storage of human skeletal remains. *The Conservator* 27: 95-106.

Brickley M, Ives R. 2008. *The bioarchaeology of metabolic bone disease.* Oxford: Academic Press.

Brickley M, Mays S, Ives R. 2005. Skeletal manifestation of vitamin D deficiency osteomalacia in documented historical collections. *International Journal of Osteoarchaeology* 15: 389-403.

Brickley M, Mays S, Ives R. 2007. An investigation of skeletal indicators of vitamin D deficiency in adults: Effective markers for interpreting past living conditions and pollution levels in 18$^{th}$ and 19$^{th}$ century Birmingham, England. *American Journal of Physical Anthropology 132: 67-79.*

Brickley M, Mays S, Ives R. 2010. Evaluation and interpretation of residuals rickets deformities in adults. *International Journal of Osteoarchaeology* 20: 54-66.

Buikstra JE, Roberts CA. 2012. *A global history of palaeopathology: pioneers and prospects*. Oxford: Oxford University Press.

Caffell AC, Roberts CA, Janaway RC and Wilson AW. 2001. Pressures on osteological collections – the importance of damage limitation. In: E. Williams, ed. *Human Remains.*

*Conservation, Retrieval and Analysis. Proceedings of a Conference held in Williamsburg, VA, 7- 11 November 1999.* BAR International Series No. 934. Oxford: Archaeopress, pp. 187-97.

Cardini A, Nagorsen D, O'Higgins P, Polly PD, Thorington Jr. RW, Tongiorgi P. 2009. Detecting biological Distinctiveness Using Geometric Morphometrics: An Example Case From the Vancouver Island Marmot. *Ethology Ecology & Evolution* 21: 209-223.

Chhibber SR, Singh I. 1970. Asymmetry in muscle weight and one-sided dominance in the human lower limbs. *Journal of Anatomy* 106(3): 553-556.

Cobb SN, O'Higgins P. 2007. The ontogeny of sexual dimorphism in the facial skeleton. *Journal of Human Evolution* 53: 176-190.

Cowie R, Bekvalac J, Kausmally T. 2008. *Late 17th- to 19th-century burial and earlier occupation at All Saints, Chelsea Old Church, Royal Borough of Kensington and Chelsea. London*, Archaeology Studies Series, Museum of London Archaeology Service.

Čuk T, Leben-Seijak P, Štefančič M. 2001. Lateral asymmetry of human long bones. *Variability and Evolution* 9: 19-32.

Danielsen K 1970 Odontodysplasia leprosa in Danish Mediaeval skeletons. *Særtryk af Tandlægebladet* 74:603-625

Elton S, Cardini A. 2008. Anthropology from the desk? The challenges of the emerging era of data sharing. *Journal of Anthropological Science* 86: 209-212.

Flessa T. 2008. The repatriation debate and the discourse of the commons. *Social & Legal Studies* 17(3): 387-405.

Franklin D, Freedman L, Milne N, Oxnard CE. 2007. Geometric morphometrics study of population variation in indigenous southern African crania. *American Journal of Human Biology* 19(1): 20-33.

Goodall C. 1991. Procrustes Methods in the Statistical Analysis of Shape.*Journal of the Royal Statistical Society*. Series B 53(2): 285-339.

Haduch E, Szczepanek A, Skrzat J, Srodek R, Brzegowy P. Residual rickets or osteomalacia: A case dating from the $16^{th}$-$18^{th}$ centuries from Krosno Ordzanskie, Poland. *International Journal of Osteoarchaeology* 19: 593-612.

Hennessy RJ, Stringer CB. 2002. Geometric morphometrics study of the regional variation of modern human form. *American Journal of Physical Anthropology* 117(1): 37-48.

Holick MF. 2003. Vitamin D: A millennium perspective. *Journal of Cellular Biochemistry* 99: 296-307.

Holick MF. 2004. Sunlight and vitamin D for bone health and prevention of autoimmune diseases, cancers, and cardiovascular disease. *American Journal of Clinical Nutrition* 80: 1678S-1688S.

Holst M. 2005. *Fishergate House artefacts and environmental evidence: The human bone*. Arch Planning Consultancy, UK. Accessed online, July 3, 2010.

Ivanhoe F. 1994. Osteometric scoring of adult residual rickets skeletal plasticity in two archaeological populations from southeastern England: Relationship to sunshine and calcium deficits and demographic stress. *International Journal of Osteoarchaeology* 4(2): 97-120.

Jans MME, Nielsen-Marsh CM, Smith CI, Collins MJ, Kars H. 2004. Characterisation of microbial attack on archaeological bone. *Journal of Archaeological Science* 31: 87-95.

Jopling WH. 1982 Clinical aspects of leprosy. *Tubercle* 63:295-305.

Kimmerle EH, Ross A, Slice D. 2008. Sexual Dimorphism in America: Geometric Morphometric Analysis of the Craniofacial Region. *Journal of Forensic Sciences* 53(1): 54-57.

Klingenberg CP. 2011. MorphoJ: An Integrated Software Package for Geometric Morphometrics. *Molecular Ecology Resources* 11: 353-357.

Kovarovic K, Aiello LC, Cardini A, Lockwood CA. 2011. Discriminant function analyses in archaeology: are classification rates too good to be true? *Journal of Archaeological Sciences* 38: 3006-18.

Kullmer O. 2008. Benefits and risks in virtual anthropology. *Journal of Anthropological Sciences* 86: 205-207.

Küstner EC, Cruz MP, Dansis CP, Iglesias HV, Rogriguez de Rivera Campillo ME, Lopez JL. 2006. Lepromatous Leprosy: A Review and Case Report. *Oral Medicine and Pathology* 11: 474-479.

Kuzminsky SC, Gardiner MS. 2012. Three-dimensional laser scanning: potential uses for museum conservation and scientific research. *Journal of Archaeological Science* 39: 2744-2751.

Lieberman DE, Carlo J, Ponce de León M, Zollikofer CP. 2007. A geometric morphometrics analysis of heterochrony in the cranium of chimpanzees and bonobos. *Journal of Human Evolution* 52: 647-662.

Macho GA. 1991. Anthropological evaluation of left-right differences in the femur of southern African populations. *Anthropologischer Anzeiger* 49(3): 207-216.

Mafart B, Guipert G, Alliez-Philip C, Brau Jean-Jacques. 2007. Virtual reconstruction and new palaeopathological study of the Magdalenian child's skull of Rochereil. *Comptes Rendus Palevol* 6: 569-579.

Magilton J. 1986. *Hospital of St. James and Mary Magdalene, Swanfield Drive.* The archaeology of Chichester and District 1986. Chichester District Council 12-15.

Magilton J. 1993. *Further excavations at the leper hospital cemetery, Swanfield Drive. The archaeology of Chichester and District 1993*. Chichester District Council 37-41.

Magilton, J., Lee, F., Boylston, A., & Council for British Archaeology 2008. *Lepers outside the gate: excavations at the cemetery of the hospital of St James and St Mary Magdalene, Chichester, 1986-87 and 1993*. York: Council for British Archaeology.

Malmström H, Stora J, Dalen L, Holmlund G, Götherström A. 2005. Extensive human DNA contamination in extracts from ancient dog bones and teeth. *Molecular Biology and Evolution* 22(10): 2040-2047.

Manchester K, Lee F. 2008. Leprosy: a review of the evidence in the Chichester sample. In: Magilton J, Lee F, Boylston A. (eds): *Lepers outside the gate: excavations at the cemetery of the hospital of St James and St Mary Magdalene, Chichester, 1986-87 and 1993*. York: Council for British Archaeology: 208-217.

Márquez-Grant N, Fibiger L. 2011. *The Routledge handbook of archaeological human remains and legislation. An international guide to laws and practice in the excavation and trearment of archaeological human remains*. New York: Routledge.

Mays S. 2010. Human osteoarchaeology in the UK 2001-2007: a bibliometric perspective. *International Journal of Osteoarchaeology* 20: 192-204.

Mays S, Smith M. 2009. Ethical dimension of reburial, retention and repatriation of archaeological human remains: a British perspective. In: Lewis M, CleggM. *Proceedings of the Ninth Annual Conference of the British Association for Biological Anthropology and Osteoarchaeology British Archaeological Reports, International Series, 1918.* Oxford: Archaeopress: 107-117.

Milner E, Ragsdale BD, Ortner DJ. 1996. Accuracy in dry bone diagnosis: a comment on palaeopathological methods. *International Journal of Osteoarchaeology* 6(3): 221-229.

Mitteroecker P, Gunz P. 2009. Advances in Geometric Morphometrics. *Evolutionary Biology* 36: 235-247.

Mitteroecker P, Gunz P, Teschler-Nicola M, Weber GW. 2004. New morphometrics methods in palaeopathology: shape analysis of a Neolithic hydrocephalus. *British Archaeological Series: Computer Applications and Quantitative Methods in Archaeology*: 96-99

Møller-Christensen, V. 1953 *Ten lepers from Naestved in Denmark. A study of skeletons from a Medieval Danish leper hospital.* Copenhagen, Danish Science Press

Møller-Christensen V. 1961. *Bone Changes in Leprosy*. Bristol: John Wright.

Møller-Christensen V. 1965. New knowledge of leprosy through palaeopathology. *International Journal of Leprosy* 33(3): 603-610.

Møller-Christensen, V. 1978. *Leprosy Changes of the Skull*. Odense: Odense University Press.

Neubauer S, Gunz P, Hublin JJ. 2009. The Patterns of Endocranial Ontogenetic Shape Changes in Humans. *Journal of Anatomy* 215: 240-255.

Neubauer S, Gunz P, Hublin JJ. 2010. Endocranial shape changes during growth in chimpanzees and humans: A morphometric analysis of unique and shared aspects. *Journal of Human Evolution* 59:555-566.

Nicholson DT, Chalk C, Funnell WRJ, Daniel SJ. 2006. Can virtual reality improve anatomy education? A randomised controlled study of a computer-generated three-dimensional anatomical ear model. *Medical Education* 40: 1081-1087.

O'Higgins P, Jones N. 1998. Facial growth in *Cercocebustorquatus*: An application of three-dimensional geometric morphometric techniques to the study of morphological variation. *Journal of Anatomy* 193: 251-272.

O'Higgins P, Jones N. 2006. *Tools for statistical shape analysis*. Hull York Medical School.

Perez SI. 2007. Artificial cranial deformation in South America: a geometric morphometrics approximation. *Journal of Archaeological Science* 34: 1649-1658.

Petersson H, Sinkvist D, Wang C, Smedby O. 2009. Web-based interactive 3D visualization as a tool for improved anatomy learning. *Anatomical Sciences Education* 2(2): 61-68.

R Development Core Team. *R: A language and environment for statistical computing*. R Foundation for Statistical Computing Vienna, Austria. ISBN 3-900051-07-0, URL http://www.R-project.org; 2012

Ridley DS, Jopling WH. 1966 Classification of leprosy according to immunity. A five-group system. *International Journal of Leprosy* 34:255-273.

Recheis W, Weber GW, Schäfer K, Prossinger H, Knapp R, Seidler H, zur Nedden D. 1999. New methods and techniques in anthropology. *Collegium Antropologicum* 23(2): 495-509.

Roberts CA. 2009. Before analysis: excavation, processing, conservation and curation. In*: Human remains in archaeology: A handbook.* York: Council for British Archaeology: Chapter 4:73-102.

Roberts CA, Mays S. 2011. Study and restudy of curated skeletal collections in bioarchaeology: a perspective on the UK and the implications for future curation of human remains. *International Journal of Osteoarchaeology* 21(5): 626-630.

Rodrigues LC, Lockwood DN. 2011 Leprosy now: epidemiology, progress, challenges, and research gaps. *Lancet Infectious Diseases* 11:464-470

Rohlf FJ. 2004. *TPSDig Version 1.40*. *Ecology and Evolution*, SUNY at Stony Brook.

Rohlf FJ. 2003. Bias and Error in Estimates of Mean Shape in Geometric Morphometrics. *Journal of Human Evolution* 44: 665-683.

Rohlf FJ, Slice D. 1990.Extensions of the Procrustes Method for the Optimal Superimposition of Landmarks. *Systematic Zoology*, 39(1):40-59.

Slice DE. 2007. Geometric Morphometrics. *Annual Review of Anthropology* 36: 261-281.

Steele J, Mays S. 1995. Handedness and directional asymmetry in the long bones of the human upper limb. *International Journal of Osteoarchaeology* 5(1): 39-49.

Stevens SD, Strand Viðarsdóttir U. 2008. Morphological Changes in the Shape of the Non-Pathological Bony Knee Joint with Age: A Morphometric Analysis of the Distal Femur and Proximal Tibia in Three Populations of Known Age at Death. *International Journal of Osteoarchaeology* 18: 352-371.

Strand Viðarsdóttir U, O'Higgins P, Stringer C. 2002. A geometric morphometrics study of regional differences in the ontogeny of the modern human facial skeleton. *Journal of Anatomy* 201(3): 211-229.

Waldron T, Rogers J. 1991. Inter-observer variation in coding osteoarthritis in human skeletal remains. *International Journal of Osteoarchaeology* 1(1): 49-56.

Wang TJ, Pencina MJ, Booth SL, Jacques PF, Ingelsson E, Lanier K, Benjamin EJ, D'Agostino RB, Wolf M, Vasan RS. Vitamin D deficiency and risk of cardiovascular disease. *Circulation* 117: 503-511.

Weber GW, Bookstein FL. 2011. *Virtual Anthropology: a guide to a new interdisciplinary field*. New York: Springer.

Weber GW, Schäfer K, Prossinger H, Gunz P, Mitteröcker P, Seidler H. 2001. Virtual anthropology: the digital evolution in anthropological sciences. *Journal of Physiological Anthropology and Applied Human Science* 20(2): 69-80.

Weber GW, Bookstein FL, Strait DS. 2011. Virtual anthropology meets biomechanics. *Journal of Biomechanics* 44: 1429-1432.

White JW, Ruttenberg BI. 2007. Discriminant Function Analysis in Marine Ecology: Some Oversights and Their Solutions. *Marine Ecology Progress Series* 329: 301-305.

Zelditch ML, Swiderski DL, Sheets HD, & Fink WL. 2004. *Geometric Morphometrics for Biologists*. Elsevier Academic Press: San Diego, CA.

# Chapter 9) Discussion:

Palaeopathological studies can provide insight into and an understanding of the life of past populations, as well as contribute to a better appreciation of the palaeoepidemiology and evolution of diseases that may be prevalent today. Archaeological human remains provide a means of analysing disease processes on large populations spanning multiple geographic and temporal ranges. Palaeopathology focuses on the skeletal manifestations of disease in the absence of soft tissue in human remains from archaeological sites, and therefore circumvents ethical issues associated with clinical research (although human remains must be treated ethically as well). The reliability, effectiveness, and accuracy of methods of recording in palaeopathology, therefore, are of wide reaching importance. Geometric morphometrics are becoming a commonly used method of analysis in biological anthropology and have only recently been adopted in bioarchaeological research, mostly on the study of sexual dimorphism in skeletal remains (Gómez-Valdés et al. 2012; Gonzalez et al. 2009; Bigoni et al. 2010; Bytheway & Ross 2010). There are few studies to date which use geometric morphometrics or virtual imaging in palaeopathological analyses, all of which have been limited to cranial deformation and knee osteoarthritis (Perez 2007; Mitteroeker et al. 2004; Mafart et al. 2007; Shepstone et al. 1999, 2001). This research project aimed to explore and identify the benefits of incorporating quantitative methods of shape analysis into a broader range of palaeopathological studies to expand the potential scope of palaeopathology by being able to answer more ambitious research questions, as well as increase the reliability and accuracy of the methods used for recording pathological lesions. The research was divided into two sections; the first analysed skeletal morphological variation in health and disease in order to identify possible morphologically related aetiological factors and the second

illustrated the use of geometric morphometrics to record, describe, and visualize palaeopathological changes. The following discussion will not focus on the findings of each study, as each manuscript includes a full discussion. Instead, it focuses on how each study contributes to the overall aims and conclusions of the thesis as a whole.

Geometric morphometrics can be used as innovative analytic methods to investigate complex relationships between skeletal morphology and pathological conditions. Palaeopathological inquiry focuses on the effect of disease on bones and geometric morphometrics afford an opportunity to explore any anatomical influence the bones themselves may have on the development or progression of pathological conditions. There are conditions which have unknown aetiologies and pathogeneses, and one aim of the current research was to identify any possible relationship between the presence of a pathological lesion and skeletal morphology.

One such lesion which is commonly identified in palaeopathology and has an unknown aetiology is Schmorl's nodes. The results of Manuscript 1 indicate that the morphology of the lower thoracic spine is strongly associated with the presence of Schmorl's nodes, with a 91.1% accuracy of identifying T12 vertebrae with severe lesions from healthy vertebrae, based solely on the shape of the neural foramen and pedicles. These shape differences were also found to be statistically significant in T10 and T11. Male affected vertebrae had larger bodies than healthy vertebrae, and both male and female affected vertebrae had a more circular body shape, influenced by the shape of the posterior vertebral margin. This finding supports those of Harrington et al. (2001) who found that vertebral bodies with Schmorl's nodes had larger radii than healthy ones. The authors suggest that this could be explained by Laplace's law which states that the ability of a fluid filled tube to withstand compression is decreased with an

increasing radius. Laplace's law could be invoked in the intervertebral disc, and the more circular and/or larger vertebral bodies could influence the ability of the disc to withstand compressional forces (Harrington et al. 2001). The pedicles play a complex role in stabilizing and buttressing the vertebral body and the pedicle shape identified as associated with Schmorl's nodes may not provide adequate support for the larger or more circular vertebral bodies (Whyne et al. 1998). The human spine has unique pressures placed on it for bipedal stance and locomotion and it is hypothesised that the vertebral shape identified in Manuscript 1 may influence the stability and function of the lower thoracic spine. The morphology of the vertebrae themselves appears to play an important role in the development of Schmorl's nodes and may be one aetiological factor predisposing individuals to the condition.

Manuscript 2 expands upon the findings presented in Manuscript 1, as the aim was to explore the relationship between vertebral morphology and Schmorl's nodes in another spinal region. Manuscript 2 analyzed the two-dimensional morphology of the thoraco-lumbar junction and lumbar spine of a single archaeological population. The results support the findings of Manuscript 1 and indicate that there is a strong correlation between vertebral morphology and the presence of Schmorl's nodes at the thoraco-junction and vertebrae L2-4 of the lumbar spine. Based on vertebral morphology, affected and healthy vertebrae were distinguished with an accuracy of 100% for both T12s and L3s, and 87.5% for L2s. The results of L1 did not display as strong a relationship as the other lumbar vertebrae (L2-4), but this could be a result of the sample size. The shape differences identified in affected lumbar vertebrae compared to healthy are also similar to those identified in affected T10 to T12 vertebrae in Manuscript 1. This indicates that there are specific morphological characteristics, such as relatively shorter pedicles and posterior translation of the posterior margin of the

vertebral body, which are associated with the presence of Schmorl's nodes throughout the lower spine.

The results presented in Manuscript 2 also indicate that the morphology associated with the lesions is a major factor in the overall morphology of the lower spine. When the group means of healthy and affected vertebrae from T12 to L4 are analyzed together, there is a separation of healthy and affected vertebrae on PC2 and PC3. This represents 5.4% of the total sample variance, which is significant when considering the analysis includes five morphologically and functionally different vertebrae. The results indicate that the shape of vertebrae in the lower spine associated with Schmorl's nodes is biologically relevant, even when considering the variation in morphology between different spinal elements. Manuscript 2 strengthens the hypothesis outlined in Manuscript 1 by indicating that the morphology associated with Schmorl's nodes represents one of the largest factors of shape variance in the lower spine. This finding could offer one explanation as to why Schmorl's nodes are such a common condition in humans and indicate an important area for both clinicians and palaeopathologists to consider when studying spinal health.

Manuscripts 1 and 2 represent an innovative analysis of a specific pathological condition and the results are of great importance for bioarchaeological research. Despite the fact that the aetiology and pathogenesis of Schmorl's nodes remains unclear in clinical studies, they are often used as skeletal indicators of strenuous physical activity in the past (Novak & Slaus 2011; Papathanasiou 2005; Robb et al 2001; Alesan et al. 1999), with some researchers even using their relative presence to draw conclusions on sexual division of labour (Slaus 2000; Klaus et al. 2009). There is an intuitive relationship between intervertebral disc herniation and physical activity, and biomechanical research has identified that loaded flexion,

extension, and torsion can result in herniation (Callaghan & McGill 2001; Wilder et al. 1988; Goto et al. 2002). However, a careful review of the clinical literature, as well as the results presented in Manuscripts 1 and 2 indicate that there are other factors also influencing the development of Schmorl's nodes. Therefore, these results are of importance both to clinicians and for bioarchaeological interpretation of these lesions.

Both studies have identified an important relationship between vertebral morphology and the health of the human spine. They also demonstrate that geometric morphometrics can be used to answer more challenging palaeopathological research questions and provide new insight into the aetiology of certain diseases. These methods can be applied to CT images, radiographs, photographs, and dry bone, making the methods applicable in both palaeopathological and clinical research. Therefore, they represent a way that the two fields can accurately communicate their research findings. Palaeopathological studies describe pathological lesions visible on dry bone, which can provide great insight into the effect of disease on the skeleton. However, it can be difficult to compare and contrast the research with clinical data, as the pathological changes visible in patients and recorded with imaging techniques are often different to those seen on dry bone. A good example of this is osteoarthritis, where there are different diagnostic criteria used by palaeopathologists and clinicians.

Clinical diagnosis of osteoarthritis relies on radiographic images of joints exhibiting joint space narrowing, subchondral cysts, subchondral sclerosis, and osteophyte formation (McGonagle et al. 2010; Jacobson et al. 2008). Joint space narrowing cannot be seen in palaeopathology; however, eburnation is often used to indicate the same manifestation, as it indicates subchondral sclerosis and a complete loss of cartilage. Osteophytes are used to

indicate joint degeneration, although there is disagreement in the palaeopathological literature whether their presence without eburnation should be considered as representing osteoarthritis (Rogers & Waldron 1995; Jurmain 1999; Wiess & Jurmain 2007). Subchondral cysts can be identified in dry bone with radiography or if the cysts open into the subchondral compact bone. The use of geometric morphometrics has the potential to bridge this gap between clinical and palaeopathological research. The methods can be used in both fields and will produce information about the relationship between joint morphology and osteoarthritis which can be used for both clinical and bioarchaeological interpretations.

Previous studies have used traditional or two-dimensional morphometrics to investigate the relationship between joint morphology and osteoarthritis (Rettig et al. 2008; Shepstone et al. 1999, 2001). Manuscript 3 expands upon these studies by using three-dimensional shape data to assess the morphology of the proximal ulna, distal humerus, and distal femur for any relationship between the shape of the joints and the presence of osteoarthritis. Three-dimensional geometric morphometrics provide more detailed information on joint morphology than the methods employed in the previous studies. The results supported the findings of Rettig et al. (2008), in that there was no identifiable relationship between distal humeral joint shape and osteoarthritis. The proximal ulnae also had no identifiable relationship. The results indicate that joint morphology is unlikely to predispose individuals to elbow osteoarthritis. These findings also indicate that osteoarthritis does not result in systematic shape deformation on these joints. The distal femur, however, did display a tentative relationship between joint morphology and osteoarthritis, with eburnated right and osteoarthritic (no eburnation) female left femora showing statistically significant shape differences when compared to healthy joints. Unfortunately, the results are inconclusive due to

the small sample size. The sample size was decreased due to the Microscribe equipment error discussed in section 4.3.14, as well as the heavy influence of non-pathological factors determining joint shape, such as asymmetry, sexual dimorphism, and allometry, all of which had to be controlled for during analyses. The limitations of Manuscript 3 highlight how future studies focusing on joint morphology need to carefully consider the influence of these factors on overall morphology.

The results of Manuscript 3 indicate that there are morphological similarities between male and female eburnated right and the osteoarthritic (without eburnation) female left distal femoral joints. However, these changes are not consistent throughout the sample and were not identified in the male left femora. It is difficult to ascertain a cause and effect relationship between joint morphology and osteoarthritic changes. Any shape differences identified between healthy and osteoarthritic joints could represent a joint shape more susceptible to developing the disease or could indicate the shape changes occur as a result of deformation due to functional adaptation. As the "pathological shapes" were not consistently identified throughout the sample, this may suggest that the shape differences relate to a change resulting from osteoarthritis. Osteoarthritic joint changes such as osteophyte development or remodelling of the joint would affect the joint shape. The morphology identified as associated with osteoarthritis may represent a systematic response to counteract the instability caused by the joint degradation. If this is the case, geometric morphometrics could be used to identify and evaluate the progression of the disease in clinical studies. The results are not positive due to sample size, but do highlight a possible area of future research into how osteoarthritis affects the knee joint.

Manuscripts 1 through 3 illustrate the benefits of using geometric morphometrics to investigate morphological skeletal variation associated with common pathological condtions. Manuscripts 1 and 2 present very significant results indicating that the morphology of the vertebrae themselves may be an important aetiological factor in the development of Schmorl's nodes. Manuscript 3 demonstrates the potential of using geometric morphometrics to explore the relationship between knee joint morphology and the presence and/or progression of osteoarthritis. However, geometric morphometrics also have the potential to strengthen palaeopathological research by providing an objective method of recording and describing pathological changes on bones.

Traditional methods used in palaeopathology rely heavily on macroscopic description of lesions, which can be highly subjective and dependent on observer experience. Manuscript 4 illustrates the potential benefits and limitations of using geometric morphometrics and virtual imaging technology in palaeopathological research. There were two pathological conditions presented, rhinomaxillary syndrome and femoral bowing due to residual rickets. Both lesions were quantifiable and the results indicate that the disease processes resulted in statistically identifiable shape deformation. These examples demonstrate the potential of using geometric morphometrics to objectively record and describe pathological lesions. The availability of accurate objective data will greatly increase the reliability and accuracy of palaeopathological recording by decreasing the reliance on subjective macroscopic descriptions. This objective data can also be easily stored and shared between research groups, a feature which is of particular importance in countries where reburial or repatriation of human remains is becoming or already is common practice (Márquez-Grant & Fibiger 2011; Mays 2010; Mays & Smith 2009; Flessas 2008). When human remains are to be repatriated or

reburied, it is vital for bioarchaeologists to obtain as much data and information as possible while they still have access to the remains (Buikstra and Ubelaker 1994).

Manuscript 4 not only demonstrated the potential of using geometric morphometrics to record lesions, but it also illustrated how virtual imaging technology can produce detailed and accurate depictions of pathological shape changes. The example in Manuscript 4 showed how geometric morphometrics data can be incorporated with scanning technology to produce 3D illustrations of the shape deformations of the face resulting from leprosy. Virtual imaging techniques can provide easy, affordable, and non-destructive ways to demonstrate pathological lesions in research or teaching. Many universities and museums worldwide do not have access to human skeletal remains and those departments that do have vast archaeological or anatomical collections have to consider that these irreplaceable bones can be contaminated and damaged over years of handling by students, instructors, and researchers (Malmström et al. 2005; Caffell et al. 2001; Roberts & Mays 2011; Bowron 2010). Ethically, bioarchaeologists should carefully consider their choices of analyses when using human skeletal material and only use destructive methods, such as isotope or DNA analysis, when the research potential outweighs the damage to the bones. Geometric morphometrics and virtual imaging technologies are both non-destructive and non-invasive, making these methods ethically sound when analyzing and interpreting pathological lesions in human remains.

**Limitations of the research:**

Although the use of geometric morphometrics in palaeopathology has great potential, there are also many limitations in using these methods. There may be financial constraints, as the techniques require equipment (i.e. Microscribes, laser scanners, and computers) which is expensive, although the software for geometric morphometric analyses is so far free and easily available. Also, in order to use shape analyses to record and describe palaeopathological lesions, the disease or condition must result in a progressive and systematic shape deformation. As illustrated with the elbow joint in Manuscript 3, if the disease does not affect the shape of the bone in a systematic manner, the affected bones will not represent an identifiable group within the sample. Another limitation to the use of geometric morphometrics in palaeopathology is one fundamental to the discipline itself: that when studying disease or injury in skeletal remains, it is the 'abnormal' which is sought. Sample sizes of data with pathological lesions are dependent on the overall health of the particular population studied and the preservation of the lesions themselves. In Manuscript 3, for example, only a very small percentage of the sample exhibited knee osteoarthritis. Osteoarthritis of the knee is generally considered to be common and the collections analysed were large. It was, therefore, expected that more adults would show evidence of the condition.

An additional limitation affecting both the sample size and accuracy of geometric morphometric studies on archaeological bone relates to preservation. Preservation of skeletal material is dependent on environmental factors, as well as excavation and handling techniques. Taphonomic damage may lead to landmarks not being present on all bones included in a sample, making it difficult to analyse large enough samples for statistical analysis. Although missing landmarks can be replaced with the centroid mean of the particular landmark after

superimposition, such substitution will introduce error in the data and is thus far from ideal. The study of rhinomaxillary syndrome in Manuscript 4 originally included 66 individuals with thirty-three 3D landmarks covering the maxilla and other facial bones. However, as each individual displayed different levels of preservation of the fragile facial bones, a subset of landmarks had to be chosen to include the largest number of individuals with adequate coverage of the affected area. This drastically reduced overall sample size and made any interpretation of the effect of the lesion on the face impossible.

The studies of vertebral morphology highlight a potential way around this limitation, as multiple datasets with varied landmark configuration can be used to investigate the same morphological features. As discussed in Manuscripts 1 and 2, the analysis of the full vertebral morphology could only include vertebrae with complete vertebral bodies and without syndesmophytes (osteophytes on the margin of the vertebral body). However, as the major shape differences between affected and healthy vertebrae were focused in the posterior vertebral elements, i.e. the pedicles and neural foramen, it was possible to increase the sample size by subsequently analyzing only the eight landmarks in this area, allowing the inclusion of vertebrae with damaged bodies. Healthy and affected vertebrae are accurately distinguished in both sets of landmarks, supporting the strength of the morphological differences between them as the results are statistically significant in both comparisons.

As illustrated in this thesis, shape analyses can identify relationships between pathological conditions and bone morphology. However, it can be difficult to determine if this relationship represents a shape which was present before the condition or if the condition itself altered the bone shape. This argument of cause and effect is illustrated in Manuscript 3, where the shape differences identified between healthy and eburnated distal femora joints are

difficult to identify as a result of functional adaptations or a joint morphology possibly influencing osteoarthritis.

Although geometric morphometric data can provide highly detailed morphological information, they do not describe other pathological bone changes, such as new bone formation, porosity, sclerotic or erosive lesions, and so forth. The intention of this research is not to replace traditional palaeopathological methods of recording and describing lesions, but instead for them to be used alongside macroscopic description and traditional morphometrics in order to provide maximum information on the skeletal remains studied and explore any complex relationships between human morphological variation and health.

# Chapter 10) Conclusions and future research

**Overall, the main research outcomes in this study were:**

- Vertebral morphology has a strong association with the presence of Schmorl's nodes in the lower spine and is likely to be a major aetiological factor in the development of the lesions (Manuscript 1 and 2).
- The vertebral morphology identified as being associated with the presence of Schmorl's nodes is a major factor in the overall morphological variation of the lower spine (Manuscript 2).
- The joint morphology of the distal humerus and proximal ulna has no identifiable relationship with the presence of osteoarthritis and likely do not predispose individuals to developing the condition (Manuscript 3).
- Osteoarthritis of the elbow does not result in systematic shape changes affecting the joint morphology (Manuscript 3).
- There are statistically identifiable shape differences between healthy and osteoarthritic knee joints, although these are not consistent throughout the sample (Manuscript 3).
- Osteoarthritis of the knee may result in systematic shape changes occurring as functional adaptations to counteract the instability of the osteoarthritic knee and warrants further investigation (Manuscript 3).
- Geometric morphometrics can be used to quantify and record pathological deformations resulting from rhinomaxillary syndrome due to a leprosy infections and femoral bowing due to residual rickets (Manuscript 4).

- Virtual imaging can be used with geometric morphometric data to illustrate pathological shape changes resulting from rhinomaxillary syndrome (Manuscript 4).

This thesis has explored the potential utility of geometric morphometrics in palaeopathological research to not only record and describe pathological changes on bones, but also to investigate the relationship between skeletal morphology and disease in a very detailed and informative manner. The overall aim was to investigate the benefits and limitations of geometric morphometrics in palaeopathological research and each individual study has fulfilled this aim. Together, all four studies have expanded the boundaries of palaeopathology by applying these methods to answer innovative research questions. The results of Manuscripts 1 and 2 indicate that the morphology of the lower vertebrae have a significant influence on the development of Schmorl's nodes, a relationship which was not previously recognized. Manuscript 3 suggests that osteoarthritis of the knee may result in systematic shape changes which can be identified using geometric morphometric techniques. And Manuscript 4 illustrates how geometric morphometrics and virtual imaging technology can be used to record, describe, and illustrate the shape deformations associated with rhinomaxillary syndrome in leprosy and femoral bowing due to residual rickets. Each manuscript provides promising groundwork for the integration of geometric morphometrics and virtual methods into future palaeopathological research.

**The main conclusions of this thesis are:**

- The data obtained with geometric morphometric methods allow for detailed analysis of the morphology of healthy and pathological bones and can indicate associations between shape and disease which were not obvious with macroscopic analysis.
- The potential of these methods has been demonstrated, as the findings in Manuscripts 1 and 2 provided insight into a pathological condition, Schmorl's nodes, which had not been previously recognized.
- Geometric morphometrics can also be used in clinical studies, which could increase the potential of collaboration between palaeopathology and medicine.
- The results of palaeopathological research, such as those found in Manuscripts 1 and 2, can aid clinical understanding of how certain diseases or conditions affect the human skeleton.
- The results in Manuscript 3 may indicate that distal femoral joints can react to osteoarthritis in a systematic way which creates identifiable morphological similarities between affected joints. This information could be useful for clinical understanding disease progression and of how osteoarthritis affects the joint.
- The use of geometric morphometrics as a recording method will greatly strengthen palaeopathological research by decreasing the subjectivity and error inherent in macroscopic description. It is a non-destructive method that has hardware that is portable for fieldwork.
- Digital data should not be used to replace traditional methods of palaeopathological recording or analysis, but instead used in combination with these in order to provide the maximum amount of information as possible about archaeological skeletons.

- The incorporation of virtual imaging and data analysis technologies into palaeopathological teaching and demonstrating will aid students and teachers who lack access to actual archaeological skeletal remains.
- The availability of digital data which can be easily stored and shared among researchers will strengthen palaeopathological research on a global scale, and is especially relevant due to the increasingly common practice of reburial and repatriation.
- Shape analyses can be used to identify relationships between skeletal morphology and disease, either as a shape resulting from or influencing the development of a disease process.

## Future directions:

Future research should focus on:

- Increasing the sample size for similar morphological studies in palaeopathology.
- Including human populations from multiple ancestral backgrounds in order to capture modern human variation and its effects on health and disease.
    - This will enable a full analysis of the conditions discussed in this thesis, such as the association of vertebral morphology and Schmorl's nodes, within the framework of modern human variation. The collections used in this project were confined to Medieval and Post-Medieval England, and incorporating individuals of various ancestries will determine if the phenomena identified in

Manuscripts 1 and 2 are consistent across space and time or if the morphological association with disc herniation found in these particular populations are more of a 'biological curiosity'.

- Using three-dimensional landmarks
    - Vertebral morphology would benefit from the use of three-dimensional landmarks, as they would allow analyses of vertebral height, articular facets, and the spinous processes. Future research expanding the work on Schmorl´s nodes to three-dimensions on the entire spine of multiple human populations would allow for a more conclusive and encompassing analysis of the importance of vertebral morphology on spinal health.
- Including comparative analyses of non-human apes and hominin fossils in analyses of 3D vertebral morphology.
    - This will enable a highly detailed investigation into the influence of bipedalism on vertebral morphology and spinal health. The human spine exhibits more spinal disease than quadrupedal animals and comparative analyses will explore the relationship between bipedalism and spinal disease.
- Incorporating clinical information, such as soft tissue lesions, body weight, and life histories into palaeopathological studies.
    - Integration of clinical information into palaeopathology would provide a full understanding of the anatomical importance of vertebral or joint morphology on the development and expression of

pathological conditions. This could be accomplished by using documented skeletal collections, CT scans, and/or biomechanical experiments using skeletal elements with soft tissue.

  - Longitudinal clinical studies looking at joint morphology and osteoarthritis would be able to fully explore the cause and effect relationship of the disease on the shape of the knee joint, as well as investigate the relationship between knee joint morphology and the progression of osteoarthritis.

- Using different landmark sets
  - Landmark choice can influence which morphological aspects are quantified, and the use of too many or too few landmarks can alter the amount and type of shape variation captured. The landmarks used in this thesis were chosen based on the limits of skeletal preservation, and during analysis landmarks which added unnecessary variance to the data (e.g. landmark on ulnar tuberosity) were removed. It is possible that different combinations of landmarks may provide insight into morphological associations with pathologies which were not found here.
- Expanding methods to other pathological lesions
  - These methods should be applied to other pathological lesions, such as congenital deformities and fractures, in order to develop standardized recording of lesions often found in archaeological contexts.

References:

Abbas J, Hamoud K, May H, Hay O, Medlej B, Masharawi Y, Peled N, Hershkovitz I. 2010. Degenerative lumbar spinal stenosis and lumbar spine configuration. *European Spine Journal* 19: 1865-1873.

Abrams SA. 2002. Nutritional rickets: An old disease returns. *Nutritional Reviews* 60: 111-115.

Acsádi G, Nemeskéri J. 1970. *History of human life span and mortality*. Akadémiai Kiadó, Budapest.

Adams MA, Freeman B, Morrison HP, Nelson IW, Dolan P. 2000. Mechanical initiation of intervertebral disc degeneration. *Spine* 25(13): 1625-1636.

Adams MA, Pollintine P, Tobias JH, Wakley GK, Donal P. 2006. Intervertebral disc degeneration can predispose to anterior vertebral fractures in the thoracolumbar spine. *Journal of Bone & Mineral Research* 21(9): 1409-1416.

Adams DC, Rohlf EJ, Slice DE. 2004. Geometric morphometrics: Ten years of progress following the 'revolution'. *Italian Journal of Zoology* 71: 5-16.

Albrecht GH. 1992. Assessing the Affinities of Fossils Using Canonical Variates and Generalized Distances. *Human Evolution* 7(4): 49-69.

Alesan A, Malgosa A, Simó C. 1999. Looking into the demography of an Iron Age population in the Western Mediterranean. I. Mortality. *American Journal of Physical Anthropology* 110: 285-301.

Ameye L.G., Young M.F. 2006. Animal models of osteoarthritis: lessons learned while seeking the 'Holy Grail'. *Current Opinion in Rheumatology* 18: 537-547.

Anakwenze OA, Kancheria V, Rendon N, Drummond DS. 2011. Adolescent disc dysplasia and back pain. *Journal of Children's Orthopaedics* 5: 49-53.

Andersen JG, Manchester K. 1987. Grooving of the proximal phalanx in leprosy: A palaeopathological and radiological study. *Journal of Archaeological Science* 14: 77-82.

Andersen JG, Manchester K. 1988. Dorsal tarsal exostoses in leprosy: A palaeopathological and radiological study. *Journal of Archaeological Science* 15:51-56.

Andersen JG, Manchester K. 1992. The rhinomaxillary syndrome in leprosy: A clinical, radiological and palaeopathological study. *International Journal of Osteoarchaeology* 2: 121-129.

Andersen JG, Manchester K, Ali R. 1992. Diaphyseal remodeling in leprosy: A radiological and palaeopathological study. *International Journal of Osteoarchaeology* 2: 211-219.

Andersen JG, Manchester K, Roberts CA. 1994. Septic bone changes in leprosy: A clinical, radiological and palaeopathological study. *International Journal of Osteoarchaeology* 4: 21-30.

Antonacci MD, Mody DR, Heggeness MH.1998. Innervation of the human vertebral body: a histologic study. *Journal of Spinal Disorders* 1:526-531.

Arriaza BT. 1993. Seronegative spondyloarthropathies and diffuse idiopathic skeletal hyperostosis in ancient northern Chile. *American Journal of Physical Anthropology* 91(3): 263-278.

Arthritis Research UK. http://www.arthritisresearchuk.org/arthritis_information/arthritis_types__ symptoms/osteoarthritis_of_the_knee.aspx#non. Accessed online April 2, 2012.

Aspden RM. 2008. Osteoarthritis: a problem of growth not decay? *Rheumatology* 47(10): 1452-1460.

Auerbach BM, Ruff CB. 2006. Limb bone bilateral asymmetry: variability and commonality among modern humans. *Journal of Human Evolution* 50(2) 203-218.

Baab KL, McNulty K, Rohlf J. 2012. The shape of human evolution: a geometric morphometrics perspective. *Evolutionary Anthropology* 21: 151-165.

Bailey, A.J., Mansell J.P., Sims T.J., Banse X. 2004. Biochemical and mechanical properties of subchondral bone in osteoarthritis. *Biorheology* 41: 349-358.

Baliunas, A.J., D.E. Hurwitz, A.B. Ryals, A. Karrar, J.P. Case, J.A. Block, & T.P. Andriachhi. 2002. Increased knee joint loads during walking are present in subjects with knee osteoarthritis. *Osteoarthritis and Cartilage* 10: 573-579.

Bass WM. 1987 (1971). *Human osteology: A laboratory and field manual*. Missouri Archaeology Society Spec Pap 2: Columbia.

Baranto A, Hellström M, Nyman R et al. 2006.. Back pain and degenerative abnormalities in the spine of young elite divers: A 5 years follow-up magnetic resonance imaging study. *Knee Surgery and Sports Traumatology Arthrose* 14: 907-14.

Baylac M, Frieβ M. 2005. Fourier descriptors, Procrustes superimposition, and datadimensionality: An example of cranial shape analysis in modern human populations. In: Slice D, ed. *Modern Morphometrics in Physical Anthropology*. New York: Springer 145-62.

Behare PB. 1981. Psychological reactions to leprosy. *Leprosy India* 53(2): 266-272.

Belcastro, M.G., V. Mariotti, F. Facchini, & O. Dutour. 2005. Leprosy in a Skeleton from the 7th Century Necropolis of Vicenne-Campochiaro (Molise, Italy). *International Journal of Osteoarchaeology* 15: 431-448.

Berry JN. 1952. Radiological signs in rickets and their differential diagnosis. *Indian Journal of Paediatrics* 19(75): 110-114.

Bienvenu T, Guy F, Coudyzer W, Gilissen E, Rouadlès G, Vignaud P, Brunet M. 2011. Assessing endocranial variations in great apes and humans using 3D data from virtual endocasts. *American Journal of Physical Anthropology* 145: 231-246.

Bigoni L, Veleminska J, Bruzek. 2010. Three-dimensional geometric morphometrics analysis of cranio-facial sexual dimorphism in a Central European sample of known sex. *HOMO Journal of Comparative Human Biology* 61(1): 16-32.

Bijkerk C, Houwing-Duistermaat JJ, Valkenburg HA, Meulenbelt I, Hofman A, Breedveld FC, Pols HAP, van Duijn C, Slagboom PE. 1999. Heritabilities of radiologic osteoarthritis in peripheral joints and of disc degeneration of the spine. *Arthritis & Rheumatism* 42(8): 1729-1735.

Bikle DD. 2012. Vitamin D and bone. *Current Osteoporosis Reports* 10: 151-159.

Blau S, Yagodin V. 2005. Osteoarchaeological evidence for leprosy from western Central Asia. *American Journal of Physical Anthropology* 126(2): 150-158.

Blondiaux J, Duvette JF, Vatteoni S, Eisenberg L. 1994. Microradiographs of leprosy from an osteoarchaeological context. *International Journal of Osteoarchaeology* 4(1): 13-20.

Boldsen JL, Mollerup L. 2006. Outside St. Jørgen: Leprosy in the Medieval Danish City of Odense. *American Journal of Physical Anthropology* 130: 344-351.

Boldsen JL. 2009. Leprosy in Medieval Denmark: Osteological and epidemiological analyses. *Anthropologischer Anzeiger* 67(4): 407-425.

Bookstein, F. 1997 (1991). *Morphometric Tools for Landmark Data: Geometry and Biology*. Cambridge University Press: Cambridge.

Bookstein F. 1997b. Landmark methods for forms without landmarks: Morphometrics of group differences in outline shape. *Medical Image Analysis* 1(3): 225-243.

Bouwman AS, Brown TA. 2005. The limits of biomolecular palaeopathology: ancient DNA cannot be used to study venereal *syphilis. Journal of Archaeological Science* 32: 703-713.

Bowron EL. 2003. A new approach to the storage of human skeletal remains. *The Conservator* 27: 95-106.

Brandt, K.D., Radin E.L, Dieppe P.A., van de Putte L. 2006. Yet more evidence that osteoarthritis is not a cartilage disease. *Annals of Rheumatic Diseases* 65: 1261-1264.

Brenner E. 2010. Recent perspectives on leprosy in Medieval Western Europe. *History Compass* 8(5): 388-406.

Brickley M, Ives R. 2008. *The bioarchaeology of metabolic bone disease.* Oxford: Academic Press.

Brickley M, Mays S, Ives R. 2005. Skeletal manifestation of vitamin D deficiency osteomalacia in documented historical collections. *International Journal of Osteoarchaeology* 15: 389-403.

Brickley M, Mays S, Ives R. 2007. An investigation of skeletal indicators of vitamin D deficiency in adults: Effective markers for interpreting past living conditions and pollution levels in 18th and 19th century Birmingham, England. *American Journal of Physical Anthropology 132: 67-79.*

Brickley M, Mays S, Ives R. 2010. Evaluation and interpretation of residuals rickets deformities in adults. *International Journal of Osteoarchaeology* 20: 54-66.

Bridges, P.S. 1991. Degenerative Joint Disease in Hunter-Gatherers and Agriculturalists From the Southeastern United States. *American Journal of Physical Anthropology* 85: 379-391.

Bridges PS. 1992. Prehistoric Arthritis in the Americas. *Annual review of Anthropology* 21: 67-91

Bridges PS. 1993. The Effect of Variation in Methodology on the Outcome of Osteoarthritic Studies. *International Journal of Osteoarchaeology* 3: 289-295.

Britton WJ, Lockwood DN. 2004. Leprosy. *Lancet* 363:1209-1219

Brooks ST, Suchey JM. 1990. Skeletal age determination based on the os pubis: Comparison of the Acsádi-Nemeskéri and Suchey-Brooks methods. *Journal of Human Evolution* 5: 227–38

Brothwell DR. 1981 (1963). *Digging up bones: the excavation, treatment and study of human skeletal remains.* Cornell University Press: Ithaca, New York.

Brown TR, Kovindna A, Wathanadikkol U, Piefer A, Smith T, Kraft GH. 1996. Leprosy neuropathy: Correlation of clinical and electrophysiological tests. *Indian Journal of Leprosy* 68(1): 1-14.

Brown KR, Pollintine P, Adams M. 2008. Biomechanical implications of degenerative joint disease in the apophyseal joints of human thoracic and lumbar vertebrae. *American Journal of Physical Anthropology* 136: 218-326.

Buikstra JE, Roberts CA. 2012. *The Global History of Paleopathology: Pioneers and Prospects*. Oxford: Oxford University Press.

Buikstra JE, Ubelaker DH. 1994. *Standards for Data Collection from Human Skeletal Remains*. Research Series, no. 44. Fayetteville, Arkansas Archaeological Survey.

Burleigh, G. 1984. Excavations at Baldock 1980–81: An interim report. *Hertfordshire's Past* 12*:* 3–17.

Burke KL. 2012. Schmorl's nodes in an American military population: Frequency, Formation, and Etiology. *Journal of Forensic Sciences* 57(3): 571-7.

Bytheway JA, Ross AH. 2010. A geometric morphometrics approach to sex determination of the human adult os coxa. *Journal of Forensic Sciences* 55(4): 859-864.

Caffell AC, Roberts CA, Janaway RC and Wilson AW. 2001. Pressures on osteological collections – the importance of damage limitation. In: E. Williams, ed. *Human Remains. Conservation, Retrieval and Analysis. Proceedings of a Conference held in Williamsburg, VA, 7- 11 November 1999.* BAR International Series No. 934. Oxford: Archaeopress, pp. 187-97.

Calais-Germain B. 2007. *Anatomy of Movement*. Seattle: Eastland Press.

Callaghan JP, McGill SM. 2001. Intervertebral disc herniation: studies on a porcine model exposed to highly repetitive flexion/extension motion with compressive force. *Clinical Biomechanics* 16:28-37.

Cardini A, Nagorsen D, O'Higgins P, Polly PD, Thorington Jr. RW, Tongiorgi P. 2009. Detecting biological distinctiveness using geometric morphometrics: An example case from the Vancouver Island Marmot. *Ethology Ecology & Evolution* 21: 209-223.

Carmichael AG. 1993. Leprosy. In: Kiple KF. *The Cambridge World History of Human Disease.* Cambridge: Cambridge University Press: 834-839.

Chhibber SR, Singh I. 1970. Asymmetry in muscle weight and one-sided dominance in the human lower limbs. *Journal of Anatomy* 106(3): 553-556.

Childs, J.D., P.J. Sparto, G.K. Fitzgerald, M. Bizzini, & J.J. Irrgang. 2004. Altertations in lower extremity movement and muscle activation patterns in individuals with knee osteoarthritis. *Clinical Biomechanics* 19: 44-49.

Cholewicki J, McGill S. 1996. Mechanical stability of the in vivo lumbar spine: Implications for injury and chronic low back pain. *Clinical Biomechanics* 11(1): 1-15.

Chen TC, Chimeh F, Lu Z, Mathieu J, Person KS, Zhang A, Kohn N, Martinello S, Berkowitz R, Holick MF. 2007. Factors that influence the cutaneous synthesis and dietary sources of vitamin D. *Archives of Biochemistry and Biophysics* 460(2): 213-217.

Clark GA, Hall NR, Armelagos GJ, Borkan GA, Panjabi MM, Wetzel FT. 1986. Poor growth prior to early childhood: Decreased healthy and life-span in the adult. *American Journal of Physical Anthropology* 70: 145-160.

Cobb SN, O'Higgins P. 2007. The ontogeny of sexual dimorphism in the facial skeleton. *Journal of Human Evolution* 53: 176-190.

Cooper C, McAlindon T, Coggon D, Egger P, Dieppe P. 1994. Occupational activity and osteoarthritis of the knee. *Annals of the Rheumatic Diseases* 53:90-93.

Cooper C., Snow S, McAlindon TE, Kellingray S, Stuart B, Coggon D, Dieppe P. 2000. Risk factors for the incidence and progression of radiographic knee osteoarthritis. *Arthritis & Rheumatism* 43(5): 995-1000.

Coughlan J, Holst M. 2001. Health Status. In: Fiorato V, Boylston A, Knusel C. *Blood Red Roses: The Archaeology of a Mass Grave from the Battle of Towton, AD 1461*. Oxford: Oxbow Books.

Covey HC. 2001. People with leprosy (Hansen's disease) during the Middle Ages. *The Social Science Journal* 38:315-321.

Cowie R, Bekvalac J, Kausmally T. 2008. *Late 17th- to 19th-century burial and earlier occupation at All Saints, Chelsea Old Church, Royal Borough of Kensington and Chelsea. London*, Archaeology Studies Series, Museum of London Archaeology Service.

Cross H. 2007. Interventions to address the stigma associated with leprosy: A perspective on the issues. *Psychology, Health & Medicine* 11(3): 367-373.

Crubezy E, Goulet J, Bruzek J, Jelinek J, Rouge D, Ludes B. 2002. Epidemiology of osteoarthritis and enthesopathies in a European population dating back 7700 years. *Joint Bone Spine* 69: 580-588.

Cule, J. The Stigma of Leprosy: It's Historic Origins and Consequences with Particular Reference to the laws of Wales. In CA Roberts, ME Lewis, & K. Manchester.eds. *The Past and Present of Leprosy: Archaeological, Historical, Palaeopathological, and Clinical Approaches*. BAR International Series 1054: 149-154.

Čuk T, Leben-Seijak P, Štefančič M. 2001. Lateral asymmetry of human long bones. *Variability and Evolution* 9: 19-32.

Cushnaghan, J. & P. Dieppe. 1991. Study of 500 patients with limb joint osteoarthritis. I. Analysis by age, sex, and distribution of symptomatic joint sites. *Annals of Rheumatic Diseases* 50: 8-13.

Dalal, S., Bull M., Stanley D. 2007. Radiographic changes at the elbow in primary osteoarthritis: A comparison with normal aging of the elbow joint. *Journal of Shoulder and Elbow Surgery* 16(3): 358-361.

Danielsen K 1970 Odontodysplasia leprosa in Danish Mediaeval skeletons. *Særtryk af Tandlægebladet* 74:603-625.

Dar G, Masharawi Y, Peleg S, Steinberg N, May H, Medlej B, Peled N,Hershkovitz I. 2010. Schmorl's nodes distribution in the human spine and its possible etiology. *European Spine Journal* 19: 670-675.

Dar G, Peleg S, Masharawi Y, Steinberg N, May H, Hershkovitz I. 2009. Demographic aspects of Schmorl's nodes. *Spine* 34(9): E312-E315.

Day, J.S., van der Linden J.C., Bank, R.A., Ding, M., Hvid I., Sumner D.R., Weinans H. 2004. Adaptation of subchondral bone in osteoarthritis. *Biorheology* 41(3): 359-368.

Davis CB, Shuler KA, Danforth ME, Herndon KE. 2012. Patterns of interobserver error in the scoring of entheseal changes. *International Journal of Osteoarchaeology early view.*

Debono L., Mafart B., Jeusel E., Guipert G. 2004. Is the incidence of elbow osteoarthritis underestimated? Insights from palaeopathology. *Joint Bone Spine* 71(5): 397-400.

Dedrick D.K., Goldstein S.A., Brandt K.D. O'Connor B.L., Goulet R.W., Albrecht M. 1993. A longitudinal study of subchondral plate and trabecular bone in cruciate-deficient dogs with osteoarthritis followed up for 54 months. *Arthritis & Rheumatism* 36: 1460-1467.

Dekker J, Boot B, van der Woude LU, Bijlsma JWJ. 1992. Pain and disability in osteoarthritis: A reiview of biobehavioral mechanisms. *Journal of Behavioral Medicine* 15(2): 189-214.

DeWitte SN. 2009. The effect of sex on risk mortality during the Black Death in London, A.D. 1349-1350. *American Journal of Physical Anthropology* 139: 222-234.

DeWitte SN. 2010. Age patterns of mortality during the Black Death in London, A.D. 1349-1350. *Journal of Archaeological Science* 37: 3394-3400.

DeWitte SN, Hughes-Morey G. 2012. Stature and frailty during the Black Death: The effect of stature on risks of epidemic mortality in London, A.D. 1348-1350. *Journal of Archaeological Science* 39:1412-1419.

DeWitte SN, Wood JW. 2008. Selectivity of Black Death mortality with respect to pre-existing health. *Proceedings of the National Academy of Science* 105(5):1436-1441.

Dieppe P, Loe L, Shepstone L, Watt I. 2006. What 'skeletal palaeopathology' can teach us about arthritis. The contributions of the late Dr. Juliet Rogers. *Reumatismo* 58(2): 79-84.

Doherty M, Spector TD, Serni U. 2000. Session 1: Epidemiology and genetics of hand osteoarthritis. *Osteoarthritis and Cartilage* 8: S14-S15.

Dominick KL, Baker TA. 2004. Racial and ethnic differences in osteoarthritis: Prevalence, outcomes, and medical care. *Ethnicity and Disease* 14(4): 558-566.

Dryden IL & Mardia KV. 1998. *Statistical Shape Analysis*. Chichester: John Wiley & Sons.

Dytham C. 2003. *Choosing and using statistics: A biologist's guide.* Chichester, West Sussex: John Wiley and Sons.

Dzierzkkray-Rogaliski T. 1980. Palaeopathology of the Ptolemaic inhabitants of Dakhleh Oasis (Egypt). *Journal of Human Evolution* 9:71-74

Eckstein, F., Lohe F., Schulte E., Muller-Gerbl M., Milz S., Putz R. 1993. Physiological incongruity of the humero-ulnar joint: a functional principal of optimized stress distribution acting upon articulating surfaces? *Anatomy & Embryology* 188: 449-455.

Eckstein F., Merz, B., Schmid P., Putz R. 1994. The influence of geometry on the stress distribution in joints – a finite element analysis. *Anatomy & Embryology* 189: 545-552.

Eckstein F, Merz B, Müller-Berbi M, Holzknecht N, Pleier M, Putz R. 1995. Morphomechanics of the humero-ulnar joint: II. Concave incongruity determines the distribution of load and subchondral mineralization. *The Anatomical Record* 243(3): 327-335.

Edmondston SJ, Singer KP. 1997. Thoracic spine: anatomical and biomechanical considerations for manual therapy. *Manual Therapy* 2(3): 132-143.

El-Khoury GY, Whitten CG. 1993. Trauma to the upper thoracic spine: Anatomy, biomechanics, and unique imaging features. *American Journal of Roentgenology* 160(1): 95-102.

Elton S, Cardini A. 2008. Anthropology from the desk? The challenges of the emerging era of data sharing. *Journal of Anthropological Science* 86: 209-212.

Faccia KJ, Williams RC. 2008. Schmorl's nodes: Clinical significance and implications for the bioarchaeological record. *International Journal of Osteoarchaeology* 18(1): 28-44.

Fahey V, Silberstein M, Anderson R, Briggs C. 1998. The pathogenesis of Schmorl's nodes in relation to acute trauma: An autopsy study. *Spine* 23(21): 2272-2275.

Fahlstrom G. 1981. The Glenohumeral joint in man; an anatomic-experimental and archaeo-osteological study on joint function. *Ossa (International Journal of Skeletal Research)*, Sumplement 1.

Felson DT. 2000. Osteoarthritis: New insights – Part 1: The disease and its risk factors. National Institute of Health Conference. *Annals of Internal Medicine* 133: 635-646.

Ferguson SJ, Steffen T. 2003. Biomechanics of the aging spine. *European Spine Journal* 12:S97-S103.

Fields AJ, Lee GL, Keaveny TM. 2010. Mechanisms of initial endplate failure in the human vertebral body. *Journal of Biomechanics* 43: 2126-3131.

Fitzpatrick S, Sheard NF, Clark NG, Ritter ML. 2000. Vitamin D deficient rickets: A multifactorial disease. *Nutrition Grand Rounds* 58(7): 218-222.

Flessa T. 2008. The repatriation debate and the discourse of the commons. *Social & Legal Studies* 17(3): 387-405.

Formicola V. 1995. X-linked hypophosphatemic rickets: a probable upper Paleolithic case. *American Journal of Physical Anthropology* 98: 403-409.

Franklin D, Freedman L, Milne N, Oxnard CE. 2007. Geometric morphometrics study of population variation in indigenous southern African crania. *American Journal of Human Biology* 19(1): 20-33.

Fras C, Kravetz P, Mody DR, Heggeness MH. 2003. Substance P-containing nerves within the human vertebral body an immunohustochemical study of the basivertebral nerve. *Spine Journal* 3(1): 63-67.

Fritz JM, Erhard RE, Hagen BF. 1998. Segmental instability of the lumbar spine. *Physical Therapy* 78: 889-896.

Frobell RB, Le Graverand MP, Buck R, Roos EM, Roos HP, Tamez-Pena J, Totterman S, Lohmander LS. 2009. The acutely ACL injured knee assessed by MRI: Changes in joint fluid, bone marrow lesions, and cartilage during the first year. *Osteoarthritis & Cartilage* 17: 161-167.

Frost H.M. 1994a. Perspectives: A vital biomechanical model of synovial joint design. *The Anatomical Record* 240: 1-18.

Frost H.M. 1994a. Perspectives: A vital biomechanical model of synovial joint design. *The Anatomical Record* 240: 1-18.

Fukuta S, Miyamoto K, Iwata A, Hosoe H, Iwata H, Shirhashi K, Shimizu K. 2009. Unusual back pain caused by intervertebral disc degeneration associated with Schmorl's node at Th11/12 in a young athlete, successfully treated by anterior interbody fusion. *Spine* 34(5): E195-E198.

Gartner LM, Greer FR. 2003. Prevention of rickets and vitamin D deficiency: New guidelines for vitamin D intake. *American Academy of Pediatrics* 111(4): 908-910.

Gendron K, Doherr MG, Gavin P, Lang J. 2011. Magnetic resonance imaging characterization of vertebral endplate changes in the dog. *Veterinary Radiology & Ultrasound* 53(1): 50-56.

Gilmore, J.K. 2008. Leprosy at the Lazaretto on St. Eustatius, Netherlands Antilles. *International Journal of Osteoarchaeology* 18: 72-84.

Girish M, Subramaniam G. 2008. Rickets in exclusively breast fed babies. *Indian Journal of Pediatrics* 75: 641-643.

Goldring M.B., Goldring S.R. 2010. Articular cartilage and subchondral bone in the pathogenesis of osteoarthritis. *Annals of the New York Academy of Sciences* 1192: 230-237.

Gomez-Valdes JA, Qunito-Sanchez M, Garmendia AM, Veleminska J, Sanchez-Mejorada G, Bruzek J. 2012. Comparison of methods to determine sex by evaluating the greater sciatic notch: visual, angular, and geometric morphometrics. *Forensic Science International* 221(1-3): 156.e1-156.e7.

Gonzalez PN, Bernal V, Perez SI. 2009. Geometric morphometrics approach to sex estimation of human pelvis. *Forensic Science International* 189(1-3): 68-74.

Good L., Odensten M., Gillquist J. 1991. Intercondylar notch measurements with special reference to anterior cruciate ligament surgery. *Clinical Orthopaedics* 263: 185-189.

Goodall C. 1991. Procrustes methods in the statistical analysis of shape. *Journal of the Royal Statistics Society*. Series B 53(2): 285-339.

Goto K, Tajima N, Chosa E, Totoribe K, Kuroki H, Arizumi Y, Arai Takashi. 2002. Mechanical analysis of the lumbar vertebrae in a three-dimensional finite element method model in which intradiscal pressure in the nucleus pulposus was used to establish the model. *Journal of Orthopaedic Science* 7: 243-246.

Gordon SJ, Yang KH, Mayer PJ, Mace AH, Kish VL, Radin EL. 1991. Mechanism of disc rupture: A preliminary report. *Spine* 16(4): 450-6.

Gower JC. 1975. Generalized procrustes analysis. *Psychometrika* 40(1): 33-51.

Grainger I, Phillpotts C. 2011. *The Cistercian abbey of St. Mary Graces, East Smithfield, London.* London, Archaeology Studies Series, Museum of London Archaeology Service.

Grainger I, Hawkins D, Cowal L, Mikulski R. 2008. *The Black Death cemetery of East Smithfield, London*. London, Archaeology Studies Series, Museum of London Archaeology Service.

Groves SE. 2003. Bodies in the Bowl Hole – An early Medieval inhumation cemetery at Bamburgh, Northumberland. *The School of Historical Studies Postgraduate Forum E-Journal*. 2nd Ed.

Groves SE. 2010. The Bowl Hole Burial Ground; A Late Anglian cemetery in Northumberland. In J. Buckberry and A. Cherryson (eds): *Burial in Later Anglo-Saxon England, c.650 to 1100AD.* 114 - 125. Oxbow Books.

Groves SE. (in press). Social and biological status in the Bowl Hole early Medieval burial ground, Bamburgh, Northumberland. In Petts D, Williams H. *Early Medieval Northumbria*. Brepols.

Gunz P. 2012. Evolutionary relationships among robust and gracile australopiths: An "evo-devo" perspective. *Evolutionary Biology*: *early view*.

Gunz P, Mitteroeker P, Bookstein F. 2005. Semilandmarks in three dimensions. In: Slice DE. *Modern morphometrics in physical anthropology. Developments in primatology: Progress and Prospects*. New York: Kluwer Academic/Plenum Publishers: 73-97.

Haduch E, Szczepanek A, Skrzat J, Srodek R, Brzegowy P. 2009. Residual rickets or osteomalacia: A case dating from the 16th-18th centuries from Krosno Ordzanskie, Poland. *International Journal of Osteoarchaeology* 19: 593-612.

Hamanashi C, Kawabata T, Yosii T, Tanaka S. 1994. Schmorl's nodes on magnetic resonance imaging: their incidence and clinical relevance. *Spine* 19: 450-453.

Hannan MT. 1996. Epidemiologic Perspectives on Women and Arthritis: An Overview. *Arthritis Care & Research* 9(6): 424- 434.

Harrington JF, Sungarian A, Rogg J, Makker VJ, Epstein MH. 2001. The relation between vertebral endplates shape and lumbar disc herniations. *Spine* 26: 2133-2138.

Hazell TJ, DeGuire JR, Weiler HA. 2012. Vitamin D: An overview of its role in a skeletal muscle physiology in children and adolescents. *Nutritional Reviews* 70(9): 520-533.

Hennessy RJ, Stringer CB. 2002. Geometric morphometrics study of the regional variation of modern human form. *American Journal of Physical Anthropology* 117(1): 37-48.

Herrero-Beaumont, G., J.A. Roman-Blas, S. Castañeda, & S.A. Jimenez. 2009. Primary Osteoarthritis no longer primary: Three subsets with distinct etiological, clinical, and therapeutic characteristics. *Seminars in Arthritis and Rheumatism* 39: 71-80.

Herzog W, Federico S. 2007. Articular Cartilage. In: Nigg BM, Herzog W. *Biomechanics of the Musculo-Skeletal System.* Chichester: John Wiley & Sons Ltd: 95-122.

Hickley DS, Hukins DWL. 1980. Vovlo Award for bioengineering: relation between the structure of the annulus fibrosus and the function and failure of the intervertebral disc. *Spine* 5: 106-116.

Hodges DC. 1991. Temporomandibular joint osteoarthritis in a British skeletal population. *American Journal of Physical Anthropology* 85: 367-377.

Holick MF. 1986. Vitamin D requirements for the elderly. *Clinical Nutrition* 5(3): 121-129.

Holick MF. 2003. Vitamin D: A millennium perspective. *Journal of Cellular Biochemistry* 99: 296-307.

Holick MF. 2004. Sunlight and vitamin D for bone health and prevention of autoimmune diseases, cancers, and cardiovascular disease. *American Journal of Clinical Nutrition* 80: 1678S-1688S.

Holick MF. 2006. Resurrection of vitamin D deficiency and rickets. *Journal of Clinical Investigation* 116(8): 2062-2072.

Holst M. 2005. *Fishergate House artefacts and environmental evidence: The human bone*. Arch Planning Consultancy, UK. Accessed online, July 3, 2010.

Holick MF, Chen TC. 2008. Vitamin D deficiency: A worldwise problem with health consequences. *American Journal of Clinical Nutrition* 87: 1080S-1086S.

Hootman, J.M., C.A. Macera, C.G. Helmick, & S.N. Blair. 2003. Influence of physical activity-related joint stress on the risk of self-reported hip/knee osteoarthritis: A new method to quantify physical activity. *Preventive Medicine* 36:636-644.

Hotelling H. 1931. The generalization of the Student's ratio. *Annals of Mathematics and Statistics 2(*3): 360-378.

Hoy D, Bain C, Williams G, March L, Brooks P, Blyth F, Woolf A, Vos T, Buchbinder R. 2012. A systematic review of the global prevalence of low back pain. *Arthritis & Rheumatism* 64(6): 2028-2037.

Hunter D.J., Zhang Y., Sokolove J., Niu J. 2005. Trapeziometacarpal subluxation predisposes to incident trapeziometacarpal osteoarthritis: the Framingham study. *Osteoarthritis & Cartilage* 13: 953-957.

Inufusa A, An HS, Lim TH, Hasegawa T, Haughton VM, Nowicki BH. 1996. Anatomical changes of the spinal canal and intervertebral foramen associated with flexion-extension movement. *Spine* 21(21): 2412-2420.

Işcan MY, Loth SR, Wright RK. 1984. Age estimation from the rib by phase analysis: White males. *Journal of Forensic Sciences* 29: 1094–104.

Işcan MY, Loth SR, Wright RK. 1985. Age estimation from the rib by phase analysis: White females. *Journal of Forensic Sciences 30*: 853–63.

Ivanhoe F. 1994. Osteometric scoring of adult residual rickets skeletal plasticity in two archaeological populations from southeastern England: Relationship to sunshine and calcium deficits and demographic stress. *International Journal of Osteoarchaeology* 4(2): 97-120.

Jacobson JA, Girish G, Jiang Y, Sabb BJ. 2008. Radiographic evaluation of arthritis: Degenerative joint disease and variations. *Radiology* 248(3): 737-747.

Jang JS, Kwan HK, Lee JJ, Hwang SM, Lim SY. 2010. Rami communicans nerve block for the treatment of symptomatic Schmorl's nodes. *Korean Journal of Pain* 23(4): 262-265

Jans MME, Nielsen-Marsh CM, Smith CI, Collins MJ, Kars H. 2004. Characterisation of microbial attack on archaeological bone. *Journal of Archaeological Science* 31: 87-95.

Johnson DR, O'Higgins P, McAndrew TJ. 1988. The relationship between age, size and shape in the upper thoracic vertebrae of the mouse. *Journal of Anatomy* 161:73-82

Jolliffe IT. 2002. *Principal Component Analysis*. 2nd Ed. New York: Springer Publishing.

Jopling WH. 1982 Clinical aspects of leprosy. *Tubercle* 63:295-305.

Jopling WH, McDougall AC. 1988. *Handbook of leprosy*. 4th Ed. New York: Sheridan Medical Books.

Jurmain R. 1999. *Stories from the Skeleton: Behavioral reconstruction in human osteology*. New York: Routledge Publishing.

Jurmain, R.D. & L. Kilgore. 1995. Skeletal Evidence of Osteoarthritis: A Palaeopathological Perspective. *Annals of Rheumatic Diseases54*: 443-450.

Karsdal, M.A., Leeming, D.J., Dam E.B., Henriksen K., Alexandersen P., Pastoureau P., Altman R.D., Christiansen C. 2008. Should subchondral bone turnover be targeted when treating osteoarthritis? *Osteoarthritis and Cartilage* 16: 638-646.

Kaufman, K.R., C. Hughes, B.F. Morrey, M. Morrey, & K. An. 2001. Gait characteristics of patients with knee osteoarthritis. *Journal of Biomechanics* 34: 907-915.

Kellergen JH, Lawrence JS, Bier F. 1963. Genetic factors in generalized osteo-arthrosis. *Annals of Rheumatic Diseases* 22: 237-255.

Kendall DG. 1984. Shape-manifolds, Procrustean metrics and complex projective spaces. *Bulletin of the London Mathematics Society* 16: 81-121.

Kendall DG. 1985. Exact distributions for shapes of random triangles in convex sets. *Advances in Applied Probability* 17: 308-329.

Kendall DG. 1977. The diffusion of shape. *Advances in Applied Probability* 9: 428-430.

Kimmerle EH, Ross A, Slice, D. 2008. Sexual dimorphism in America: Geometric morphometric analysis of the craniofacial region. *Journal of Forensic Sciences* 53(1): 54-57.

King, G.J.W., Morrey B.F., An, K. 1993. Stabilizers of the elbow. *Journal of Shoulder and Elbow Surgery* 2: 165-174.

Kjellström, A. 2012. Possible Cases of Leprosy and Tuberculosis in Medieval Sigtuna, Sweden. *International Journal of Osteoarchaeology* 22(3): 261-283.

Klaus HD, Larsen CS, Tam ME. 2009. Economic intensification and degenerative joint disease: Life and labor on the postcontact north coast of Peru. *American Journal of Physical Anthropology* 139: 204-21.

Klepinger LL. 1983. Differential diagnosis in palaeopathology and the concept of disease evolution. *Medical Anthropology: Cross-Cultural Studies in Health and Illness* 7(1): 73-77.

Klingenberg CP. 2011. MorphoJ: An integrated software package for geometric morphometrics. *Molecular Ecology Resources* 11: 353-357.

Klingenberg CP, Monteiro LR. 2005. Distances and Directions in Mulltidimensional Shape Spaces: Implications for Morphometric Applications. *Systematic Biology* 54(4): 678-688.

Knüsel CJ, Göggel S, Lucy D. 1997. Comparative degenerative joint disease of the vertebral column in the medieval monastic cemetery of the Gilbertine Priory of St. Andrew, Fishergate, York, England. *American Journal of Physical Anthropology* 103: 481-495.

Kooh SW, Fraser D, Reilly BJ, Hamilton JH, Gall DG, Bell L. 1977. Rickets due to calcium deficiency. *New England Journal of Medicine* 297: 1264-1266.

Kovarovic K, Aiello LC, Cardini A, Lockwood CA. 2011. Discriminant function analyses in archaeology: are classification rates too good to be true? *Journal of Archaeological Sciences* 38: 3006-18.

Kreiter SR, Schwartz RP, Kirkman HN, Charlton PA, Calikoglu AS, Davenport ML. 2000. Nutritional rickets in African American breast-fed infants. *Journal of Pediatrics* 137: 153-157.

Krishnan SG, Harkins DC, Pennington SD, Harrison DK, Burkhead WZ. 2007. Arthroscopic ulnohumeral arthroplasty for degenerative arthritis of the elbow in patients under fifty years of age. *Journal of Shoulder and Elbow Surgery* 16(4): 443-448.

Krismer M, Haid C, Rabl, W. 1996. The Contribution of the Anulus Fibers to Torque Resistance. *Spine* 21: 2551-2557.

Kullmer O. 2008. Benefits and risks in virtual anthropology. *Journal of Anthropological Sciences* 86: 205-207.

Küstner, E.C., M.P. Cruz, C.P. Dansis, H.V. Iglesias, M.E. Rogriguez de Rivera Campillo, J.L. Lopez. 2006. Lepromatous Leprosy: A Review and Case Report. *Oral Medical Pathology* 11: 474-479.

Kuzminsky SC, Gardiner MS. 2012. Three-dimensional laser scanning: potential uses for museum conservation and scientific research. *Journal of Archaeological Science* 39: 2744-2751.

L'Abbe EN, Steyn M. 2007. Health status of the Venda, a post-antibiotic community in rural South Africa. *International Journal of Osteoarchaeology* 17: 492-503.

Lahiri R, Krahebuhl JL. 2008. The role of free-living pathogenic amoeba in the transmission of leprosy: A proof of principle. *Leprosy Review* 79: 401-409.

Lai P, Lovell NC. 1992. Skeletal markers of occupational stress in the fur trade: A case study from a Hudson's Bay Company fur trade post. *International Journal of Osteoarchaeolology* 2*:* 221–234.

LaPrade, R.F., Burnett Q.M. 1994. Femoral intercondylar notch stenosis and correlation to anterior cruciate ligament injuries. *The American Journal of Sports Medicine* 22(2): 198- 203.

Larsen CS. 1997. *Bioarchaeology: Interpreting Behavior From the Human Skeleton.* Cambridge: Cambridge University Press.

Lee F, Manchester K. 2008. Leprosy: A review of the evidence in the Chichester sample. In: Magilton J, Lee f, Boylston A (eds): *Lepers outside the gate: excavations at the cemetery of*

*the hospital of St James and St Mary Magdalene, Chichester, 1986-87 and 1993*. York: Council for British Archaeology: 208-217.

Legendre P, Legendre L.1998. *Numerical Ecology: Developments in Environmental Modelling 2*0. 2nd Ed. Amsterdam: Elsevier Publishing.

Letić M. 2012. Feeling wall tension in an interactive demonstration of Laplace's law. *Advances in Physiology Education* 36(2): 176

Lewek M.D., Rudolph K.S, Snyder-Mackler L. 2004. Control of frontal knee laxity during gait in patients with medial compartment knee osteoarthritis. *Osteoarthritis & Cartilage* 12:745-751.

Lewis ME. 2002. Impact of industrialization: Comparative study of child health in four sites from Medieval and Postmedieval England (AD 850-1859). *American Journal of Physical Anthropology* 119: 211-223.

Lewis ME, Roberts CA, Manchester K. 1994. Comparative study of the prevalence of maxillary sinusitis in later Medieval urban and rural populations in Northern England. *American Journal of Physical Anthropology* 98(4): 497-506.

Lewis ME . 2007. *The bioarchaeology of children: Perspectives from biological and forensic anthropology*. Cambridge: Cambridge University Press .

Li Y, Xu L, Olsen BR. 2007. Lessons from genetic forms of osteoarthritis for the pathogenesis of the disease. *Osteoarthritis and Cartilage* 15: 1101-1105.

Lieberman DE, Carlo J, Ponce de León M, Zollikofer CP. 2007. A geometric morphometrics analysis of heterochrony in the cranium of chimpanzees and bonobos. *Journal of Human Evolution* 52: 647-662.

Lieverse AR, Weber AW, Bazalilskiy VI, Goriunova OI, Savel'ev NA. 2007. Osteoarthritis in Siberia's Cis-Baikal: Skeletal indicators of hunter-gatherer adaptation and cultural change. *American Journal of Physical Anthropology* 132: 1-16.

Likovskỳ, J., M. Urbanova, M. Hajek, V. Cerny, & P. Cech. Two Cases of Leprosy from Žatec (Bohemia), Dated to the Turn of the 12th Century and Confirmed by DNA Analysis for *Mycobacterium leprae. Journal of Archaeological Science* 33: 1276-1283.

Lockwood DNJ, Reid AJC. 2001. The diagnosis of leprosy is delayed in the United Kingdom. *Quarterly Journal of Medicine* 94: 207-212.

Lohmander LS, Felson D. 2004. Can we identify a 'high risk' patient profile to determine who will experience rapid progression of osteoarthritis. *Osteoarthritis & Cartilage* 12: S49-S52.

Loughlin J. 2001. Genetic Epidemiology of Primary Osteoarthritis. *Current Opinions in Rheumatology* 13: 111-116.

Lovell NC. 1990. *Patterns of injury and illness in great apes: A skeletal analysis*. Smithsonian Institutional Press.

Lovell N. 1994. Spinal Arthritis and Physical Stress at Bronze Age Harappa. *American Journal of Physical Anthropology* 93: 149-164.

Lovejoy CO, Meindl RS, Pryzbeck TR, Mensforth RP. 1985. Chronological metamorphosis of the auricular surface of the ilium: A new method for the determination of age at death. *American Journal of Physical Anthropology* 68: 15–28.

Lunt, D.A. 2011. The First Evidence for Leprosy in Early Medieval Scotland: Two Individuals from Cemeteries in St. Andrews, Fife, Scotland, with Evidence for Normal Burial Treatment. *International Journal of Osteoarchaeology* (early view).

Maat GJR, Mastwijk RW, Van Der Velde EA. 1995. Skeletal Distribution of Degenerative Changes in Vertebral Osteophytosis, Vertebral Osteoarthritis and DISH. *International Journal of Osteoarchaeology* 5: 289-298.

Macfarlane GJ, Beasley M, Jones EA, Precott GJ, Docking R, Keeley P, McBeth GT, MUSICIAN study team. 2012. The prevalence and management of low back pain across adulthood: Results from a population-based cross-sectional study (MUSICAN study). *Pain* 153: 27-32.

Macho GA. 1991. Anthropological evaluation of left-right differences in the femur of southern African populations. *Anthropologischer Anzeiger* 49(3): 207-216.

Mafart B, Guipert G, Alliez-Philip C, Brau Jean-Jacques. 2007. Virtual reconstruction and new palaeopathological study of the Magdalenian child's skull of Rochereil. *Comptes Rendus Palevol* 6: 569-579.

Magilton J. 2008a. A history of the hospital. In J Magilton, F Lee, A Boylston (eds): *Lepers outside the gate: excavations at the cemetery of the hospital of St James and St Mary Magdalene, Chichester, 1986-87 and 1993*. York: Council for British Archaeology, pp. 57-68.

Magilton J. 2008a. The cemetery. In J Magilton, F Lee, A Boylston (eds): *Lepers outside the gate: excavations at the cemetery of the hospital of St James and St Mary Magdalene, Chichester, 1986-87 and 1993*. York: Council for British Archaeology, pp.84-132.

Magilton, J., Lee, F., Boylston, A., & Council for British Archaeology 2008. *Lepers outside the gate: excavations at the cemetery of the hospital of St James and St Mary Magdalene, Chichester, 1986-87 and 1993*. York: Council for British Archaeology.

Magilton J. 1986. *Hospital of St. James and Mary Magdalene, Swanfield Drive*. The archaeology of Chichester and District 1986. Chichester District Council 12-15.

Magilton J. 1993. *Further excavations at the leper hospital cemetery, Swanfield Drive.* The archaeology of Chichester and District 1993. Chichester District Council 37-41.

Magilton J, Kenny J, Boylston A, & Council for British Archaeology. 2008. *Lepers outside the gate: excavations at the cemetery of the hospital of St James and St Mary Magdalene, Chichester, 1986-87 and 1993*. York: Council for British Archaeology.

Maly, M.R., P.A. Costigan, S.J. Olney. 2008. Mechanical factors relate to pain in knee osteoarthritis. *Clinical Biomechanics* 23: 796-805.

Malmström H, Stora J, Dalen L, Holmlund G, Götherström A. 2005. Extensive human DNA contamination in extracts from ancient dog bones and teeth. *Molecular Biology and Evolution* 22(10): 2040-2047.

Manchester K. 1991. Tuberculosis and leprosy: Evidence for interaction of disease. In: Ortner D, Aufderheide AC. *Human Palaeopathology. Current Synthesis and Future Options*. Washington: Smithsonian Institute Press: 23-35.

Manchester K, Lee F. 2008. Leprosy: a review of the evidence in the Chichester sample. In: Magilton J, Lee F, Boylston A. (eds): *Lepers outside the gate: excavations at the cemetery of the hospital of St James and St Mary Magdalene, Chichester, 1986-87 and 1993*. York: Council for British Archaeology: 208-217.

Manchester K. 1981. A leprous skeleton of the 7th century from Eccles, Kent, and the present evidence of leprosy in early Britain. *Journal of Archaeological Science* 8: 205-209.

Manchester K, Roberts CA. 1989. The paleaopathology of leprosy in Britain: A review. *World Archaeology* 21(2): 265-272.

Mandelbaum BR, Browne JE, Fu F, Micheli L, Mosely B, Erggelet C, Minas T, Peterson L. 1998. Articular cartilage lesions of the knee. *American Journal of Sports Medicine* 26(6): 853-861.

Manek, N.J., D. Hart, T.D. Spector, & A. J. MacGregor. 2003. The association of body mass index and osteoarthritis of the knee joint. *Arthritis and Rheumatism* 48(4): 1024-1029.

Maniadakis N, Gray A. 2000. The economic burden of back pain in the UK. *Pain* 84(1): 95-103.

Mankin HJ. 1974. Rickets, osteomalacia, and renal osteodystrophy part 1. *Journal of Bone and Joint Surgery* 56(1): 101-128.

Mankin HJ, Brandt KD, Shulman LE. 1986. Workshop on Ethiopathogenesis of Osteoarthritis: Proceedings and Recommendations. *Journal of Rheumatology* 13(6): 1130-1160.

Mantini S, Ripani M. 2009. Modern Morphometrics: New Perspectives in Physical Anthropology. *New Biotechnology* 25(5): 325-330.

Martin RB, Burr DB, Sharkey NA. 1998. *Skeletal Tissue Mechanics*. London: Springer.

Márquez-Grant N, Fibiger L. 2011. *The Routledge handbook of archaeological human remains and legislation. An international guide to laws and practice in the excavation and trearment of archaeological human remains.* New York: Routledge.

Masharawi Y. 2012. Lumbar shape characterization of the neural arch and vertebral body in spondylolysis: A comparative skeletal study. *Clinical Anatomy* 25: 224-230.

Masharawi Y, Salame K. 2011. Shape variation of the neural arch in the thoracic and lumbar spine: Characterization and relationship with the vertebral body shape. *Clinical Anatomy* 24(7): 858-867.

Masharawi Y, Dar G, Peleg S, Steinberg N, Medlej B, May H, Abbas J, Hershkovitz I. 2010. A morphological adaptation of the thoracic and lumbar vertebrae to lumbar hyperlordosis in young and adult females. *European Spine Journal* 19: 768-773.

Masharawi Y, Salame K, Mirovsky Y, Peleg S, Dar G, Steinberg N, Hershkovitz I. 2008. Vertebral body shape variation in the thoracic and lumbar spine: Characterization of its asymmetry and wedging. *Clinical Anatomy* 21: 46-54.

Masharawi Y, Rothschild B, Salame K, Dar G, Peleg S, Hershkovitz I. 2005. Facet tropism and interfacet shape in the thoracolumbar vertebrae: Characterizations and biomechanical interpretation. *Spine* 30(11): E281-E292.

Masharawi Y, Rothschild B, Dar G, Peleg S, Robinson D, Been E, Hershkovitz I. 2004. Facet orientation in the thoracolumbar spine. *Spine* 29(16): 1755-1763.

Mays S. 2010. Human osteoarchaeology in the UK 2001-2007: a bibliometric perspective. *International Journal of Osteoarchaeology* 20: 192-204.

Mays S, Smith M. 2009. Ethical dimension of reburial, retention and repatriation of archaeological human remains: a British perspective. In: Lewis M, CleggM. *Proceedings of the Ninth Annual Conference of the British Association for Biological Anthropology and Osteoarchaeology British Archaeological Reports, International Series, 1918*. Oxford: Archaeopress: 107-117.

Mays S, Brickley M, Ives R. 2006. Skeletal manifestations of rickets in infants and young children in a historic population from England. *American Journal of Physical Anthropology* 129: 362-374.

Mays S, Brickley M, Ives R. 2009. Growth and vitamin D deficiency in a population from 19th century Birmingham, England. *International Journal of Osteoarchaeology* 19: 406-415.

Mazzuca SA, Brandt KD, Buckwalter KA. 2003. Detection of radiographic joint space narrowing in subjects with knee osteoarthritis: longitudinal comparison of the metatarsophalangeal and semiflexed anteroposterior views. *Arthritis & Rheumatism* 48(2): 385-390.

McAlindon TE, Wilson PW, Aliabadi P, Weissman B, Felson DT. 1999. Level of physical activity and the risk of radiographic and symptomatic knee osteoarthritis in the elderly: the Framingham study. *The American Journal of Medicine* 106(2): 151-157.

McGonagle, D., Tan AL, Carey J. Benjamin M. 2010. The anatomical basis for a novel classification of osteoarthritis and allied disorders. *Journal of Anatomy* 216: 279-291.

McNulty KP. 2012. Evolutionary developmental in *Australopithecus africanus*. *Evolutionary Biology early view*.

Meijer GJM, Homminga J, Hekman EEG, Veldhuizen AG, Verkerke GJ. 2010. The effect of three-dimensional geometrical changes during adolescent growth on the biomechanics of a spinal motion segment. *Journal of Biomechanics* 43: 1590-1597.

Merbs CF. 1983. *Patterns of activity-induced pathology in a Canadian Inuit population*. Vol 119. Ottawa: National Museums of Canada.

Merbs CF, Euler RC. 1985. Atlanto-occipital fusion and spondylolisthesis in an Anasazi skeleton from bright angel ruin, Grand Canyon National Park, Arizona. *American Journal of Physical Anthropology* 67(4): 381-391.

Merz, B., Eckstein, F., Hillebrand, S., Putz, R. 1997. Mechanical implications of humero-ulnar incongruity- finite element analysis and experiment. *Journal of Biomechanics* 30(7): 713-721.

Meyers KM. 2010. *Early modern London and rickets: Resolving the discrepancies between the historical and skeletal evidence*. Unpublished MSc thesis. University of Edinburgh.

Miller E, Ragsdale BD, Ortner DJ. 1996. Accuracy in dry bone diagnosis: A comment on palaeopathological methods. *International Journal of Osteoarchaeology* 6: 221-229.

Milner GR. 1992. *Determination of skeletal age and sex: A manual prepared for the Dickson Mound reburial team.* Dickson Mound Museum, Lewiston, Illinois.

Mitteroecker P, Gunz P. 2009. Advances in geometric morphometrics. *Evolutionary Biology* 36: 235-247.

Mitteroecker P, Gunz P, Teschler-Nicola M, Weber GW. 2004. *New morphometrics methods in palaeopathology: shape analysis of a Neolithic hydrocephalus.* British Archaeological Series: Computer Applications and Quantitative Methods in Archaeology: 96-99

Mok F, Samartzis D, Karppinen J, Luk K, Fong D, Cheung K. 2010. Prevalence, determinants, and association of Schmorl's nodes of the lumbar spine with disc degeneration: A population-based study of 2449 Individuals. *Spine* 35(21): 1944-1952.

Møller-Christensen V. 1953 *Ten lepers from Naestved in Denmark. A study of skeletons from a Medieval Danish leper hospital.* Copenhagen, Danish Science Press

Møller-Christensen V. 1961. *Bone Changes in Leprosy*. Bristol: John Wright.

Møller-Christensen V. 1965. New knowledge of leprosy through palaeopathology. *International Journal of Leprosy* 33(3): 603-610.

Møller-Christensen V. 1978. *Leprosy Changes of the Skull*. Odense: Odense University Press.

Molnar P, Ahlstrom TP, Leden I. 2009.Osteoarthritis and activity – An analysis of the relationship between ebunarion, musculoskeletal stress markers (MSM) and age in two Neolithci hunter-gatherer populations from Gotland, Sweden. *International Journal of Osteoarchaeology* 21(3): 283-291.

Molnar P, Ahlstrom TP, Leden I. 2011. Osteoarthritis and activity – an analysis of the relationship between eburnation, musculoskeletal stress markers (MSM) and age in two Neolithic Hunter-Gatherer populations from Gotland, Sweden. *International Journal of Osteoarchaeology* 21: 283-291.

Monot M, Honore N, Garnier T, Araoz R, Coppee JY, Lacroix C, Sow S, Spencer JS, Truman RW, Williams DL, Gelber R, Virmond M, Flageul B, Cho SN, Ji B, Paniz-Mondolfi A, Convit J, Young S, Fine PE, Rasolofo V, Brennan PJ, Cole ST. 2005. On the origin of leprosy. *Science* 308: 1040-1042.

Morrey, B.F., An, K. 1983. Articular and ligamentous contributions to the stability of the elbow joint. *The American Journal of Sports Medicine* 11(5): 315- 319.

Morrey B.F., An, K. 2005. Stability of the elbow: Osseous constraints. *Journal of Shoulder and Elbow Surgery* 14(1): S174-S178.

Moskowitz RW. 2004. Specific Gene Defects Leading to Osteoarthritis. *Journal of Rheumatology* 31(S70): 16-21.

Munnus CF, Simm PJ, Rodda CP, Garnett CP, Zacharin MR, Ward LM, Geddes , Cherian S, Zurynski Y, Cowell CT. 2012. Incidence of vitamin D deficiency rickets among Australian children: An Australian paediatric surveillance unit study. *Medical Journal of Australia* 196(7): 466-468.

Nambu T., Gasser B., Schneider E., Bandi W., Perren S.M. 1991. Deformation of the distal femur: A contribution towards the pathogenesis of osteochondrosis dissecans in the knee joint. *Journal of Biomechanics* 24(6): 421-423, 425-433.

Neubauer S, Gunz P, Mitteroecker P, Weber GW. 2004. Three-dimensional digital imaging of the partial *Australopithecus africanus* endocranium MLD 37/38. *Canadian Association of Radiologists* 55(4): 271-278.

Neubauer S, Gunz P, Hublin JJ. 2010. Endocranial shape changes during growth in chimpanzees and humans: A morphometric analysis of unique and shared aspects. *Journal of Human Evolution* 59:555-566.

Neubauer S, Gunz P, Hublin JJ. 2009. The patterns of endocranial ontogenetic shape changes in humans. *Journal of Anatomy* 215: 240-255.

Nicholson DT, Chalk C, Funnell WRJ, Daniel SJ. 2006. Can virtual reality improve anatomy education? A randomised controlled study of a computer-generated three-dimensional anatomical ear model. *Medical Education* 40: 1081-1087.

Novak M, Šlaus M.2011.Vertebral pathologies in two early modern period ($16^{th}$-$19^{th}$ Century) populations from Croatia. *American Journal of Physical Anthropology* 145: 270-281.

O'Higgins P. 2000. The study of morphological variation in the hominid fossil record: Biology, landmarks and geometry. *Journal of Anatomy* 197(1): 103-120.

O'Higgins P, Chadfield P, Jones N. 2001. Facial growth and the ontogeny of morphological variation within and between *Cebus apella* and *Cercocebus torquatus*. *Journal of Zoology* 254:337–357.

O'Higgins P, Cobb SN, Fitton LC, Groning F, Phillips R, Liu J, Fagan MJ. 2012. Combining geometric morphometrics and functional simulation: an emerging toolkit for virtual functional analyses. *Journal of Anatomy* 218: 3-15.

O'Higgins P, Fitton LC, Phillips R, Shi J, Liu J, Groning D, Cobb S, Fagan MJ. 2011. Virtual functional morphology: novel approaches to the study of craniofacial form and function. *Evolutionary Biology early view*.

O'Higgins P, Jones N. 2006. *Tools for statistical shape analysis*. Hull York Medical School.

O'Higgins P, Jones N. 1998. Facial growth in Cercocebus torquatus: An application of three-dimensional geometric morphometric techniques to the study of morphological variation. *Journal of Anatomy* 193: 251-272.

O'Higgins P, Strand Viðarsdóttir U. 1999. New approaches to the quantitative analysis of craniofacial growth and variation. In: Hoppa RD, Fitzgerald CM. *Human growth in the past: Studies from bones and teeth.* Cambridge: Cambridge University Press: 128-160.

Ortner D. 1968. Description and classification of degenerative bone changes in the distal joint surfaces of the humerus. *American Journal of Physical Anthropology* 28: 139-156.

Ortner D. 2007 (2003). *Identification of pathological conditions in human skeletal remains*. $2^{nd}$ Ed. London: Academic Press.

Ornter DJ, Mays S. 1998. Dry-bone manifestations of rickets in infancy and early childhood. *International Journal of Osteoarchaeology* 8: 45-55.

Ortner DJ, Manchester K, Lee F. 1991. Metastatic carcinoma in a leper skeleton from a Medieval cemetery in Chichester, England. *International Journal of Osteoarchaeology* 1(2): 91-98.

Ortner DJ, Utermohle CJ. 1981. Polyarticular inflammatory arthritis in a Pre-Columbian skeleton from Kodiak Island, Alaska, USA. *American Journal of Physical Anthropology* 56: 23-31.

Overvliet GM, Beuls EAM, ter Laak-Poort M, Cornips EMJ. 2009. Two brothers with a symptomatic thoracic disc herniation at T11-T12: Clincial report. *ActaNeurochir* 151: 393-396.

Owen JG, Chmielewski MA. 1985. On canonical variates analysis and the construction of confidence ellipses in systematic studies. *Systematic Zoology* 34(3): 366-374.

Papathanasiou A. 2005. Health status of the Neolithic population of Alepotrypa Cave, Greece. *American Journal of Physical Anthropology* 126: 377-390.

Paterson DE, Rad M. 1961. Bone changes in leprosy, their incidence, progress, prevention, and arrest. *International Journal of Leprosy* 29: 393-422.

Pearson O.M., Lieberman D.E. 2004. The aging of Wolff's "Law": Ontogeny and responses to mechanical loading in cortical bone. *Yearbook of Physical Anthropology* 47: 63-99.

Peat G, McCarney R, Croft P. 2001. Knee pain and osteoarthritis in older adults: A review of community burden and current use of primary health care. *Annals of Rheumatic Diseases* 60: 91-97.

Peng B, Wu W, Hou S, Shang W, Wang X, Yang Y. 2003. The pathogenesis of Schmorl's nodes. *Journal of Bone and Joint Surgery* 85 B: 879-882.

Perez SI. 2007. Artificial cranial deformation in South America: a geometric morphometrics approximation. *Journal of Archaeological Science* 34: 1649-1658.

Perez SI, Valeria B, Gonzalez PN. 2007. Evolutionary relationships among prehistoric human populations: An evaluation of relatedness patterns based on facial morphometrics data using molecular data. *Human Biology* 79(1): 25-50.

Petersson IF. 1996. Occurrence of osteoarthritis of the peripheral joints in European populations. *Annals of the Rheumatic Diseases* 55: 659-664.

Phenice TW. 1969. A newly developed visual method of sexing the os pubis. *American Journal of Physical Anthropology* 30: 297–302

Pfeiffer S, Crowder C. 2004. An ill child among mid-Holocene foragers of Southern Africa. *American Journal of Physical Anthropology* 123(1): 23-29.

Pfirrmann C, Resnick D. 2001. Schmorl's nodes of the thoracic and lumbar spine: Radiographic-pathologic study of prevalence, characterization, and correlation with degenerative changes of 1,650 spinal levels in 100 cadavers. *Radiology* 219: 368-374.

Pitt M. 1995. Rickets and osteomalacia. In: Resnick D, Niwayama G. *Diagnosis of bone and joints disorders*. Philadelphia: Saunders Publishing: 1885-1922.

Plomp KA, Roberts CA, Strand Viðarsdóttir U. 2012. Vertebral morphology influences the development of Schmorl's nodes in the lower thoracic vertebrae. *American Journal of Physical Anthropology* 149(4): 572-582.

Pooni JS, Hukins DWL, Harris PF, Hilton RC, Davies KE. 1986. Comparison of the Structure of Human Intervertebral Discs in the Cervical, Thoracic and Lumbar Regions of the Spine. *Surgical Radiologic Anatomy* 8:175-182.

Prentice A. 2008. Vitamin D deficiency: A global perspective. *Nutrition Review* 66(S2):S153-S164.

Prescher A. 1998. Anatomy and Pathology of the Aging Spine. *European Journal of Radiology* 27: 181-195.

Pritzker KPH. 1998. Pathology of Osteoarthritis. In: Brandt KD, Doherty M, Stefan L. *Osteoarthritis.* Oxford: Oxford University Press: 50-61.

Quasnichka H.L., Anderson-MacKenzie J.M., Tarlton J.F. Sims T.J., Billingham M.E. Bailey A.J. 2005. Cruciate ligament laxity and femoral intercondylar notch narrowing in early-stage knee osteoarthritis. *Arthritis & Rheumatism* 52(10): 3100-3109.

Qui TX, Teo EC, Zhang QH. 2006. Comparisons of kinematics between thoracolumbar T11-T12 and T12-L1 functional spinal units. *Journal of English Medicine* 220: 493-504.

R Development Core Team. 2012. *R: A language and environment for statistical computing*. R Foundation for Statistical Computing Vienna, Austria. ISBN 3-900051-07-0, URL http://www.R-project.org

Rafferty J. 2005. Curing the stigma of leprosy. *Leprosy Review* 76: 119-126.

Rando C, Waldron T. 2012. TMJ osteoarthritis: A new approach to diagnosis. *American Journal of Physical Anthropology* 148: 45-53.

Rannou F, Corvol M, Revel M, Poiraudeau S. 2001. Disk degeneration and disk herniation: the contribution of mechanical stress. *Joint Bone Spine* 68: 543-46.

Rathbun TA. 1987. Health and disease at a South Carolina plantation: 1840-1870. *American Journal of Physical Anthropology* 74: 239-253.

Rawcliffe, C. 2006. *Leprosy in Medieval England.* The Boydell Press: Suffolk, UK.

Recheis W, Weber GW, Schafer K, Prossinger H, Knapp R, Seidler H, zur Nedden D. 1999. New methods and techniques in anthropology. *Collegium Antropologicum* 23(2): 495-509.

Resnick D, Niwayama G. 1978. Intervertebral disc herniations: cartilaginous (Schmorl's) nodes. *Radiology* 126(1): 57-65.

Resnick D, Niwayama G. 1995. Osteoporosis. In Resnick D. *Diagnosis of bone and joint disorders.* Philadelphia: Saunders Publishing Vol 4, Chapter 5: 11783-1853.

Rettig LA, Hastings H, Feinberg JR. 2008. Primary osteoarthritis of the elbow: Lack of radiographic evidence for morphological predisposition, results of operative debridement at intermediate follow-up, and basis for a new radiographic classification system. *Journal of Shoulder and Elbow Surgery* 17: 97-105.

Reyment RA. 1985. Multivariate morphometrics and analysis of shape. *Mathematical Geology* 17(6): 591-609.

Richards P. 1977. *The medieval leper and his northern heirs*. Cambridge, DS Brewer

Ridley DS, Jopling WH. 1966 Classification of leprosy according to immunity. A five-group system. *International Journal of Leprosy* 34:255-273.

Roas S, Gorole V, Walawalker S, Khot S, Karandikar N. 1996. Gender differentials in the social impact of leprosy. *Leprosy Review* 67(3): 190-199.

Robb J. 1994. Skeletal signs of activity in the Italian Metal Ages: Methodological and interpretative notes. *Human Evolution* 9(3): 215-29.

Robb J, Bigazzi R, Lazzarini L, Scarsini C, Sonego F. 2001. Social "status" and biological "status": A comparison of grave goods and skeletal indicators from Pontecagnano. *American Journal of Physical Anthropology* 115: 213-22.

Robbin A, Skalli W, Lavaste F. 1994. Influence of geometrical factors on the behavior of lumbar spine segments: a finite element analysis. *European Spine Journal* 3: 84-90.

Robbins, G., V.M. Tripathy, V.N. Misra, R.K. Mohanty, V.S. Shinde, K.M. Gray, & M.D. Schug. 2009. Ancient Skeletal Evidence for Leprosy in India (2000 B.C.). *PLoS ONE* 4(5): e5669.

Roberts CA. 2002. The antiquity of leprosy in Britain: the skeletal evidence. In Roberts, CA., M. Lewis, & K. Manchester eds. *The Past and Present of Leprosy: Archaeological, Historical, Palaeopathological, and Clinical Approaches*. BAR International Series 1054:213-221

Roberts CA. 1984a. *The human skeletal report from Baldock, Herfordshire*. Bradford, Calvin Wells laboratory, University of Bradford, North Hertfordshire District Council Archaeology Services. *Unpublished.*

Roberts CA. 1984b. *The Barratt inhumation cemetery, Baldock, Hertfordshire (A11/BAL 11), human skeletal material*. Bradford, Calvin Wells laboratory, University of Bradford, North Hertfordshire District Council Archaeology Services. *Unpublished.*

Roberts CA. 2007. A bioarchaeological study of maxillary sinusitis. *American Journal of Physical Anthropology* 133: 792-807.

Roberts CA. 2009. *Human remains in archaeology: A handbook.* York: Council for British Archaeology.

Roberts CA. 2011. The bioarchaeology of leprosy and tuberculosis: A comparative study of perceptions, stigma, diagnosis, and treatment. In: Agarwal SC, Glencross BA. *Social Bioarchaeology*. London: John Wiley and Sons.

Roberts CA, Ingham S. 2008. Using ancient DNA analysis in palaeopathology: a critical analysis of published papers, with recommendations for future work. *International Journal of Osteoarchaeology* 18: 600-613.

Roberts CA, Manchester K. 2007. *The archaeology of disease*. New York: Cornell University Press.

Roberts CA, Lewis ME, Manchester K. 2002. *The past and present of leprosy: archaeological, historical, palaeopathological and clinical approaches.* International Congress on the Evolution and Palaeoepidemiology of the Infectious Diseases. Oxford: Archaeopress.

Roberts CA, Mays S. 2011. Study and restudy of curated skeletal collections in bioarchaeology: a perspective on the UK and the implications for future curation of human remains. *International Journal of Osteoarchaeology* 21(5): 626-630.

Roberts J, Burch TA. 1966. Osteoarthritis prevalence in adults by age, sex, race, and geographic area. *National Center of Health Statistics Series* 11(15): 1-27.

Robson Brown K, Pollintine P, Adams M. 2008. Biomechanical implications of degenerative joint disease in the apophyseal joints of human thoracic and lumbar vertebrae. *American Journal of Physical Anthropology* 136: 218-326.

Rodrigues LC, Lockwood DN. 2011. Leprosy now: epidemiology, progress, challenges, and research gaps. *Lancet Infectious Disease* 11:464-470.

Rogers J, Dieppe P. 2003. Palaeopathology of osteoarthritis. In: Brandt K, Doherty M, Lohmander S. *Osteoarthritis* 2nd Edition. Oxford: Oxford University Press.

Rogers J, Waldron T. 1995. *A field guide to joint disease in archaeology*. Chichester; New York: J. Wiley.

Rogers J, Shepstone L, Dieppe P. 1997. Bone formers: Osteophyte and enthesophyte formation are positively associated. *Annals of Rheumatic Diseases* 56: 85-90.

Rogers J, Shepstone L, Dieppe P. 2004. Is osteoarthritis a systematic disorder of bone? *Arthritis & Rheumatism* 50(2): 452-457.

Rogers, J. Watt, I, Dieppe P. 1990. Comparison of visual and radiographic detection of bony changes at the knee joint. *British Medical Journal* 300(6721): 367-368.

Rogers J, Waldron T, Dieppe P, Watt I. 1987. Arthropathies in palaeopathology: the basis of classification according to the most probable cause. *Journal of Archaeological Science* 14: 179-193.

Rohlf FJ. 2000. Statistical power comparisons among alternative morphometrics methods. *American Journal of Physical Anthropology* 111(4): 463-478.

Rohlf FJ. 2004. TPSDig Version 1.40. *Ecology and Evolution*, SUNY at Stony Brook.

Rohlf FJ. 2003. Bias and error in estimates of mean shape in geometric morphometrics. *Journal of Human Evolution* 44: 665-683.

Rohlf FJ, Marcus LF. 1993. A revolution in morphometrics. *Trends in Ecology and Evolution* 8(4): 129-132.

Rohlf FJ, Slice D. 1990. Extensions of the Procrustes method for the optimal superimposition of landmarks. *Systematic Zoology* 39(1):40-59.

Rothschild, B.M. 1997. Porosity: A curiosity without diagnostic significance. *American Journal of Physical Anthropology* 104(4): 529-533.

Rothschild BM, Woods RJ. 1991. Spondyloarthropathy: Erosive arthritis in representative defleshed bones. *American Journal of Physical Anthropology* 85: 125-134.

Rubini M. Zaio P. 2009. Lepromatous leprosy in an early Medieval cemetery in Central Italy (Morrione, Campochiaro, Morlise, $6^{th}$-$8^{th}$ Century AD). *Journal of Archaeological Science* 36: 2771-2779.

Ruff , C.B. 1988. Hindlimb articular surface allometry in hominoidea and Macaca, with comparisons to diaphyseal scaling. *Journal of Human Evolution* 17 (7):687-714

Ruff C.B. 2000. Body size, body shape and long bone strength in modern humans. *Journal of Human Evolution* 38: 269-290.

Ruff C.B., Runestad J.A. 1992. Primate limb bone structural adaptations. *Annual Review of Anthropology* 21: 407-433.

Ruff, C.B., Holt B., Trinkaus E. 2006. Who's afraid of the big bad Wolff?: "Wolff's Law" and bone functional adaptation. *American Journal of Physical Anthropology* 129(4): 484-498.

Saluja G, Fitzpatrick K, Bruce M, Cross J. 1986. Schmorl's nodes (intervertebral herniations of intervertebral disc tissue) in two historic British populations. *Journal of Anatomy* 145: 87-96.

Sandness KL, Reinhard KJ. 1992. Vertebral pathology in prehistoric and historic skeletons from Northeastern Nebraska. *Plains Anthropologist* 37(141): 299-309.

Scheuer L, Black S. 2000. *Developmental juvenile osteology*. Academic Press: London, UK.

Schmorl G. Die pathologische Anatomie der Wirbelsaule. 1927. *Archrives of Orthopaedic and Trauma Surgery* 21:3–41

Schmorl G, Junghans H. 1971. *The human spine in health and disease*. New York: Grune & Stratton.

Schrader SA. 2012. Activity patterns in New Kingdom Nubia: An examination of enthseal remodeling and osteoarthritis at Tombos. *American Journal of Physical Anthropology* 149: 60-70.

Schultz M, Timme U, Schmidt-Schultz TH. 2007. Infancy and childhood in the Pre-Columbian North American Southwest – first results of the palaeopathological investigation of the skeletons from the Grasshopper Pueblo, Arizona. *International Journal of Osteoarchaeology* 17: 369-279.

Schwab, G.H., Bennett J.B., Woods G.W., 1980. Biomechanics of elbow instability: the role of the medial collateral ligament. *Clinical Orthopaedics* 146: 42-52.

Scollard DM, Adams LB, Gillis TP, Krahenbuhl JL, Truman RW, Williams DL 2006 The continuing challenge of leprosy. *Clinical Microbiology Review* 19:338-381

Sharma, L., J. Song, D.T. Felson, S. Cahue, E. Shamiyeh, & D.D. Dunlop. 2001. The role of knee alignment in disease progression and functional decline in knee osteoarthritis. *The Journal of the American Medical Association* 286(2): 188-195.

Shepstone, L., J. Rogers, J. Kirwan, & B. Silverman. 1999. The Shape of the Distal Femur: A Palaeopathological Comparison of Eburnated and Non-Eburnated Femora. *Annals of Rheumatic Diseases* 58: 72-78.

Shepstone L, Rogers J, Kirwan JR, Silverman BW. 2001. Shape of the Intercondylar Notch of the Human Femur: A Comparison of Osteoarthritic and Non-Osteoarthritic bones from a Skeletal Sample. *Annals of Rheumatic Diseases* 60: 968-973.

Shiozaki, H., Y. Koga, G. Omori, G. Yamamoto, & H.E. Takahashi. 1999. Epidemiology of osteoarthritis of knee in a rural Japanese population. *The Knee* 6:183-188.

Sidlauskas BL, Mol JH, Vari RP. 2011. Dealing with allometry in linear and geometric morphometrics: a taxonomic case study in the *Leporinus cylindriformis* group (Characiformes: Anostomidae) with description of a new species from Suriname. *Zoological Journal of the Linnean Society* 162: 103-130.

Silberstein M, Opeskin K, Fahey V. 1999. Spinal Schmorl's nodes: Sagittal sectional imaging and pathological examination. *Australasia Radiology* 43: 27-30.

Šlaus M. 2000. Biocultural analysis of sex differences in mortality profiles and stress levels in late Medieval populations from Nova Rača, Croatia. *American Journal of Physical Anthropology* 111: 193-209.

Slice DE. 2001. Landmark coordinate aligned by Procrustes analysis do not lie in Kendall's shape space. *Systematic Biology* 50(1): 141-149.

Slice DE. 2005. *Modern Morphometrics*. In: Slice DE. *Modern Morphometrics in Physical Anthropology*. New York: Kluwer Academic/Plenum Publishers: 1-46.

Slice DE. 2007. Geometric morphometrics. *Annual Review of Anthropology* 36: 261-281.

Solovieva S, Vehmas T, Riihimaki H, Luoma K, Leino-Arjas P. 2005. Hand use and patterns of joint involvement in osteoarthritis. A comparison of female dentists and teachers. *Rheumatology* 44: 521-528.

Somers KM. 1986. Multivariate allometry and removal of size with principal components analysis. *Systematic Biology* 35(3): 359-368.

Somers TJ, Keefe FJ, Pells JJ, Dixon KE, Waters SJ, Riordan PA, Blumenthal JA, McKee DC, LaCaille L, Tucker JM, Schmitt D, Caldwell DS, Kraus VB, Sims EL, Shelby A, Rice JR. 2009. Pain catastrophizing and pain-related fear in osteoarthritis patients: Relationships to pain and disability. *Journal of Pain and Symptom Management* 37(5): 863-872.

Souryal T.O., Moore H.A., Evans J.P. 1988. Bilaterality in anterior cruciate ligament injuries: Associated intercondylar notch stenosis. *American Journal of Sports Medicine* 16: 449-454.

Sparre S, Nielsen B, Jensen TK, Gram J, Brixen K, Brock-Jacobsen B. 2009. Nutritional rickets in Denmark: A retrospective review of children's medical records from 1985 to 2005. *European Journal of Pediatrics* 168: 941-949.

Spector T.D., Hart D.J. Doyle D.V. 1994. Incidence and progression of osteoarthritis in women with unilateral knee disease in the general population: the effect of obesity. *Annals of the Rheumatic Diseases* 53: 565-568.

Spector T.D., Cicuttini F., Baker J., Loughlin J., Hart D. 1996. Genetic influences on osteoarthritis in women: a twin study. *British Medical Journal* 312: 940-944.

Spector, T.D., & Hart, D.J. 1992. How serious is knee osteoarthritis? *Annals of the Rheumatic Diseases* 51: 1105-1106.

Spector TD, MacGregor AJ. 2004. Risk Factors for Osteoarthritis: Genetics. *Osteoarthritis & Cartilage* 12: S39-S44.

SPSS Inc. 2007. *SPSS Base 8.0 for Windows User's Guide*.SPSS Inc., Chicago IL.

Steele J, Mays S. 1995. Handedness and directional asymmetry in the long bones of the human upper limb. *International Journal of Osteoarchaeology* 5(1): 39-49.

Steen SL, Lane RW. 1998. Evaluation of habitual activities among two Alaskan Eskimo populations based on musculoskeletal stress markers. *International Journal of Osteoarchaeology* 8(5): 341-353.

Stevens SD, Strand Viðarsdóttir U. 2008. Morphological changes in the shape of the non-pathological bony knee joint with age: A morphometric analysis of the distal femur and proximal tibia in three populations of known age at death. *International Journal of Osteoarchaeology* 18: 352-371.

Stone, A.C., A. K. Wilbur, J. E. Buikstra & C.A. Roberts. 2009. Tuberculosis and Leprosy in Perspective. *Yearbook of Physical Anthropology* 52: 66-94.

Stone R, Appleton-Fox N. 1996. *A view of Hereford's past: Report on the archaeological excavation of Hereford Cathedral Close in 1993*. Hereford: Logaston Press.

Strand Viðarsdóttir U, Cobb S. 2004. Inter- and intra-specific variation in the ontogeny of the hominoid facial skeleton: testing assumptions of ontogenetic variability. *Annals of Anatomy* 186(5-6): 423-428.

Strand Viðarsdóttir U, O'Higgins P, Stringer C. 2002. A geometric morphometrics study of regional differences in the ontogeny of the modern human facial skeleton. *Journal of Anatomy* 201(3): 211-229.

Stroud G. *The human skeletal remains from Hickleton, South Yorkshire*. Unpublished skeletal report, held at the Biological Anthropology Research Centre, Archaeological Sciences, University of Bradford. *unpublished*

Suzuki K, Takigawa W., Tanigawa K, Nakamura K, Ishido Y, Kawashima A, Wu H, Sue M, Yoshihara A, Mori S, Ishii N. 2010. Detection of *Mycobacterium leprae* DNA from archaeological skeletal remains in Japan using whole genome amplification and polymerase chain reaction. *PLoS One* 5(8).

Sydes B. 1984. *The excavation of St. Wilfrid's church, Hickleton: An intrim report, September 1984.* Unpublished report. Shefflied: South Yorkshire County Council Archaeology.

Takahashi K., Miyazaki T, Ohnari H, Takino T, Tomita K. 1995. Schmorl's nodes and low-back pain. *European Spine Journal* 4: 56-59.

Tan, A.L., Toumi H., Benjamin M., Grainger A.J., Tanner S.F., Emery P., McGonagle D. 2006. Combined high-resolution magnetic resonance imaging and histological examination to explore the role of ligaments and tendons in the phenotypic expression of early hand osteoarthritis. *Annals of Rheumatic Diseases* 65: 1267-1272.

Taylor GM, Watson CL. Bouwman AS, Lockwood DN, Mays SA. 2006. Variable nucleotide tandem repeat (VNTR) typing of two palaeopathological cases of lepromatous leprosy from Medieval England. *Journal of Archaeological Science* 33(11): 1569-1579.

Taylor GM, Mays SA, Huggett JF. 2010. Ancient DNA (aDNA) studies of man and microbes: general similarities and specific differences. *International Journal of Osteoarchaeology* 20(6): 747-751.

Thandrayen K, Pettifor JM. 2010. Maternal vitamin D status: Implications for the development of infantile nutritional rickets. *Endocrinology Metabolism Clinics of North America* 39(2): 303-320.

Tukker A, Visscher TLS, Picavet HSJ. 2009. Overweight and health problems of the lower extremities: osteoarthritis, pain and disability. *Public Health & Nutrition* 12: 359-368.

Ulrich M, Zulueta AM, Caceres-Dittmar G, Sampson C, Pinardi ME, Rada Em, Aranzazu N. Leprosy in women: Characteristics and repercussions. *Social Science & Medicine* 37(4): 445-456.

Üstündağ H. 2009. Schmorl's nodes in a Post-Medieval skeletal sample from Klostermarienberg, Austria. *International Journal of Osteoarchaeology* 19: 695-710.

Van Brakel WH. 2006. Measuring health-related stigma: A literature review. *Psychology, Health & Medicine* 11(3): 307-334.

Van der Kraan PM, van der Berg WB. 2008. Osteoarthritis in the context of ageing and evolution loss of chondrocyte differentiation block during ageing. *Ageing Research Reviews* 7: 106-113.

VanPool TL, Leonard RD. 2011. *Quantitative Analysis in Archaeology*. London: Wiley-Blackwell Publishing.

Vernon-Roberts B. 1989. Pathology of intervertebral discs and apophyseal joints. In: Jayson MIV, editor. *The lumbar spine and back pain*. Edinburgh: Churchill Livingstone. p 37-55.

Vernon-Roberts B, Moore RJ, Fraser D. 2007. The Natural History of Age-Related Disc Degeneration: The Pathology and Sequelae of Tears. *Spine* 32(25): 2797-2804.

Von Hunnis T. 2009. Using microscopy to improve a diagnosis: an isolated case of tuberculosis-induced hypertrophic osteopathy in archaeological dog remains. *International Journal of Osteoarchaeology* 19(3): 397-405.

Von Porat, Ross EM, Roos H. 2004. High prevalence of osteoarthritis 14 years after an anterior cruciate ligament tear in male soccer players: a study of radiographic and patient relevant outcomes. *Annals of Rheumatic Disease* 63: 269-273.

Wada M, Tatsuo H., Baba H., Asamoto K., Nojyo Y. 1999. Femoral intercondylar notch measurements in osteoarthritic knees. *Rheumatology* 38(6): 554-558.

Walker BF. 2000. The prevalence of low back pain: A systematic review of the literature from 1966-1998. *Journal of Spinal Disorders* 13(3): 205-217.

Waldron T. 1991. The Prevalence of, and the Relationship Between Some Spinal Diseases in a Human Skeletal Population from London. *International Journal of Osteoarchaeology* 1: 103-110.

Waldron T. 1992. Osteoarthritis in a Black Death cemetery in London. *International Journal of Osteoarchaeology* 2(3): 235-240.

Waldron T. 1994. *Counting the Dead: The Epidemiology of Skeletal Populations*. Chichester: J. Wiley.

Waldron T. 2009. *Palaeopathology*. Cambridge: Cambridge University Press.

Waldron T, Rodwell W. 2007. *St. Peter's Barton-upon-Humber, Lincolnshire: A parish church and its community*. Oxford: Oxbow.

Waldron T, Rogers J. 1991. Inter-observer variation in coding osteoarthritis in human skeletal remains. *International Journal of Osteoarchaeology* 1(1): 49-56.

Wagner CL, Greer FR. 2008. Prevention of rickets and vitamin D deficiency in infants, children, and adolescents. *Pediatrics* 122: 1142- 1152.

Wang TJ, Pencina MJ, Booth SL, Jacques PF, Ingelsson E, Lanier K, Benjamin EJ, D'Agostino RB, Wolf M, Vasan RS. Vitamin D deficiency and risk of cardiovascular disease. *Circulation* 117: 503-511.

Watkins R. 2012. Variation in healthy and socioeconomic status within the W. Montague Cobb skeletal collection: Degenerative joint disease, trauma and cause of death. *International Journal of Osteoarchaeology* 22: 22-44.

Watts R. 2010. Non-specific indicators of stress and their association with age at death in Medieval York: Using stature and vertebral neural canal size to examine the effects of stress occurring during different periods of development. *International Journal of Osteoarchaeology* 21(5): 568-576.

Webb AR, Kline L, Holick MF. 1988. Influence of season and latitude on the cutaneous synthesis of vitamin $D_3$: Exposure of winter sunlight in Boston and Edmonton will not promote vitamin $D_3$ synthesis in human skin. *Journal of Clinical Endocrinololgy & Metabolism* 67(2): 373-378.

Webb R, Brammah T, Lunt M, Urwin M, Allison T, Symmons D. 2003. Prevalence and predictors of intense, chronic, and disabling neck and back pain in the UK general population. *Spine* 28(11): 1195-1202.

Weber GW, Bookstein FL. 2011. *Virtual Anthropology: a guide to a new interdisciplinary field*. New York: Springer.

Weber GW, Schäfer K, Prossinger H, Gunz P, Mitteröcker P, Seidler H. 2001. Virtual anthropology: the digital evolution in anthropological sciences. *Journal of Physiological Anthropology and Applied Human Science* 20(2): 69-80.

Weiss E. 2005 Understanding osteoarthritis patterns: and examination of aggregate osteoarthritis. *Journal of Paleopathology* 16: 87-98.

Weiss E. 2006. Osteoarthritis and body mass. *Journal of Archaeological Science* 33: 690-695.

Weiss, E. & R. Jurmain. 2007. Osteoarthritis Revisited: A Contemporary Review of Aetiology. *International Journal of Osteoarchaeology* 17(5): 437-450.

Weston D, Boylston A, Ogden AR. (in prep) *The Mappa Mundi Excavation at Hereford Cathedral in 1993: Report on the Human Skeletal Remains*. Unpublished.

White JW, Ruttenberg BI. 2007. Discriminant function analysis in marine ecology: Some oversights and their solutions. *Marine Ecology Progress* 329: 301-305.

Whyne CM, Hu SS, Klisch S, Lotz J. 1998. Effect of the pedicle and posterior arch on vertebral body strength predictions in finite element modeling. *Spine* 23(8): 899-907.

Wilder DG, Pope MH, Frymoyer JW. 1988. The biomechanics of lumbar disc herniations and the effect of overload and instability. *Journal of Spinal Disorders* 1(1):16-32.

Williams FMK, Manek NJ, Sambrook P, Spector TD, MacGregor AJ. 2007. Schmorl's nodes: Common, highly heritable, and related to lumbar disc disease. *Arthritis & Rheumatism* 57(5): 855-60.

Wilkins KE. 1986. Bowlegs. *Pediatric Clinics of North America* 33(6): 1429-1438.

Woods RJ. *Biomechanics and osteoarthritis of the knee*. Unpublished PhD thesis. The Ohio State University.

Woolf AD. 2002. *Bone and Joint Futures*. London: BMJ Books.

Wren KT. 2007. *Methodological Considerations: Osteoarthritis and the Significance of Porosity in the William M. Bass Donated Skeletal Collection*. Unpublished Master's thesis, University of Tennessee.

Wright AA, Cook C, Abbott JH. 2009. Variables associated with the progression of hip osteoarthritis: a systematic review. *Arthritis Care & Research* 61(7): 925-936.

Zelditch ML, Swiderski DL, Sheets HD, Fink. 2004. *Geometric morphometrics for biologists: A primer*. Elsevier Academic Press: San Diego, CA.

Zhai, G., D.J. Hart, B.S. Kato, A. MacGregor, & T.D. Spector. 2007. Genetic influence on the progression of radiographic knee osteoarthritis: A longitudinal twin study. *Osteoarthritis & Cartilage* 15: 222-225.

Zhang N, Li F, Huang Y, Teng C, Chen W. 2010. Possible key role of immune system in Schmorl's nodes. *Medical Hypotheses* 74: 552-554.